UNCLASSIFIED

AD 404 072

Reproduced
by the

DEFENSE DOCUMENTATION CENTER

FOR

SCIENTIFIC AND TECHNICAL INFORMATION

CAMERON STATION, ALEXANDRIA, VIRGINIA

UNCLASSIFIED

NOTICE: When government or other drawings, specifications or other data are used for any purpose other than in connection with a definitely related government procurement operation, the U. S. Government thereby incurs no responsibility, nor any obligation whatsoever; and the fact that the Government may have formulated, furnished, or in any way supplied the said drawings, specifications, or other data is not to be regarded by implication or otherwise as in any manner licensing the holder or any other person or corporation, or conveying any rights or permission to manufacture, use or sell any patented invention that may in any way be related thereto.

AD 404 072

GRAPHIC DI
GEOMAGNET

RM 63TMP-2
DASA 1372
1 APRIL 1963

GENERAL ELECTRIC COMPANY
SANTA BARBARA,
CALIFORNIA

1

CATALOGED BY ASTIA
AS AD No. 404072

HIC DISPLAYS OF
AGNETIC GEOMETRY

DDC
MAY 20 1963

CTRIC COMPANY
A,

63-3-4

GRAPHIC DISPL
GEOMAGNETIC

RM 63TMP-2
DASA 1372
1 APRIL 1963

Walter F. Dudziak
David D. Kleinecke
Theodore J. Kostigen

Submitted to: Defense Atomic Support Agency
Washington 25, D.C.

Under Contract: DA 49-146-XZ-109

TECHNICAL MILITARY
PLANNING OPERATION
GENERAL ELECTRIC COMPANY
SANTA BARBARA, CALIFORNIA

APHIC DISPLAYS OF
)MAGNETIC GEOMETRY

TMP-2
1372
L 1963

ORIGINAL CONTAINS COLOR PLATES: ALL DDC REPRODUCTIONS WILL BE IN BLACK AND WHITE. ORIGINAL MAY BE SEEN IN DDC HEADQUARTERS.

Dudziak
Kleinecke
J. Kostigen

Atomic Support Agency
gton 25, D.C.

146-XZ-109

IICAL MILITARY
'ING OPERATION
AL ELECTRIC COMPANY
BARBARA, CALIFORNIA

2

ABSTRACT

This report contains sixty maps presenting computational data pertaining to the geometric properties of the geomagnetic field and a brief related theoretical description to make this material more meaningful. The maps display (1) the values of total field intensity (B) and McIlwain's magnetic shell parameter (L) for altitudes from zero to two thousand kilometers, (2) the detailed value of total field intensity near the South Atlantic anomaly, (3) the traces in both hemispheres of points with a fixed value of B and L and (4) some other geomagnetic properties. The description includes tables of the geomagnetic coefficients used and a description of the codes utilized.

The maps have been carefully checked. Because of the magnitude of this task and the wide distribution, notification of any detectable errors which may have been overlooked would be appreciated.

ACKNOWLEDGMENTS

It is difficult in a brief summary to justly acknowledge the help of everyone whose work played a part in molding the ideas that have led to the presentation of the results of this study. To all of those who are not mentioned we apologize, for to all we are equally indebted.

It is a pleasure to express our sincerest appreciation to Lt. Col. Billy McCormac of DASA for his encouragement and stimulating discussions. Similarly it is our pleasure to express our sincere appreciation to Major R. Pennington of DDRE and Dr. C. E. McIlwain of U. C. San Diego for contributing their computer codes, as well as the help of E. W. Klingenberg for his aid in the development of the plotting routines.

WFD

DCK

TJK

TABLE OF CONTENTS

ABSTRACT	II
ACKNOWLEDGEMENTS	II
LIST OF ILLUSTRATIONS	III
LIST OF TABLES	V
DESCRIPTIVE MATERIAL	VI
I. Introduction	VI
II. Physical Background	VI
III. Description of Maps	XXI
REFERENCES	XXIII
MAPS	
A. Contours of B and L	1
B. Contours of B Near the South Atlantic Anomaly	17
C. Contours of B and L (Jensen and Whitaker Coefficients)	33
D. Comparison Between Contours (as calculated from the Jensen and Cain Coefficients and as calculated from the Jensen and Whitaker Coefficients)	35
E. Constant B-L Traces	39
F. Differences Between Constant B-L Traces	45
G. Pairs of Conjugate B-L Traces	49
H. The Geomagnetic Equator	51
I. Approximate Geomagnetic Shell Latitudes	52
J. Conjugate Auroral Grids	53

LIST OF ILLUSTRATIONS

Figure	Title	Page
A	MAGNETIC SHELL FUNCTION F	XIX
	Constant Magnetic Field Intensity, B(Gauss), and Constant Magnetic Shell Parameter, L (Earth Radii), at Altitude...	
1	...0 Kilometers	1
2	...100 Kilometers	2
3	...200 Kilometers	3
4	...300 Kilometers	4
5	...400 Kilometers	5
6	...500 Kilometers	6
7	...600 Kilometers	7
8	...700 Kilometers	8
9	...800 Kilometers	9
10	...900 Kilometers	10
11	...1000 Kilometers	11
12	...1200 Kilometers	12
13	...1400 Kilometers	13
14	...1600 Kilometers	14
15	...1800 Kilometers	15
16	...2000 Kilometers	16

LIST OF ILLUSTRATIONS (cont.)

Constant Magnetic Field Intensity, B(Gauss), in the Region of the South Atlantic Anomaly at Altitude...

17 ...0 Kilometers 17

18 ...100 Kilometers 18

19 ...200 Kilometers 19

20 ...300 Kilometers 20

21 ...400 Kilometers 21

22 ...500 Kilometers 22

23 ...600 Kilometers 23

24 ...700 Kilometers 24

25 ...800 Kilometers 25

26 ...900 Kilometers 26

27 ...1000 Kilometers 27

28 ...1200 Kilometers 28

29 ...1400 Kilometers 29

30 ...1600 Kilometers 30

31 ...1800 Kilometers 31

32 ...2000 Kilometers 32

33 Constant Magnetic Field Intensity, B(Gauss), and Constant Magnetic Shell Parameter, L(Earth Radii), at altitude 0 Kilometers (Jensen and Whitaker Coefficients) 33

34 Constant Magnetic Field Intensity, B(Gauss), and Constant Magnetic Shell Parameter, L(Earth Radii), at altitude 500 Kilometers (Jensen and Whitaker Coefficients) 34

35 Constant Magnetic Field Intensity, B(Gauss), Using the 48 Coefficients of Jensen & Crain and the 512 coefficients of Jensen & Whitaker at Altitude 0 Kilometers. 35

36 Constant Magnetic Shell Parameter L(Earth Radii), Using the 48 Coefficients of Jensen & Cain and the 512 Coefficients of Jensen & Whitaker at Altitude 0 Kilometer 36

LIST OF ILLUSTRATIONS (cont.)

Figure	Title	Page
37	Constant Magnetic Field Intensity, B(Gauss), Using the 48 Coefficients of Jensen & Cain and the 512 Coefficients of Jensen & Whitaker at Altitude 500 Kilometers.	37
38	Constant Magnetic Shell Parameter, L(Earth Radii), Using the 48 Coefficients of Jensen & Cain and the 512 Coefficients of Jensen & Whitaker at Altitudes 500 Kilometers	38
39	Constant B-L Traces in the Northern Hemisphere at Initial Latitude 17.5°N, Initial Longitude 190°E at Various Initial Altitudes where B is the Magnetic Field Intensity (Gauss) and L is the Magnetic Shell Parameter (in Earth Radii)	39
40	Constant B-L Trace in the Northern Hemisphere at Initial Latitude 17.5°N, Initial Longitude 190°E at Initial Altitude 1500km where B is the Magnetic Field Intensity (Gauss) and L is the Magnetic Shell Parameter (in Earth Radii)	40
41	Constant B-L Traces in the Southern Hemisphere of the Conjugate to the Traces at Initial Latitude 17.5 N, Initial Longitude 190°E at Various Initial Altitudes where B is the Magnetic Field Intensity (Gauss) and L is the Magnetic Shell Parameter (in Earth Radii)	41
42	Constant B-L Trace in the Southern Hemisphere at the Conjugate to the Traces at Initial Latitudes 17.°5 N Initial Longitude 190°E at Initial Altitude 1500km where B is the Magnetic Field Intensity (Gauss) and L is the Magnetic Shell Parameter (in Earth Radii)	42
43	Constant B-L Traces in the Northern Hemisphere at Initial Latitudes 46°N, Initial Longitudes 72°E at Various Initial Altitudes where B is the Magnetic Field Intensity (Gauss) and L is the Magnetic Shell Parameter (in Earth Radii)	43

LIST OF ILLUSTRATIONS (cont.)

Figure	Title	Page
44	Constant B-L Traces in the Southern Hemisphere at the Conjugates to the Traces at Initial Latitude 46 N Initial Longitude 72 E at Various Initial Altitudes where B is the Magnetic Field Intensity (Gauss) and L is the Magnetic Shell Parameter (in Earth Radii)	44
45	Northern Hemisphere--Differences in Latitude verses Longitude Angles from the Constant B-L Trace at Initial Altitude of 1500km and those traces having the same Initial Latitudes 17.5 N, Longitude 190 E but Different Initial Altitudes.	45
46	Southern Hemisphere--Differences in Latitude verses Longitude Angles from the Constant B-L Conjugate Trace at Initial Altitude of 1500km and those Conjugate Traces having the same Initial Latitude 17.5 N, Longitude 190 E but at Different Initial Altitudes.	46
47	Northern Hemisphere--Differences in Latitude verses Longitude Angles from the Constant B-L Trace at Initial Altitudes 1500km and those traces having the same Initial Latitude 46 N, Longitude 72 E but Different Initial Altitudes	47
48	Southern Hemisphere--Differences in Latitude. verses Longitude Angles from the Constant B-L Conjugate Trace at Initial Altitude 1500km and those Conjugate traces having the same Initial Latitude 46 N, Longitude 72 E but at Different Initial Altitudes	48
49	Constant B-L Trace in the Northern Hemisphere for Initial Altitude of 1500km, Initial Latitude 17.5 N and Initial Longitude 190 E also its Conjugate Trace in the Southern Hemisphere	49
50	Constant B-L Trace in the Northern Hemisphere for Initial Altitude of 1500km, Initial Latitude 46 N and Initial Longitude 72 E also its Conjugate Trace in the Southern Hemisphere	50
51	Position of the Geomagnetic Equator at 100km Altitude	51
52	Approximate Geomagnetic Shell Latitudes	52

LIST OF ILLUSTRATIONS (cont.)

Figure	Title	Page
	Auroral Conjugate Grids for...	
53	... Pacific Area at 70 Kilometers	53
54	100 Kilometers	54
55	... North Eurasian Area at 70 Kilometers	55
56	100 Kilometers	56
57	... West 70 Kilometers	57
58	100 Kilometers	58
59	... East 70 Kilometers	59
60	100 Kilometers	60

LIST OF TABLES

A. Geomagnetic Coefficients as Given by Jensen and Cain XI

B. Geomagnetic Coefficients as given by Jensen and Whitaker XII

C. Coefficients In Polynomial Fits to McIlwain's f XX

DESCRIPTIVE MATERIAL

I INTRODUCTION

The earth's magnetic field has been studied since the dawn of modern physics. There are authoritative descriptions of the older work in references (1) and (2). Naturally enought the earlier students were interested only in the field on the surface of the earth--field which affected the compass. This interest led Gauss to devise the method of expansion in spherical harmonics which has dominated descriptions of the geomagnetic field for a century and a half.

More recently, inspired by Birkelund's terrella experiments which so spectacularly simulate auroral displays, geophysicists began to investigate the causes of the aurora and so initiated the study of the behavior of charged particles in space. There is an excellent description of the older work on this problem in reference (3) and the newer ideas are collected in reference (4).

Astrophysicists soon recognized the importance of this work to problems of stellar evolution and related astronomical phenomena. The background to modern work in this direction is well summarized in reference (5). More recently still it has been widely recognized that these effects, originally observed in an astronomic context, could be of great use in practical applications of fusion processes. The literature on plasma physics is already immense and mostly not too relevant to geomagnetic phenomena but some work which originated in plasma physics is of great importance (for example, references (6) and (19).

Finally, the work of Van Allen and his collegues (see, for example, reference (7) has clarified the physical picture involved in radiation belt and shell formation and placed the mathematical models of charged particles in space on a firm observational basis.

II PHYSICAL BACKGROUND

For an adequate description of the graphs in this report there are three separate stages in the development of the subject which must be considered - first, the basic geometry of the earth's geomagnetic field; second, the motion of charged particles in that field; and third, those special properties of the geomagnetic field of particular interest to studies of particle motion. Each of these is discussed separately below.

The Geomagnetic Field

The geomagnetic field unquestionably exists but its fundamental cause has not been satisfactorily explained. Paleomagnetic studies (9) indicate that it has been present since the beginning of geologic history. In the absense of any fundamental theoretical derivation it has been necessary to determine the geomagnetic field strictly from observational data. This is permissible because good observations exist over a wide range of time and location.

The geomagnetic induction $\vec{B}$ is a vector quantity which is conventionally measured in a variety of ways. $\vec{B}$ is related to the force $\vec{F}$ exerted on a particle of charge e moving with velocity $\vec{u}$ by

$$\vec{F} = e\vec{u} \otimes \vec{B} .$$

The geomagnetic field $\vec{H}$ is equal to $\vec{B}$ divided by the permeability of free space which is equal to one in electromagnetic units. Thus in electromagnetic units $\vec{H}$ and $\vec{B}$ are numerically equal but physically distinct fields. In this discussion the three magnetic induction components

$$B_r, B_\theta, B_\varphi$$

are used where r, θ, and φ are spherical coordinates with respect to the earth's center. The polar axis will be identified with the geographic axis in such a way that $\theta=0$ at the north pole (thus θ measures south co-latitude rather than

latitude). The azimuthal coordinate φ is taken as geographic longitude, east of Greenwich meridian. The earth's radius is symbolized by R and was taken to be 6371.2 kilometers in these calculations.

Charts of the magnetic field at different epochs are available from various agencies. The United States Naval Hydrographic Office has undertaken to produce up-to-date compilations at regular intervals. The data on these charts are used as input to analyses described below. Other agencies (especially in the Soviet Union) have also produced up-to-date charts of the

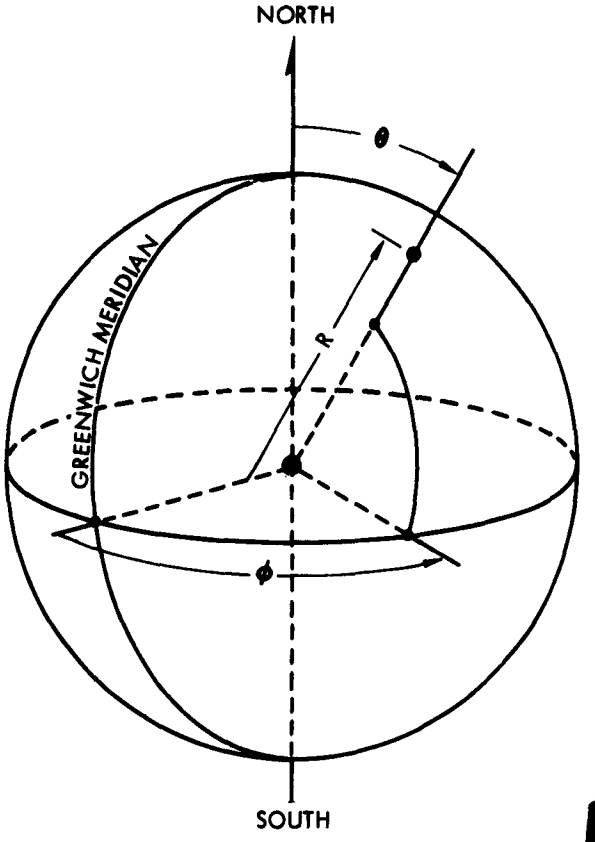

Spherical Coordinate System

magnetic field and these charts have sometimes been used to modify the standard navy charts. Satellite information has also been used to modify surface observations (see reference (10)).

The classical Gaussian analysis of the geomagnetic field requires the use of some rather ponderous classical mathematical analysis since it works with expansions in series of spherical surface harmonics. These classical mathematical techniques are presented in various manners in many different sources. The discussion in reference (11) is rigorous and complete and provides an excellent introduction to the literature. A more conventional description is given in reference (12).

The spherical surface harmonics are a double series of functions defined on the surface of a unit sphere with coordinates θ and φ

$$G_{mn} = \cos(m\varphi) P_n^m(\cos\theta) ,$$

$$H_{mn} = \sin(m\varphi) P_n^m(\cos\theta) ,$$

where P_n^m are associated Legendre polynomials as described below; n ranges from zero to infinity and m from 0 to n. It should be noted that $H_{0n} = 0$ for all n. These functions are all mutually orthogonal over the surface of the unit sphere, that is for all m, m', n and n'

$$\int \partial\theta \sin\theta \int \partial\varphi \, G_{mn} H_{m'n'} = 0,$$

$$\int \partial\theta \sin\theta \int \partial\varphi \, G_{mn} G_{m'n'} = 0 \text{ if } m' \neq m \text{ or } n' \neq n,$$

$$\int \partial\theta \sin\theta \int \partial\varphi \, H_{mn} H_{m'n'} = 0 \text{ if } m' \neq m \text{ or } n' \neq n,$$

Thus any function on the surface of the sphere can be expressed as the sum of series in terms of these functions

$$f(\theta, \varphi) = \sum_{n=o}^{\infty} \left(\sum_{m=o}^{n} g_{mn} G_{mn} + \sum_{m=1}^{n} h_{mn} H_{mn} \right)$$

and this expression is unique (with the usual restrictions on discontinuities). As is shown below the coefficients g_{mn} and h_{mn} are easily obtained by integration.

The associated Legendre polynomials are defined in many different ways. Perhaps the most convenient form is the Rodrigues' formula

$$P_n^m(\cos\theta) = (-)^n \frac{(n-m)!}{2n!} \sin^m\theta \left(\frac{\partial}{\partial\cos\theta}\right)^{m+n} \sin^n\theta.$$

The normalization factor $(n-m)!/2n!$ is that of reference (13) which has become conventional in a large part of geophysical literature. A factor of $1/2^n n!$ is used in references (11) (also with a $(-)^m$ multiplier) and (12) and most standard references. A change in normalization does not effect the basic procedure but it does change the values of the geomagnetic coefficients g_{mn} and h_{mn}; for example, the more usual normalization would lead to coefficients which are

$$\frac{2^n\, n!\,(n-m)!}{2n!}$$

times the conventional geomagnetic coefficients.

The coefficients g_{mn} and h_{mn} can be obtained in the standard fashion

$$\int\partial\theta \sin\theta \int\partial\varphi f(\theta,\varphi)\, G_{mn} = g_{mn} \int\partial\theta \sin\theta \int\partial\varphi G_{mn}^2$$

$$= g_{mn} \frac{2\pi}{2n+1} \frac{(n+m)!}{(n-m)!^3} \frac{2n!^2}{2^{2n} n!^2}$$

so that

$$g_{mn} = \frac{\int\partial\theta \sin\theta \int\partial\varphi G_{mn} f(\theta,\varphi)}{\frac{2\pi}{2n+1} \frac{(n+m)!}{(n-m)!^3} \frac{2n!^2}{2^{2n} n!^2}},$$

$$h_{mn} = \frac{\int\partial\theta \sin\theta \int\partial\varphi H_{mn} f(\theta,\varphi)}{\frac{2\pi}{2n+1} \frac{(n+m)!}{(n-m)!^3} \frac{2n!^2}{2^{2n} n!^2}}$$

The particular application of these mathematical results which is of interest here is the case where $f(\theta,\varphi)$ is one of the geomagnetic quantities.

Since all of the various forces and inductions can be obtained from a geomagnetic potential (if one exists) it is conventional to take f as the geomagnetic potential V on the surface of the earth and use "geomagnetic coefficient" to mean the coefficients in the expansion of V. For example, Gauss described the earth's magnetic field (in Gauss) in the year 1835 by

$$g_{00} = 0 \quad , \qquad g_{01} = +.3235, \qquad g_{11} = -.0311, \qquad g_{02} = -.0051,$$

$$g_{12} = -.0292, \qquad g_{22} = +.0002, \qquad h_{11} = -.0625,$$

$$h_{12} = -.0012, \qquad h_{22} = -.0157.$$

The geomagnetic potential V is not itself directly observable. The individual forces and inductions, however, are observable and, in electromagnetic units,

$$B_r = -\frac{\partial}{\partial r} V ,$$

$$B_\theta = -\frac{1}{r}\frac{\partial}{\partial \theta} V ,$$

$$B_\varphi = -\frac{1}{r\sin\theta}\frac{\partial}{\partial \varphi} V ,$$

Since

$$V = \sum_{n=o}^{\infty} \sum_{m=o}^{n} (g_{mn} G_{mn} + h_{mn} H_{mn}) ;$$

it follows, for example, that

$$B_\varphi = -\frac{1}{R \sin\theta} \sum_{n=o}^{\infty} \sum_{m=o}^{n} (g_{mn} \frac{\partial}{\partial \varphi} G_{mn} + h_{mn} \frac{\partial}{\partial \varphi} H_{mn}) ,$$

and, since $\frac{\partial}{\partial \varphi} G_{mn} = - m H_{mn}$, and $\frac{\partial}{\partial \varphi} H_{mn} = m G_{mn}$,

$$B_\varphi = -\frac{1}{R\sin\theta}\sum_{n=o}^{\infty}\sum_{m=o}^{n} m(-g_{mn}H_{mn} + h_{mn}G_{mn}) ,$$

so that

$$g_{mn} = \frac{R\sin\theta}{m}\,\frac{\int\partial\theta\sin\theta\int\partial\varphi G_{mn}B_\varphi}{\frac{2\pi}{2n+1}\,\frac{(n+m)!}{(n-m)!^3}\,\frac{2n!^2}{2^2 n_{n!}^2}} ,$$

and so on. There is a similar approach based on B_θ. For B_r as will be discussed below it is necessary to introduce a radial dependence.

The analysis just described is an excellent means of studying the geomagnetic field and its changes so long as attention is confined to the surface of the earth. In order to describe the behavior of charged particles in space it is necessary to extend this knowledge above the earth's surface. For this purpose, some additional assumptions are required because the analysis given above is valid for any function whatsoever defined over the earth's surface. If there were no geomagnetic potential the only defect in the surface analysis would be that the coefficients derived from B_θ would not equal those from B_φ. Since Maxwell's equations virtually insure the existence of a potential this is a priori unlikely to occur and experience shows that the minor differences which do arise are well within the observational uncertainties.

In order to make an extension of the analysis into space (or to evaluate B_r) it is necessary to assume that the values on the surface are boundary values of some field which fills space and whose behavior is known. If the field is constant and there are no magnetic sources in space then the potential must, by Maxwell's equations, be magnetostatic and satisfy Laplace's equation

$$0 = \frac{\partial}{\partial r}\left(r^2\frac{\partial}{\partial r}V\right) + \frac{1}{\sin^2\theta}\frac{\partial^2}{\partial\varphi^2}V + \frac{1}{\sin\theta}\frac{\partial}{\partial\theta}\left(\sin\theta\frac{\partial}{\partial\theta}V\right) .$$

The solutions of Laplace's equation (and related material) are well known as the subject matter of potential theory (see, for example, reference (14)). One of the theorems of potential theory states that the potential is uniquely determined by its boundary values.

The magnetic field is definitely not constant. However, the hope is that it can be assumed (a) to be approximately constant (an adiabatic constant in the sense used in the discussion below on the behavior of charged particles) with respect to very long term changes and (b) to smooth over short term changes. The smoothing has not been very carefully standardized--"it is usual to take an annual mean based on quiet days as the value of the main field at any station" (reference (2)). Many of the irregularities arise because the second assumption---no sources in space---is also invalid. Ionospheric currents are easily detectable but these alone do not cause all the variations; some sources of irregularity have never been explained. It is the hope that smoothing will permit the discussion of any adiabatic constant geomagnetic field. In the absence of a definitive treatment of this problem it seems best to proceed with the magnetostatic assumption.

The computer codes used in making these computations apply equally well to all the points on the earth's surface. For this reason the data has been extended into close proximity to the magnet and geographic poles. Many geophysicists believe that computations based on the magnetostatic assumption are very inaccurate in the "auroral zone" (say, above about 50° in latitude) because this zone is subject to interference from interplanetary magnetic disturbances and the lines of force originating here extend so far into space that they may not close or may be persistently broken. Until this question is settled the data presented here for the region near the poles should be used with caution.

In this case the extension from boundary value to potential in space is formally immediate because

$$V = \sum_{n=o}^{\infty} \frac{R^{n+1}}{r^{n+1}} \sum_{m=o}^{n} (g_{mn} G_{mn} + h_{mn} H_{mn})$$

is the unique solution of Laplace's equation which vanishes at infinity such that

$$V = \sum_{n=o}^{\infty} \sum_{m=o}^{n} (g_{mn}G_{mn} + h_{mn}H_{mn})$$

on the surface. This shows how B_r can be used to determine the coefficients since

$$B_r = -\frac{\partial V}{\partial r} = \sum_{n=o}^{\infty} (n+1) \frac{R^{n+1}}{r^{n+2}} \sum_{m=o}^{n} (g_{mn}G_{mn} + h_{mn}H_{mn})$$

in general and on the surface

$$B_r = \frac{1}{R} \sum_{n=o}^{\infty} (n+1) \sum_{m=o}^{n} (g_{mn}G_{mn} + h_{mn}H_{mn}) ,$$

so that

$$g_{mn} = \frac{R}{n+1} \frac{\int \partial\theta \sin\theta \int \partial\varphi G_{mn} B_r}{\frac{2\pi}{2n+1} \frac{(n+m)!}{(n-m)!^3} \frac{2n!^2}{2^{2n} n!^2}} ,$$

and so on. The general formulas for B_φ and B_θ are easily obtained and closely resemble those for points on the surface.

$$B_\varphi = -\frac{1}{R\sin\theta} \sum_{n=o}^{\infty} \frac{R^{n+1}}{r^{n+.}} \sum_{m=o}^{n} m(-g_{mn}H_{mn} + h_{mn}G_{mn}) ,$$

$$B_\theta = -\frac{1}{R} \sum_{n=o}^{\infty} \frac{R^{n+1}}{r^{n+1}} \sum_{m=o}^{n} (g_{mn} \frac{\partial}{\partial\theta} H_{mn} + h_{mn} \frac{\partial}{\partial\theta} G_{mn}) .$$

It is most convenient to work with a system of units which measure r in earth radii so that R=1 in all the equations given above.

It is easy to conceive how the formulas given could be embodied in a computer program. There is such a program--a subroutine called MAGNET--which originated with Air Force Special Weapons Center,

Kirtland A. F. B. This subroutine exists in several different versions depending on the values used for the geomagnetic coefficients. Another form of this subroutine utilizing identical mathematical procedures but written in FAP for speed and convenience in changing geomagnetic coefficients has been prepared at TEMPO. These versions give identical (to five significant figures) results when used with the same coefficients except at poles where the AFSWC version fails to compute B_θ correctly.

Most of the computations reported here used a set of 48 coefficients obtained by D.C. Jensen and J.C. Cain (reference (15)) for epoch 1960; these were compared in some computations to a set of 512 (nominally, actually 568 were used) due to D.C. Jensen and W.A. Whitaker (reference (16)) for epoch 1955. The difference is relatively small. The 48 coefficients of Jensen and Cain are shown in Table A; the Jensen and Whitaker coefficients are shown in Table B. The Jensen and Whitaker coefficients are also reproduced in reference (10); the version in Table B differs slightly but the difference is probably not significant.

Motion of Charged Particles

The motion of charged paticles in a magnetic field is a well-known phenomena. In particular, all the experience of plasma physics is available as well as work in aurora and stellar physics. The motion has been studied in detail (see, for example, reference (17)). Suppose a particle has relativistic mass m and charge e and it moves with (vector) velocity $\vec{u}$ in a magnetic (induction) field $\vec{B}$ then its acceleration $\vec{a}$ is given (in rational electromagnetic units) by

$$\vec{a} = \frac{e}{m} \vec{u} \vec{\otimes} \vec{B}$$

where $\vec{\otimes}$ is the vector outer product. If $\vec{B}$ is uniform of strength B in the direction of the z-axis then

$$a_x = \frac{e}{m} B u_y \quad ,$$

X

Table A. Geomagnetic Coefficients as give

$g_{00} = 0$

$g_{01} = +.304112$

$g_{02} = +.024035$

$g_{03} = -.031518$

$g_{04} = -.041794$

$g_{05} = +.016256$

$g_{06} = -.019523$

$g_{11} = +.021474$	$h_{11} = -.057989$
$g_{12} = -.051253$	$h_{12} = +.033124$
$g_{13} = +.062130$	$h_{13} = +.014870$
$g_{14} = -.045298$	$h_{14} = -.011825$
$g_{15} = -.034407$	$h_{15} = -.000796$
$g_{16} = -.004853$	$h_{16} = -.005758$

ficients as given by Jensen and Cain (in gauss)

$g_{22} = -.013381$	$h_{22} = -.001579$
$g_{23} = -.024898$	$h_{23} = -.004075$
$g_{24} = -.021795$	$h_{24} = +.010006$
$g_{25} = -.019447$	$h_{25} = -.002000$
$g_{26} = +.003212$	$h_{26} = -.008735$
$g_{33} = -.006496$	$h_{33} = +.000210$
$g_{34} = +.007008$	$h_{34} = +.000430$
$g_{35} = -.000608$	$h_{35} = +.004597$
$g_{36} = +.021413$	$h_{36} = -.003406$
$g_{44} = -.002044$	$h_{44} = +.001385$
$g_{45} = +.002775$	$h_{45} = +.002421$
$g_{46} = +.001051$	$h_{46} = -.000118$
$g_{55} = +.000697$	$h_{55} = -.001218$
$g_{56} = +.000227$	$h_{56} = -.001116$
$g_{66} = +.001115$	$h_{66} = -.000325$

Table B. Geomagnetic Coefficients as given by Jensen an

G 0 0 =	-1.81868757E-04
G 0 1 =	3.03954965E-01
G 0 2 =	2.33116880E-02
G 0 3 =	-2.94613826E-02
G 0 4 =	-3.84925836E-02
G 0 5 =	1.40194169E-02
G 0 6 =	-5.53376138E-04
G 0 7 =	-2.82791689E-02
G 0 8 =	3.96758285E-02
G 0 9 =	-5.80275220E-02
G 010 =	7.16070324E-02
G 011 =	-1.42793787E-01
G 012 =	6.65231597E-02
G 013 =	2.59923062E-02
G 014 =	-3.89992028E-01
G 015 =	4.54625410E-01
G 016 =	-7.67623520E-01
G 017 =	1.13768254E+00
G 018 =	6.71064389E-01
G 019 =	-4.41675669E-01
G 020 =	2.55144835E+00
G 021 =	9.11195302E-01
G 022 =	6.29949319E+00
G 023 =	1.80562043E+01
G 024 =	-1.43265873E+01

G 2 2=	-1.44362517E-02	H 2 2=	-.39770
G 2 3=	-2.18119371E-02	H 2 3=	-.40692
G 2 4=	-2.30735725E-02	H 2 4=	.87596
G 2 5=	-9.90265870E-03	H 2 5=	-.68792
G 2 6=	-1.33617684E-02	H 2 6=	-.19722
G 2 7=	2.80319178E-02	H 2 7=	-.31370
G 2 8=	-5.54907614E-02	H 2 8=	-.50937
G 2 9=	5.79421985E-02	H 2 9=	-.23562
G 210=	-9.57042813E-02	H 210=	-.44653
G 211=	1.10184102E-01	H 211=	-.26703
G 212=	-3.07802543E-01	H 212=	-.17468
G 213=	3.15454930E-01	H 213=	-.11858
G 214=	-7.38183868E-01	H 214=	.19509
G 215=	1.29783694E+00	H 215=	-.59673
G 216=	-1.59470893E+00	H 216=	.17438
G 217=	6.86960286E+00	H 217=	-.40989
G 218=	-3.88578549E+00	H 218=	.44624
G 219=	-4.33715057E-01	H 219=	.25762
G 220=	-4.51282966E+00	H 220=	.52052
G 221=	4.81428140E+00	H 221=	-.29131
G 222=	-1.02758293E+01	H 222=	.12025
G 223=	1.54551627E+01	H 223=	-.90117
G 224=	-2.61509347E+01	H 224=	.28835

G 1 1=	1.95516829E-02	H 1 1 =	-.56772422E-01
G 1 2=	-5.00696254E-02	H 1 2 =	.31326689E-01
G 1 3=	5.67198098E-02	H 1 3 =	.13461722E-01
G 1 4=	-4.29228514E-02	H 1 4 =	-.42734104E-02
G 1 5=	-3.92501289E-02	H 1 5 =	.60307883E-03
G 1 6=	-1.51519343E-02	H 1 6 =	.69540757E-02
G 1 7=	9.88630116E-04	H 1 7 =	.21372991E-02
G 1 8=	-2.60652316E-02	H 1 8 =	.22308741E-01
G 1 9=	-1.36711310E-02	H 1 9 =	-.38442398E-01
G 110=	7.58558434E-02	H 110 =	.47657927E-01
G 111=	-2.36752740E-01	H 111 =	-.13708930E+00
G 112=	3.28001598E-01	H 112 =	.87569359E-01
G 113=	-4.07894486E-01	H 113 =	.11263226E+00
G 114=	-1.21878576E-02	H 114 =	.35060196E+00
G 115=	9.51373816E-01	H 115 =	.13410333E+00
G 116=	-1.60000132E+00	H 116 =	.94253541E+00
G 117=	1.62543717E+00	H 117 =	.44449853E+00
G 118=	1.87724178E-01	H 118 =	-.16294888E+00
G 119=	-8.28943944E-01	H 119 =	-.22336922E+00
G 120=	1.30357011E+00	H 120 =	-.10106994E+01
G 121=	-2.85698953E-01	H 121 =	.52921404E-02
G 122=	-1.25369941E+00	H 122 =	-.10813708E+01
G 123=	9.11831880E+00	H 123 =	.95924255E+00
G 124=	-1.21354425E+01	H 124 =	.25457914E+01

G 3 3=	-7.87599021E-03	H 3 3=	.37069
G 3 4=	7.69684792E-03	H 3 4=	.29573
G 3 5=	4.64784771E-03	H 3 5=	-.82332
G 3 6=	1.83292185E-02	H 3 6=	.34563
G 3 7=	1.16323982E-02	H 3 7=	-.92663
G 3 8=	-1.21336505E-02	H 3 8=	.13198
G 3 9=	6.20017439E-02	H 3 9=	.44506
G 310=	-1.04773767E-02	H 310=	-.17950
G 311=	1.69627547E-01	H 311=	.13344
G 312=	-3.33588099E-02	H 312=	-.13154
G 313=	3.93287235E-01	H 313=	.27327
G 314=	8.75455499E-02	H 314=	-.45138
G 315=	6.29087347E-01	H 315=	.72092
G 316=	-7.85736656E-01	H 316=	-.21753
G 317=	2.54874733E+00	H 317=	.38167
G 318=	-1.06856495E+01	H 318=	.14819
G 319=	7.36168706E+00	H 319=	-.85143
G 320=	-9.39381993E+00	H 320=	.13051
G 321=	2.17313221E+01	H 321=	-.23914
G 322=	-8.09967613E+00	H 322=	.10810
G 323=	5.67008585E+01	H 323=	-.63910
G 324=	4.85954058E+00	H 324=	-.72432

Coefficients as given by Jensen and Whitaker

7E-02	H 2 2=	-.39770070E-02	G 4 4=	-2.68995824E-03	H 4 4=	.14357304E-02
1E-02	H 2 3=	-.40692630E-02	G 4 5=	2.36998877E-03	H 4 5=	.19446669E-02
5E-02	H 2 4=	.87596376E-02	G 4 6=	2.07940811E-03	H 4 6=	.26233475E-02
0E-03	H 2 5=	-.68792437E-02	G 4 7=	1.26910639E-03	H 4 7=	-.57251951E-02
4E-02	H 2 6=	-.19722961E-01	G 4 8=	-6.11431164E-03	H 4 8=	.69763496E-02
8E-02	H 2 7=	-.31370295E-02	G 4 9=	-1.14259993E-04	H 4 9=	-.19227442E-02
4E-02	H 2 8=	-.50937451E-02	G 410=	-1.78115948E-02	H 410=	.14025690E-01
5E-02	H 2 9=	-.23562953E-01	G 411=	2.49092811E-02	H 411=	.14587651E-02
3E-02	H 210=	-.44653744E-01	G 412=	-9.04762042E-03	H 412=	.32060851E-01
2E-01	H 211=	-.26703096E-01	G 413=	3.46934888E-02	H 413=	.21117154E+00
3E-01	H 212=	-.17468439E+00	G 414=	7.19249713E-02	H 414=	-.65312709E-01
0E-01	H 213=	-.11858796E+00	G 415=	1.61639129E-01	H 415=	.13883826E+01
8E-01	H 214=	.19509618E+00	G 416=	1.09987515E+00	H 416=	-.98344058E+00
4E+00	H 215=	-.59673567E+00	G 417=	-1.69762634E-01	H 417=	.42977376E+01
3E+00	H 216=	.17438091E+01	G 418=	3.46227095E-01	H 418=	-.27706360E+01
6E+00	H 217=	-.40989000E+01	G 419=	2.12356859E+00	H 419=	-.24920900E+01
9E+00	H 218=	.44624547E+01	G 420=	-8.26668859E+00	H 420=	.37605141E+01
7E-01	H 219=	.25762977E+00	G 421=	2.20897472E+01	H 421=	-.24900554E+02
6E+00	H 220=	.52052133E+01	G 422=	-4.82690144E+01	H 422=	.30410382E+02
0E+00	H 221=	-.29131021E+01	G 423=	9.25412357E+01	H 423=	-.10742829E+03
3E+01	H 222=	.12025600E+02	G 424=	-1.74685910E+02	H 424=	.11363591E+03
7E+01	H 223=	-.90117842E+01				
7E+01	H 224=	.28835645E+02				

1E-03	H 3 3=	.37069506E-03	G 5 5=	1.90808070E-04	H 5 5=	-.39044273E-03
2E-03	H 3 4=	.29573649E-02	G 5 6=	-3.41266379E-04	H 5 6=	-.57703760E-03
1E-03	H 3 5=	-.82332600E-03	G 5 7=	1.80337308E-03	H 5 7=	.84937564E-03
5E-02	H 3 6=	.34563800E-02	G 5 8=	-3.72495374E-03	H 5 8=	-.45125045E-02
2E-02	H 3 7=	-.92663568E-02	G 5 9=	6.54090440E-03	H 5 9=	-.20082999E-02
5E-02	H 3 8=	.13198289E-01	G 510=	-3.22639897E-02	H 510=	.16581872E-01
9E-02	H 3 9=	.44506361E-03	G 511=	3.00731552E-02	H 511=	.33973354E-01
7E-02	H 310=	-.17950016E-01	G 512=	-8.50520551E-02	H 512=	.36425515E-01
7E-01	H 311=	.13344460E+00	G 513=	1.81601094E-01	H 513=	.66510495E-01
9E-02	H 312=	-.13154834E+00	G 514=	-3.09801957E-01	H 514=	.20757329E+00
5E-01	H 313=	.27327400E+00	G 515=	2.51311260E-01	H 515=	-.36455151E+00
9E-02	H 314=	-.45138622E+00	G 516=	-9.52850389E-01	H 516=	.12680572E+00
7E-01	H 315=	.72092323E+00	G 517=	1.24242945E+00	H 517=	-.17643484E+01
6E-01	H 316=	-.21753822E+00	G 518=	-6.84175873E+00	H 518=	-.44801130E+01
3E+00	H 317=	.38167326E+00	G 519=	5.04973274E+00	H 519=	.15298184E+01
5E+01	H 318=	.14819237E+02	G 520=	-1.06697671E+00	H 520=	.46542019E-01
6E+00	H 319=	-.85143019E+01	G 521=	9.45154250E+00	H 521=	.14300774E+01
3E+00	H 320=	.13051635E+02	G 522=	-6.90077794E-01	H 522=	.16019346E+02
1E+01	H 321=	-.23914570E+02	G 523=	1.28977227E+01	H 523=	-.13329579E+02
3E+00	H 322=	.10810833E+02	G 524=	-3.41950521E+01	H 524=	.11937782E+03
5E+01	H 323=	-.63910954E+02				
8E+00	H 324=	-.72432314E+01				

Table B. Continued

G 6 6=	3.72382683E-04	H 6 6=	.31110748E-03
G 6 7=	2.48866597E-04	H 6 7=	.11967165E-03
G 6 8=	-4.30195636E-04	H 6 8=	.13508165E-03
G 6 9=	2.13727152E-03	H 6 9=	-.59623941E-03
G 610=	3.92002609E-04	H 610=	-.39774839E-02
G 611=	5.91470301E-03	H 611=	.14304200E-01
G 612=	-3.50500008E-02	H 612=	-.75366375E-02
G 613=	1.14717758E-01	H 613=	.16425152E-01
G 614=	-6.67961460E-02	H 614=	.19044402E+00
G 615=	2.63254735E-01	H 615=	-.18118073E+00
G 616=	-4.68508679E-01	H 616=	.77385639E+00
G 617=	3.93588877E-01	H 617=	-.93185308E+00
G 618=	-9.46770525E-01	H 618=	.11830100E+01
G 619=	-2.15334615E+00	H 619=	.45361664E+00
G 620=	4.70842755E+00	H 620=	.12137469E+01
G 621=	-3.23913029E+00	H 621=	.51886065E+00
G 622=	1.22418870E+01	H 622=	.34168698E+01
G 623=	-3.41499013E+00	H 623=	-.22478455E+01
G 624=	3.47551903E+01	H 624=	.21725370E+02

G 7 7=	-3.38034552E-04	H 7 7=	.21221215E-03
G 7 8=	3.12339079E-04	H 7 8=	.40195247E-03
G 7 9=	-1.64081767E-04	H 7 9=	-.32573011E-03
G 710=	-3.54309604E-05	H 710=	-.44602487E-03
G 711=	8.74138987E-03	H 711=	-.40131347E-02
G 712=	-2.31940338E-02	H 712=	.11920718E-01
G 713=	9.79040563E-03	H 713=	-.21646387E-02
G 714=	-7.82577634E-03	H 714=	-.25150594E-01
G 715=	4.23793578E-02	H 715=	-.47148820E-01
G 716=	3.14093077E-01	H 716=	-.70200782E-01
G 717=	2.35095525E-01	H 717=	-.63394758E+00
G 718=	-2.27362189E-01	H 718=	.77351442E+00
G 719=	-8.55997884E-01	H 719=	-.22506956E+01
G 720=	2.11810184E-01	H 720=	.60293251E+00
G 721=	-6.79813421E+00	H 721=	.24065237E+01
G 722=	1.59271164E+00	H 722=	.40884249E+01
G 723=	-2.05063617E+01	H 723=	.16366798E+02
G 724=	4.66132146E+00	H 724=	.11242851E+02

G 8 8=	-7.84447628E-05	H 8 8=	.78618
G 8 9=	3.58204448E-04	H 8 9=	.26507
G 810=	-3.29865205E-04	H 810=	.31687
G 811=	6.18262714E-04	H 811=	-.24796
G 812=	-5.38137847E-03	H 812=	.27419
G 813=	-9.67857158E-03	H 813=	.46908
G 814=	-1.77339838E-02	H 814=	-.14796
G 815=	5.60007304E-02	H 815=	-.25111
G 816=	1.26031697E-01	H 816=	-.15439
G 817=	-1.30248885E-01	H 817=	-.10635
G 818=	2.65852699E-01	H 818=	.15451
G 819=	3.02515981E+00	H 819=	-.27101
G 820=	-1.31322975E+00	H 820=	-.16310
G 821=	1.68301795E+00	H 821=	-.20618
G 822=	-6.81312644E+00	H 822=	-.18742
G 823=	1.87334432E+01	H 823=	-.28089
G 824=	-2.00761449E+01	H 824=	.51845

G 9 9=	2.27598068E-05	H 9 9=	.10934
G 910=	4.48861927E-04	H 910=	.21485
G 911=	-5.43971902E-04	H 911=	-.51823
G 912=	1.20773913E-06	H 912=	-.10370
G 913=	-4.17231458E-03	H 913=	-.18675
G 914=	-2.40911657E-02	H 914=	.12845
G 915=	1.53373276E-02	H 915=	.43221
G 916=	-3.40123063E-03	H 916=	.68572
G 917=	-1.36573054E-01	H 917=	.73340
G 918=	5.69084722E-01	H 918=	-.13342
G 919=	-3.58062005E-01	H 919=	.25583
G 920=	-1.42951311E+00	H 920=	.32768
G 921=	3.46892813E-01	H 921=	-.17114
G 922=	-1.14053144E+00	H 922=	.26847
G 923=	1.70650628E+00	H 923=	-.56829
G 924=	5.27083588E+00	H 924=	-.96297

Table B. Continued

28E-05	H 8 8=	.78618141E-04	G1010=	2.26452458E-05	H1010=	.45036482E-04
48E-04	H 8 9=	.26507891E-03	G1011=	2.33529708E-04	H1011=	-.36810529E-04
05E-04	H 810=	.31687960E-03	G1012=	-8.91741598E-04	H1012=	-.29591757E-03
14E-04	H 811=	-.24796961E-02	G1013=	-1.56877363E-04	H1013=	.22745711E-02
47E-03	H 812=	.27419954E-02	G1014=	-4.35126334E-03	H1014=	.66920146E-03
58E-03	H 813=	.46908004E-02	G1015=	-3.51159173E-03	H1015=	-.17879607E-01
38E-02	H 814=	-.14796194E-01	G1016=	3.32822767E-03	H1016=	.33127994E-01
04E-02	H 815=	-.25111580E-01	G1017=	-5.77071053E-03	H1017=	-.82620066E-01
97E-01	H 816=	-.15439786E+00	G1018=	-4.54620612E-02	H1018=	.41995889E-01
85E-01	H 817=	-.10635683E+00	G1019=	2.35214061E-01	H1019=	.21141051E-01
99E-01	H 818=	.15451624E+00	G1020=	-5.10877770E-01	H1020=	.96197826E-01
81E+00	H 819=	-.27101147E+01	G1021=	-2.98460230E+00	H1021=	.26562107E+00
75E+00	H 820=	-.16310960E+01	G1022=	-4.12052613E+00	H1022=	.20263140E+01
95E+00	H 821=	-.20618759E+01	G1023=	-7.74724239E+00	H1023=	.81069597E+00
44E+00	H 822=	-.18742205E+01	G1024=	-9.34438992E+00	H1024=	.43509346E+01
32E+01	H 823=	-.28089741E+02				
49E+01	H 824=	.51845120E+01				

68E-05	H 9 9=	.10934553E-03	G1111=	3.11853099E-07	H1111=	.19943533E-04
27E-04	H 910=	.21485281E-03	G1112=	4.61401331E-05	H1112=	.65685716E-04
02E-04	H 911=	-.51823650E-03	G1113=	7.00662887E-04	H1113=	-.57514181E-03
13E-06	H 912=	-.10370259E-04	G1114=	-1.49686325E-03	H1114=	.19025045E-02
58E-03	H 913=	-.18675102E-02	G1115=	6.20740569E-03	H1115=	-.38037015E-02
57E-02	H 914=	.12845599E-01	G1116=	-4.78811705E-03	H1116=	.87781070E-02
76E-02	H 915=	.43221558E-02	G1117=	5.05607700E-02	H1117=	-.11860078E-01
53E-03	H 916=	.68572128E-01	G1118=	2.96481013E-02	H1118=	-.75516208E-02
54E-01	H 917=	.73340895E-01	G1119=	3.37778446E-02	H1119=	-.27742110E+00
22E-01	H 918=	-.13342141E+00	G1120=	2.49035451E-01	H1120=	.40644831E+00
05E-01	H 919=	.25583037E+00	G1121=	5.81554365E-01	H1121=	-.62613786E+00
11E+00	H 920=	.32768912E+01	G1122=	3.69804353E-01	H1122=	.96574415E+00
13E-01	H 921=	-.17114816E+01	G1123=	2.05693766E+00	H1123=	-.49260746E+00
04E+00	H 922=	.26847065E+01	G1124=	2.26466373E+00	H1124=	.58899468E+01
28E+00	H 923=	-.56829415E+01				
88E+00	H 924=	-.96297451E+01				

G1212=	4.97031879E-06	H1212=	-.11532726E-04
G1214=	9.32817745E-05	H1213=	.66208218E-04
G1215=	-1.50069757E-03	H1214=	-.11560561E-03
G1216=	-3.29807943E-03	H1215=	.13216347E-02
G1217=	-2.42404020E-02	H1216=	.39858468E-02
G1218=	-1.18340293E-02	H1217=	.71293963E-03
G1219=	-2.97000375E-02	H1218=	.54699325E-01
G1220=	-8.72789907E-02	H1219=	-.45257668E-01
G1221=	-1.24087340E-01	H1220=	.24349356E+00
G1222=	-3.67687169E-01	H1221=	-.43559620E+00
G1223=	3.53759694E-01	H1222=	.86030682E+00
G1224=	-4.95835471E+00	H1223=	-.40262476E+00
		H1224=	.17689044E+01

G1414=	1.63016976E-05	H1414=	-.3250
G1415=	-2.59073138E-04	H1415=	.4950
G1416=	3.40091488E-04	H1416=	.4822
G1417=	-1.41947019E-03	H1417=	.2834
G1418=	5.83098143E-04	H1418=	.3215
G1419=	-2.62405512E-03	H1419=	.2033
G1420=	7.40987337E-03	H1420=	.5794
G1421=	-5.14948857E-02	H1421=	.1546
G1422=	-2.18633866E-02	H1422=	-.9805
G1423=	-7.10342449E-01	H1423=	-.5823
G1424=	6.16288781E-01	H1424=	-.6828

G1313=	1.53294280E-05	H1313=	-.38266698E-05
G1314=	7.45644820E-05	H1314=	.38828054E-03
G1315=	-1.44238126E-04	H1315=	-.20612176E-04
G1316=	-5.87090564E-04	H1316=	.24693960E-02
G1317=	1.70755588E-05	H1317=	.21962900E-02
G1318=	-5.34952754E-03	H1318=	.91944685E-02
G1319=	-6.67326641E-03	H1319=	.21478447E-01
G1320=	8.30221927E-02	H1320=	-.83588941E-01
G1321=	-3.26044178E-01	H1321=	-.11314857E+00
G1322=	7.52621979E-01	H1322=	.23812565E+00
G1323=	-8.81060314E-01	H1323=	-.85692165E+00
G1324=	8.95327234E-01	H1324=	.43386539E+00

G1515=	1.21820159E-05	H1515=	.2617
G1516=	-1.57948726E-04	H1516=	.3083
G1517=	8.58468127E-06	H1517=	.2832
G1518=	-3.73096913E-04	H1518=	.1969
G1519=	-2.27779779E-04	H1519=	.1024
G1520=	1.47155267E-02	H1520=	-.6471
G1521=	2.42504528E-02	H1521=	.5167
G1522=	1.42425814E-01	H1522=	.9672
G1523=	2.49694762E-03	H1523=	.4383
G1524=	4.54553312E-02	H1524=	-.4858

76E-05	H1414=	-.32505932E-05	G1616=	-5.84503371E-06	H1616= .89085426E-05
38E-04	H1415=	.49502956E-04	G1617=	-1.27970049E-04	H1617= -.96542149E-04
88E-04	H1416=	.48223895E-03	G1618=	-8.93225408E-05	H1618= .70450073E-03
19E-03	H1417=	.28346161E-02	G1619=	-6.86292642E-04	H1619= .17460934E-02
43E-04	H1418=	.32151694E-02	G1620=	9.36995876E-04	H1620= .19562971E-02
12E-03	H1419=	.20337665E-01	G1621=	1.42977914E-02	H1621= .23798996E-01
37E-03	H1420=	.57944611E-01	G1622=	4.30475062E-02	H1622= .23377695E-01
57E-02	H1421=	.15466959E-01	G1623=	-4.11517870E-02	H1623= .15745310E+00
66E-02	H1422=	-.98059527E-01	G1624=	8.54049182E-02	H1624= -.14426384E+00
49E-01	H1423=	-.58232037E+00			
81E-01	H1424=	-.68287732E+00			

59E-05	H1515=	.26172433E-04	G1717=	3.58879706E-06	H1717= .12514104E-04
26E-04	H1516=	.30831242E-04	G1718=	-8.84852993E-06	H1718= .15768269E-03
27E-06	H1517=	.28322050E-03	G1719=	-6.74888104E-04	H1719= .23150870E-03
13E-04	H1518=	.19695519E-02	G1720=	-2.30968866E-05	H1720= .18252449E-02
79E-04	H1519=	.10243259E-01	G1721=	1.10360624E-03	H1721= .44591573E-02
67E-02	H1520=	-.64714580E-02	G1722=	1.92448065E-02	H1722= -.80043459E-02
28E-02	H1521=	.51676833E-01	G1723=	8.30055857E-02	H1723= .41447697E-01
14E-01	H1522=	.96725937E-01	G1724=	-4.15158582E-03	H1724= -.60527826E-02
62E-03	H1523=	.43839802E-01			
12E-02	H1524=	-.48587178E+00			

$$a_y = \frac{e}{m} B u_x ,$$

$$a_z = 0 ,$$

and the particle moves in the trajectory (assuming it is initially at the origin with velocity $\vec{w}$)

$$x = (w_y + w_x \sin \lambda t - w_y \cos \lambda t)/\lambda ,$$

$$y = (-w_x + w_y \sin \lambda t - w_x \cos \lambda t)/\lambda ,$$

$$z = w_z t ,$$

where the angular frequency $\lambda = \frac{e}{m} B$. The projection on the x-y plane is a circle with its center at $x = w_y/\lambda$, $y = -w_x/\lambda$ and radius $w_\perp/\lambda$ where

$$w_\perp^2 = w_x^2 + w_y^2 .$$

The projected motion in the x-y plane is therefore a circular path with period $2\pi/\lambda$. If the angular frequency λ is very large the particle can then be smoothed out over its circular path and viewed as a ring current of (electromagnetic) intensity $e\lambda/2\pi$ and radius $w_\perp/\lambda$ moving along the z-axis with constant velocity w_z. For the geomagnetic field near the earth B is on the order of 0.1 gauss (equals 10^{-5} kg/sec-coulombs) and since e/m for electrons is approximately 2×10^{11} coulombs/kg it follows that λ is about 2×10^6 revolutions per sec. Since λ depends inversely on particle mass the period of a proton is about 2000 times longer than that of an electron but this is still only a few milliseconds so that the smoothing into a ring current seems to be a valid physical approximation for both particles. The size of ring is quite modest--even if $w_\perp$ is taken as the speed of light the radius for an electron is only a few hundred meters. For protons the radius is considerable if the energy is large and the theory given here must break down for very high energy protons, say above 1 Bev where the radius is about 10 km.

Thus the charged particle will behave like a small current whirl with the usual dipole moment (in inductive units)

$$M = \tfrac{1}{2} m w_\perp^2 / B_o ,$$

directed, of course, in such a way as to oppose the field.

The physical picture just described is often called the "guiding center approximation". The particle is replaced by a moving dipole whose position describes the trajectory of the guiding center. In the uniform field for which the picture was developed it is exact but it is also applied to situations in which the field is not uniform. If non-uniformity is introduced slowly enough the motion should be adiabatic (see reference (18) for a more complete discussion; a really thorough rigorous discussion of this point is still needed), and the dipole moment should behave like a physical invariant. Since the field does no work on the particle the total velocity is a true invariant. If w is the total velocity then, under the adiabatic assumption,

$$w^2 = w_\parallel^2 + w_\perp^2 ,$$

($w_\parallel$ is the velocity along the lines of force of the field and $w_\perp$ is the velocity "perpendicular" to these lines) so that

$$w^2 = w_\parallel^2 + \frac{BM}{\frac{1}{2} m} .$$

Hence if B becomes as large as $\frac{1}{2} m w^2 / M$ it is necessary for $w_\parallel$ to go to zero.

If a charged particle is introduced into space in the geomagnetic region, say with initial velocity $w_\parallel$ parallel to magnetic field and $w_\perp$ perpendicular to it, then it acquires a magnet moment

$$M = \tfrac{1}{2} m w_\perp^2 / B$$

if B_o is the initial field strength. It will move along the field lines as determined by the initial component $w_\parallel$. In general the geomagnetic field is such that higher altitudes correspond to smaller fields but each line of force rises to a maximum and then returns to the surface of the earth. This

where

$$B^2 = B_r^2 + B_\theta^2 = (4\cos^2\theta + \sin^2\theta)\,(m/4\pi r^3)^2 ,$$

so that B is total field strength. If the equation for a line of force is utilized the field strength at colatitude θ along a line of force is seen to be

$$B = \frac{(3\cos^2\theta + 1)^{\frac{1}{2}}\, m}{4\pi L^3 \sin^6\theta} .$$

The derivative of this expression with respect to φ is proportional to

$$\cos\theta(3 + 2\cos^2\theta)$$

so that there is a unique minimum B at $\theta = \pi/2$ where $B = m/4\pi L^3$. In this situation the pairs of points with equal latitudes (with colatitudes θ and $\pi/2 - \theta$) are mirror points. The equator can be characterized as those points which mirror to themselves.

There is no a priori reason why there should be only a minimum of B along any line of force but observation and calculations have not uncovered any locations where multiple minima occur. If such multiple minima were found it would mean that some particles could go from mirror point to mirror point about one minimum without even coming into contact with particles moving around another minimum.

The oscillation of a particle between mirror points is accompanied by an additional motion as the guiding center drifts across the magnetic field. This motion is rather slow (in the geomagnetic case) and more difficult to study than the basic case outlined above. The basic reasons for the drift arise from the non-uniformity of the geomagnetic force; other fields also contribute to drift but their contributions are very small; a more detailed discussion is given below. Plainly it is necessary to find some other "constant" of motion to describe the process. An adiabatic "invariant" I has been proposed (by M. N. Rosenbluth, see reference (19) for this purpose. It appears to be based on the analogy between a particle oscillating between mirror points and a pendulum-type motion in a one-dimensional potential where it corresponds to the action integral

$$J = \oint \partial x \sqrt{2(E-V(x))} \quad ,$$

where E is energy and V(x) is potential energy.

Since $w^2 = w_{||}^2 + \frac{M}{\frac{1}{2}m} B$ can be written in terms of energy as

$$\tfrac{1}{2}mw^2 = \tfrac{1}{2}mw_{||}^2 + MB \ ,$$

where $\frac{1}{2}mw^2$ can be interpreted as the total energy available for motion and $\frac{1}{2}mw_{||}^2$ as kinetic energy of motion, it follows that MB can be interpreted as potential energy available for motion. Then

$$J = \oint \partial s \sqrt{2(\tfrac{1}{2}mw^2 - \tfrac{1}{2}mw^2 \frac{B}{B_o})}$$

$$= \sqrt{m}\ w \oint \partial s \sqrt{1 - \frac{B}{B_o}} \quad ,$$

because $M = \frac{1}{2}mw^2/B_o$ if B_o is the field at a mirror point. Since $\sqrt{m}w$ is a constant these can be dropped and

$$I = \oint \partial s \sqrt{1 - \frac{B}{B_o}}$$

(where the integral extends over arc-length from mirror point to mirror point) is an adiabatic invariant (if J is such an invariant, see reference (19)). A proof that I is an adiabatic invariant is presented in reference (7). Since the argument just presented is highly heuristic such a proof is clearly needed.

The two quantities B_o and I define a pair of lines (each containing the mirror points of the other) around the world and therefore would be adequate to describe the drifting of particles geometrically but not kinematically. That is, they determine where the particles go but not the rate of movement. For many purposes the geometry alone is adequate and it is this geometry which is presented in the graphs of this report. For the sake of completeness, a brief sketch of the details of motion follows (based on Alfvén, reference (5) see also reference (20)).

There are two main causes for drift perpendicular to the magnetic field which operate in the absence of other fields--a free dipole with movement M in a non-uniform field will drift as it is acted upon by a force

$$\vec{\nabla}\,(\vec{M}\cdot\vec{B})\,.$$

In the present case, however, the dipole is not free since it is constrained to move along a line of force and another force term must be included to account for the centripedal effect of this constraint. This centrifugal force is given by:

$$m w_{\parallel}^2 \frac{\partial^2 \vec{x}}{\partial s^2}$$

where $\vec{x}$ is the position of the guiding center. Since $\vec{x}$ follows a line of force

$$\frac{\partial \vec{x}}{\partial s} = \frac{\vec{B}}{B}$$

and, therefore

$$\frac{\partial^2 \vec{x}}{\partial s^2} = \frac{1}{B}\,\vec{\nabla} B - \frac{1}{B^3}\,(\vec{B}\,\vec{\nabla} B)\,\vec{B}\ .$$

When the non-uniformity force and the constraint force are combined the total effective force is

$$(M + \frac{m w_{\parallel}^2}{B})\,\vec{\nabla} B - \frac{m w_{\parallel}^2}{B^3}\,(\vec{B}\,\vec{\nabla} B)\,\vec{B}\ .$$

The second term of the expression acts along the line of force and does not contribute to the drift.

In order to evaluate the drift consider a change of frame to a system moving with drift velocity $\vec{v}$. In this new frame the magnetic field will appear to contribute an electric force given, to the first order approximation of the relativistic correction by

$$\vec{E}' = \frac{1}{c}\,\vec{v}\otimes\vec{B}\ .$$

Then the force on the particle has been changed to

$$\vec{F} + ce\vec{E}' = \vec{F} + e\vec{v}\otimes\vec{B}\ ;$$

and this can be made to vanish by taking

$$\vec{v} = \frac{1}{eB^2} \vec{F} \otimes \vec{B} \quad ,$$

which is, therefore, the particle drift velocity.

In terms of the force obtained above

$$\vec{v} = \frac{1}{eB^2} (M + \frac{mw_\perp^2}{B}) (\vec{\nabla} B \otimes \vec{B}) = \frac{m}{eB^3} (\frac{1}{2} w_\perp^2 + w_{||}^2) (\vec{\nabla} B \otimes \vec{B}) \quad .$$

Note especially that since the charge e appears it follows that positive and negative particle will drift in opposite directions--electrons move eastward and protons westward in the earth's field. Detailed calculations of the drift velocity for a dipole earth have been made several times (see reference (20)). There it is shown that a 1 MEV electron requires about 30 minutes to orbit the earth.

Geomagnetic Geometry

Since the geometry of motion of trapped particles is governed by the quantities B and I (the subscript zero at mirror point field strengths will be omitted if there is no chance for confusion) it can be visualized in terms of these quantities. I is, however, somewhat awkward to work with; for example, there does not seem to be any closed form expression for

$$I_{DP} = L \int_{\theta_o}^{\frac{1}{2}\pi - \theta_o} \partial\theta \sin\theta [3\cos^2\theta + 1]^{\frac{1}{2}} [1 - \frac{(3\cos^2\theta + 1)^{\frac{1}{2}}}{(3\cos^2\theta_o + 1)^{\frac{1}{2}}} \quad \frac{\sin^6\theta_o}{\sin^6\theta}]^{\frac{1}{2}}$$

the value of I for a particle mirroring at colatitude θ_o in a dipole field. This is not especially objectionable on the basis of applications because the earth is not exactly a dipole -- the deviation about 5%--but rather because it interferes with intuitive understanding. Such understanding is based, naturally enough, on the traditional dipole representation of the earth which has proved very useful. In an effort to preserve the value of such understanding McIlwain (reference (21)) proposed another quantity L be used instead. Roughly speaking L is the radial distance at the equator which a line of force would have if it were a dipole line rather than a realistic one.

Suppose $\Phi(\theta)$ is the function defined by the integral just quoted so that

$$I_{DP} = L\Phi(\theta) \quad .$$

Since, as shown earlier

$$B = \frac{H}{L^3 \sin^6\theta} \quad (1 + 3\cos^2\theta)^{\frac{1}{2}} \ ,$$

$$L^3 B/H = \Phi(\theta) = (1 + 3\cos^2\theta)^{\frac{1}{2}} / \sin^6\theta \ ,$$

and, therefore, if Ω is the functional inverse of Φ

$$I^3 B/H = L^3 B/H\, \Phi(\theta) = L^3 B/H\, \Phi(\Omega(L^3 B/H))$$

so that there is a functional relationship between $I^3 B/H$ and $L^3 B/H$. This can be inverted so that, for some function f,

$$L^3 B/H = f(I^3 B/H) \ .$$

Thus, if I is known L can be calculated. McIlwain (reference (21)) gives an approximate formula for f and table which is presented in Figure A. A more exact formula, also due to McIlwain (reference (22)) gives

$$\lambda = \log\left(\frac{L^3 B}{H} - 1\right)$$

as a function of $\mu = \log\left(\frac{I^3 B}{H}\right)$ in the form

$$\lambda = \sum_{n=0}^{9} \alpha_n \mu^n \ ,$$

where the α_n are as shown in Table C. This formula improves that of reference (21) and was used (with one small change) for all the calculations reported here. There is a very recent change included in Table C which was not present in the calculations--it seems that the difference due to this change should be quite small (less than 1%) and then only in the immediate neighborhood of the geomegnetic equator.

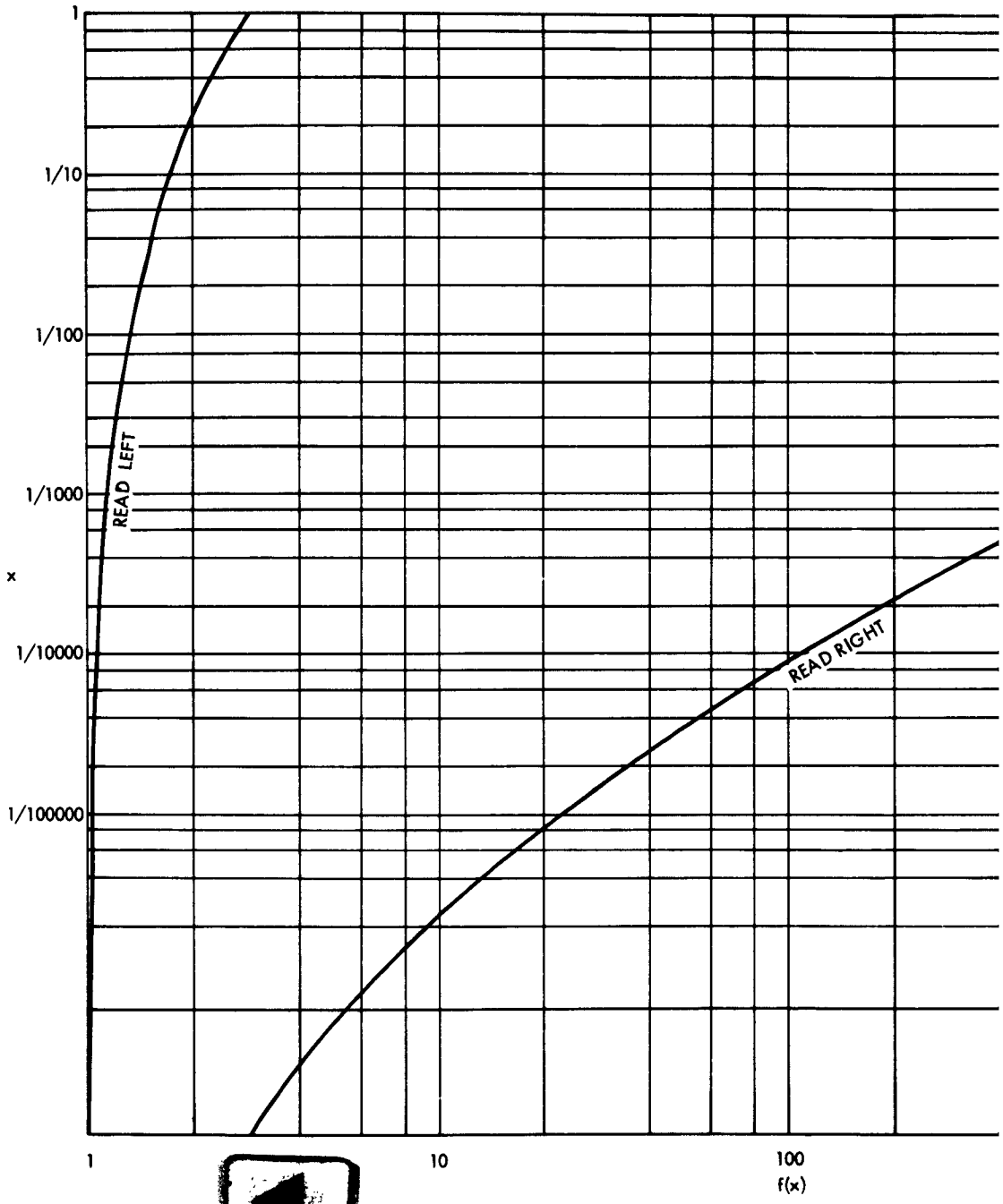

Figure A. Magnetic Shell Function

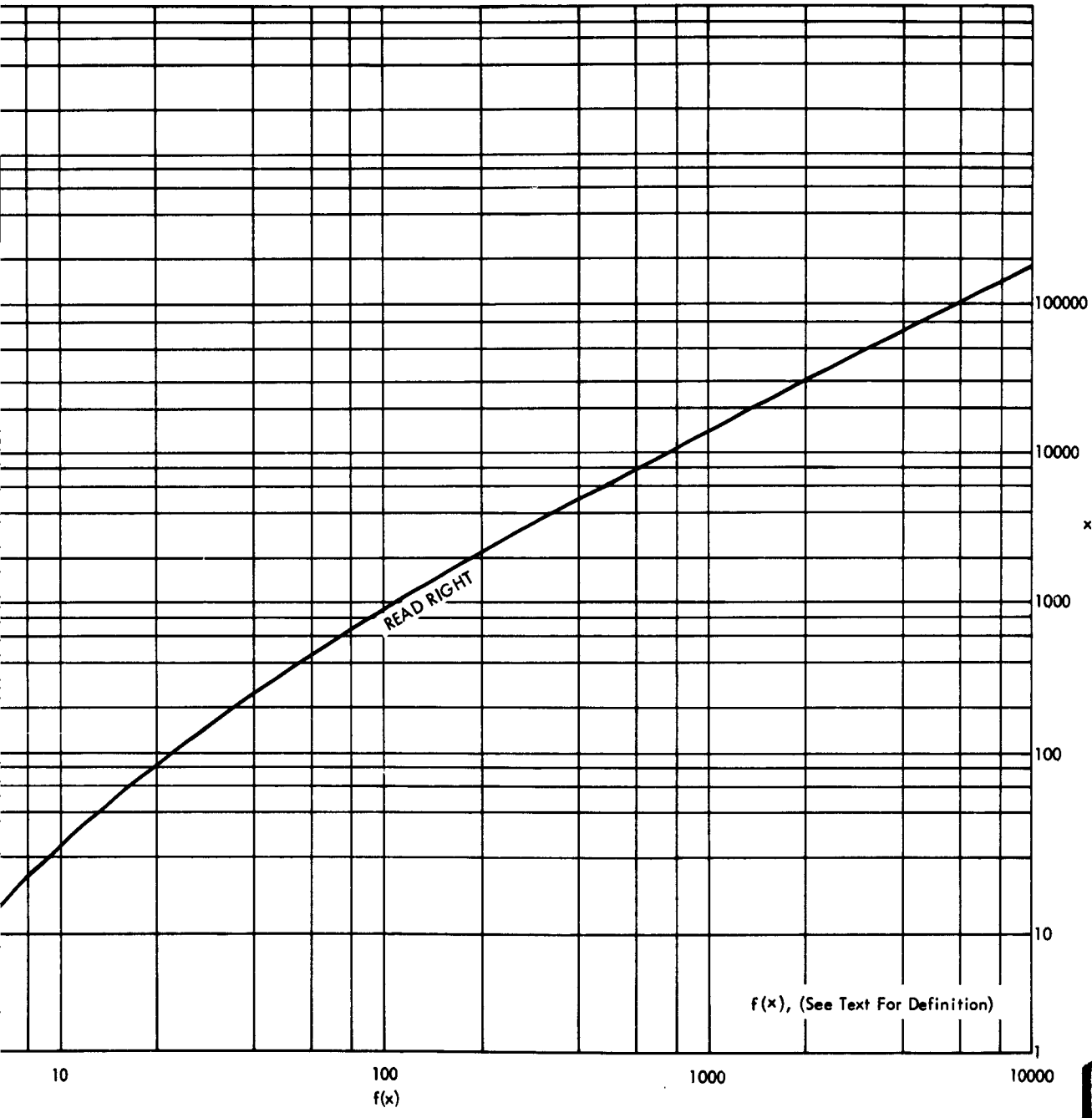

Figure A. Magnetic Shell Function

2

Table C. Coefficients in polynomial to McIlwain's f

If $\mu \leq -22.0$

$\alpha_0 = +.30062102$ $\alpha_1 = +.333338$

if $-22.0 < \mu \leq -3.0$

$\alpha_0 = +.62337691$ $\alpha_1 = +.43432642$ $\alpha_2 = +.15017245 \cdot 10^{-1}$

$\alpha_3 = +.13714667 \cdot 10^{-2}$ $\alpha_4 = +.82711096 \cdot 10^{-4}$ $\alpha_5 = +.32916354 \cdot 10^{-5}$

$\alpha_6 = +.81048663 \cdot 10^{-7}$ $\alpha_7 = +.10066362 \cdot 10^{-8}$ $\alpha_8 = +.83232531 \cdot 10^{-12}$

$\alpha_9 = -.81537735 \cdot 10^{-13}$

if $-3.0 < \mu \leq +3.0$

$\alpha_0 = +.6228644$ $\alpha_1 = +.43352788$ $\alpha_2 = +.14492441 \cdot 10^{-1}$

$\alpha_3 = +.11784234 \cdot 10^{-2}$ $\alpha_4 = +.38379917 \cdot 10^{-4}$ $\alpha_5 = -.33408822 \cdot 10^{-5}$

$\alpha_6 = -.53977642 \cdot 10^{-6}$ $\alpha_7 = -.21997983 \cdot 10^{-7}$ $\alpha_8 = +.23028767 \cdot 10^{-8}$

$\alpha_9 = +.26047023 \cdot 10^{-9}$

if $+3.0 < \mu \leq +11.7$

$\alpha_0 = +.6222355$ $\alpha_1 = +.43510529$ $\alpha_2 = +.12817956 \cdot 10^{-1}$

$\alpha_3 = +.21680398 \cdot 10^{-2}$ $\alpha_4 = -.32077032 \cdot 10^{-3}$ $\alpha_5 = +.79451313 \cdot 10^{-4}$

$\alpha_6 = -.12531932 \cdot 10^{-4}$ $\alpha_7 = +.99766148 \cdot 10^{-6}$ $\alpha_8 = -.3958306 \cdot 10^{-7}$

$\alpha_9 = +.63271665 \cdot 10^{-9}$

if $+11.7 < \mu \leq 23$

$\alpha_0 = +2.0007187$ $\alpha_1 = -.18461796$ $\alpha_2 = .12038224$

$\alpha_3 = -.67310339 \cdot 10^{-2}$ $\alpha_4 = +.2170224 \cdot 10^{-3}$ $\alpha_5 = -.38049276 \cdot 10^{-5}$

$\alpha_6 = +.28212095 \cdot 10^{-7}$

if $23 < \mu$

$\alpha_0 = -3.0460681$ $\alpha_1 = +1.0$

The idea behind using L instead of I is that L is geometrically simplier than I but carries all the physical significance of I. This happens because L is almost constant along lines of force--McIlwain reports a maximum percentage deviation of 1%. All the particles which begin to move from any one point spread themselves along the line of force through that point. Then as they drift perpendicular to the field their mirror points sweep out a surface defined by all the lines of constant B and L passing through the initial line of force. In general, lines of force do not lie in this surface and the particles moving between the mirror points do not move on the surface. The separation away from the surface is small however and the concept of "magnetic shell" is valid if it is allowed to have a finite, though small thickness. This shell is uniquely characterized by L up to the variation of L along a line of force. Hence L is called the "magnetic shell radius" or "magnetic shell parameter". This parameter is displayed in detail by the graphs in this report.

The first set of maps (1 through 38) show contours of constant B and L at fixed altitudes. These graphs allow data be reduced in the B and L coordinate system and then replotted in geographic coordinate and conversely. The next set of maps (39 through 48) show curves defined by a fixed pair of B and L values.

The B-L mirror point traces show an unexpected geometric feature which deserves emphasis. All the points above any particular point on the earth's surface belong to different traces depending on the values of B and L at these points. There is not a priori reason why the different traces should not circle the world essentially independently of each other. In matter of fact, however, the different traces all pass over virtually the same points on the surface. What is even more startling is that the opposite mirror points to these points also show the same consistency and "stack" over on another.

Thus, the geometry can be visualized by a set of irregular cones originating at the center of the earth. These cones are paired by containing all the mirror

points of one another and can be said to form a system of geomagnetic shell latitudes (these latitudes are illustrated on map 52). The equatorial cone is its own conjugate and is defined as the geomagnetic equator; it is shown on map 51.

III. DESCRIPTION OF MAPS

All of the maps in this collection are plotted on a straight forward projection of the earth which permits extension ot the poles without unduly distorting the remainder of the earth's surface. On the worldwide maps there is a superimposed grid of geomagnetic "meridians". These meridians indicate the general trend of lines of force as given by the Jensen and Cain coefficients. No individual lines of force can be taken as typical because they either do not reach high latitudes above the surface or extend too far into space for really trustworthy calculations. The approximate meridians shown were obtained by following a "line of force" constrained to maintain a constant altitude of one hundred kilometers. That is, it represents the path of the guiding center of a charged particle constrained to this altitude; so that it is not especially useful in itself but it does represent a convenient approximation to all the true lines of force at different altitudes. These meridians are not exact and should be supplemented by precise calculations if accurate meridians are required.

The maps are divided into sections, (A through G) each of which included a set of similar displays. The individual sections are described in detail below. The programs used are described very briefly, more detailed descriptions will appear in a forthcoming TEMPO report. All of the programs are available from the DASA Computer Library at General Electric TEMPO.

Section A Contours of B and L

Figures 1 through 16 are maps showing the contours of constant values of B (the total magnetic field intensity in gauss) and L (the magnetic shell

parameter in earth radii) at various fixed altitudes above the surface of the earth. These maps were obtained from a modified version of the computer program TEST due to C. E. McIlwain which obtains the value of B and L at any specified location. The computations in this section were all based on the Jensen and Cain set of 48 geomagnetic coefficients. The modifications introduced included a linear interpolation scheme to locate contours and a direct plotter output subroutine which provide input for a Benson-Lehner tape-driven off-line plotter.

Section B Contours of B Near the South Atlantic Anomaly

Figures 17 through 32 are maps showing the contours of constant values of B (the total magnetic field intensity) in the South Atlantic region where the intensity is minimized. These detailed maps were prepared because the intensity changes very slowly in this region and the large scale of the worldwide maps obscures the structure of the B contours. The L contours are omitted because they show no special features in this region. The computational methods used were identical to these used in Section A.

Section C Contours of B and L (Jensen and Whitaker Coefficients)

Figures 33 and 34 show the same material as section A (for a restricted portion of the earth's surface) for two altitudes (0 and 500 km) with the difference that these maps were calculated using the Jensen and Whitaker coefficients. Otherwise the methods are the same as those used in Section A.

Section D Comparison between Contours (as calculated using the Jensen and Cain Coefficients and as calculated using the Jensen and Whitaker Coefficients)

Figures 35 through 38 show cross plots of the data in Section A and that in Section C for both altitudes (0 and 500 km) and both quantities (B and L). These plots allow the user to compare the differences between the two sets of coefficients used. On a world-wide scale the difference is quite small.

Section E Constant B-L Traces

Figures 39 through 44 show the position and latitude of the lines defined by a fixed pair of B and L for a variety of starting conditions. These lines were obtained from a slightly modified version of the program MIRROR due to R. Pennington; MIRROR is, in turn, a modification of the TEST program used in Section A so that all the calculations are based on the same basic codes. These calculations used only the Jensen and Cain coefficients. As noted above the lines originating over a single point (and their conjugate lines) "stack" one over another so that a single latitude versus longitude line represents all the traces between 100 and 1500 kilometers to within 1.5° (in the regions where they are above the surface of the earth). Superimposed on the world map showing the surface projection of the position is a plot of the altitude versus longitude.

Section F Difference between Constant B-L Traces

Figures 45 through 48 show the longitude versus latitude dependency of the B-L traces for different altitudes in much greater detail. This material is a replotting of the data presented on a world-wide scale in Section E.

Section G Pairs of Conjugate B-L Traces

Figures 49 and 50 are also replots of material in Section E and show the two conjugate traces simultaneously on the same map.

Section H The Geomagnetic Equator

Figure 51 shows a map of the geomagnetic equator ot 100 kilometers altitude; the equator at an altitude of 1500 km is not materially different. This map was obtained by a special code which utilized the subroutine MAGNET with the Jensen and Cain coefficients. The equator was obtained by searching iteratively at every longitude step for that point at the set altitude which was a minimum of B along the line of force through itself. The lines of force considered here were true lines of force and since they are not constrained to a given altitude it was necessary to constantly

correct the calculation to return to the set altitude. The equator as defined here is that point which is a mirror point of itself; each pair of mirror points lie one on each side of this equator.

Section I Approximate Geomagnetic Shell Latitudes

Figure 52 shows a map with the latitude versus longitude projections of a number of different traces of constant B and L computed for different purposes. All the computations used the MIRROR code utilized in Section E but there was no particular consistency in the choice of altitudes. Because of the miscellaneous nature of the data these traces can only be considered as an approximate definition of the structure involved in the geomagnetic latitude system. The pairs of conjugate cones are not indicated on this display but can be inferred approximately from Figures 49 and 50.

Section J Conjugate Auroral Grids

Figures 53 through 60 are a set of grids showing the transformation from (almost) rectangular grids in the northern hemisphere into grids in the southern hemisphere. The points shown are at equal altitudes (70 and 100 kilometers) at the two ends of a common line of force. The data using the Jensen and Whitaker were obtained from computations carried out by the Air Force Special Weapons Center (reference (23)). The data using the Jensen and Cain coefficients were obtained from a simple line following code utilizing the MAGNET subroutine. The altitudes in question are especially interesting because auroral displays occur at these altitudes and the grid shows where coupled aurora borealis and aurora australis pairs will occur simultaneously.

REFERENCES

1. Chapman, S. and Bartels, J. Geomagnetism Oxford 1940

2. Runcorn, S. K. "The Magnetism of the Earth's Body" in (pp. 498-533) Handbuch der Physik XLVII "Geophysik I " Springer 1956

3. Störmer, C. The Polar Aurora Oxford 1955

4. Chamberlain, J.W. Physics of the Aurora and Airglow Academic Press 1961

5. Alfvén, H. Cosmical Electrodynamics Oxford 1950

6. Christofilos, N. C. "The Argus Experiment" Jour. Geophysical Res. 64 (1959) 869-875

7. Northrup, T. G. and Teller, E. "Stability of the Adiabatic Motion of Charged Particles in the Earth's Field" Phy. Rev. 117 (1960) 215-225

8. Van Allen, J. A., Ludwig, G. H, Ray, E. C. and McIlwain, C.E. "Observation of High Intensity Radiation by Satellites 1958 Alpha and Gamma" Jet Propulsion 28 (1958) 588-592

9. Runcorn, S. K. "Magnetization of Rocks" in (pp. 470-497) Handbuck der Physik XLVII "Geophysik I" Springer 1956

10. Cain, J. E., Shapiro, I. R., Stolarik, J. D. and Heppner, J. P. "Measurements of the Geomagnetic Field by the Vanguard III Satellite" NASA TN D-1418 October 1962

11. Erdélyi, A. (ed) Higher Transcendental Functions McGraw-Hill 1953-5 (3 volumes)

12. Morse, P. M. and Feshbach, H. Methods of Theoretical Physics McGraw-Hill 1953 (2 volumes)

13. Schmidt, A. D. Tafeln der normierten Kugelfunktionen Engelhard-Reyher 1935

14. Kellogg, O. D. Foundations of Potential Theory Dover (reprint) 1953

15. Jensen, D. C. and Cain, J. C. unpublished, presented at April 1962 meeting of the American Geophysical Union, Washington, D. C.

16. Jensen, D. C. and Whitaker, W. A. unpublished, presented at April 1960 meeting of the American Geophysical Union, Washington, D. C.

17. Welch, J. A. and Whitaker, W. A. "Theory of Geomagnetically Trapped Electrons from an Artificial Source" Jour. Geophysical Res. 64 (1959) pp. 909-922

18. Chandrasekhar, S. "Adiabatic Invariants in the Motions of Charged Particles" in (p. 3-22) The Plasma in a Magnetic Field R.K.M. Landshoff (ed) Standford 1958

19. Tuck, J. L. (ed) "Series of Lectures on Physics of Ionised Gases" LA-2055 October 24, 1956

20. Lew, J. S. "Drift Rate in a Dipole Field" Jour. Geophysical Res. 66 (1961) pp. 2681-2686

21. McIlwain, C. E. "Coordinates for Mapping the Distribution of Magnetically Trapped Particles" Jour. Geophysical Res. 66(1961) 3681-3691

22. McIlwain, C. E. personal communication

23. McCormac, B. personal communication

A. CONTOURS OF B AND L

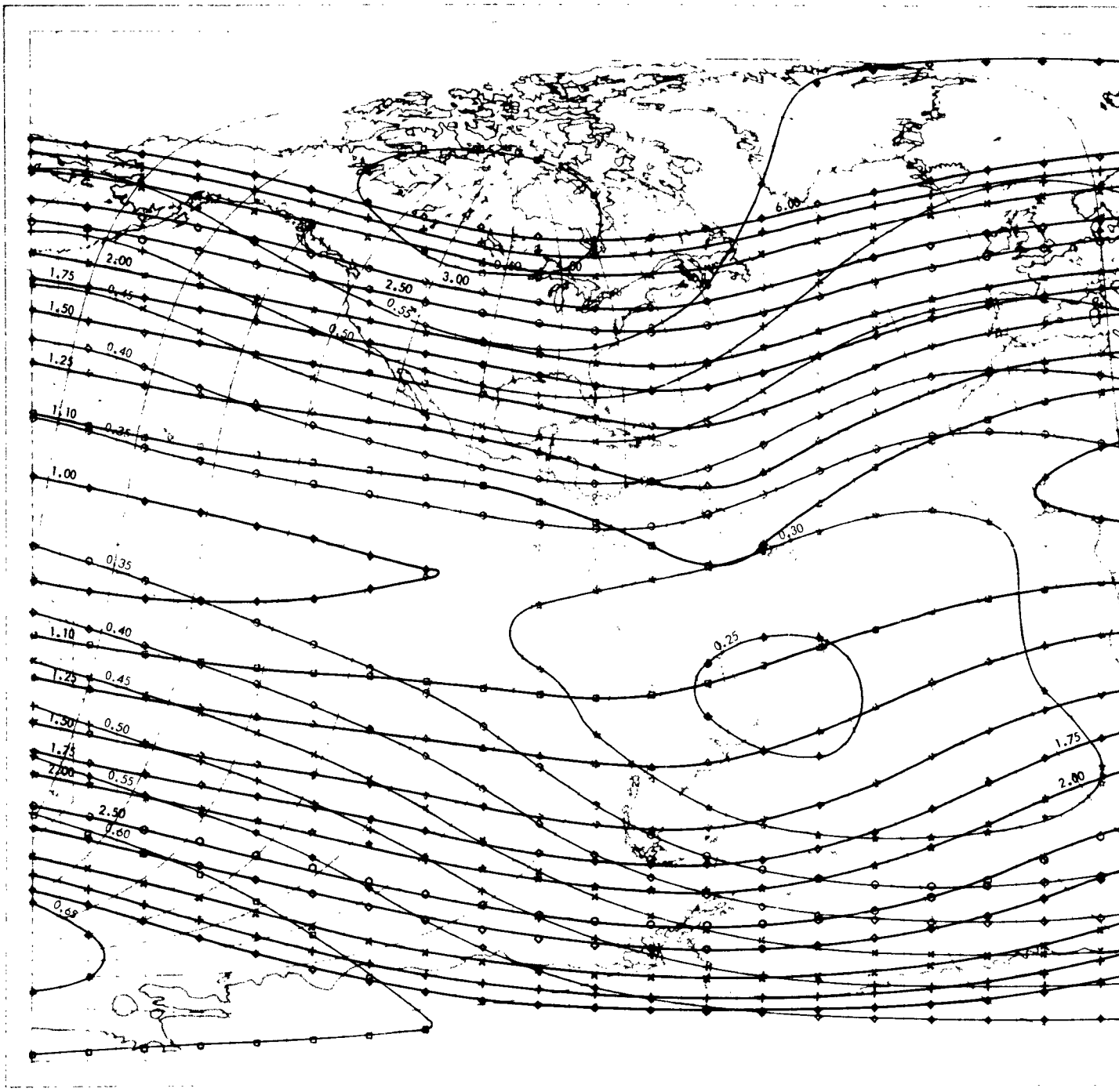

Figure 1. Constant Magnetic Field Intensity, B (Gauss), and Constant Magenti

2

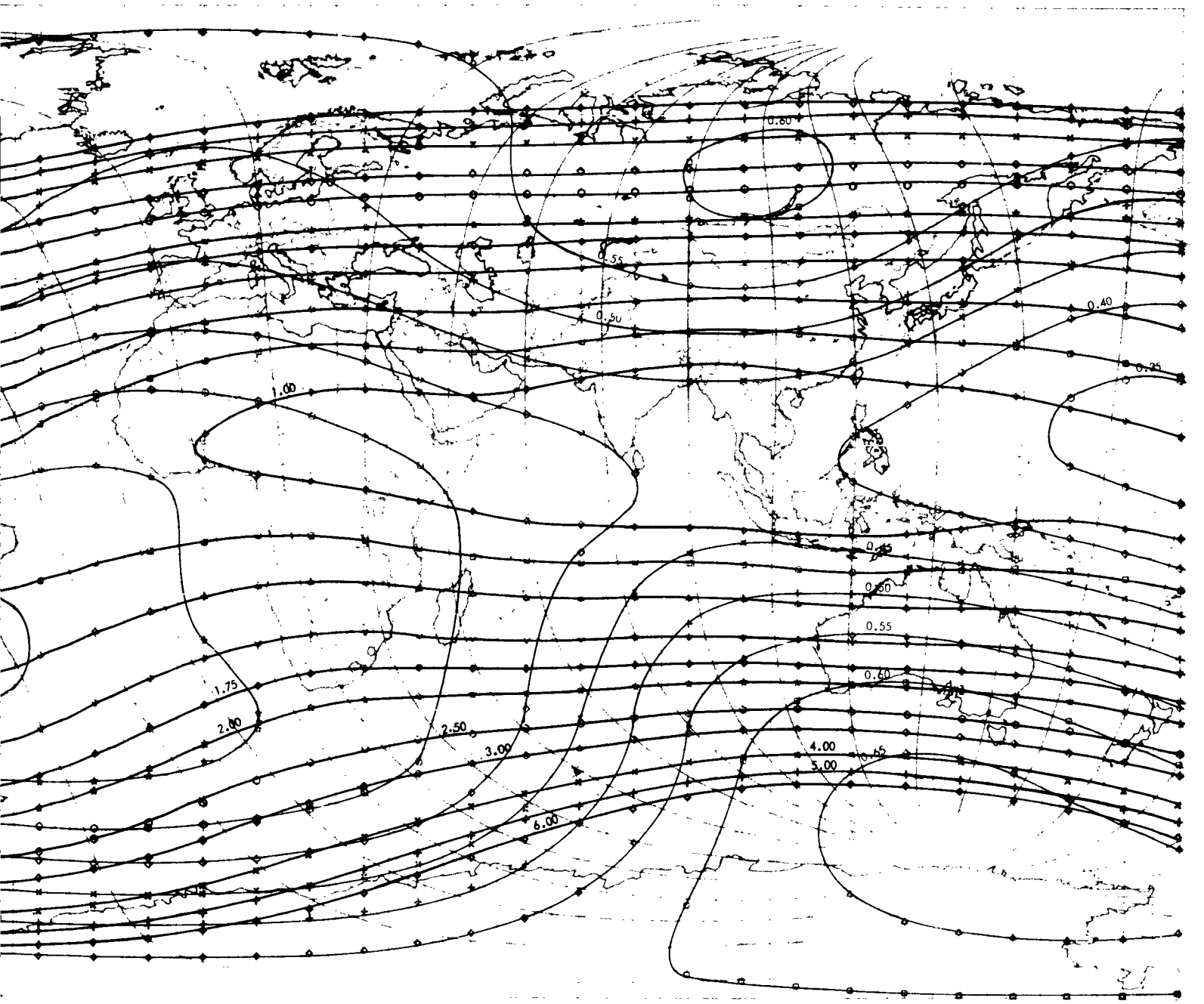

y, B (Gauss), and Constant Magentic Shell Parameter, L (Earth Radii), At Altitude 0 Kilometers.

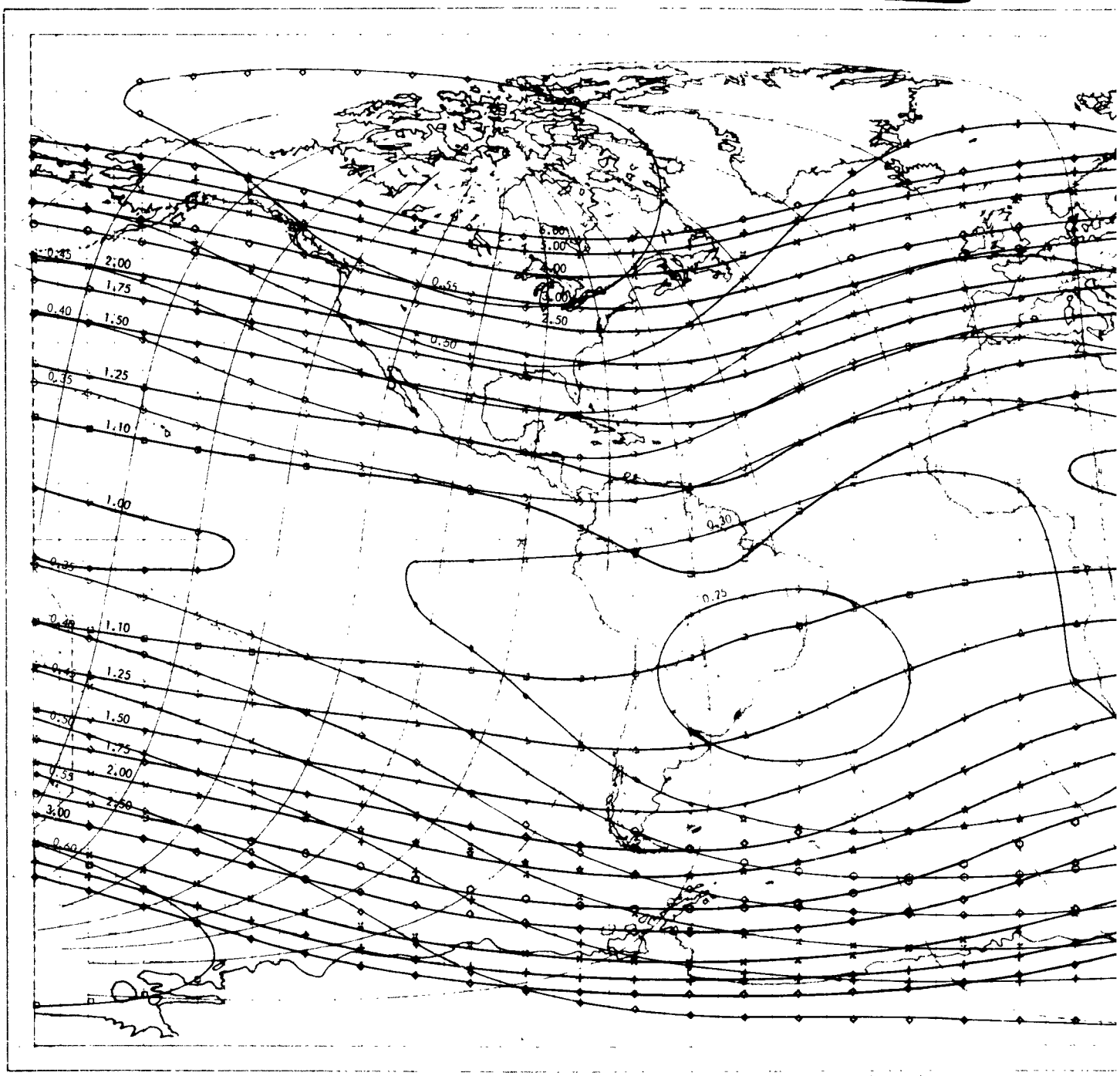

Figure 2. Constant Magnetic Field Intensity, B(Gauss), and Constant Magnetic

2

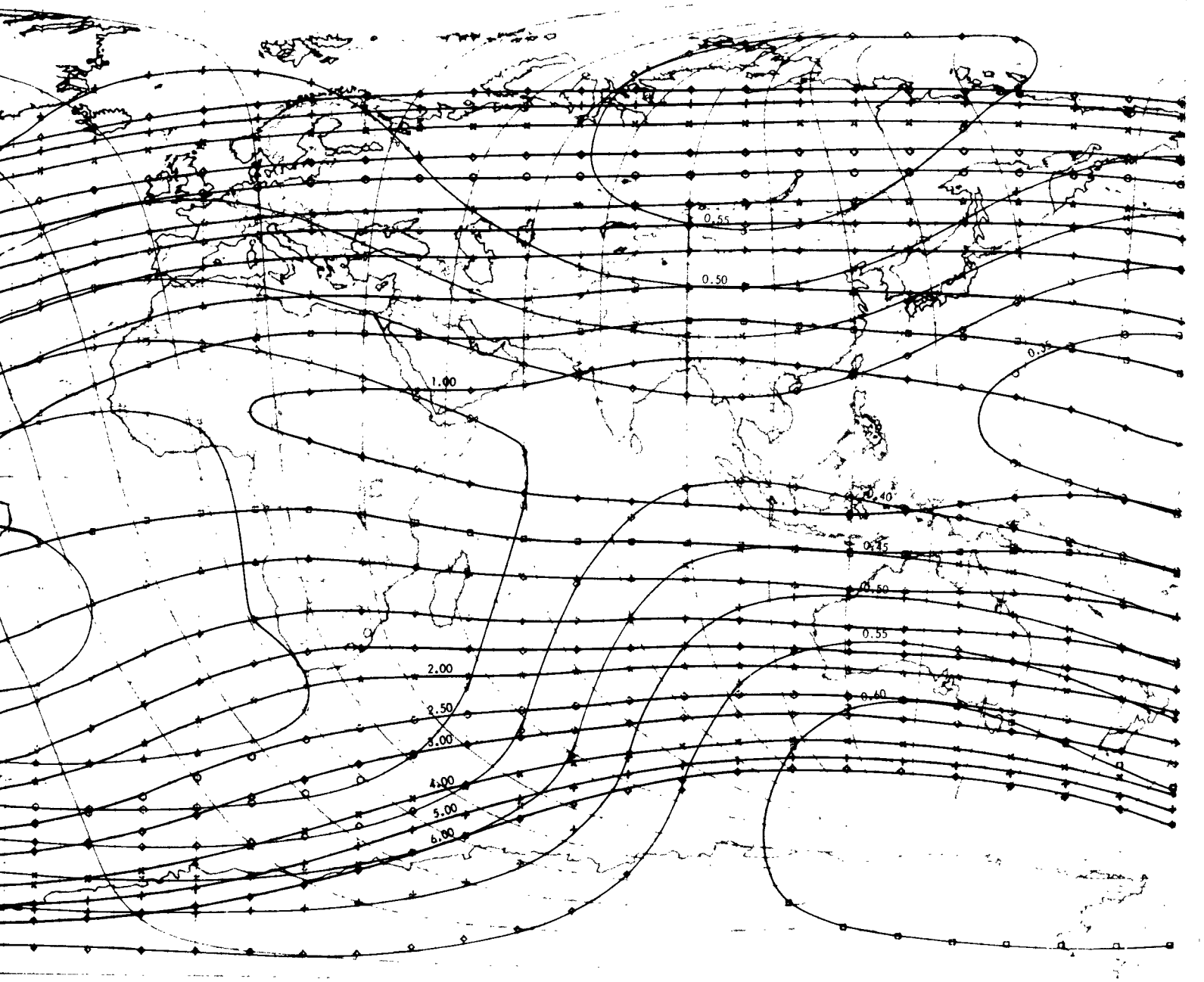

ity, B(Gauss), and Constant Magnetic Shell Parameter, L (Earth Radii), At Altitude 100 Kilometers.

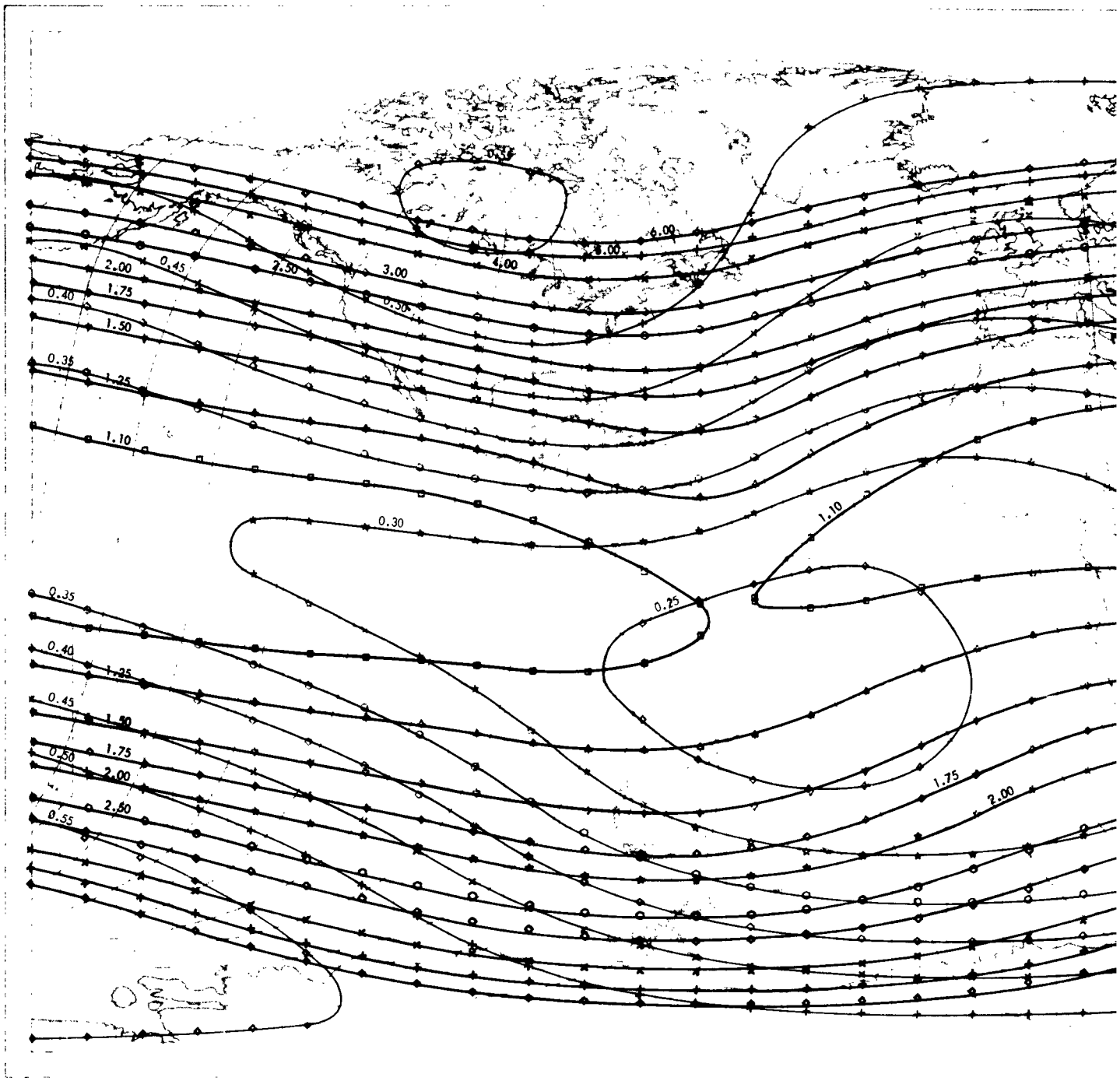

Figure 3. Constant Magnetic Field Intensity, B (Gauss), and Constant Magnetic Shell Para

2

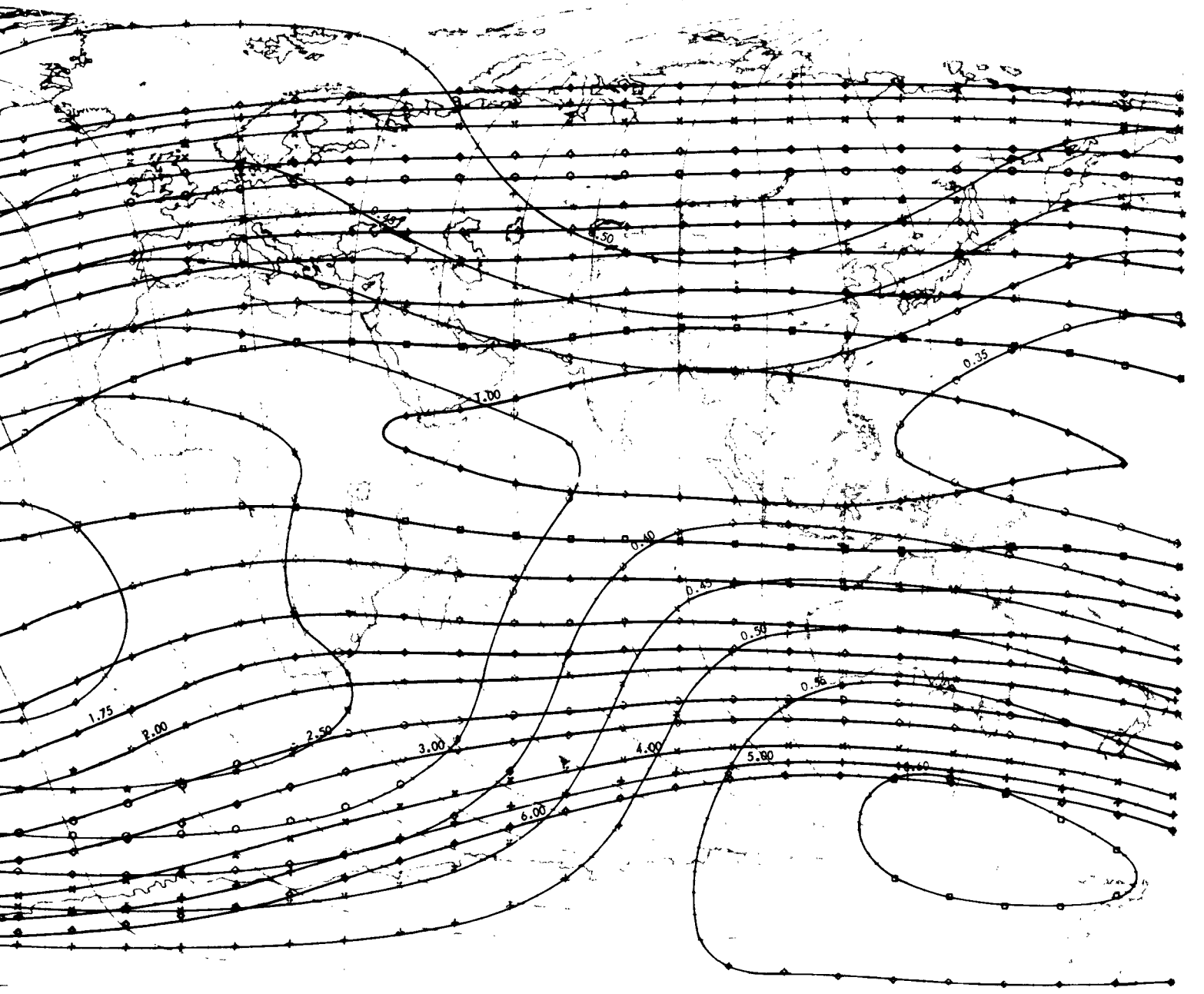

and Constant Magnetic Shell Parameter, L (Earth Radii), At Altitude 200 Kilometers.

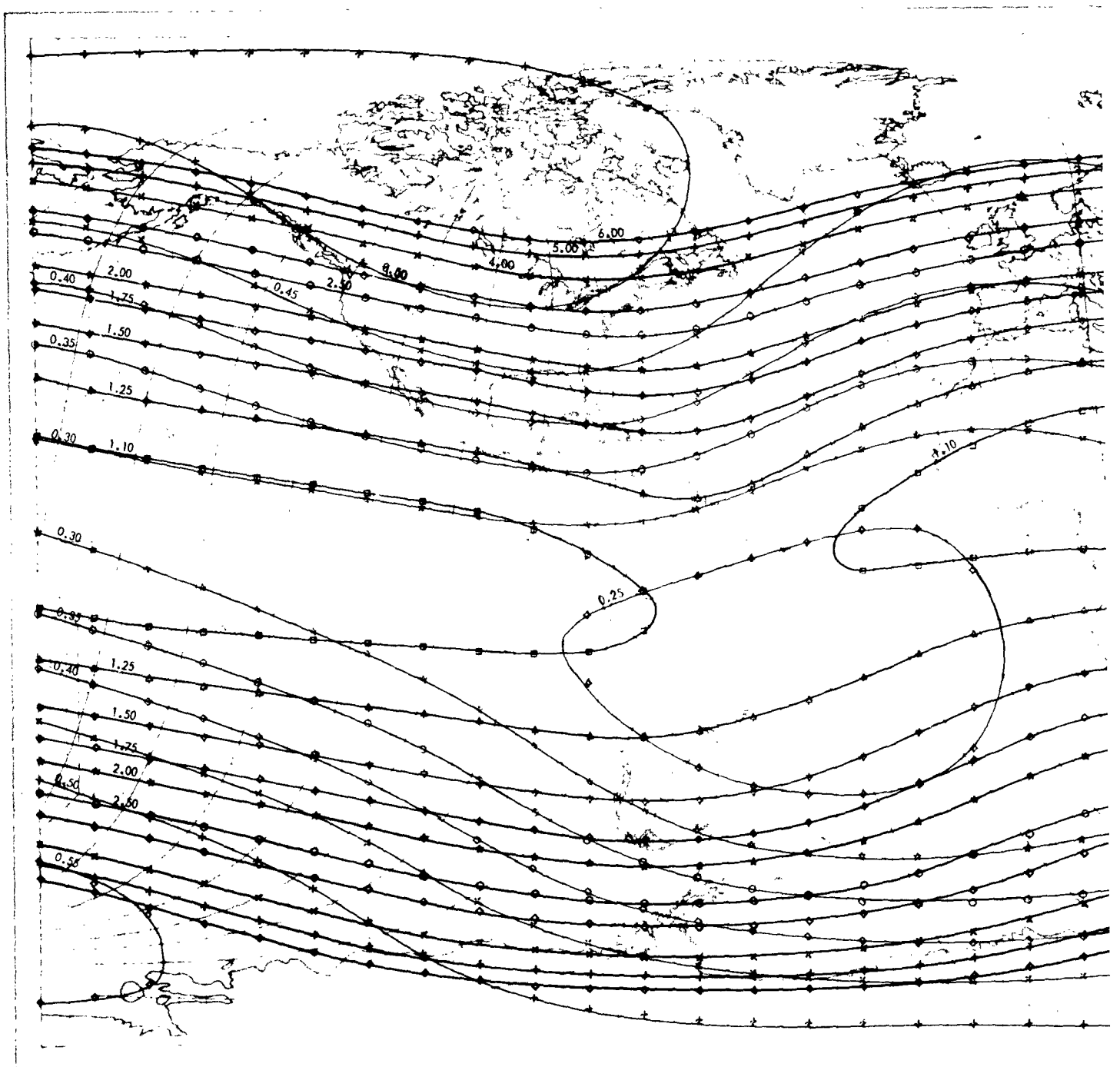

Figure 4. Constant Magentic Field Intensity, B (Gauss), and Constant Magnet

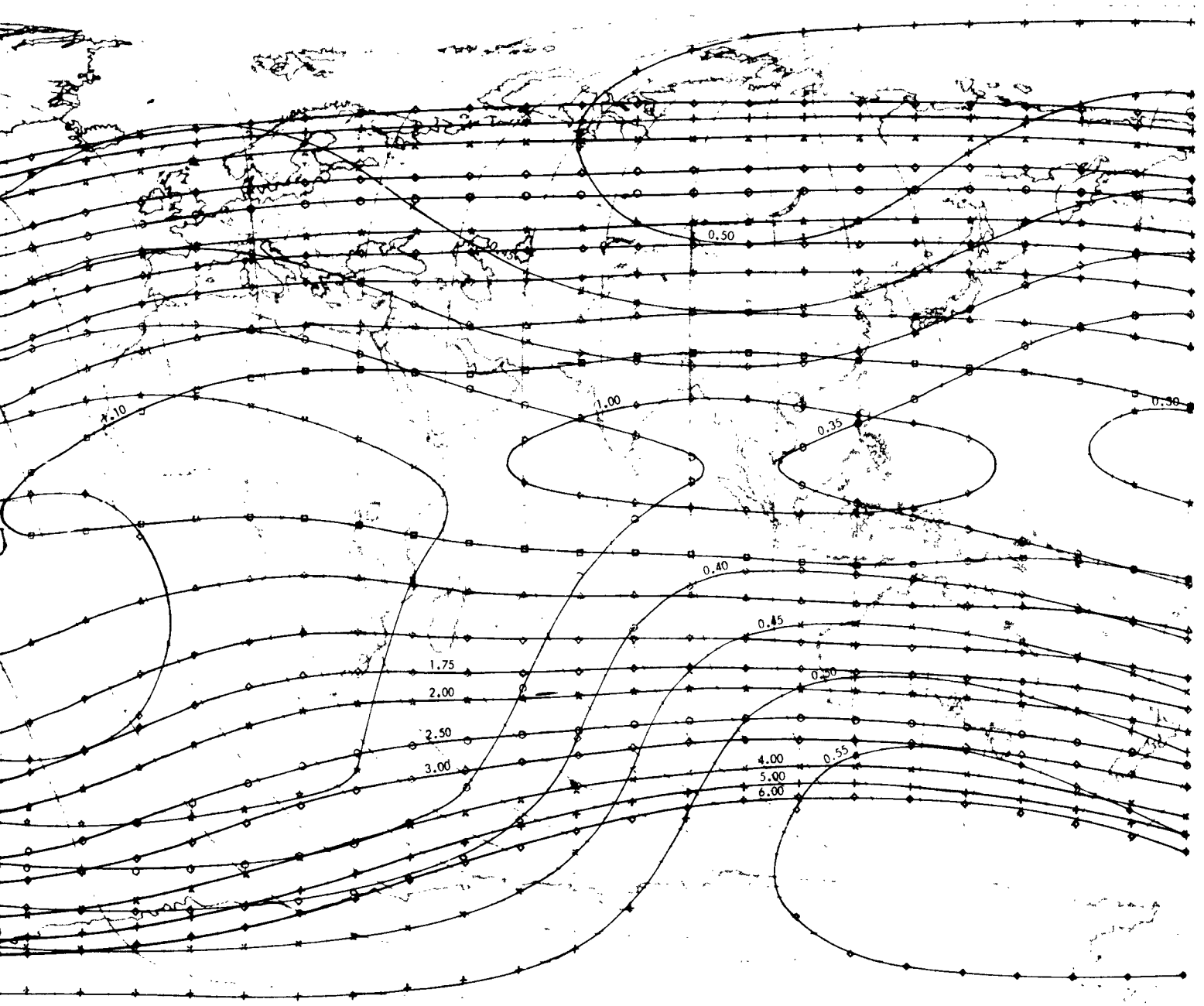

, B (Gauss), and Constant Magnetic Shell Parameter, L (Earth Radii), At Altitude 300 Kilometers.

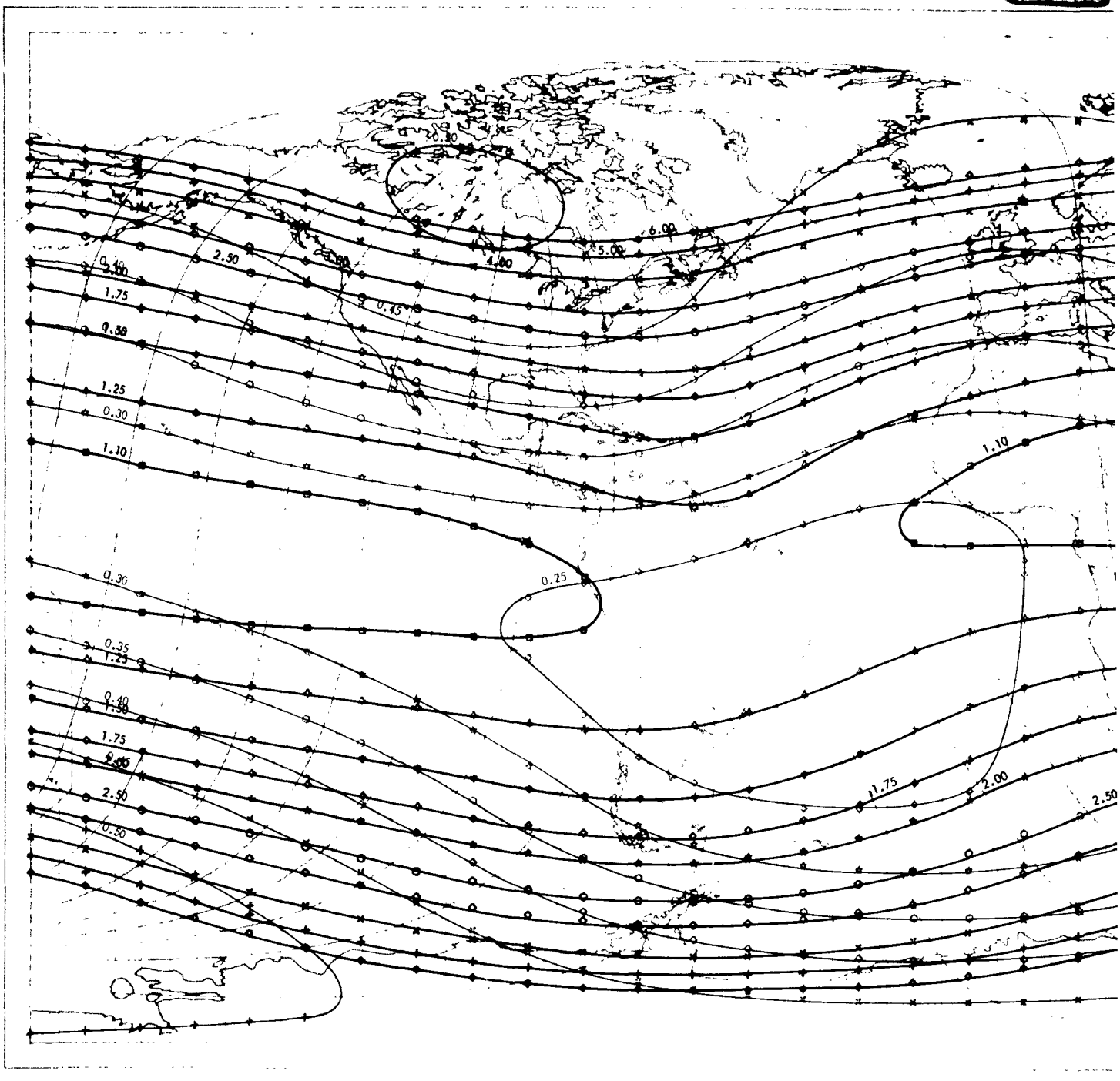

Figure 5. Constant Magnetic Field Intensity, B (Gauss), and Constant Magnetic

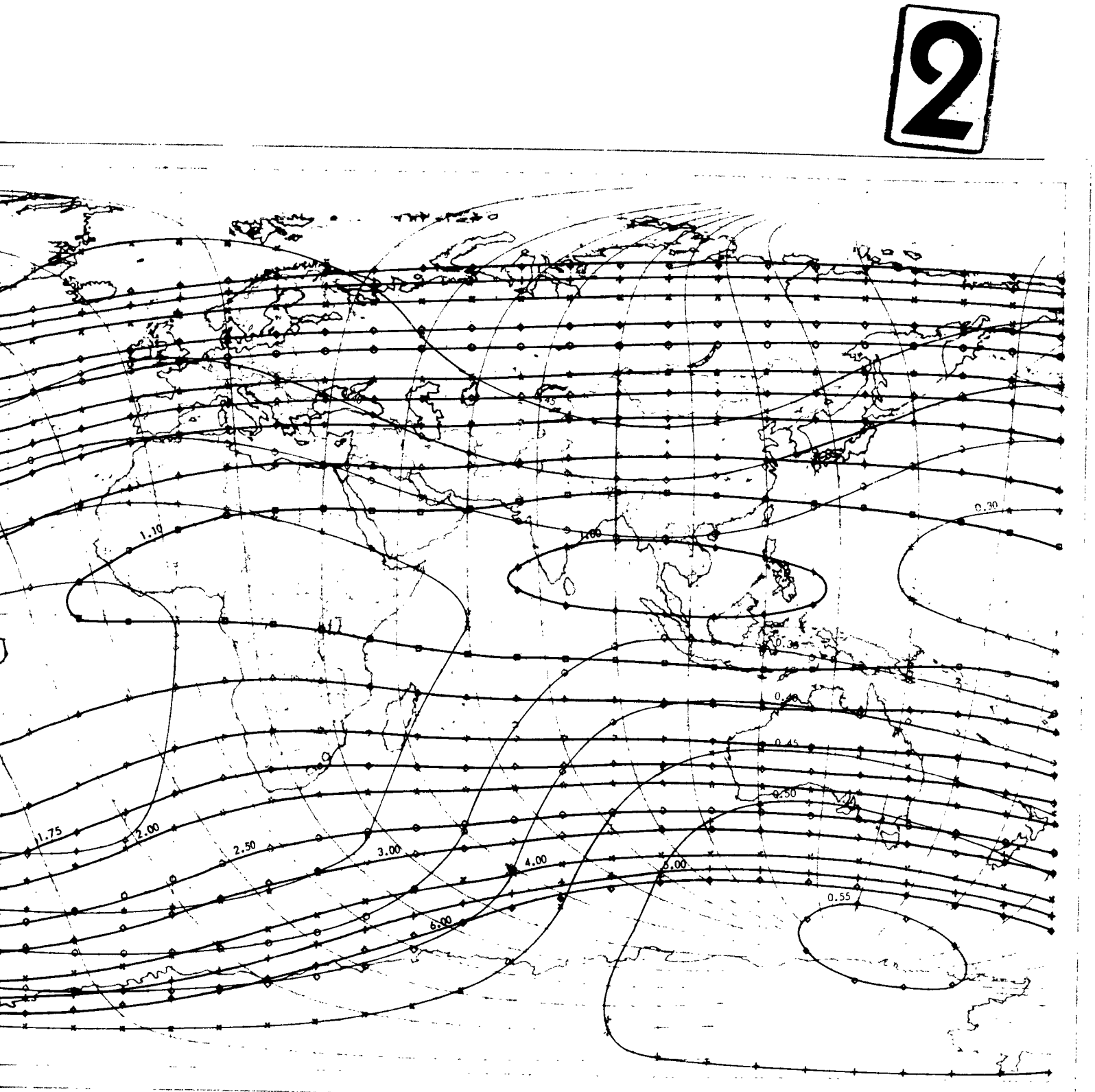

B (Gauss), and Constant Magnetic Shell Parameter, L (Earth Radii), At Altitude 400 Kilometers.

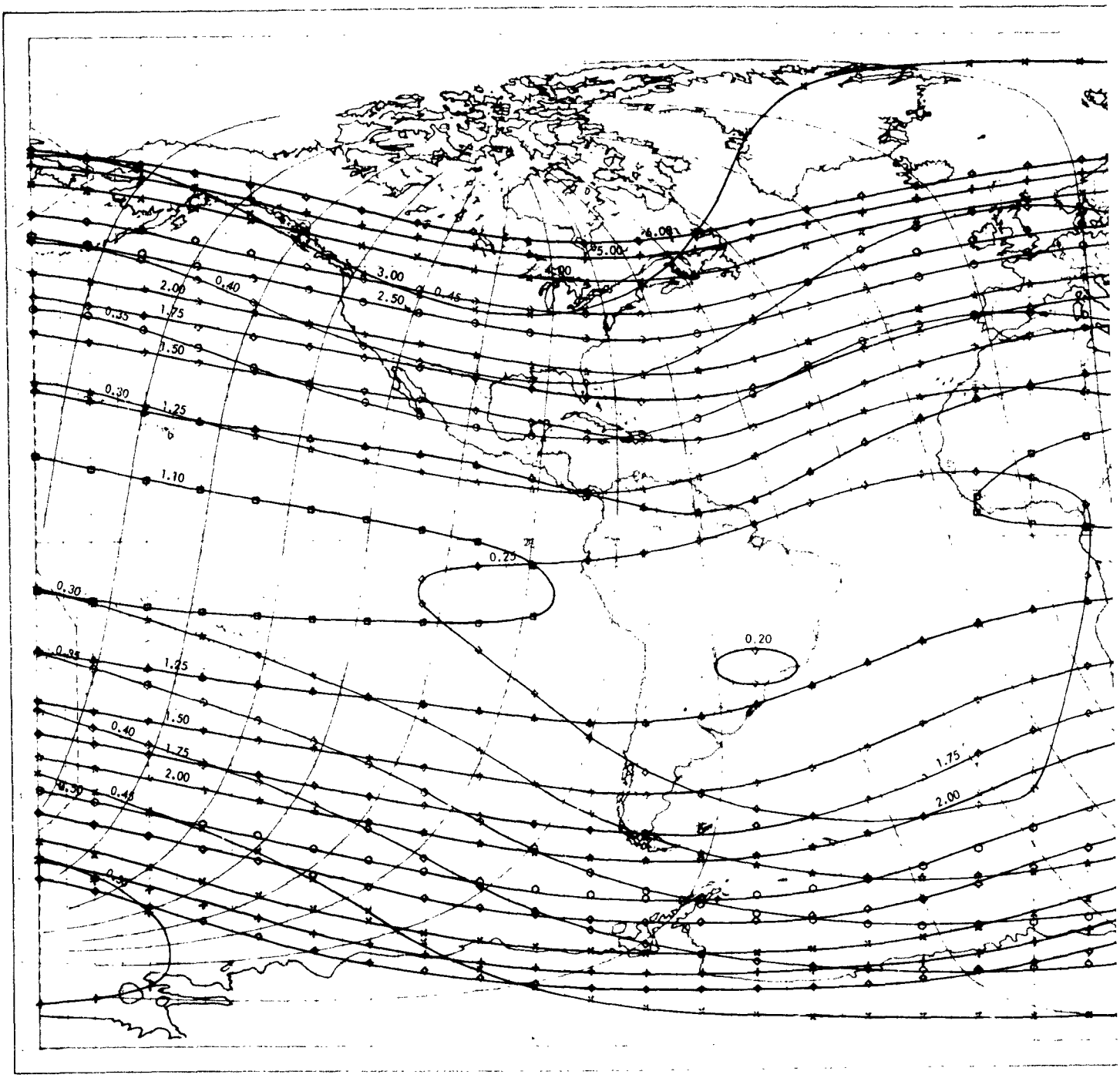

Figure 6. Constant Magnetic Field Intensity, B (Gauss), and Constant Magnetic

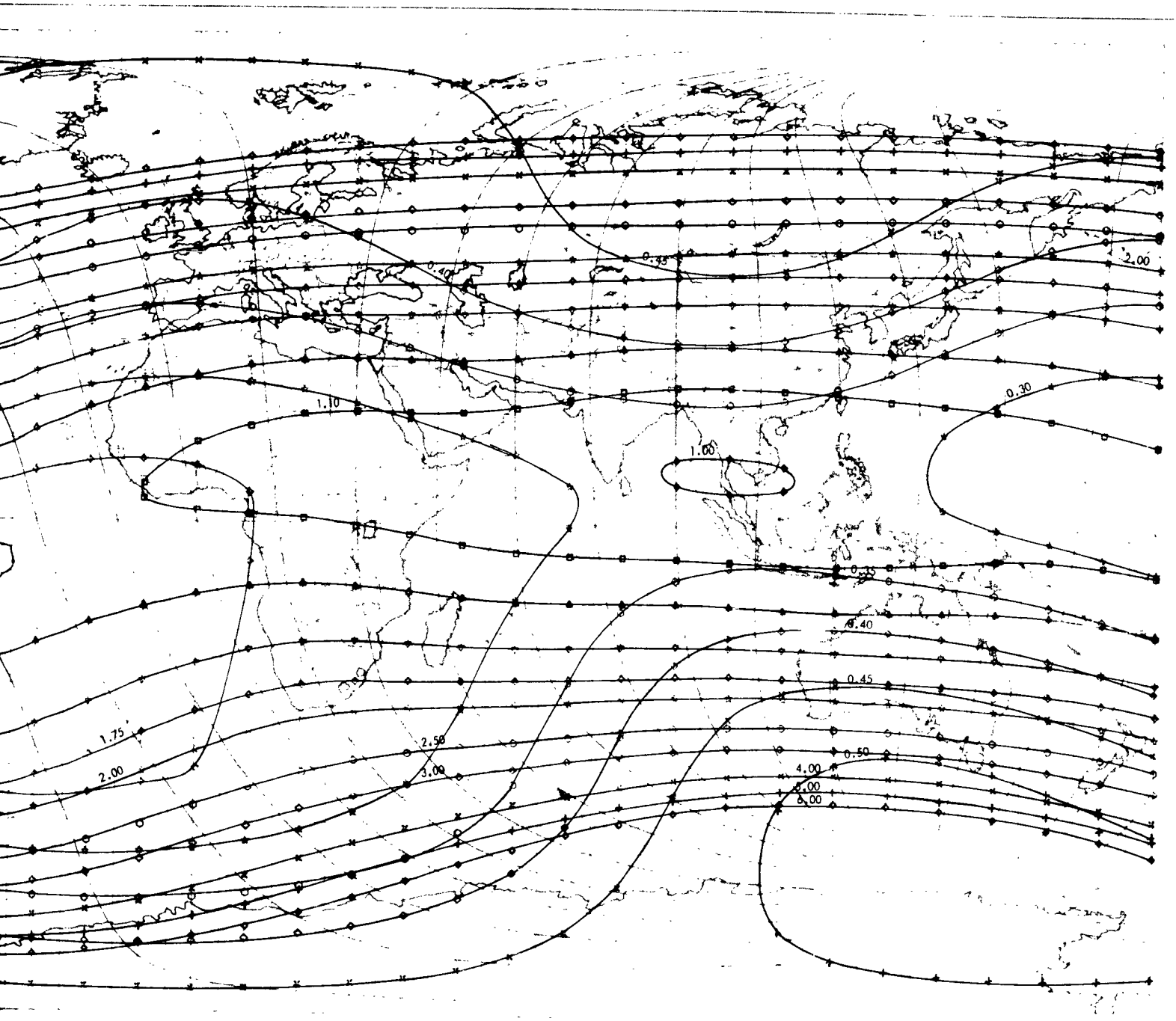

, B (Gauss), and Constant Magnetic Shell Parameter, L (Earth Radii), At Altitude 500 Kilometers.

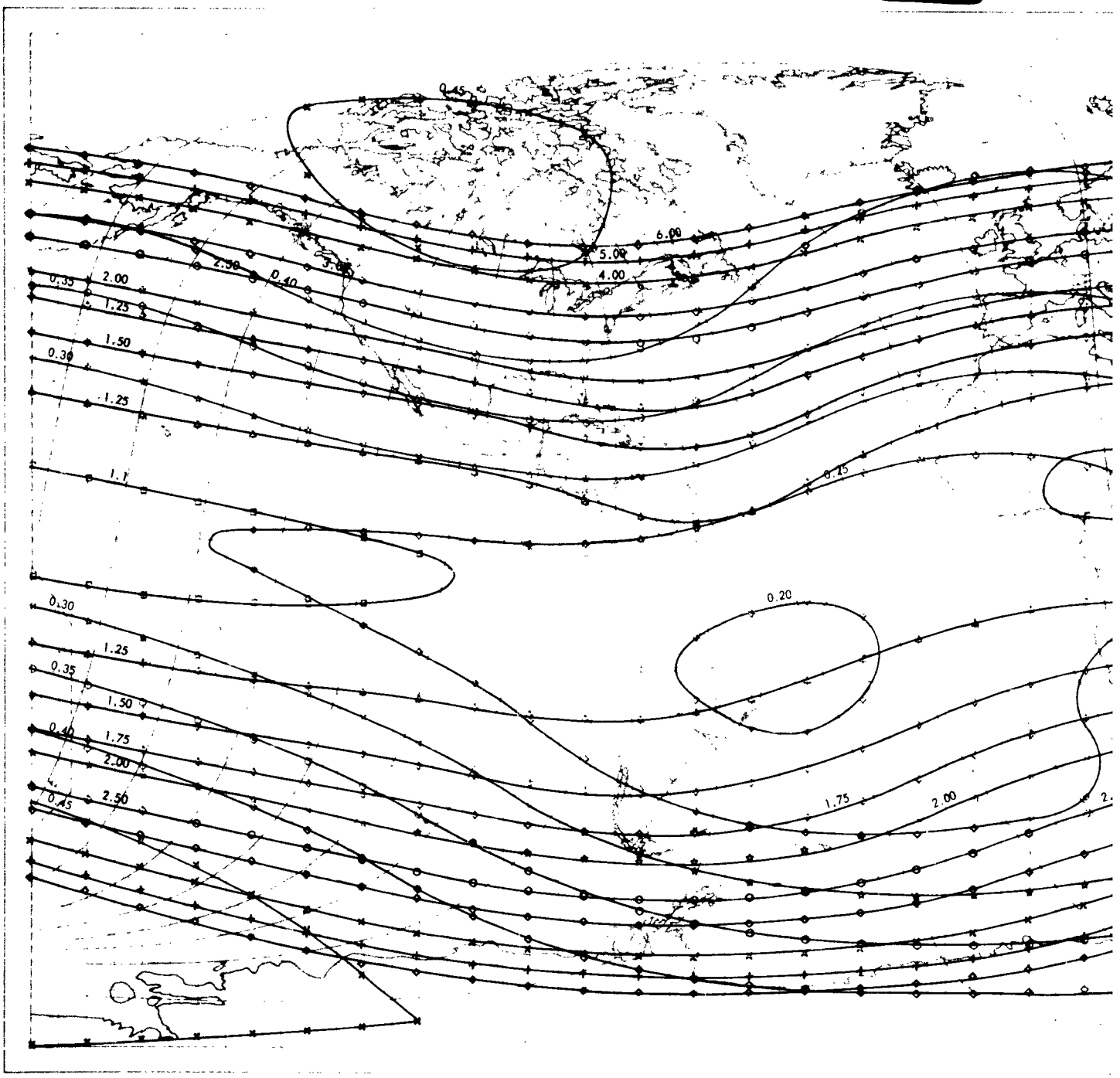

Figure 7. Constant Magnetic Field Intensity, B (Gauss), and Constant Magnet

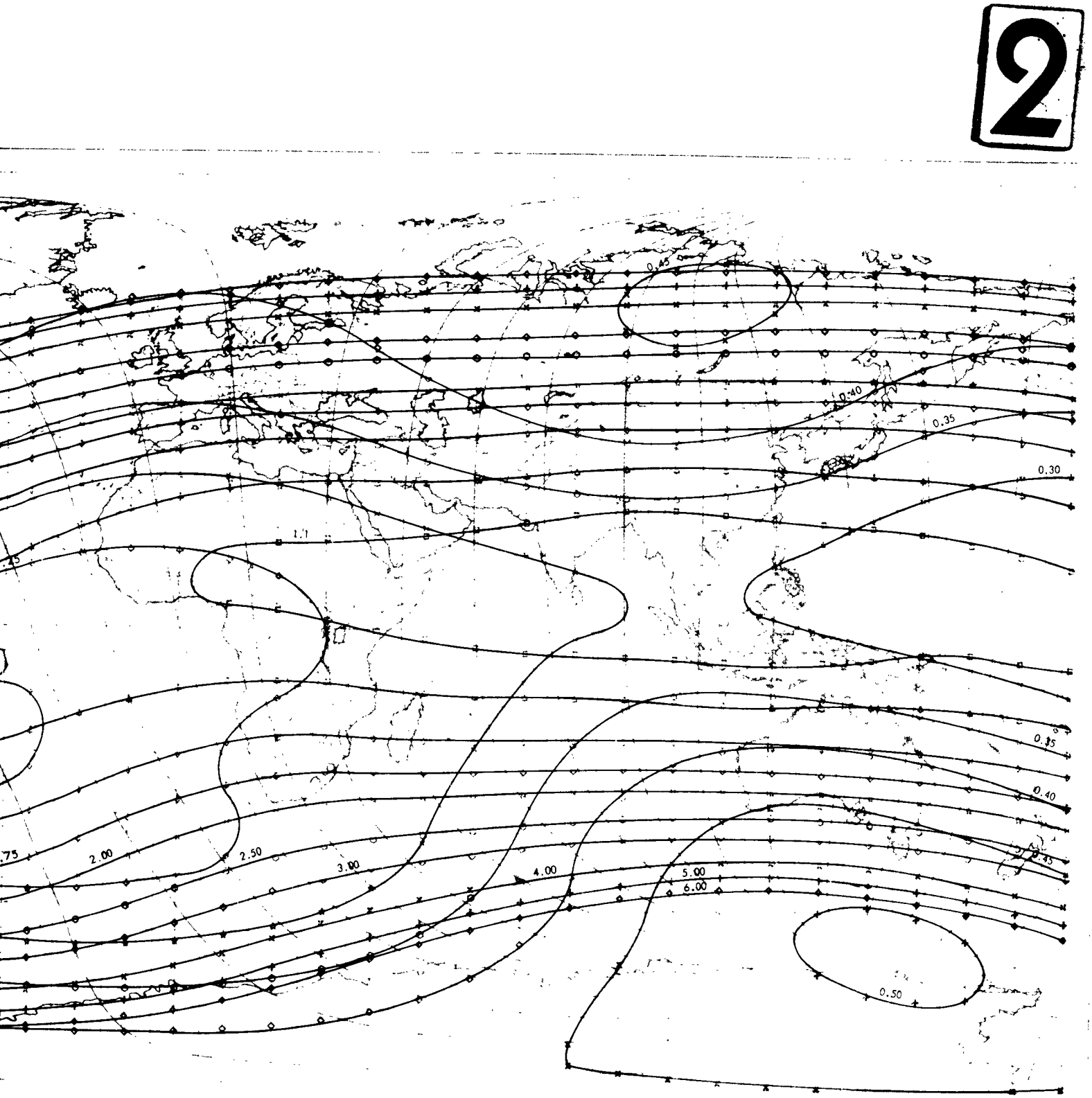

, B (Gauss), and Constant Magnetic Shell Parameter, L (Earth Radii), At Altitude 600 Kilometers.

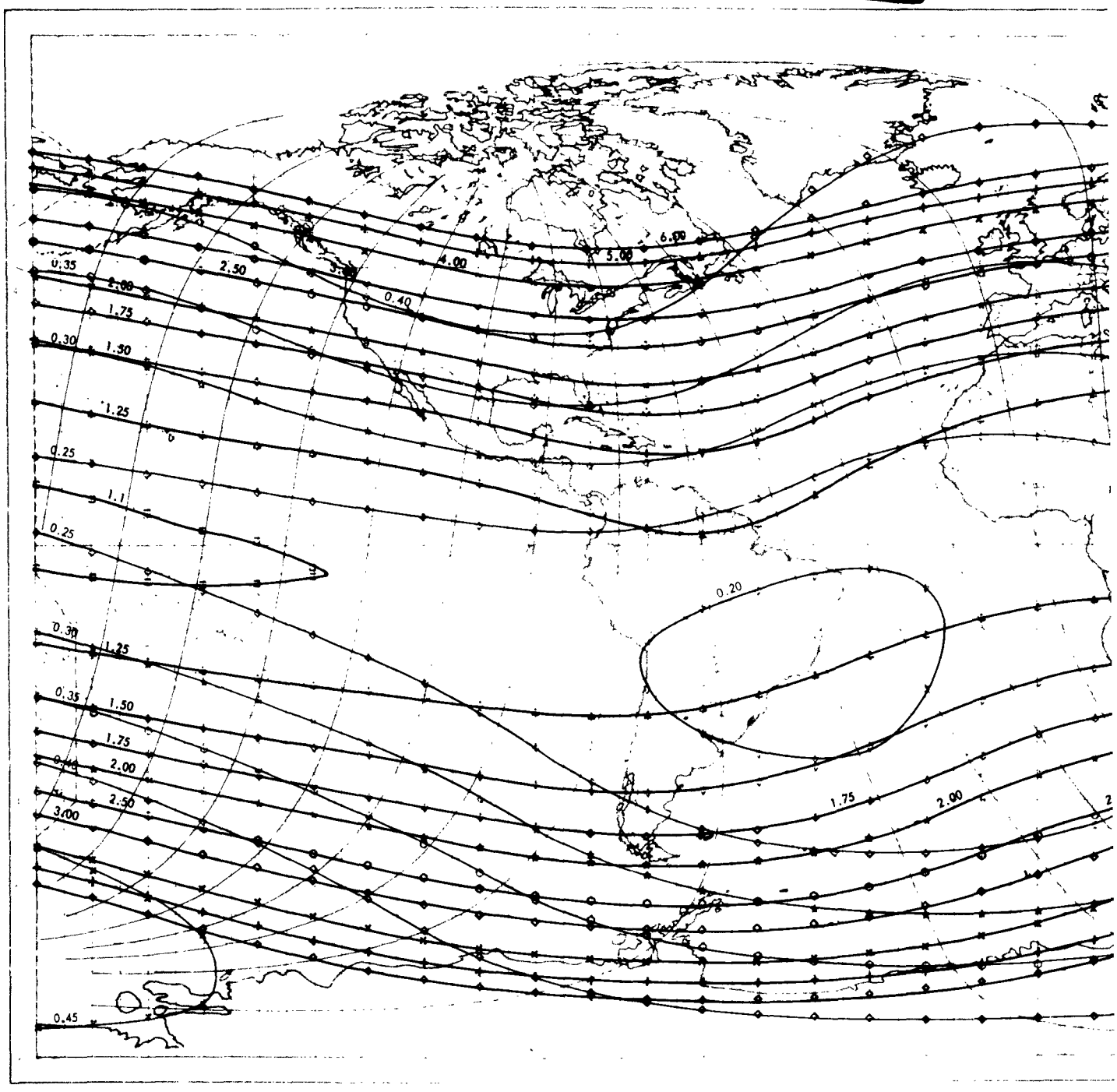

Figure 8. Constant Magnetic Field Intensity, B (Gauss), and Constant Magnet

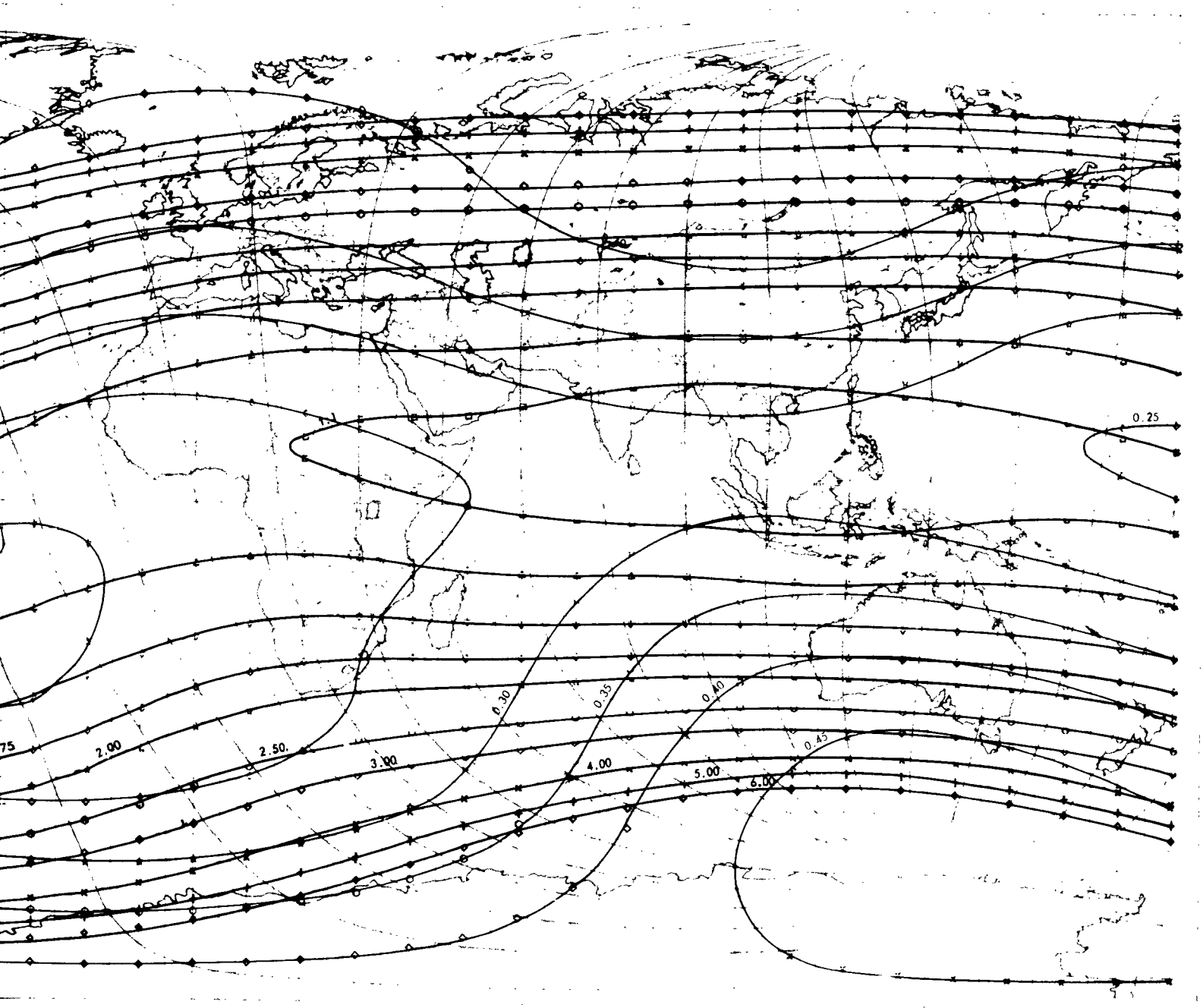

, B (Gauss), and Constant Magnetic Shell Parameter, L (Earth Radii), At Altitude 700 Kilometers.

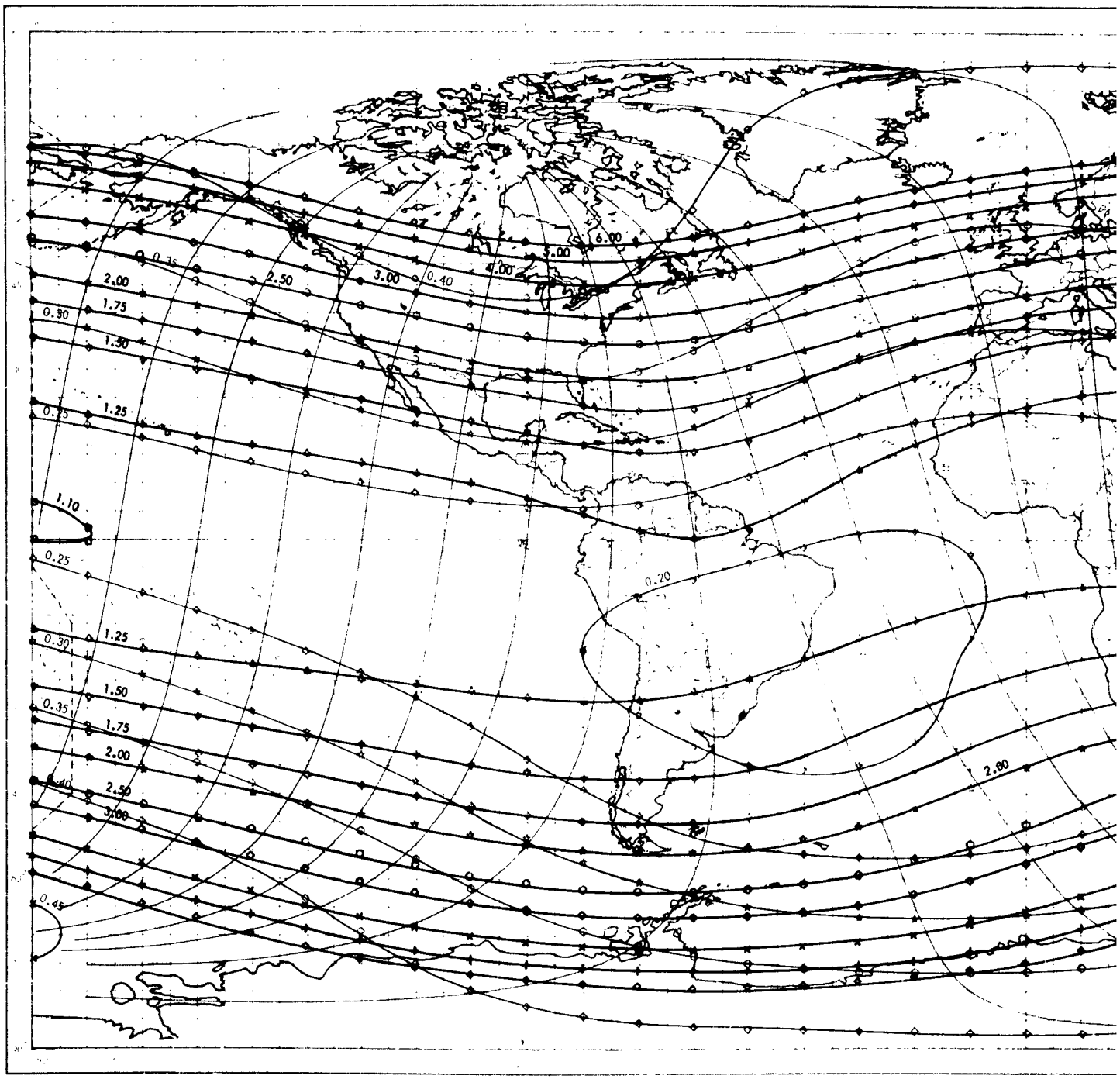

Figure 9. Constant Magnetic Field Intensity, B (Gauss), and Constant Magnetic

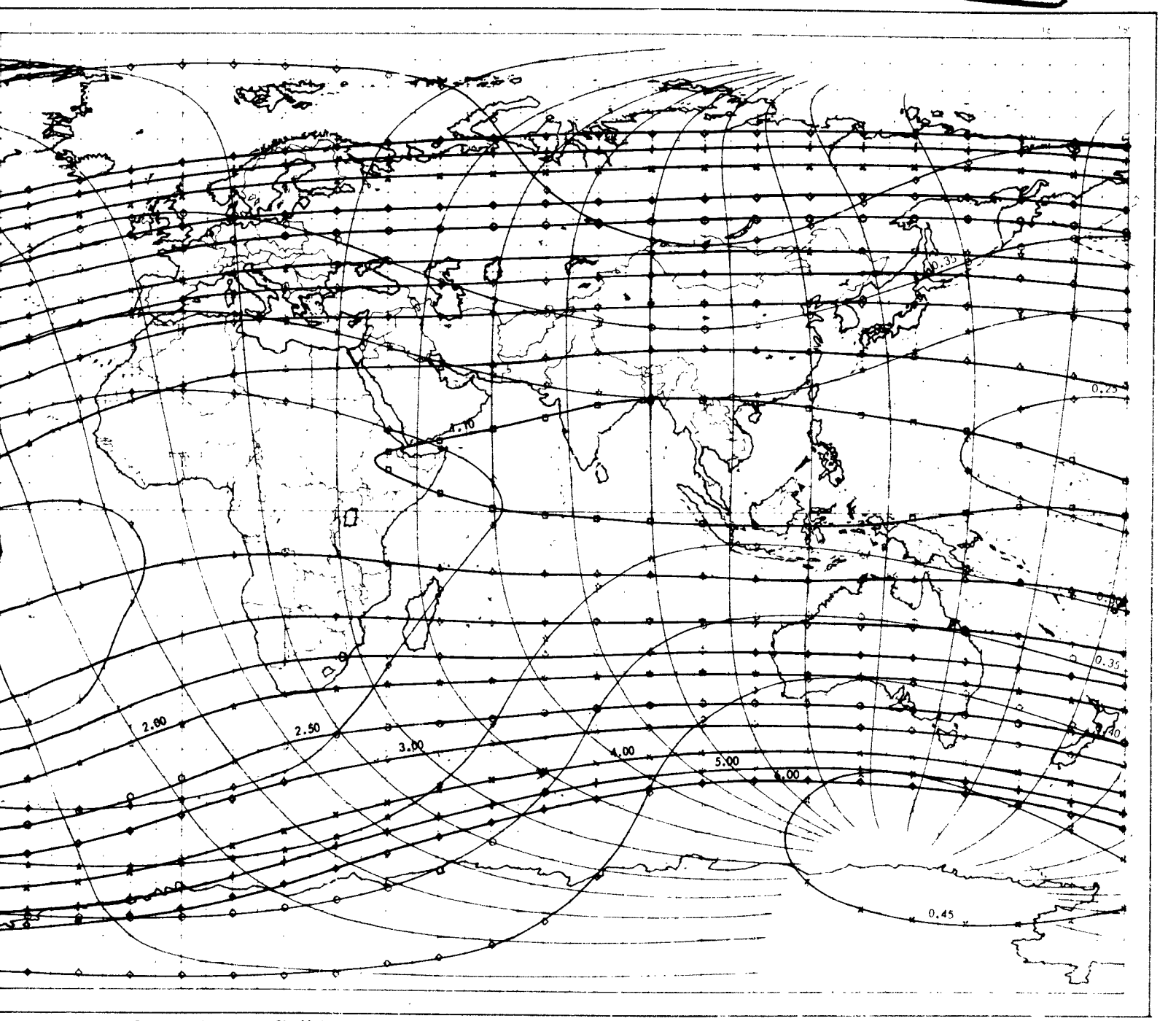

, B (Gauss), and Constant Magnetic Shell Parameter, L (Earth Radii), At Altitude 800 Kilometers.

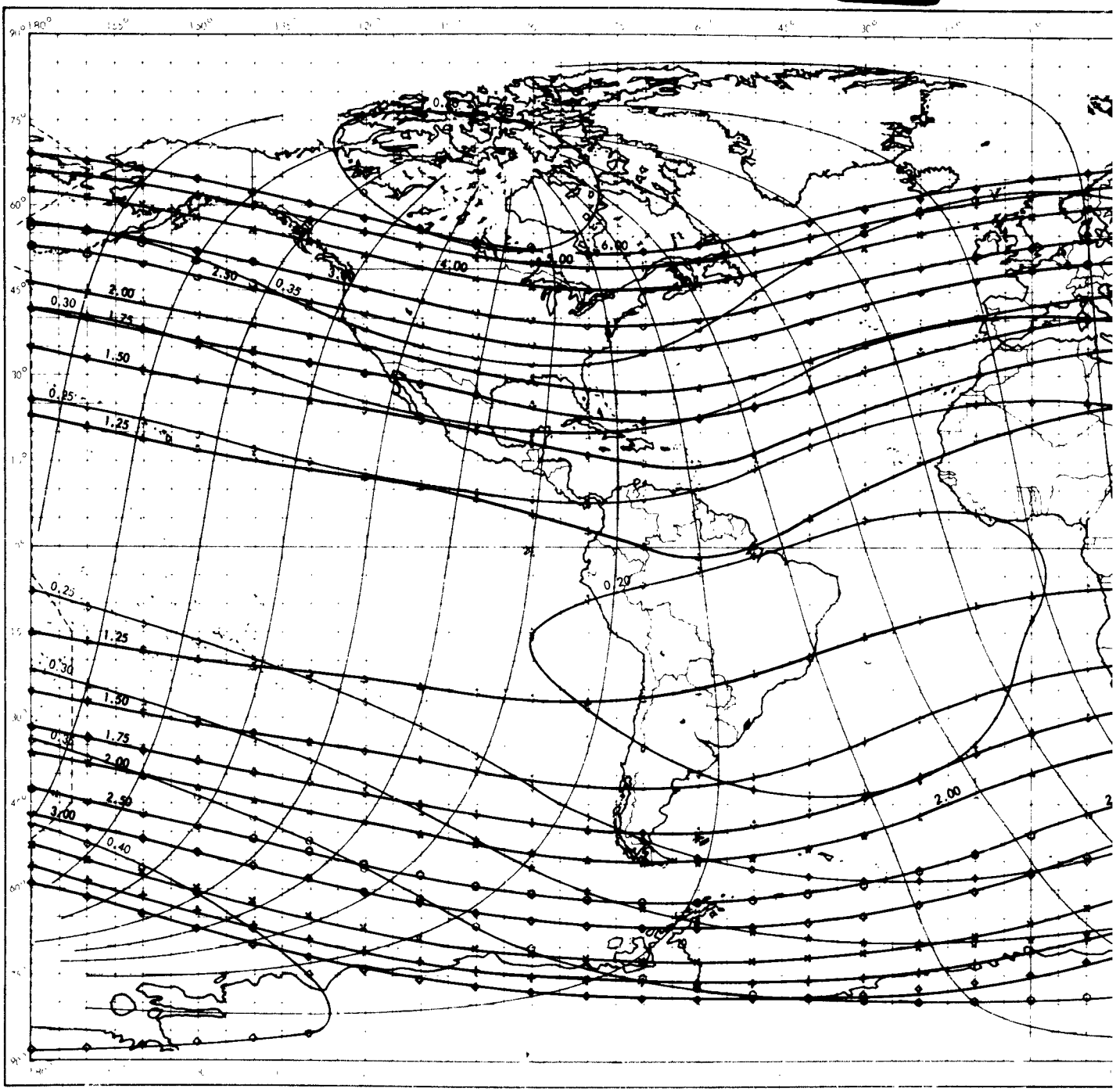

Figure 10. Constant Magnetic Field Intensity, B (Gauss), and Constant Magnetic S

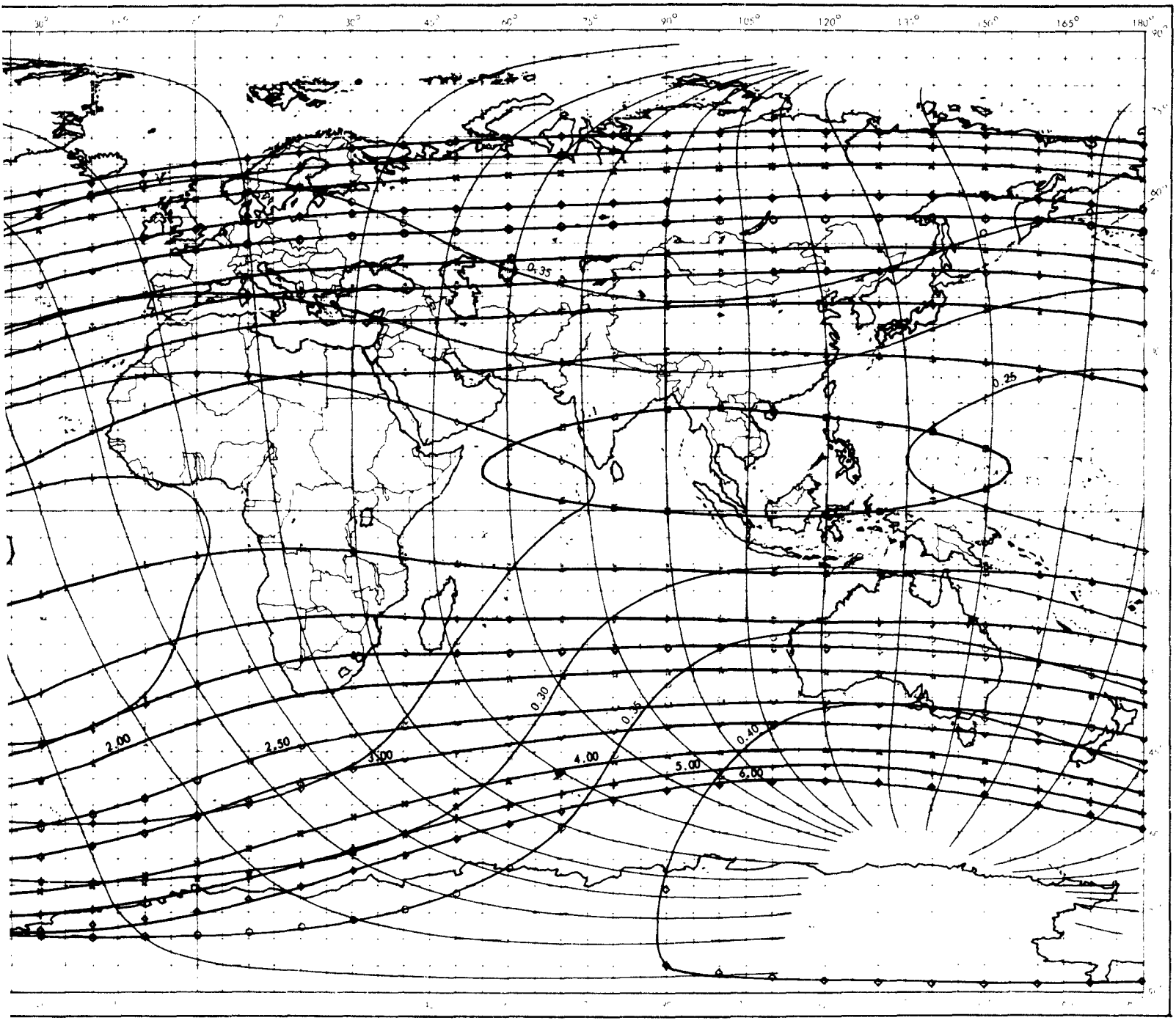

B (Gauss), and Constant Magnetic Shell Parameter, L (Earth Radii), At Altitude 900 Kilometers.

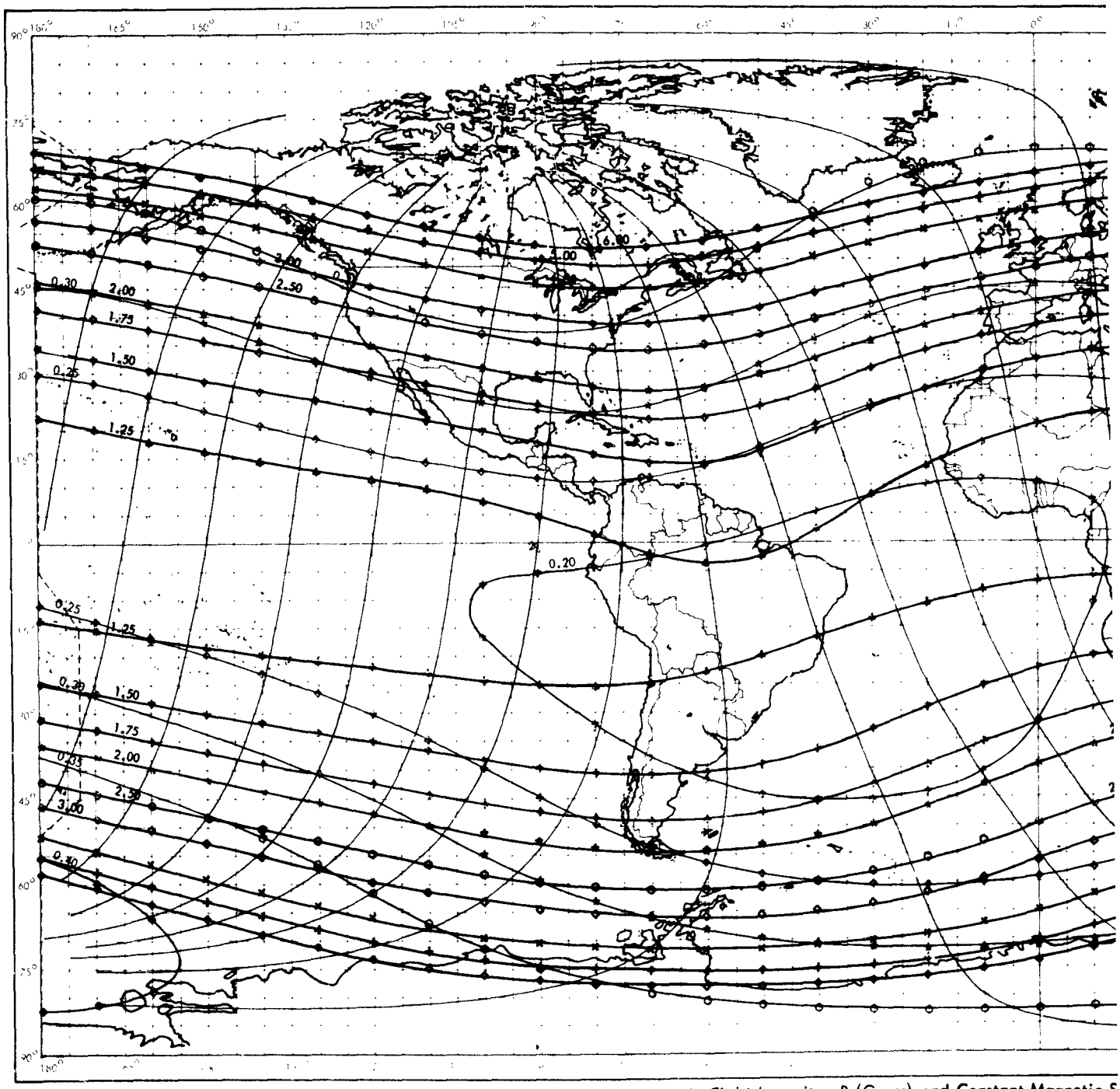

Figure 11. Constant Magnetic Field Intensity, B (Gauss), and Constant Magnetic S

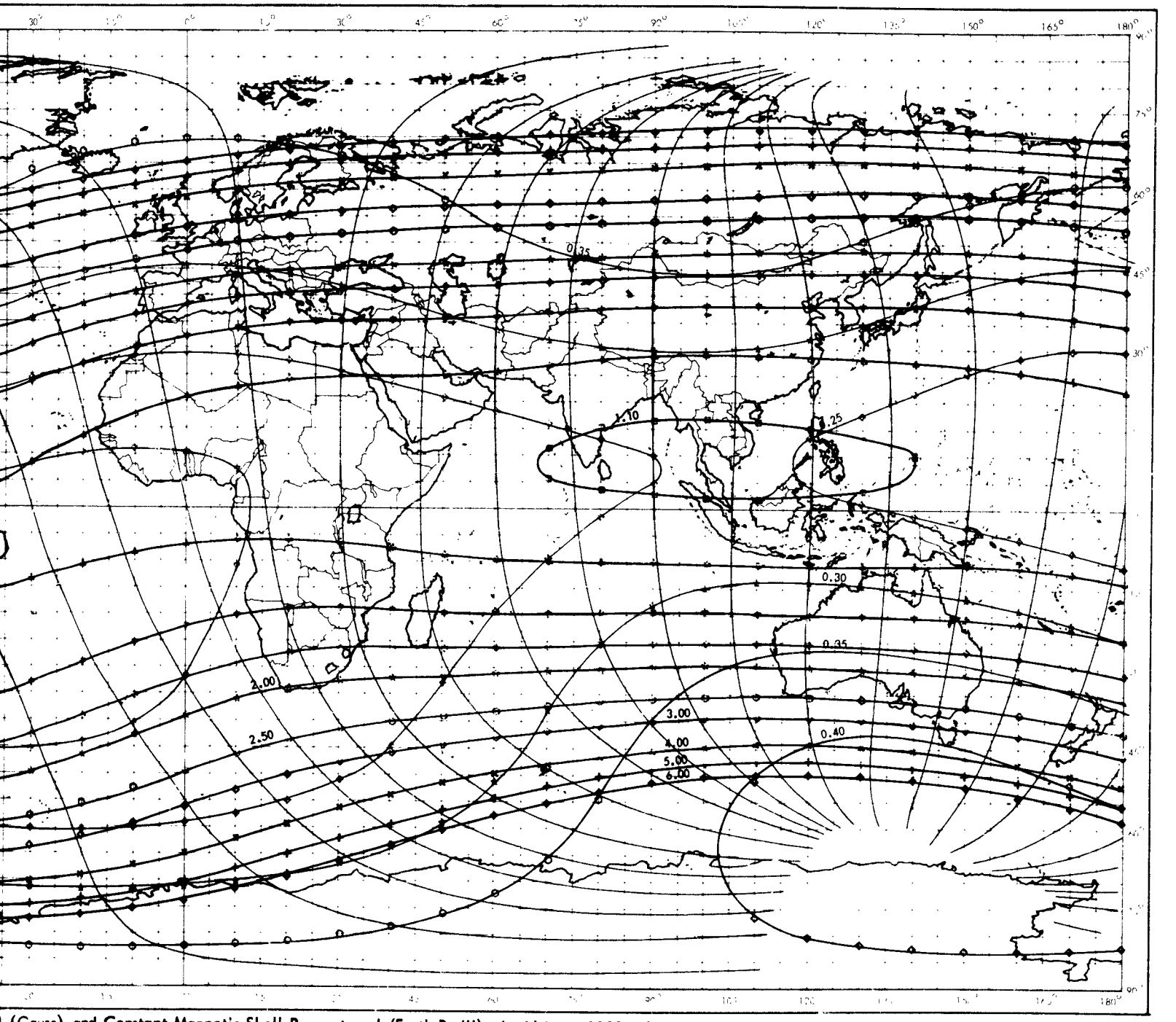

(Gauss), and Constant Magnetic Shell Parameter, L (Earth Radii), At Altitude 1000 Kilometers.

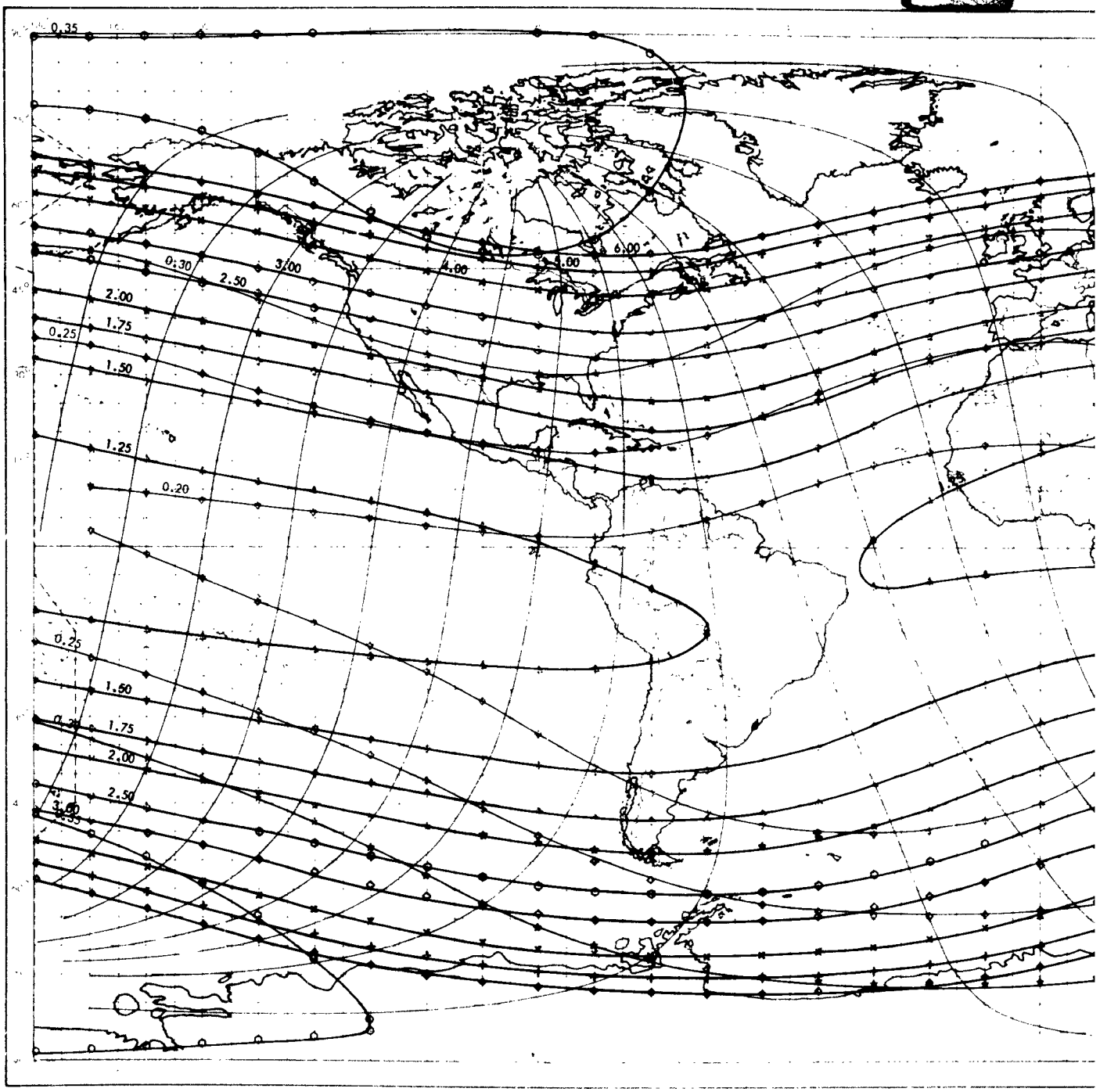

Figure 12. Constant Magnetic Field Intensity, B (Gauss), and Constant Magneti

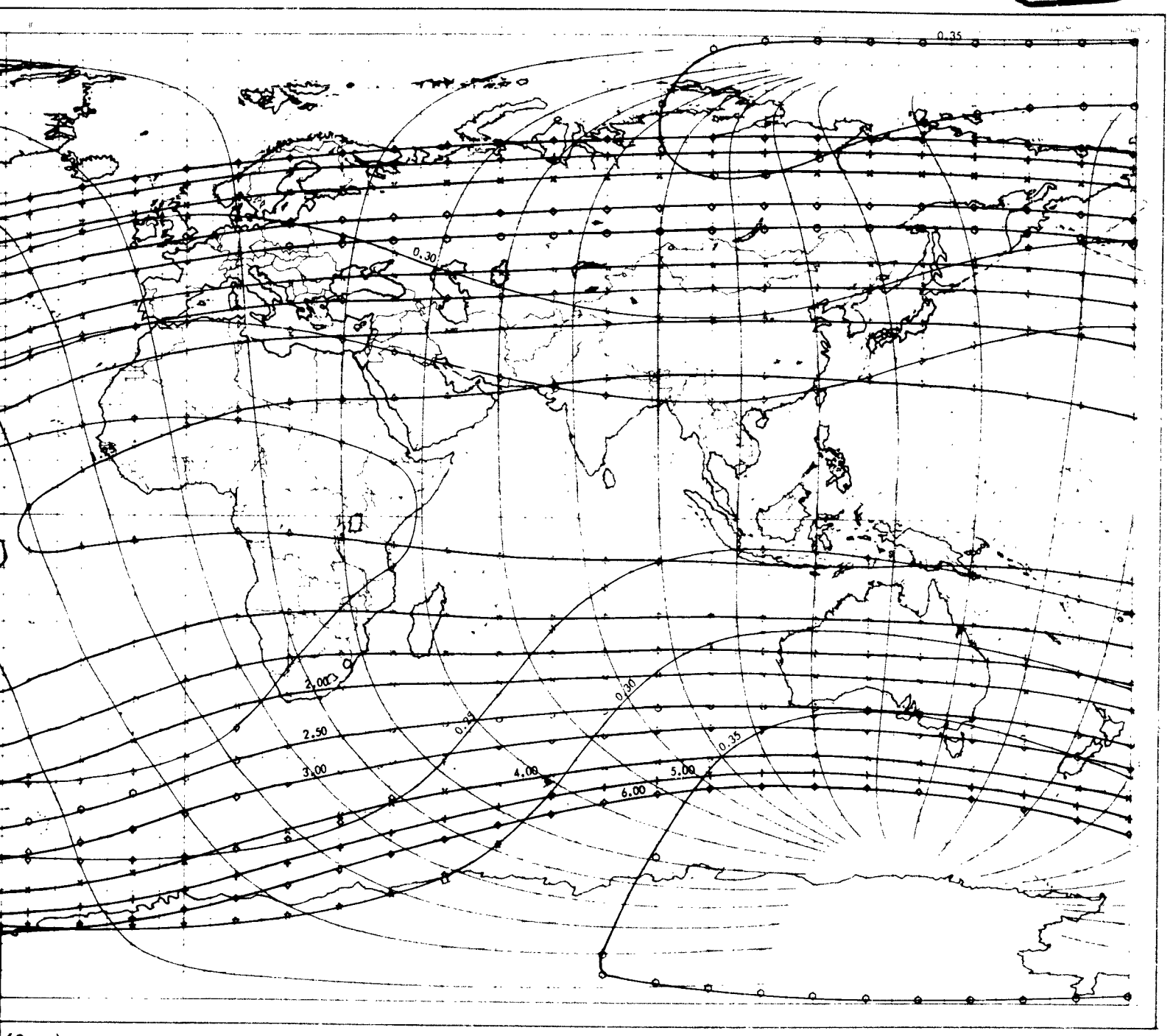

(Gauss), and Constant Magnetic Shell Parameter, L (Earth Radii), At Altitude 1200 Kilometers.

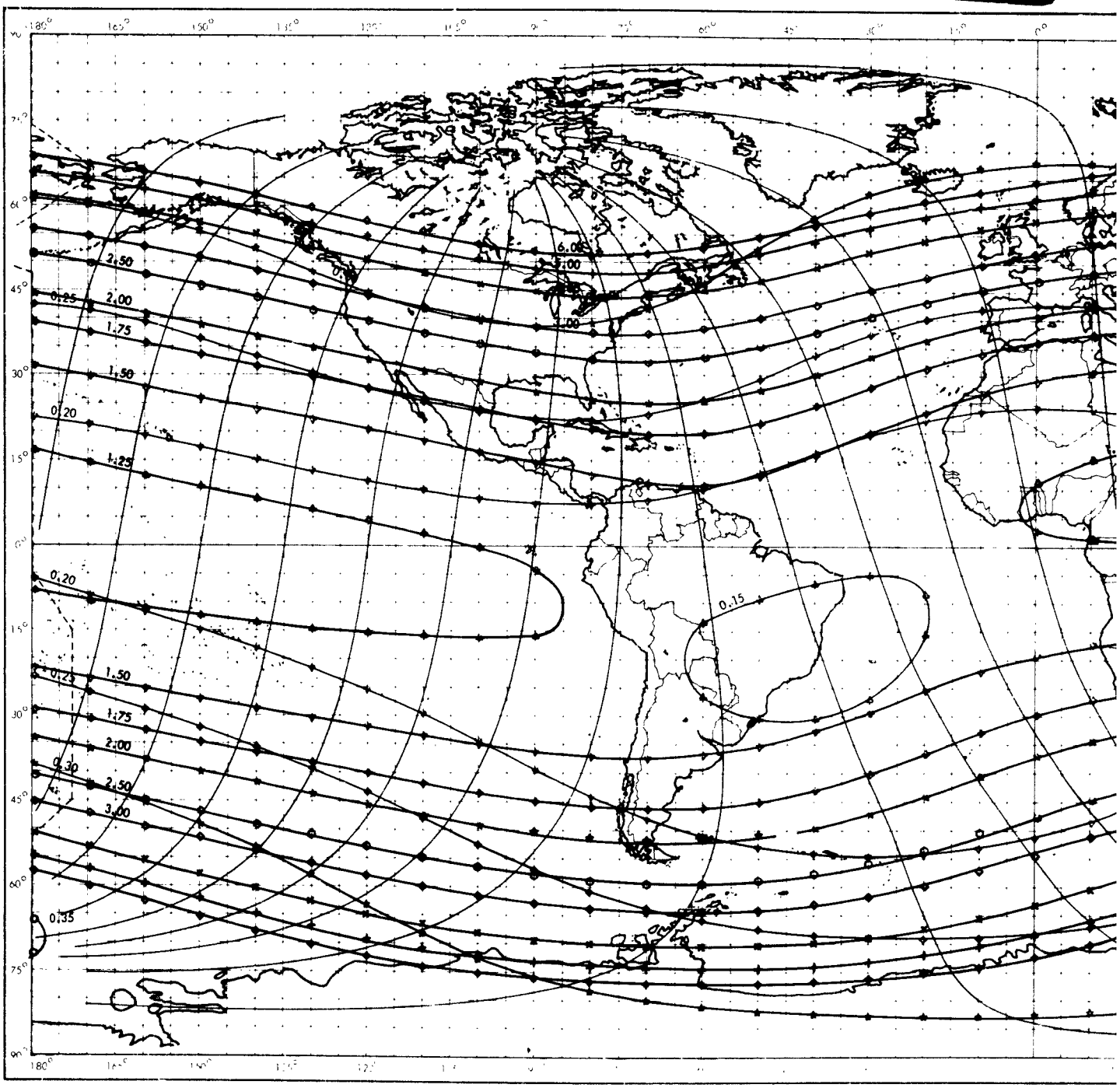

Figure 13. Constant Magnetic Field Intensity, B (Gauss), and Constant Magnetic

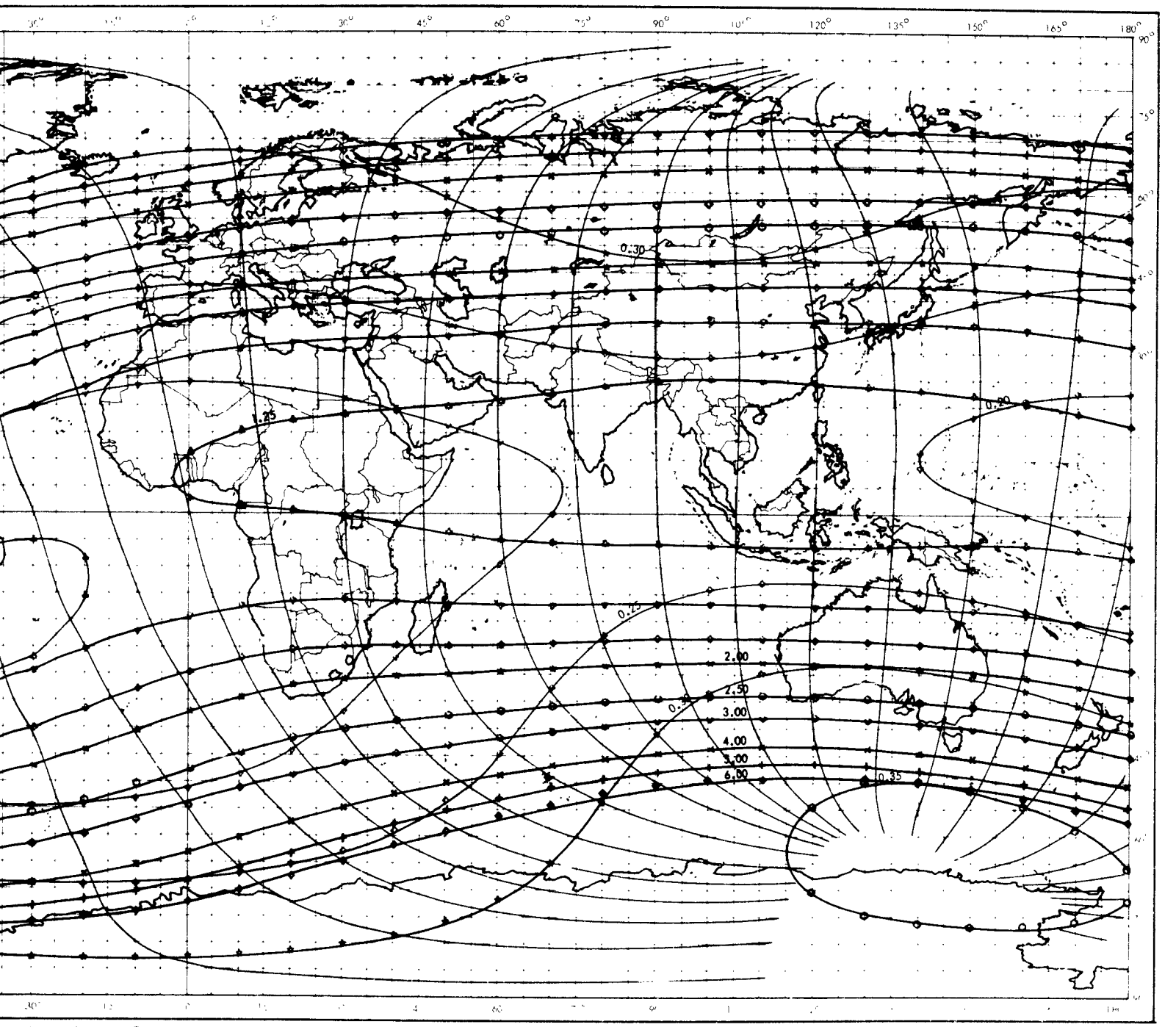

B (Gauss), and Constant Magnetic Shell Parameter, L (Earth Radii), At Altitude 1400 Kilometers.

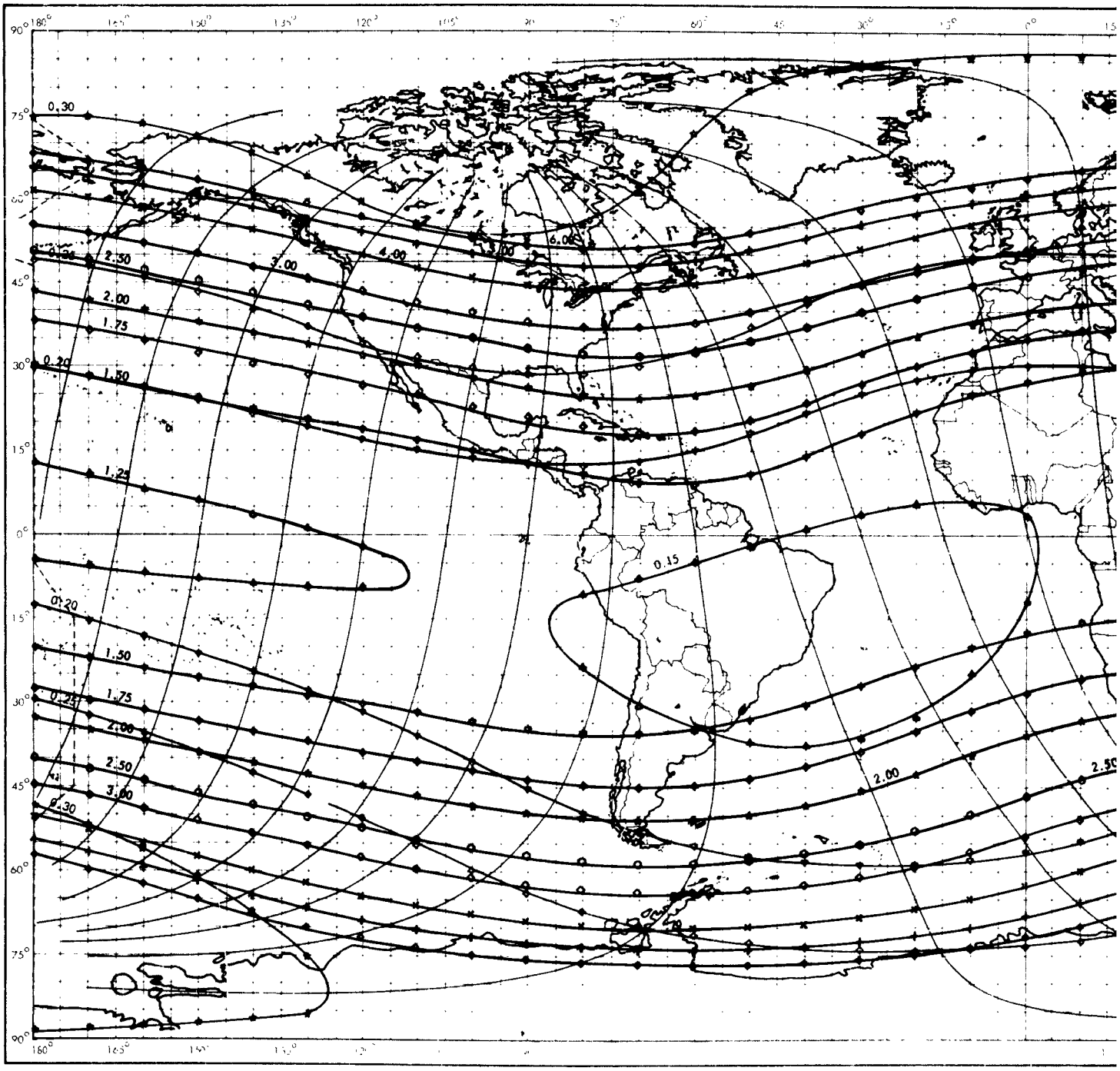

Figure 14. Constant Magnetic Field Intensity, B (Gauss), and Constant Magnetic

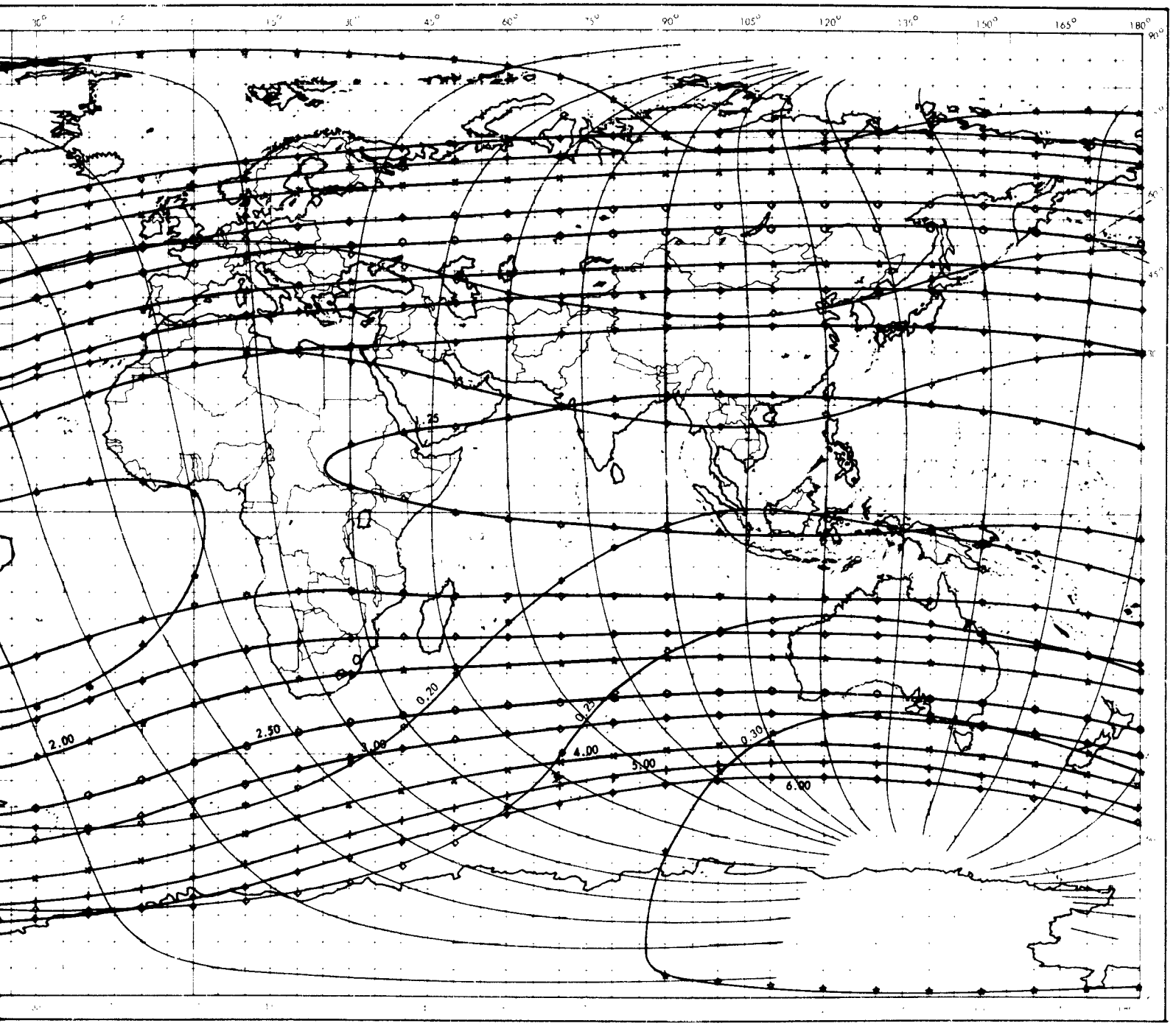

, B (Gauss), and Constant Magnetic Shell Parameter, L (Earth Radii), At Altitude 1600 Kilometers.

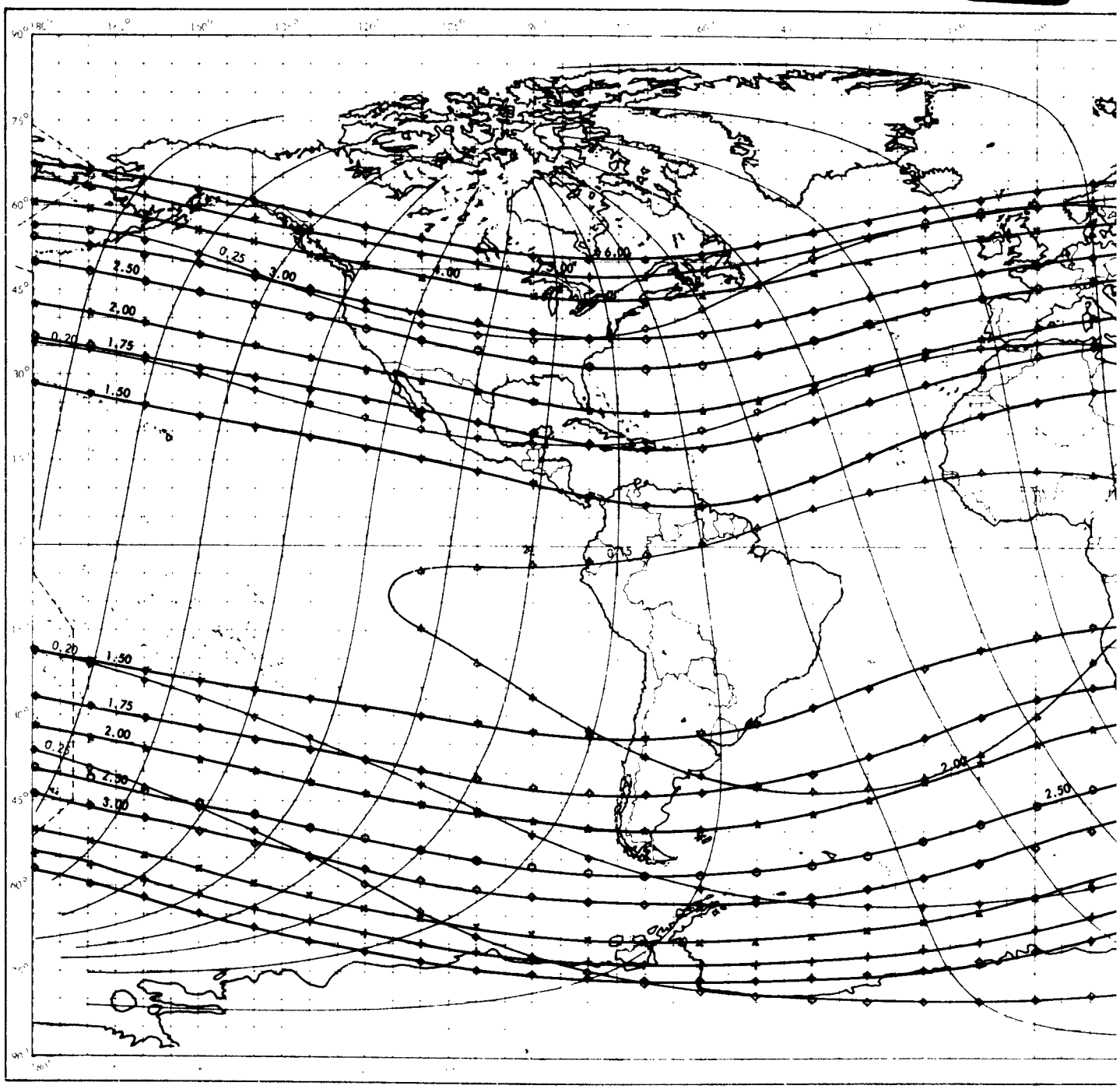

Figure 15. Constant Magnetic Field Intensity, B (Gauss), and Constant Magnetic

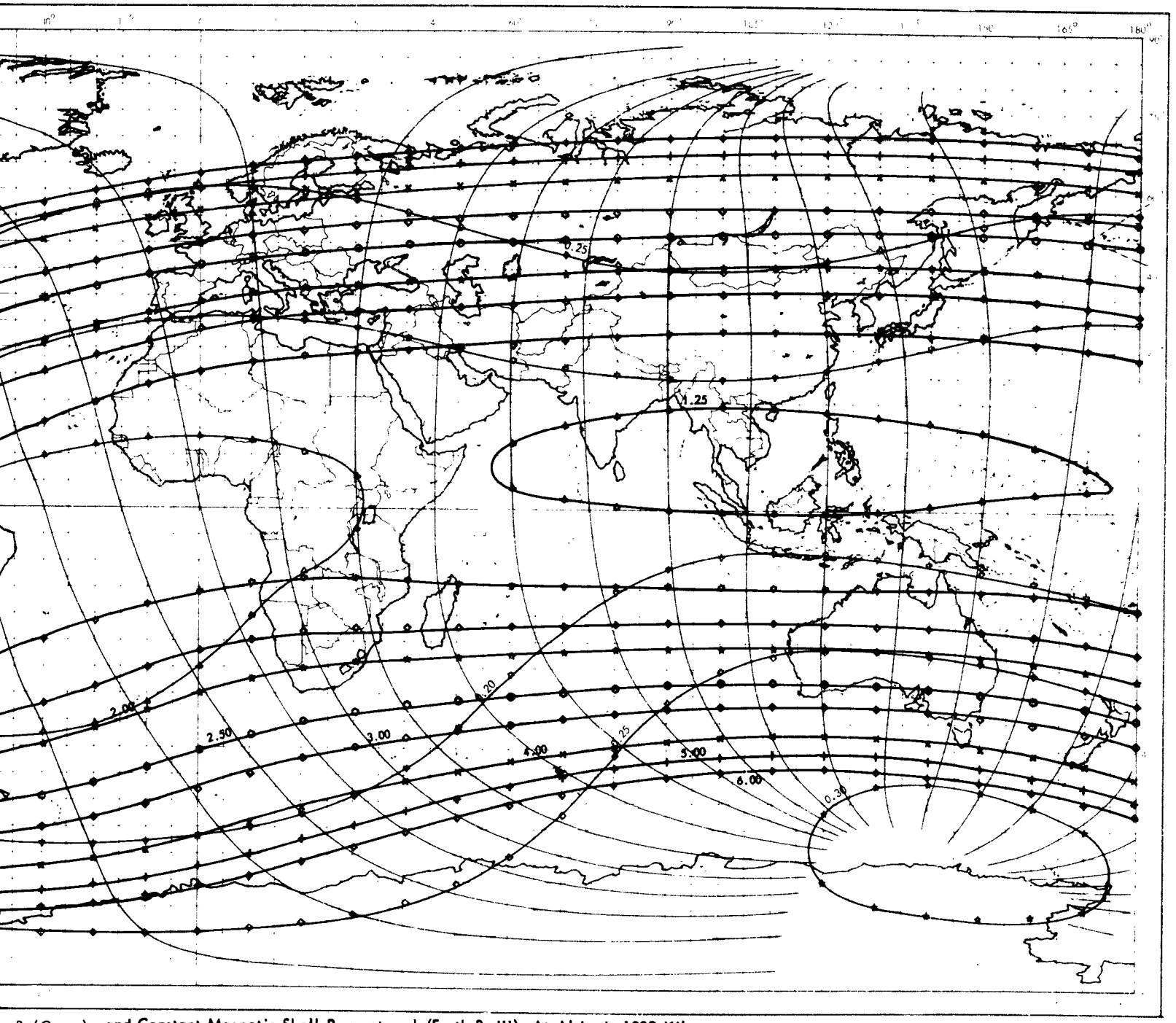

, B (Gauss), and Constant Magnetic Shell Parameter, L (Earth Radii), At Altitude 1800 Kilometers.

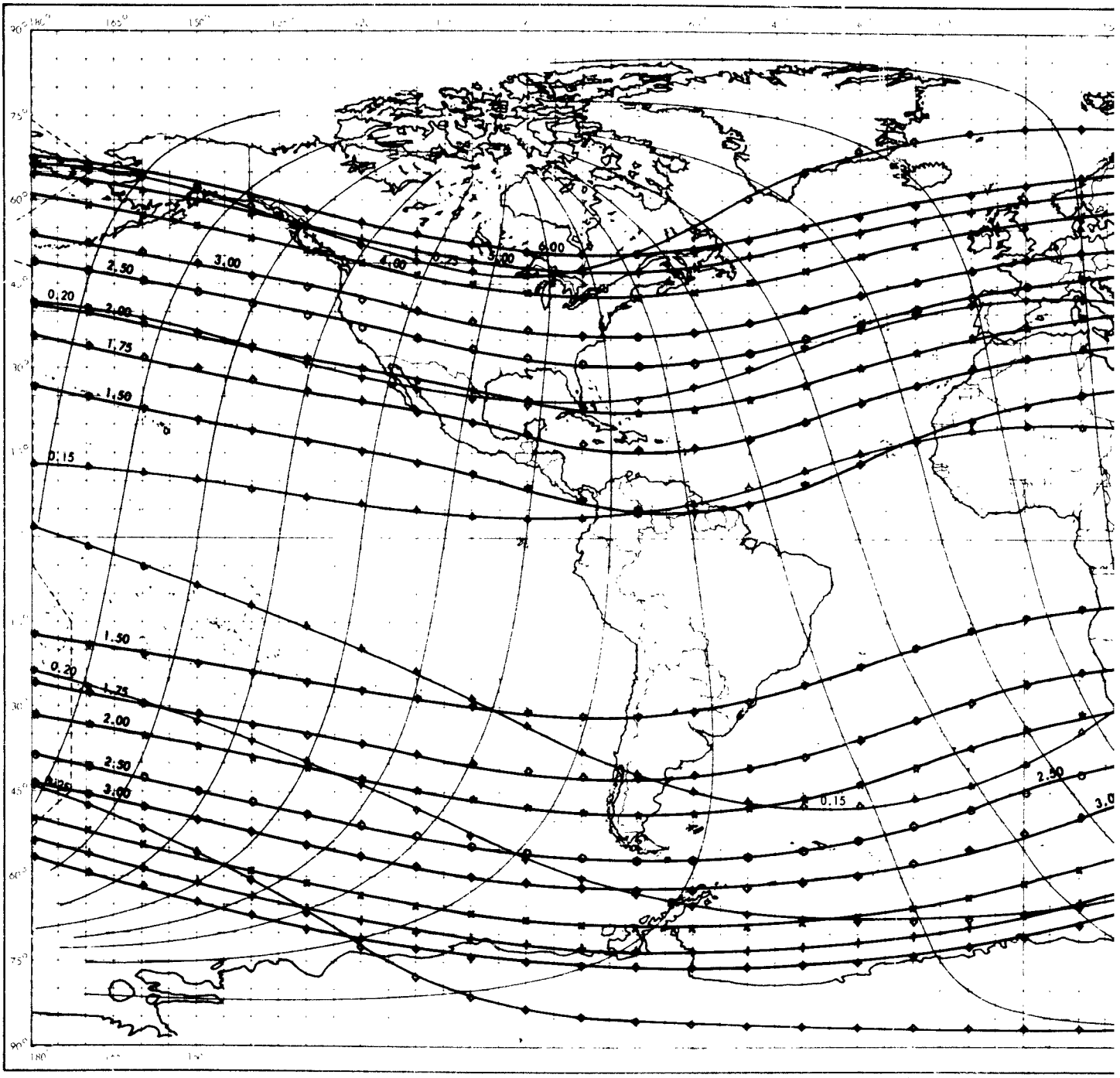

Figure 16. Constant Magnetic Field Intensity, B (Gauss), and Constant Magnetic

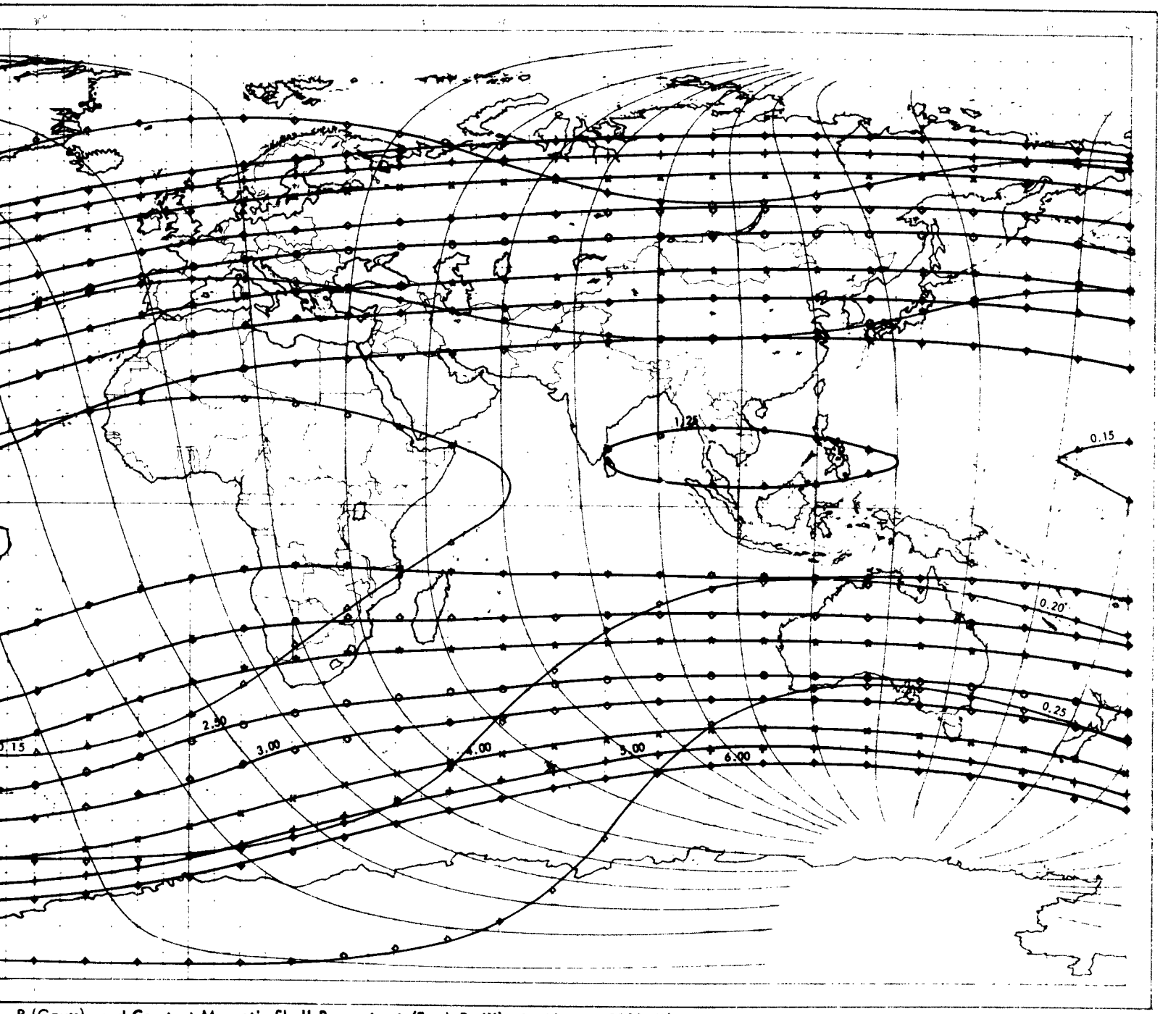

B (Gauss), and Constant Magnetic Shell Parameter L (Earth Radii), At Altitude 2000 Kilometers.

B. CONTOURS OF B NEAR THE SOUTH ATLANTIC ANOMALY

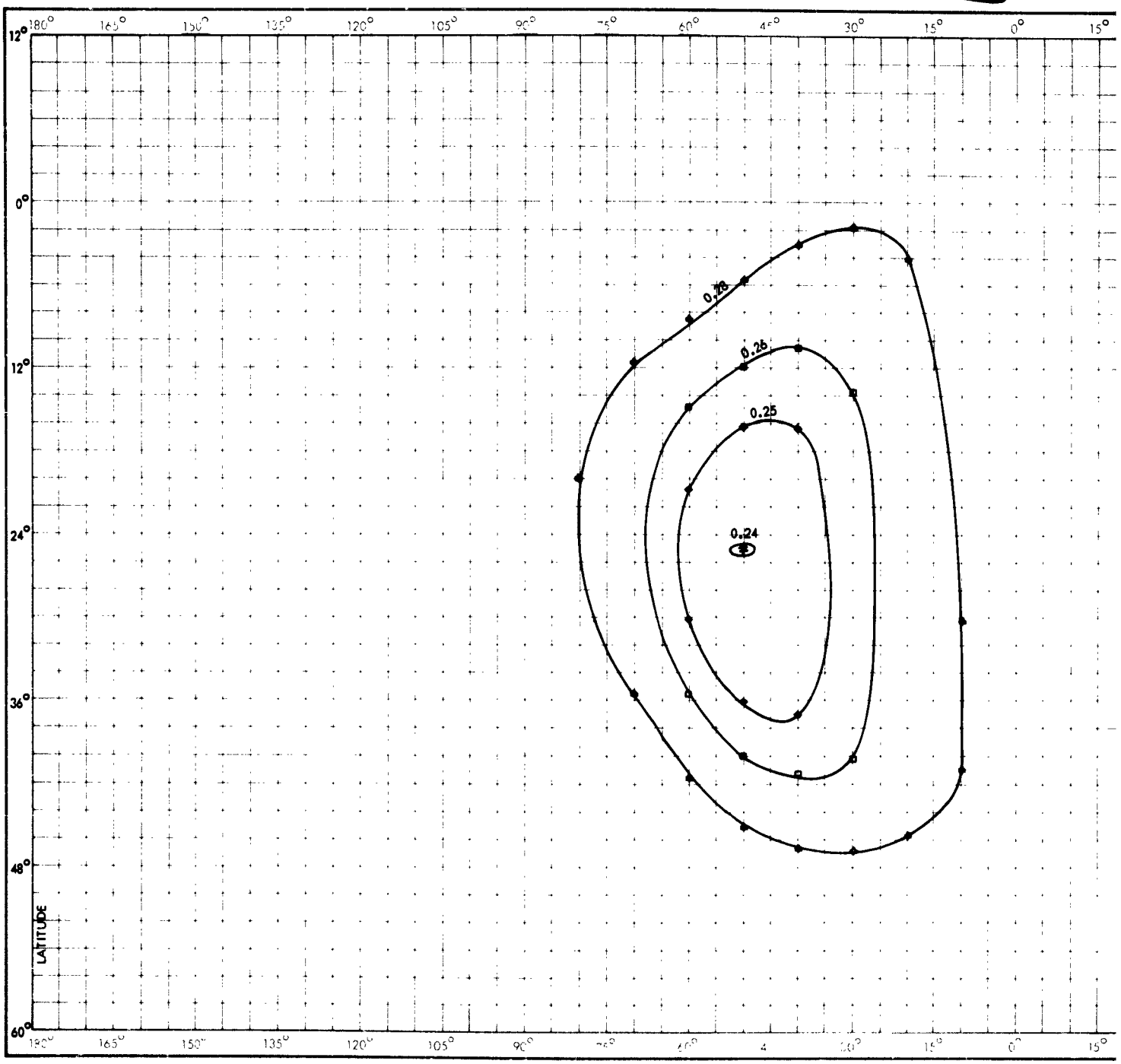

Figure 17. Constant Magnetic Field Intensity, B (Gauss), in the Region of th

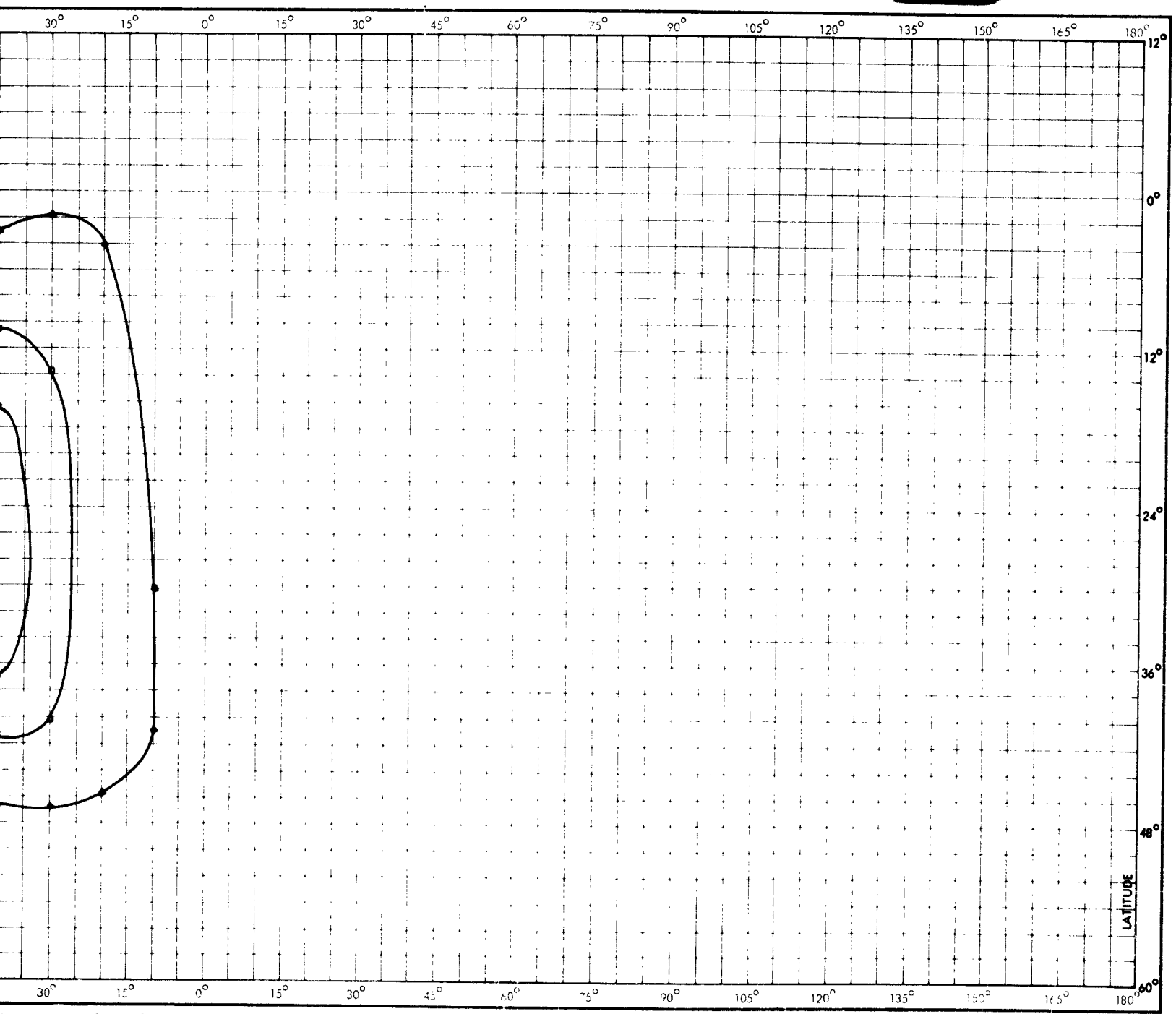

Intensity, B (Gauss), in the Region of the South Atlantic Anomaly at Altitude 0 km

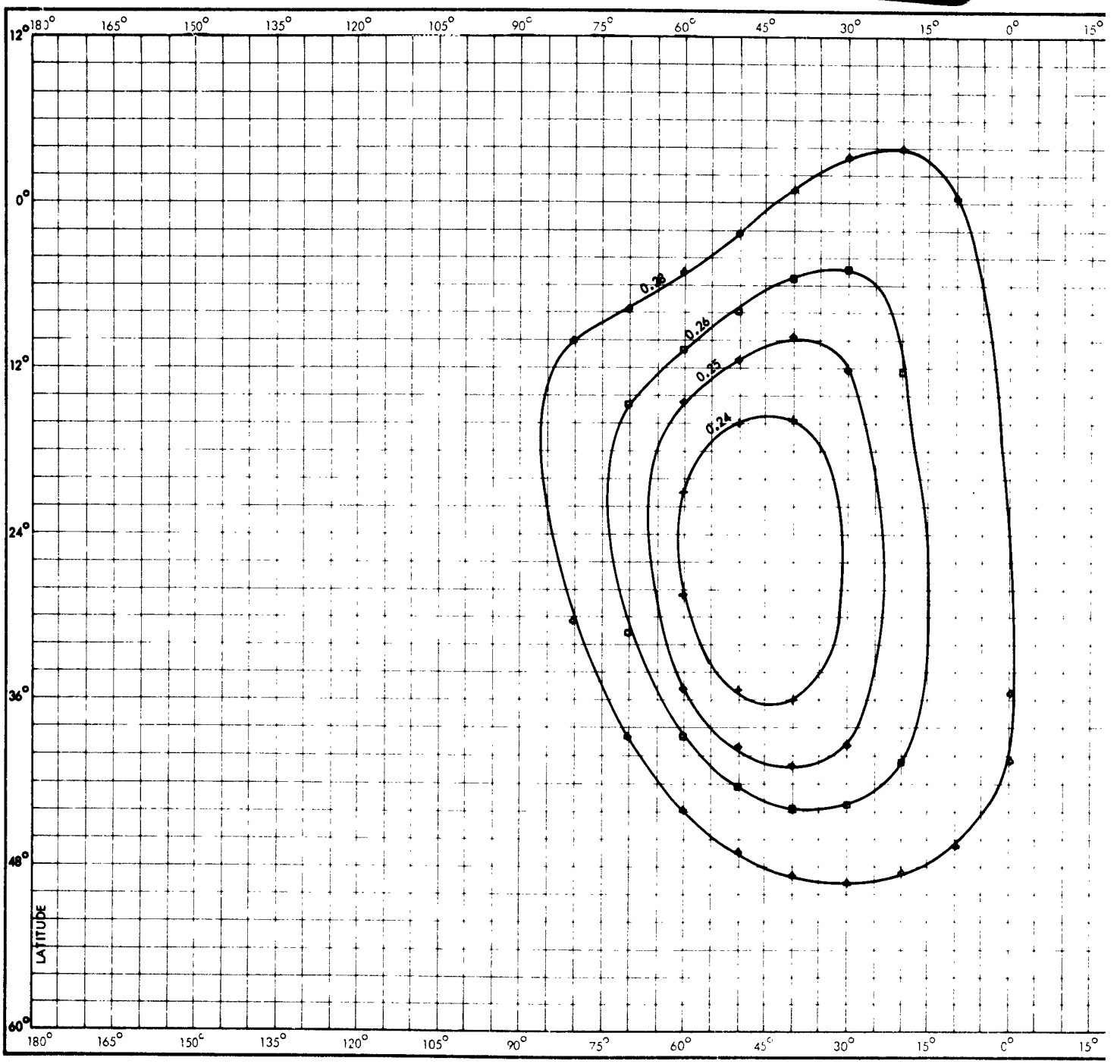

Figure 18. Constant Magnetic Field Intensity, B (Gauss), in the Region of the

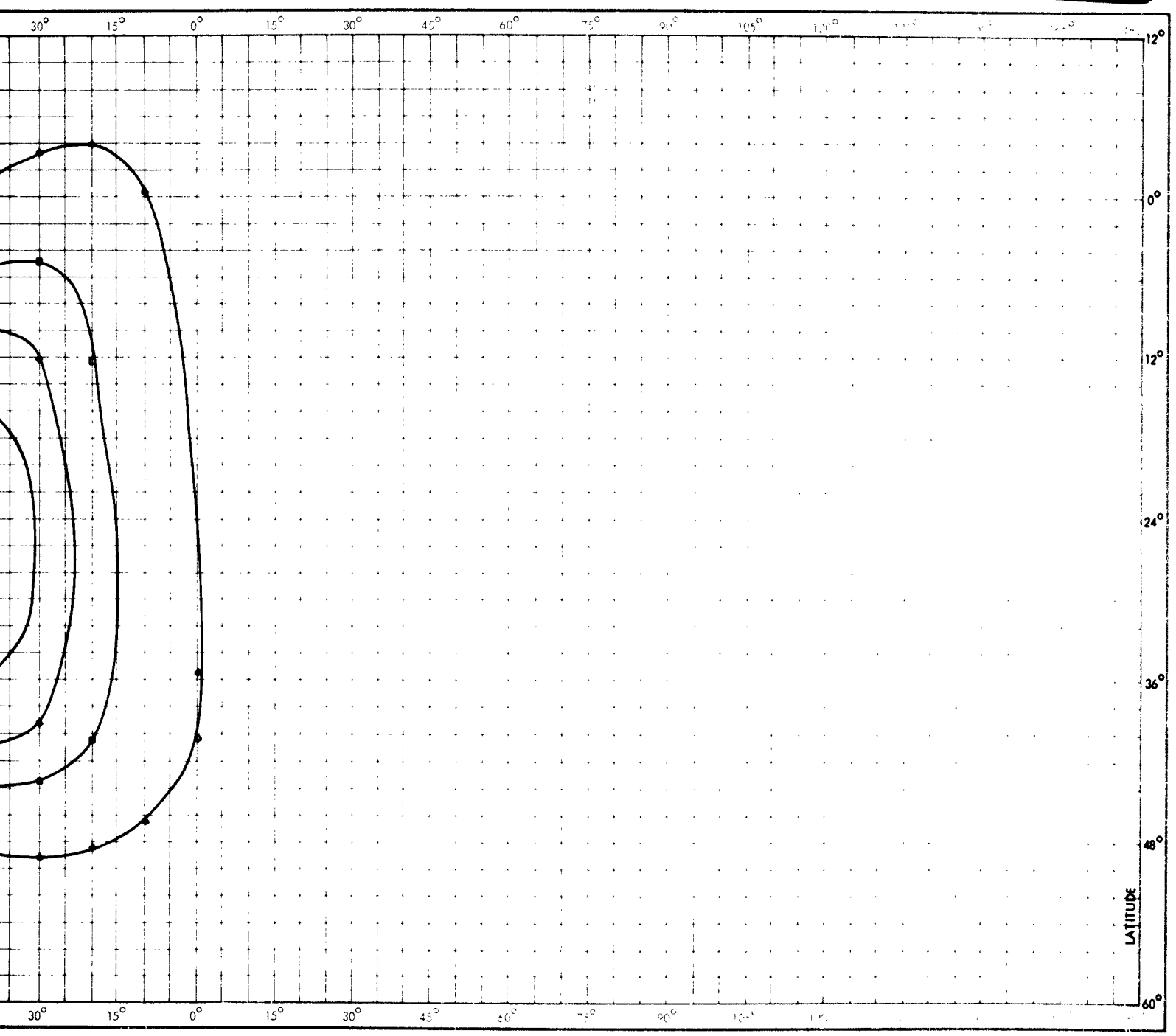

nsity, B (Gauss), in the Region of the South Atlantic Anomaly at Altitude 100 km

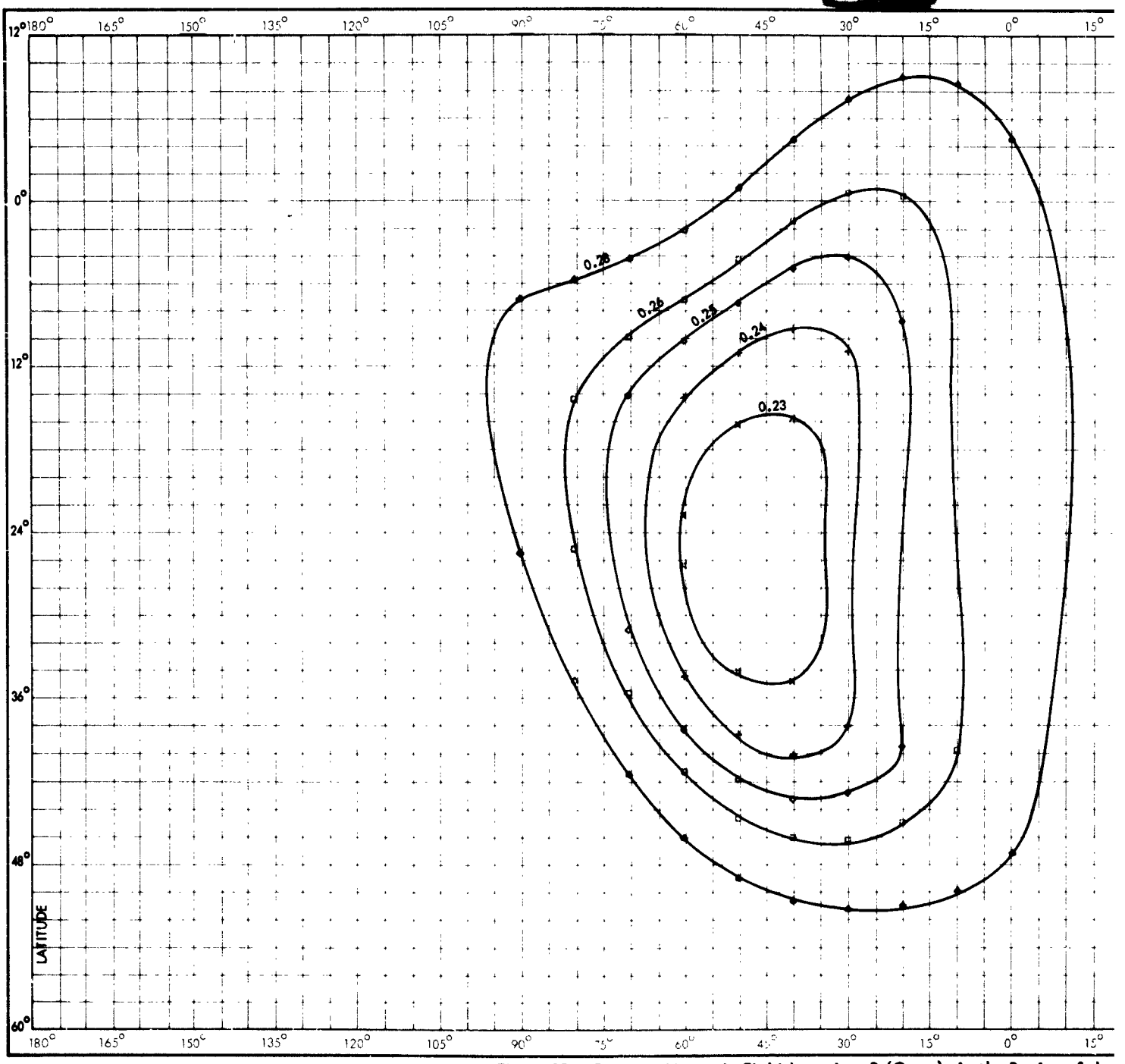

Figure 19. Constant Magnetic Field Intensity, B (Gauss), in the Region of the

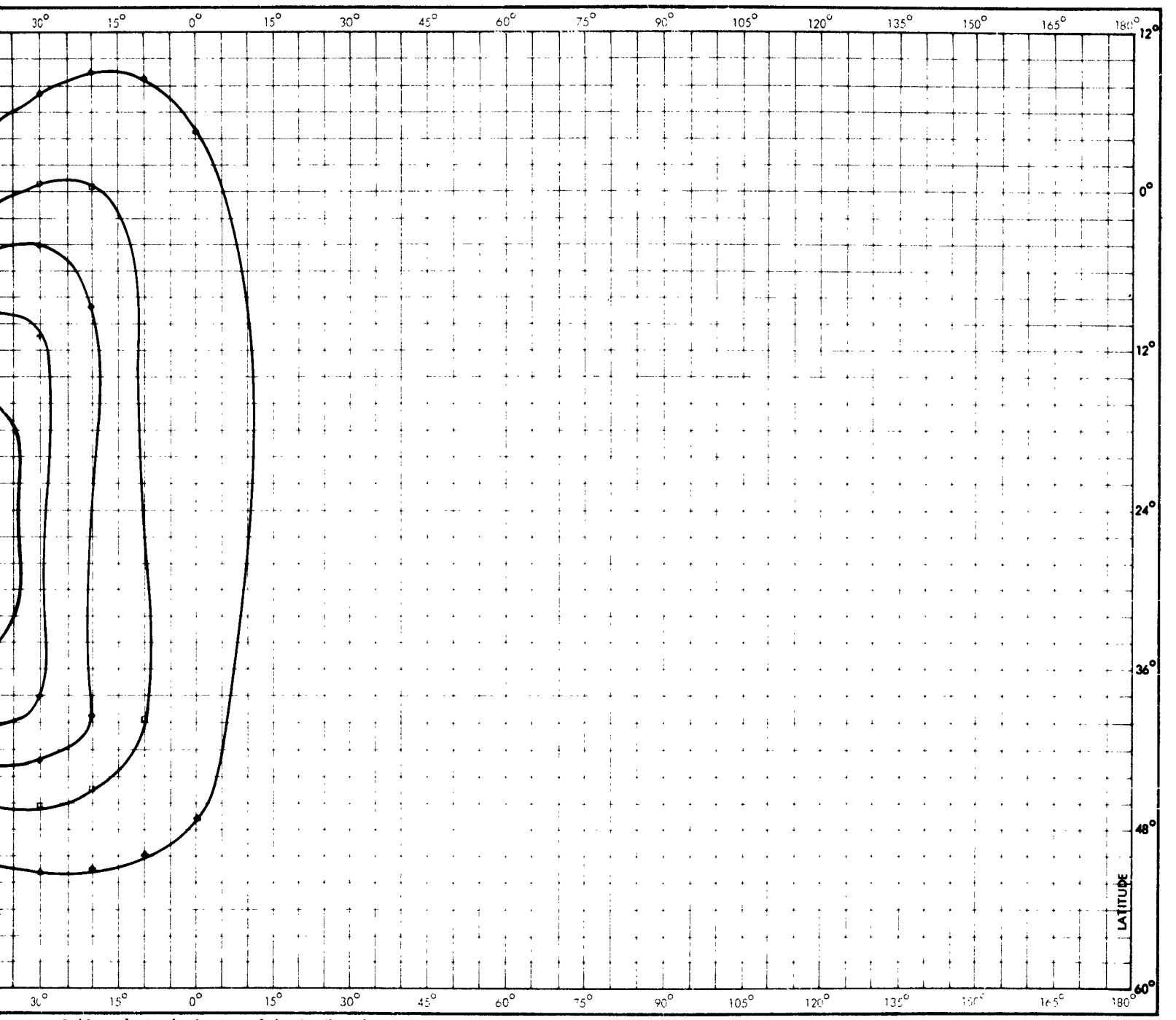

ensity, B (Gauss), in the Region of the South Atlantic Anomaly at Altitude 200 km

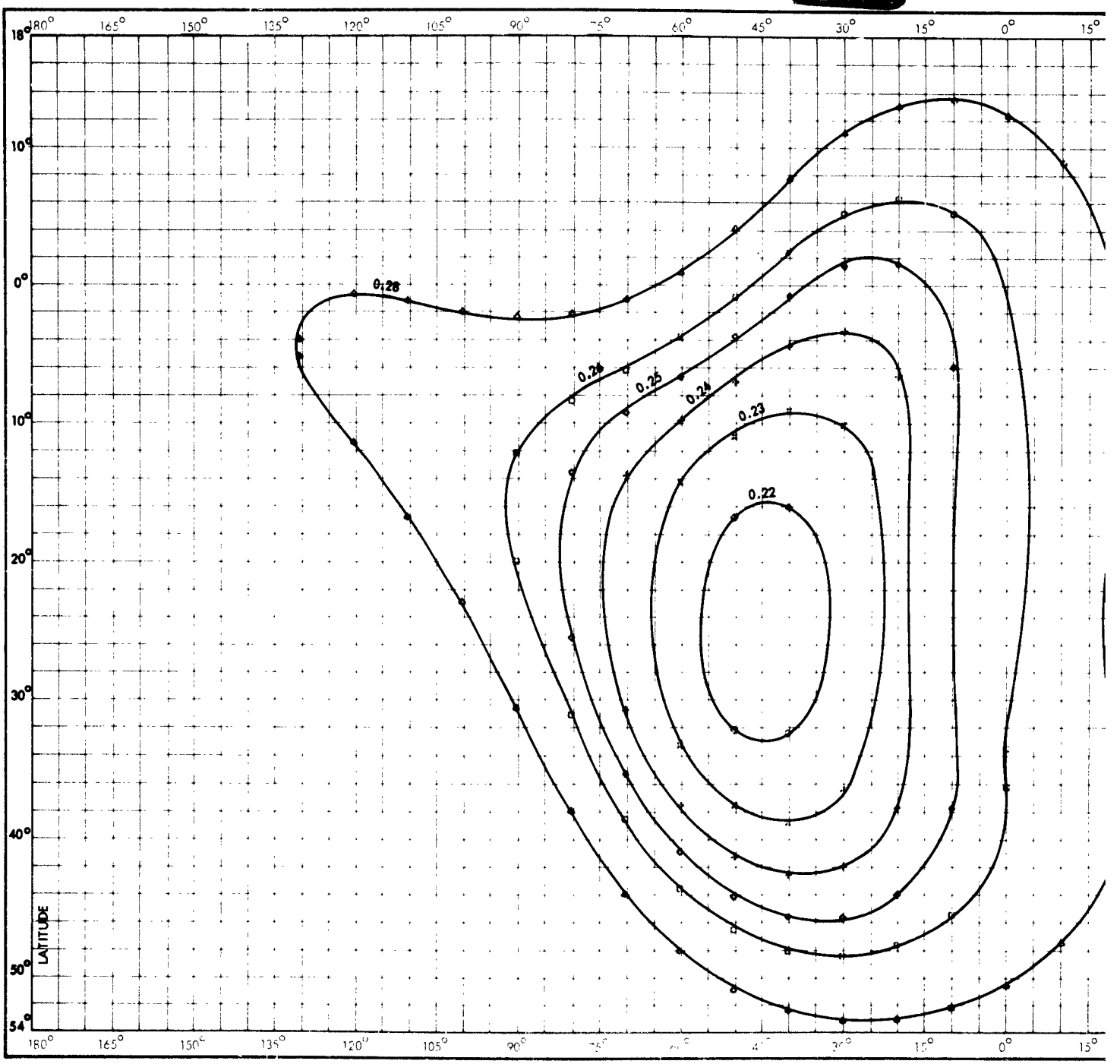

Figure 20. Constant Magnetic Field Intensity, B (Gauss), in the Region of th

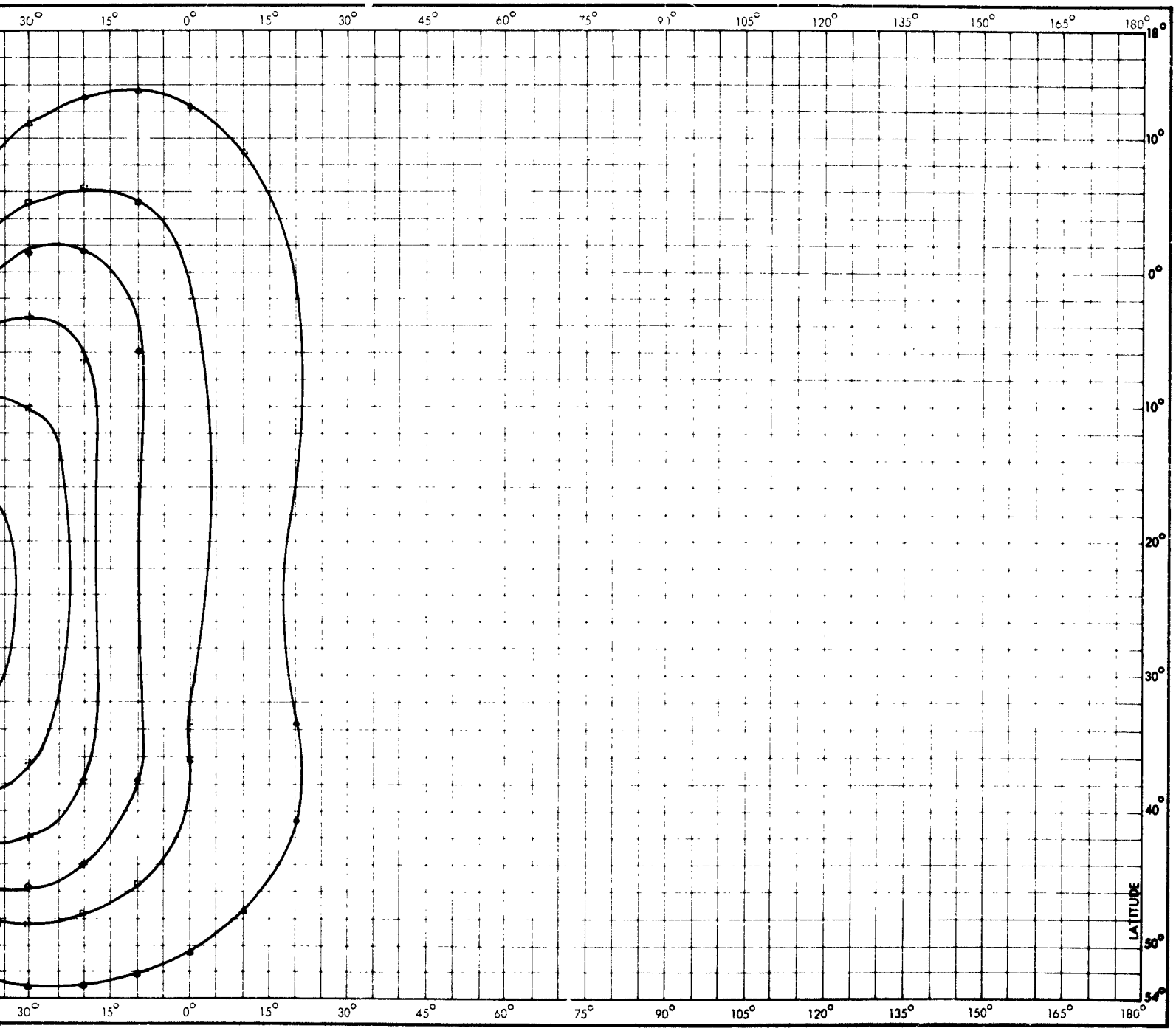

nsity, B (Gauss), in the Region of the South Atlantic Anomaly at Altitude 300 km

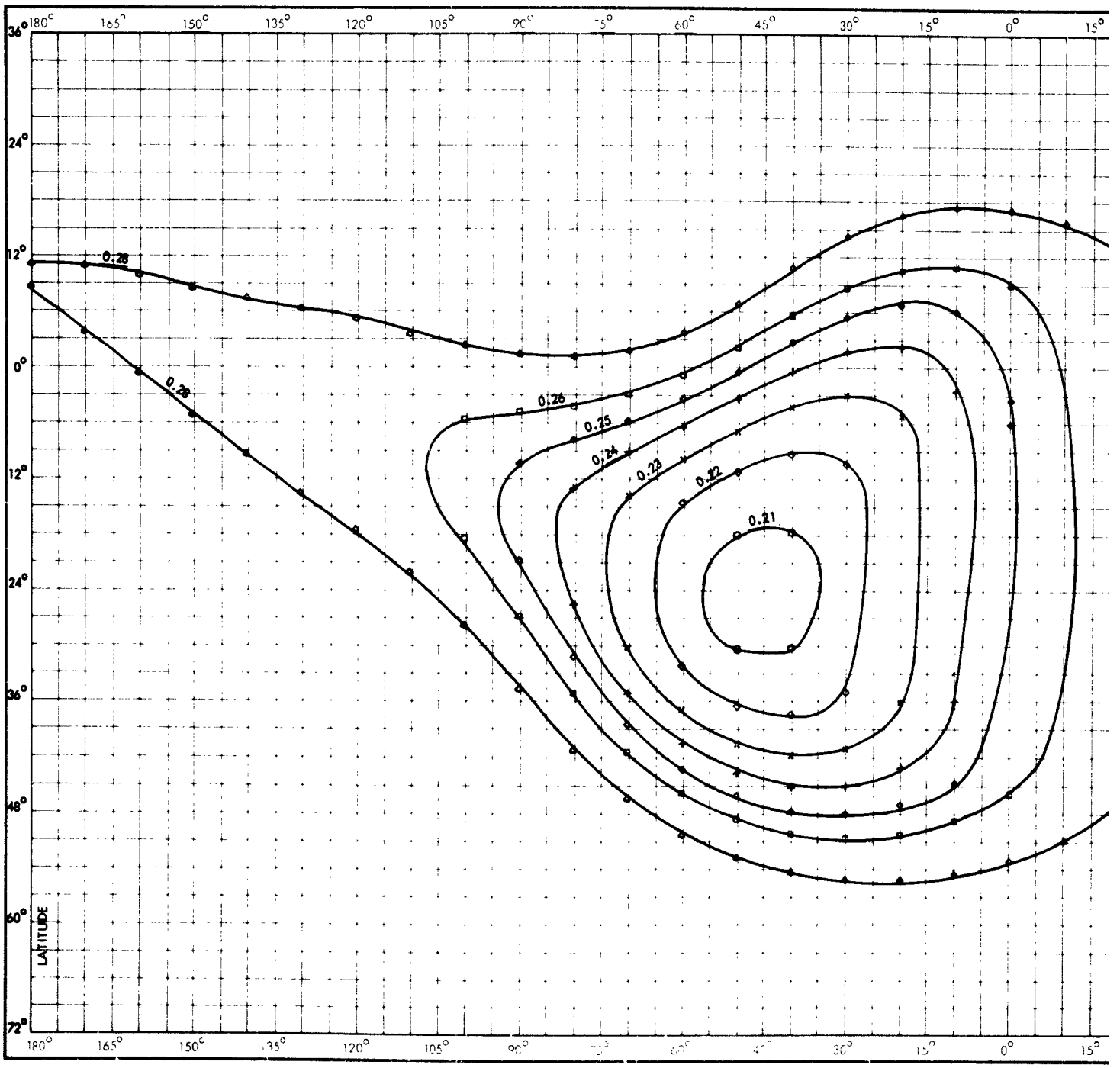

Figure 21. Constant Magnetic Field Intensity, B (Gauss), in the Region of the

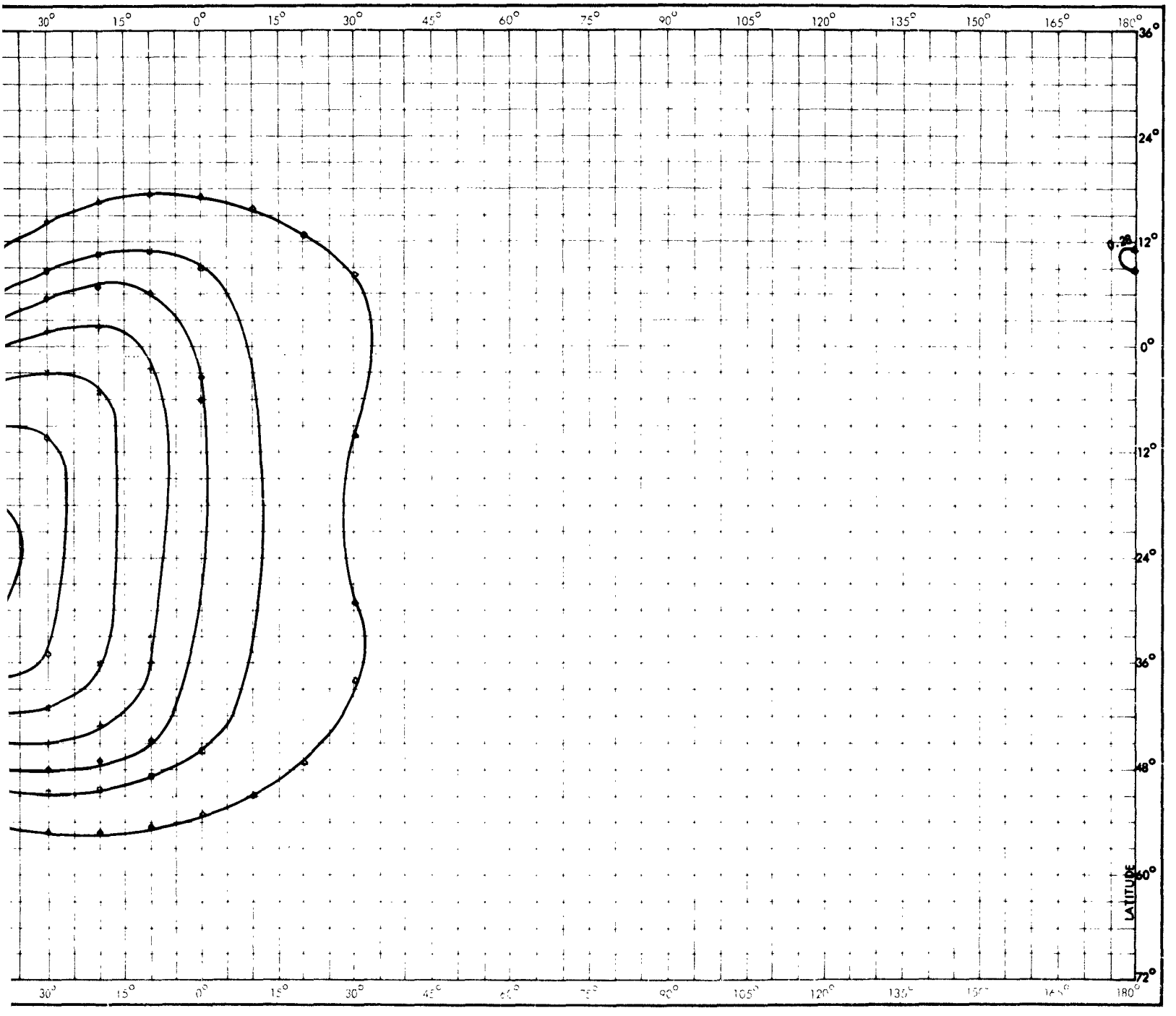

ensity, B (Gauss), in the Region of the South Atlantic Anomaly at Altitude 400 Kilometers.

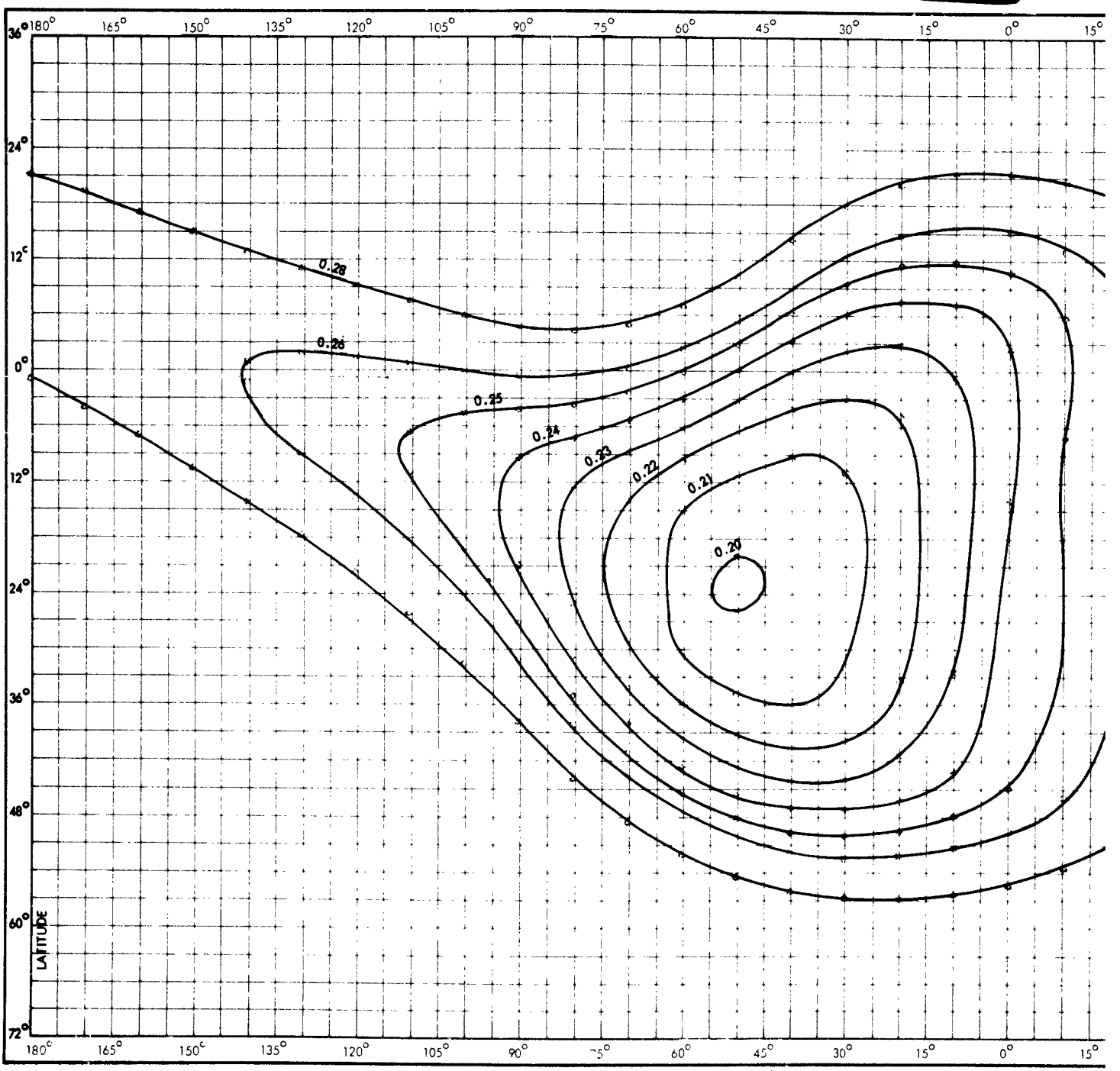

Figure 22. Constant Magnetic Field Intensity, B (Gauss), in the Region of th

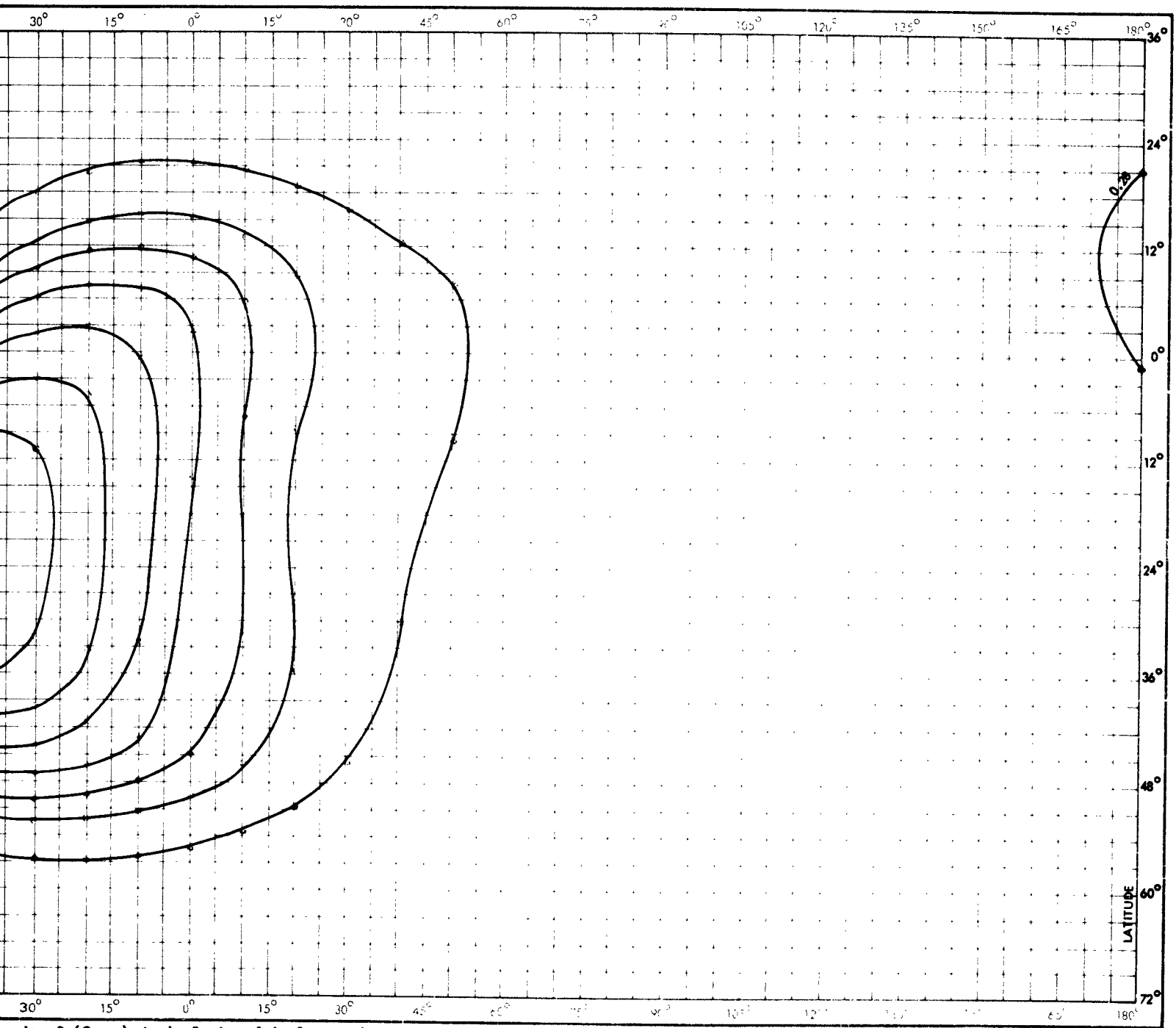

ensity, B (Gauss), in the Region of the South Atlantic Anomaly at Altitude 500 Kilometers.

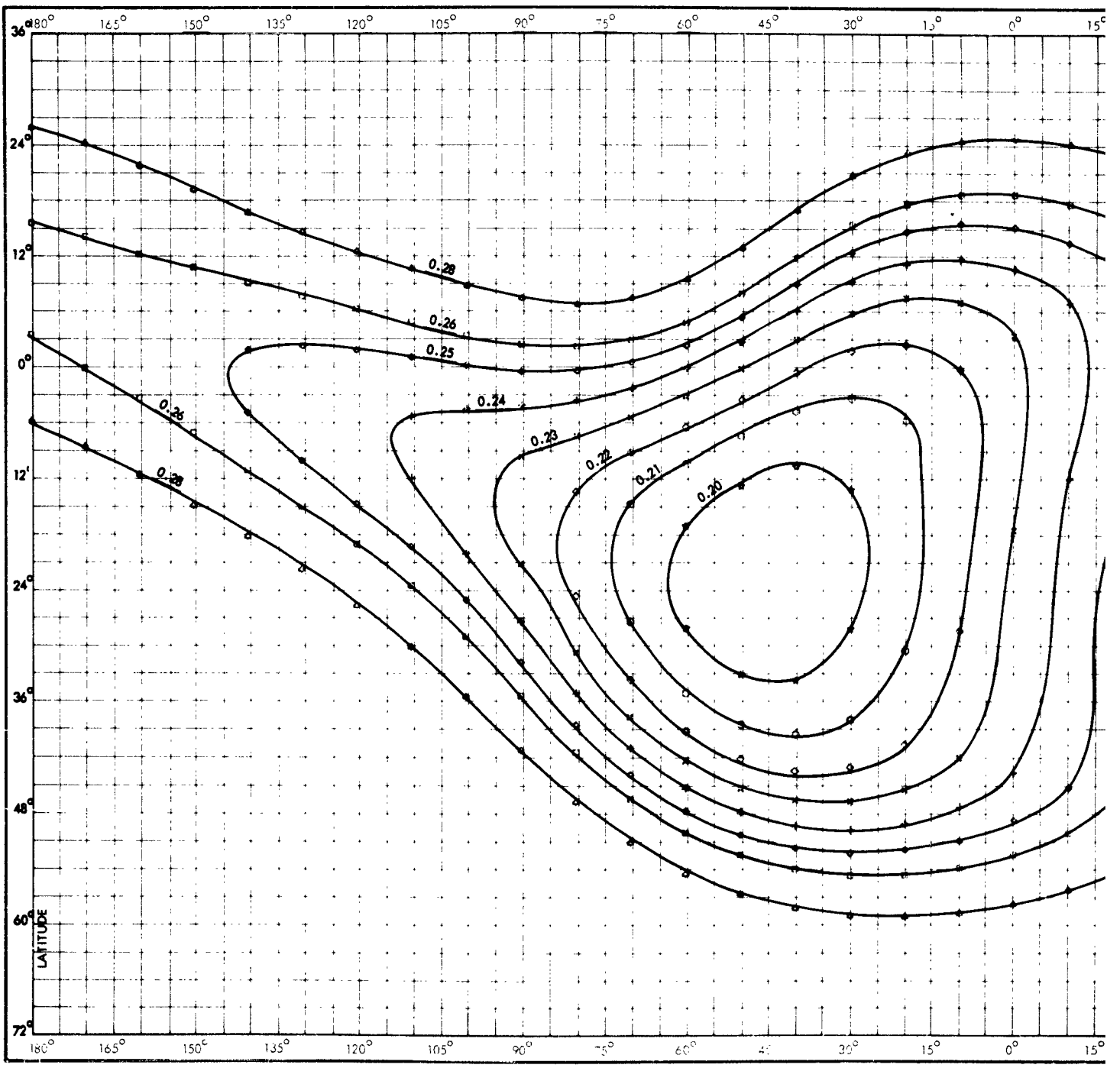

Figure 23. Constant Magnetic Field Intensity, B (Gauss), in the Region of th

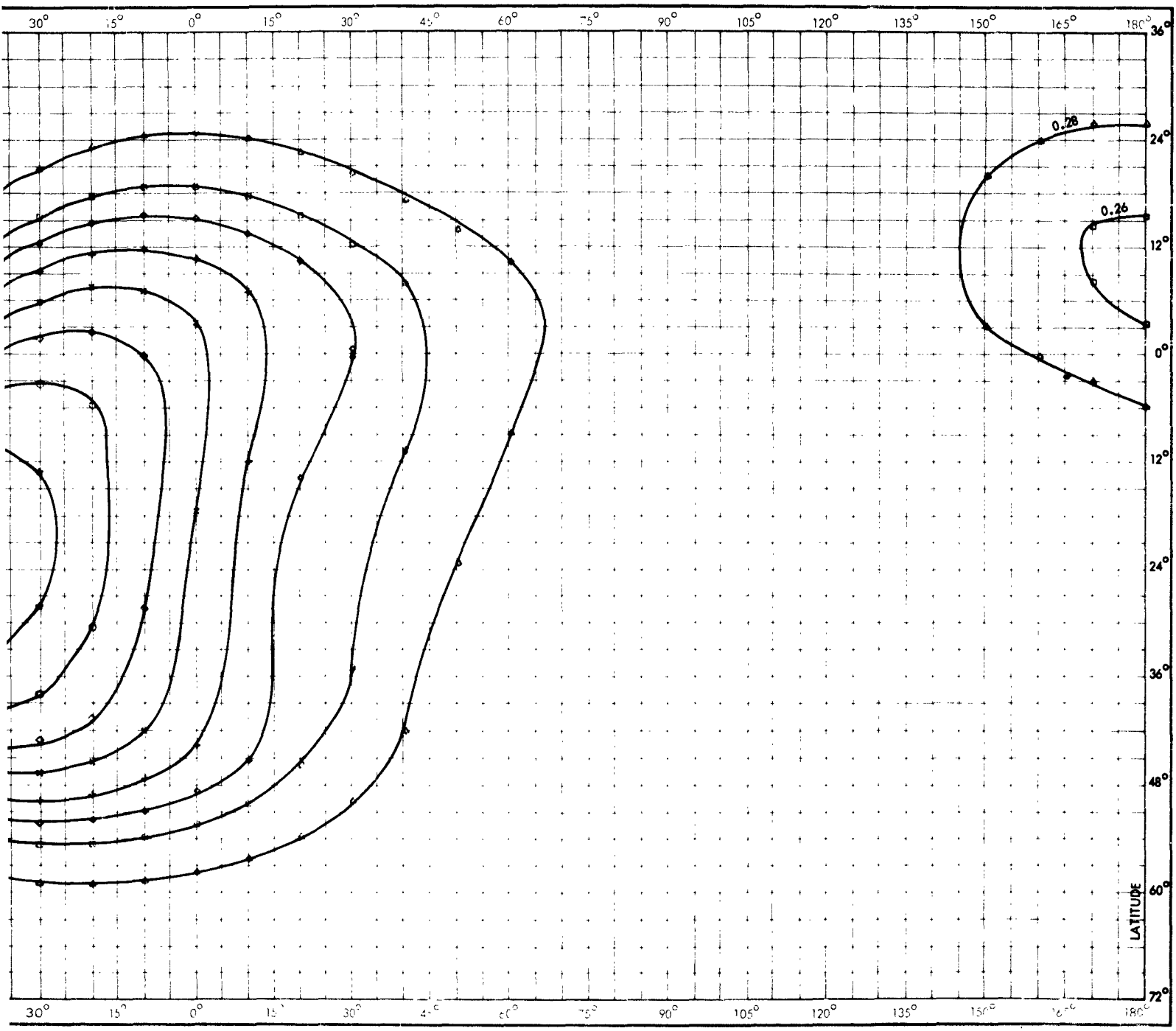

ɲsity, B (Gauss), in the Region of the South Atlantic Anomaly at Altitude 600 Kilometers.
)

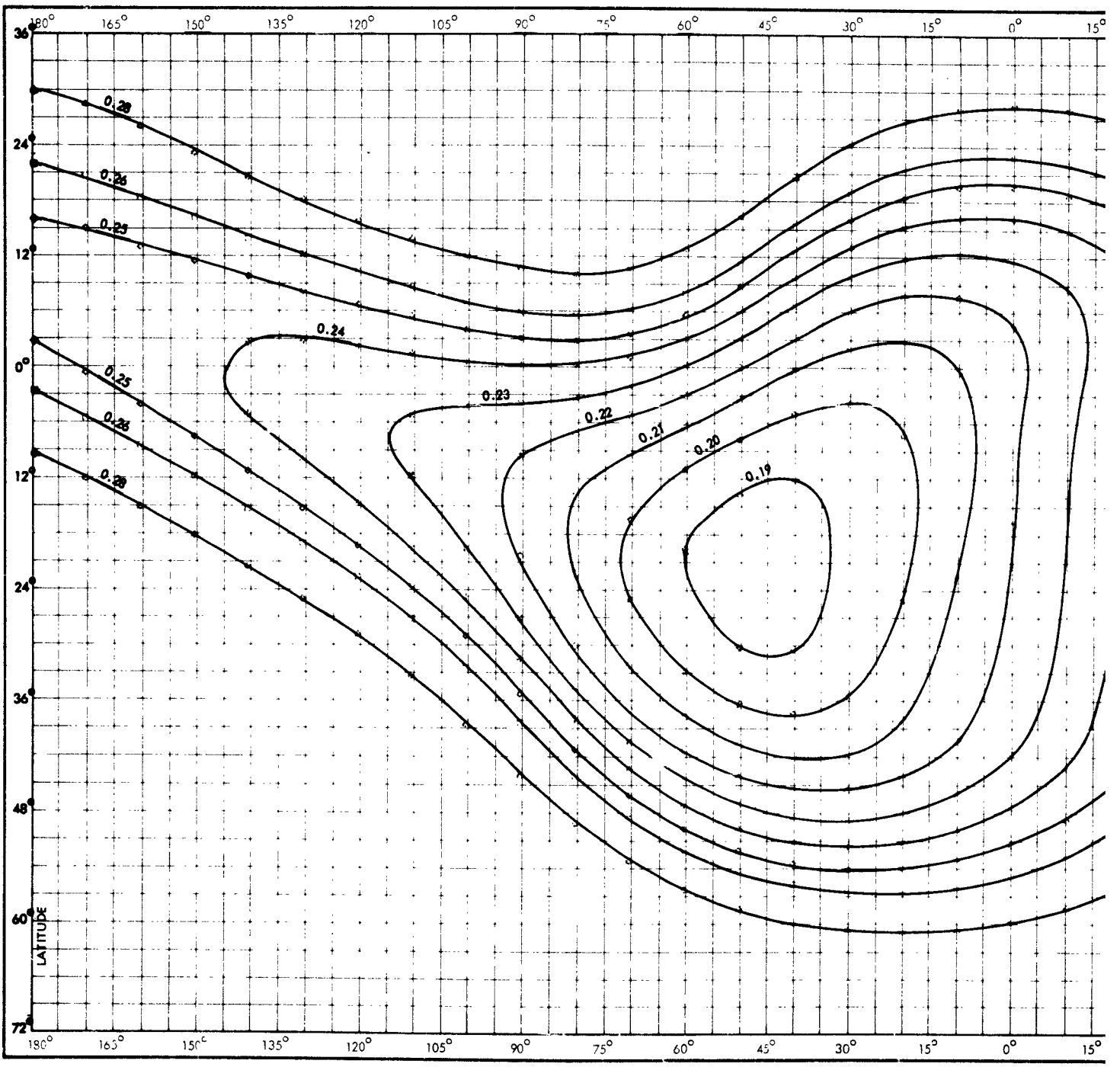

Figure 24. Constant Magnetic Field Intensity, B (Gauss), in the Region of th

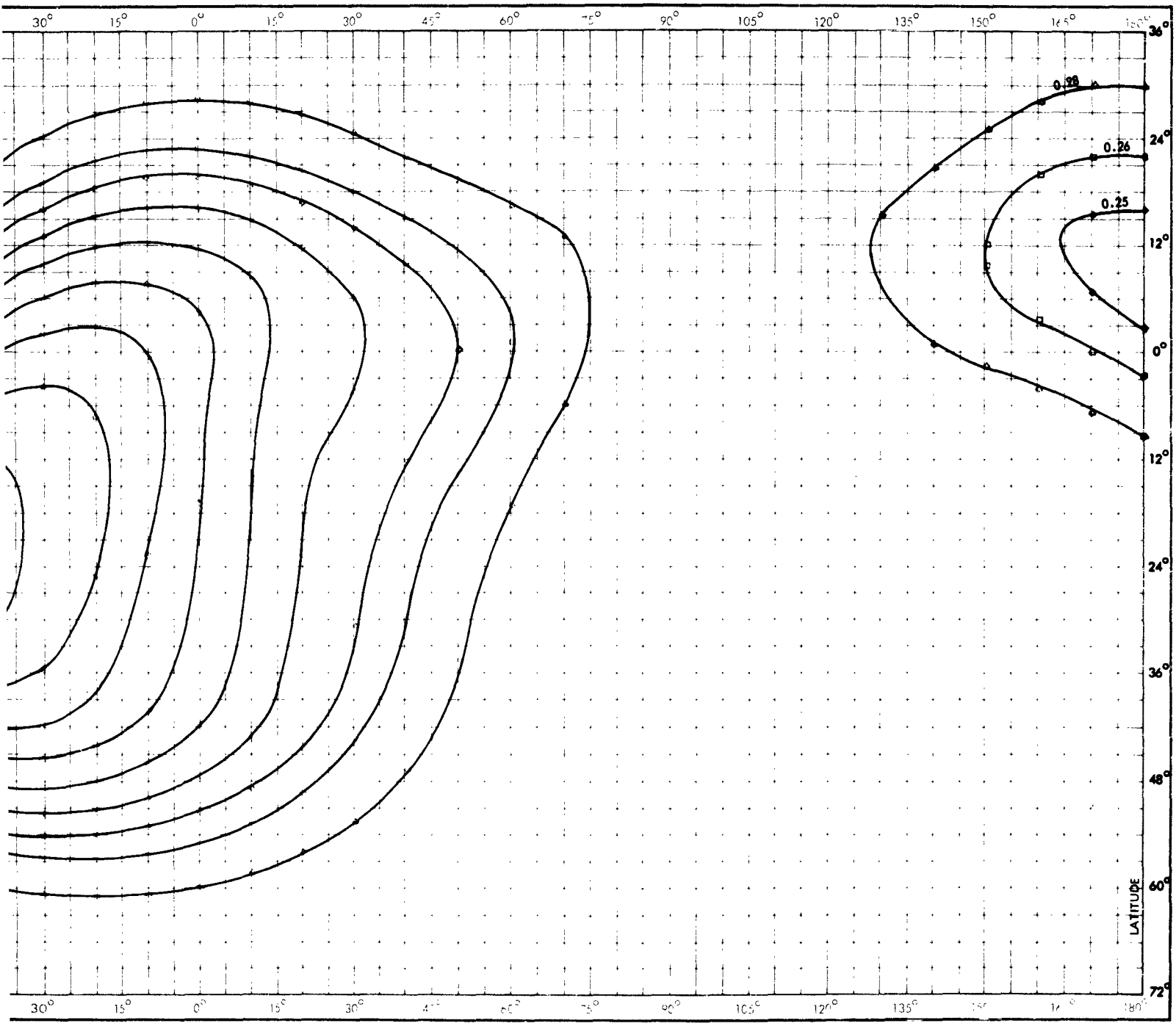

tensity, B (Gauss), in the Region of the South Atlantic Anomaly at Altitude 700 Kilometers.

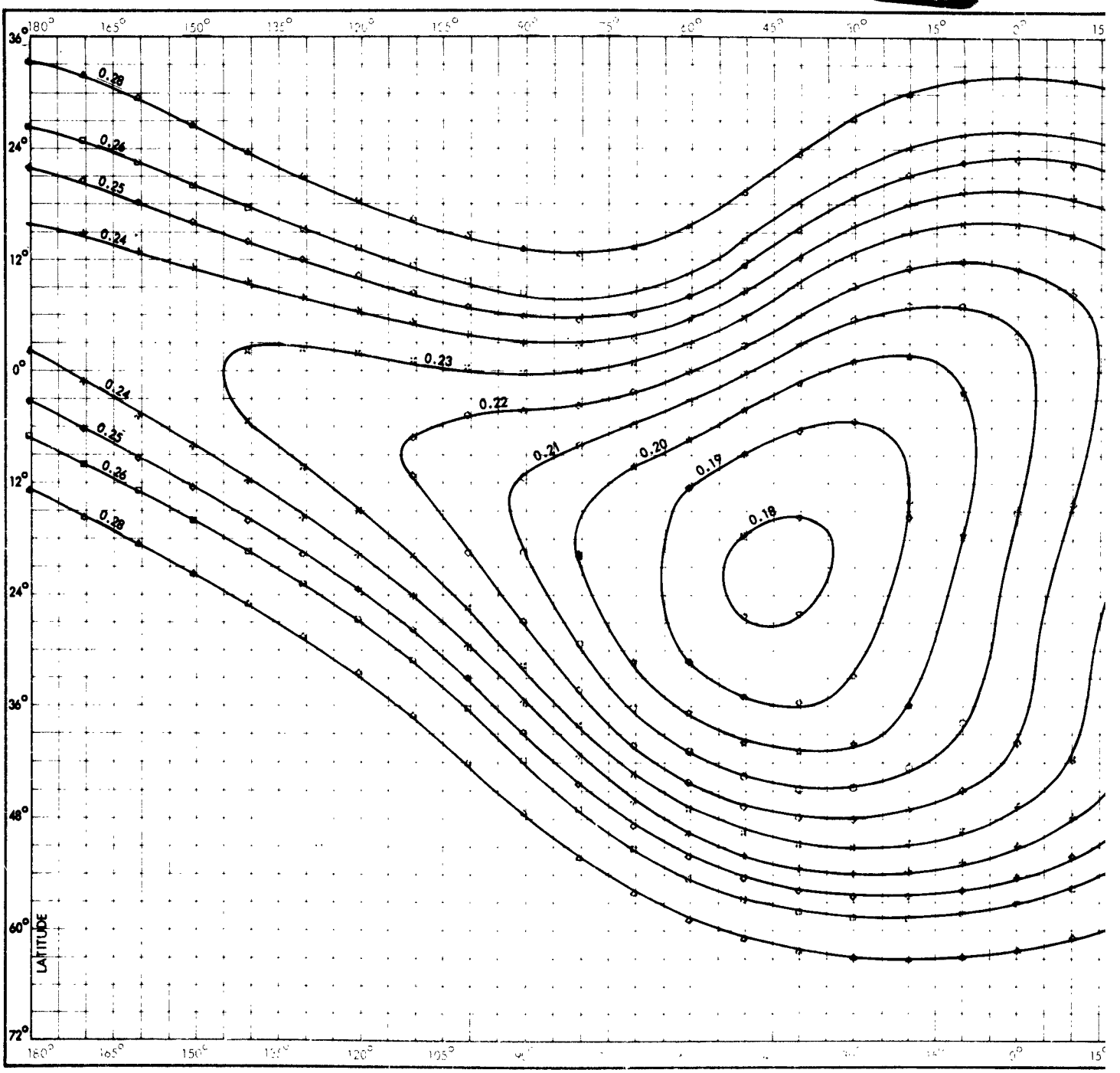

Figure 25. Constant Magnetic Field Intensity, B (Gauss), in the Region of

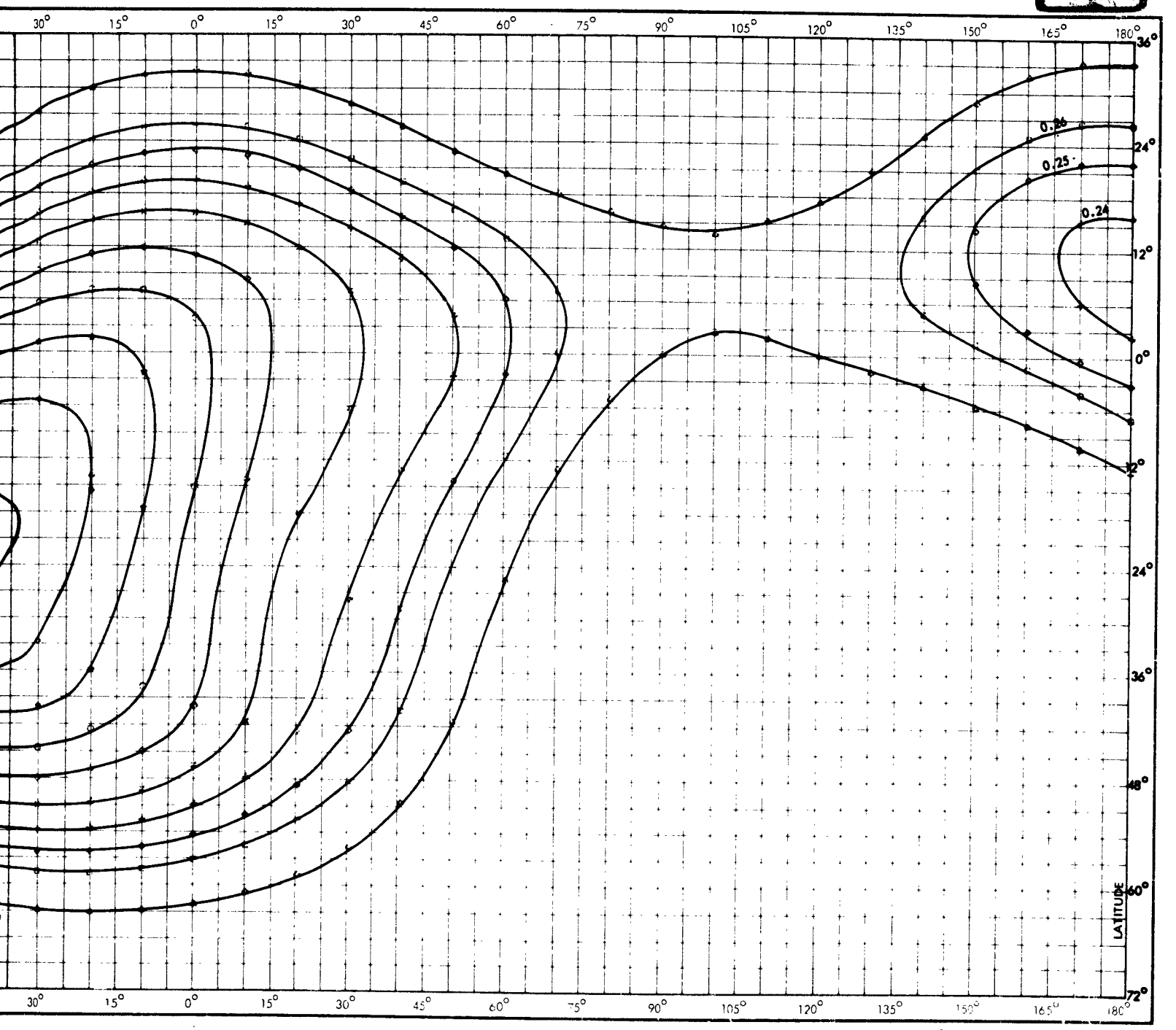

ensity, B (Gauss), in the Region of the South Atlantic Anomaly at Altitude 800 Kilometers.

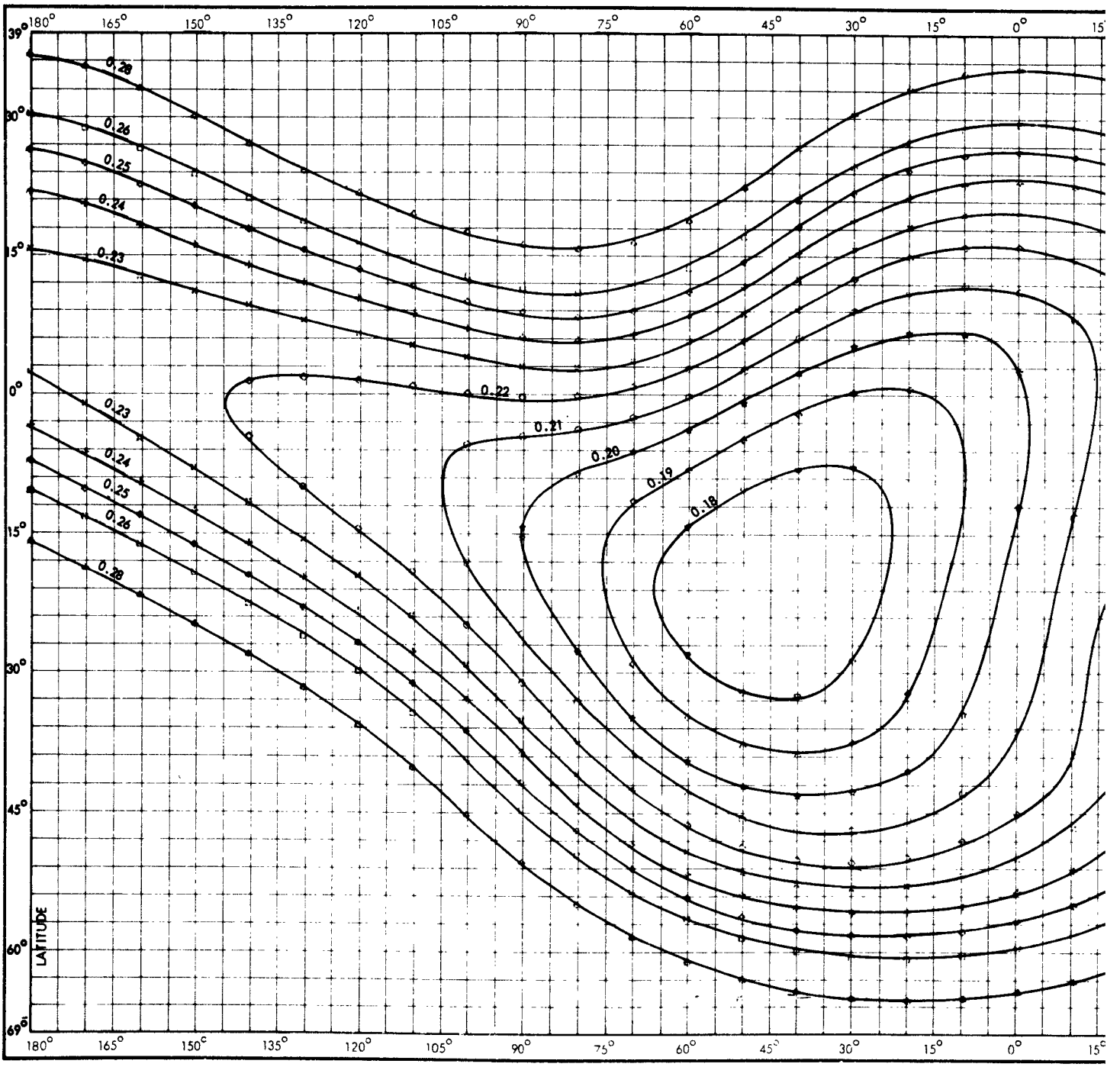

Figure 26. Constant Magnetic Field Intensity, B (Gauss), in the Region of th

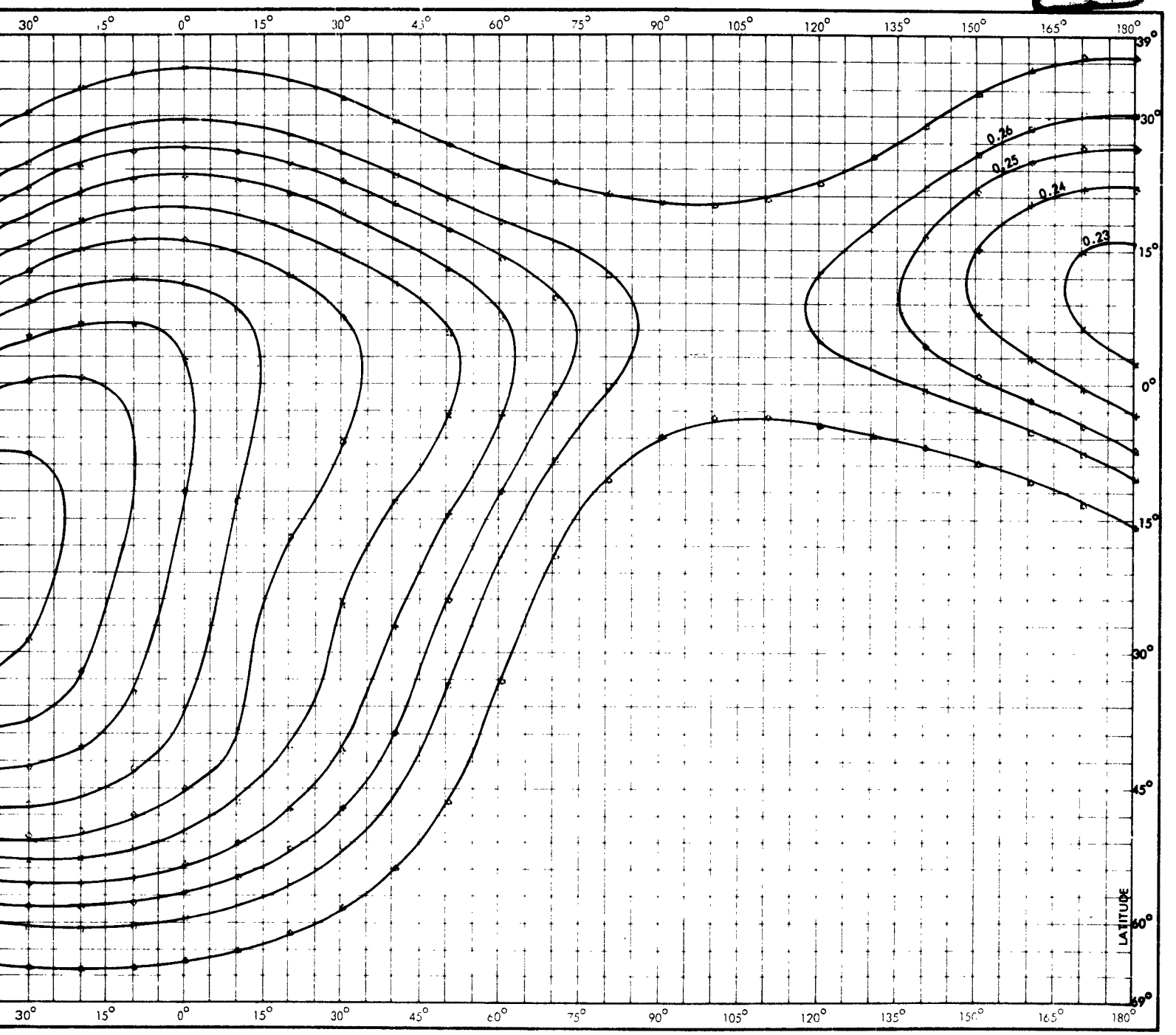

sity, B (Gauss), in the Region of the South Atlantic Anomaly at Altitude 900 Kilometers.

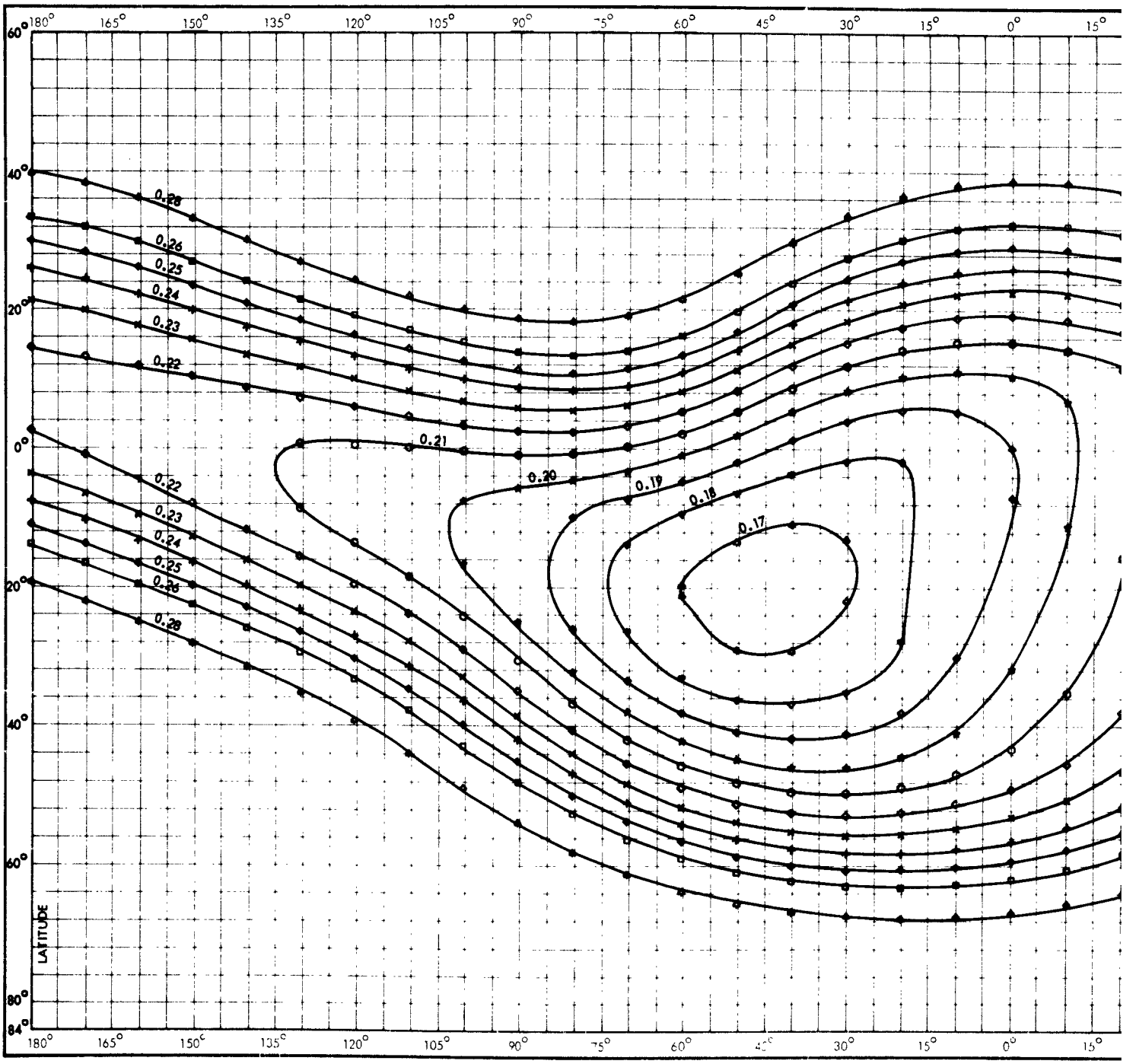

Figure 27. Constant Magnetic Field Intensity, B (Gauss), in the Region of the So

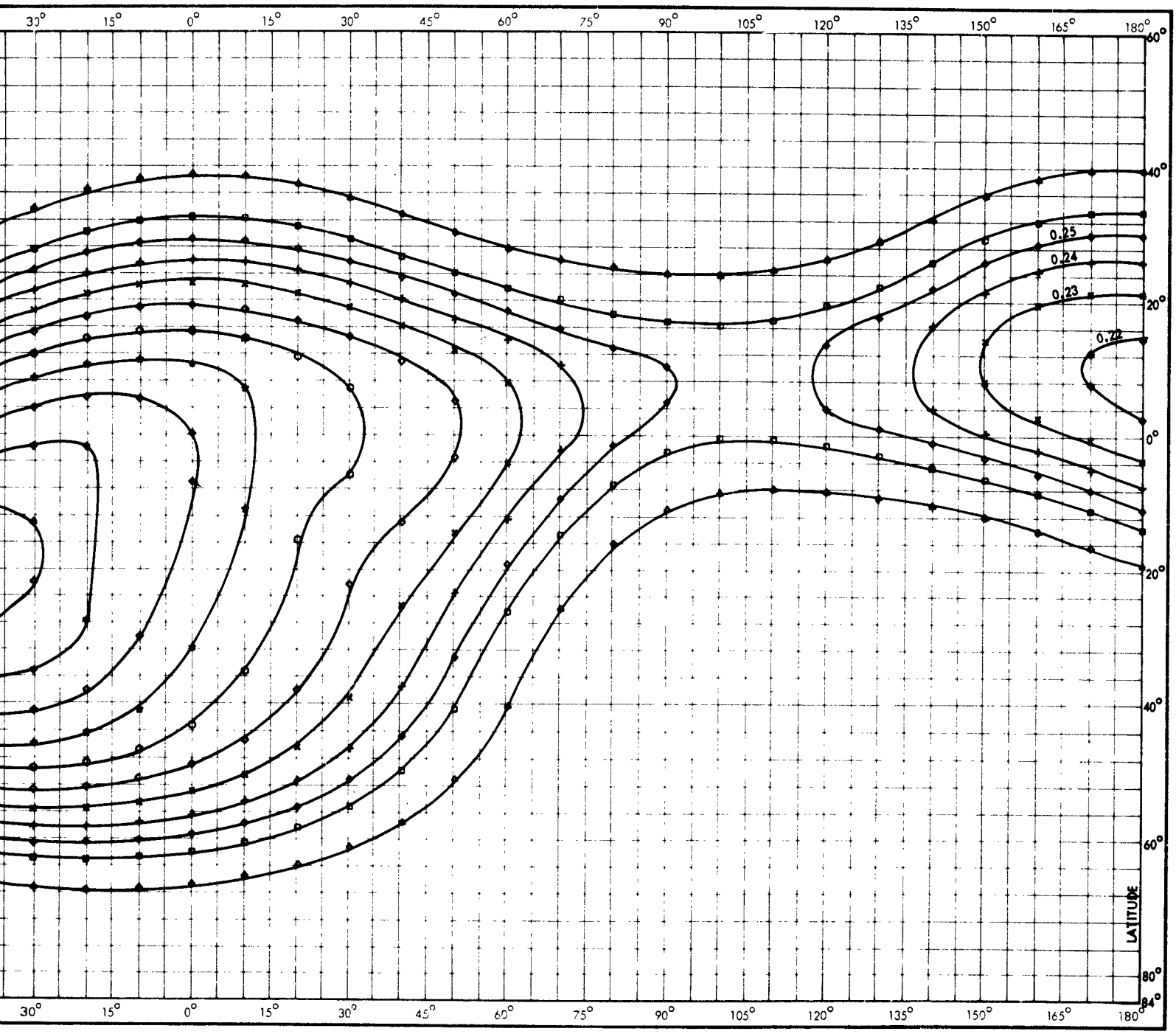

ity, B (Gauss), in the Region of the South Atlantic Anomaly at Altitude 1000 km

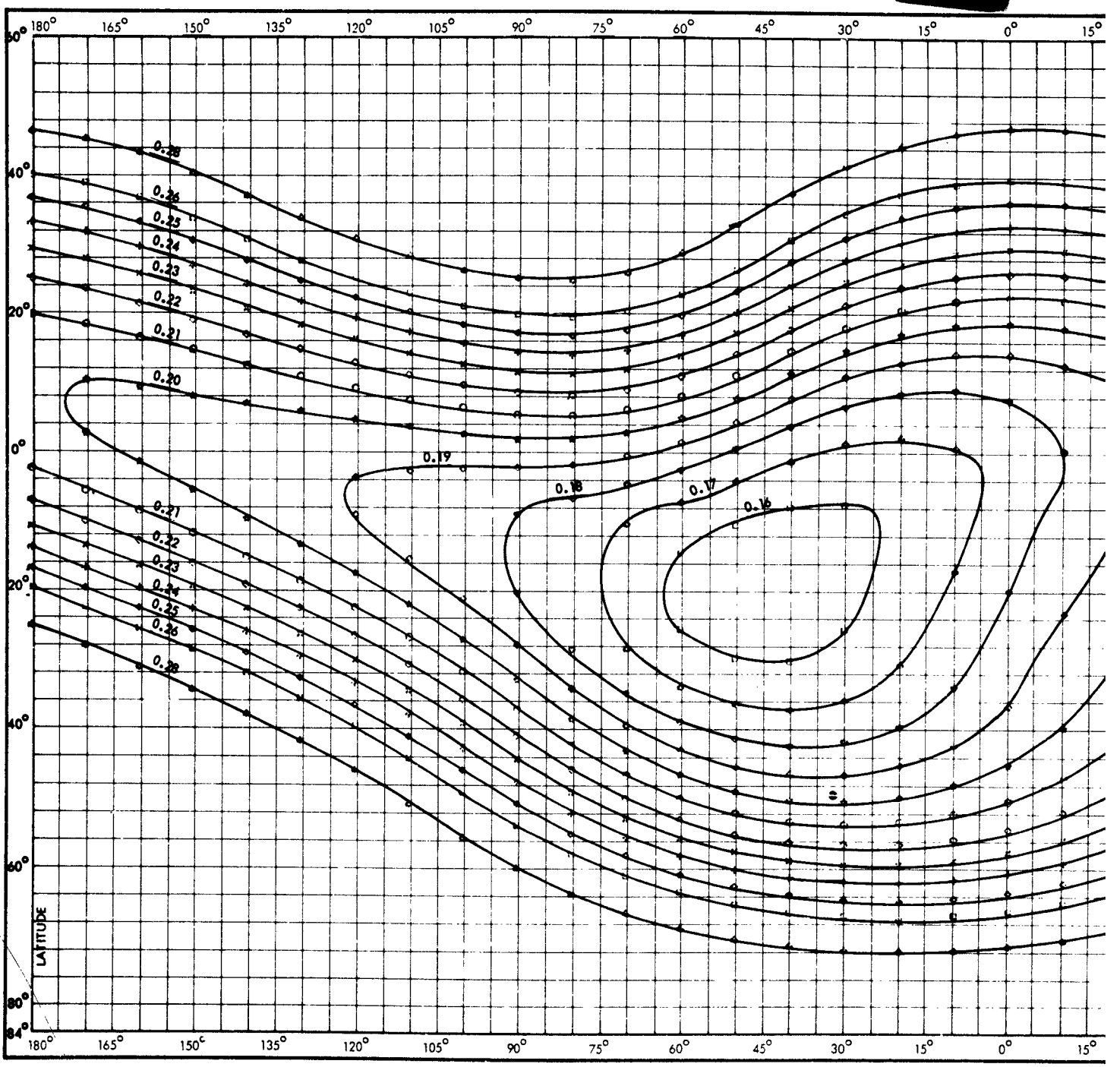

Figure 28. Constant Magnetic Field Intensity, B (Gauss), in the Region of the

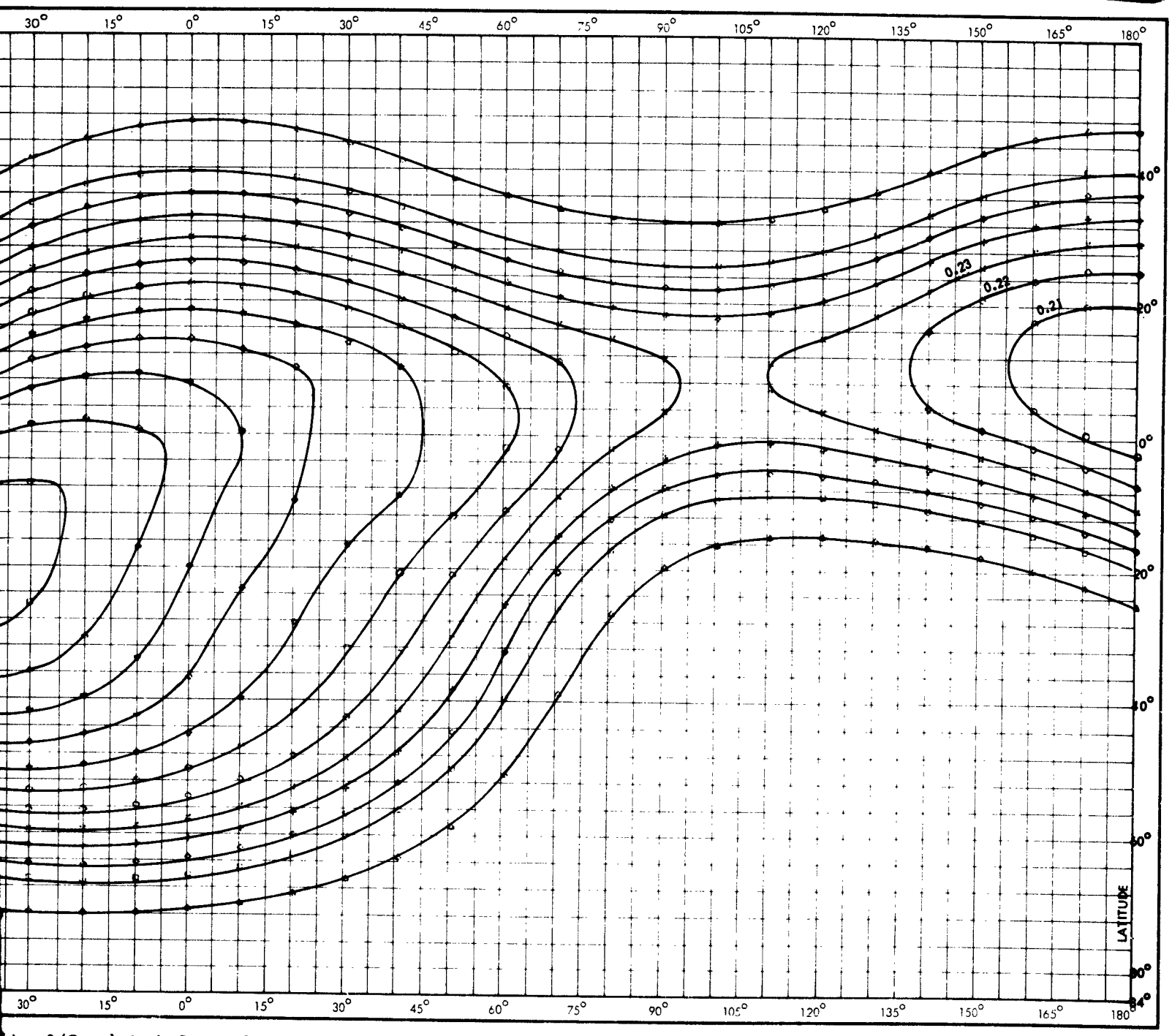

ity, B (Gauss), in the Region of the South Atlantic Anomaly at Altitude 1200 Kilometers.

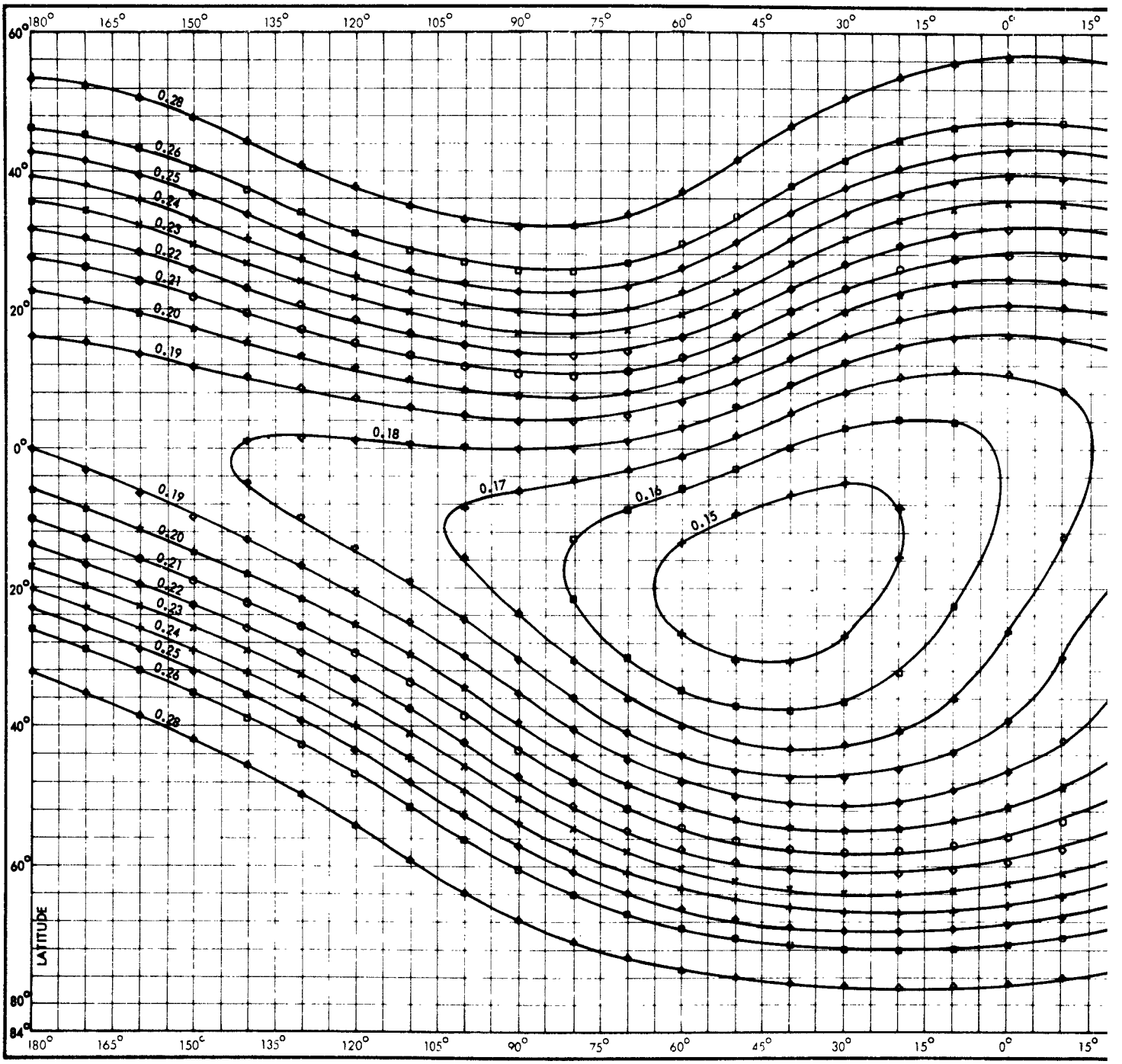

Figure 29. Constant Magnetic Field Intensity, B (Gauss), in the Region of the S

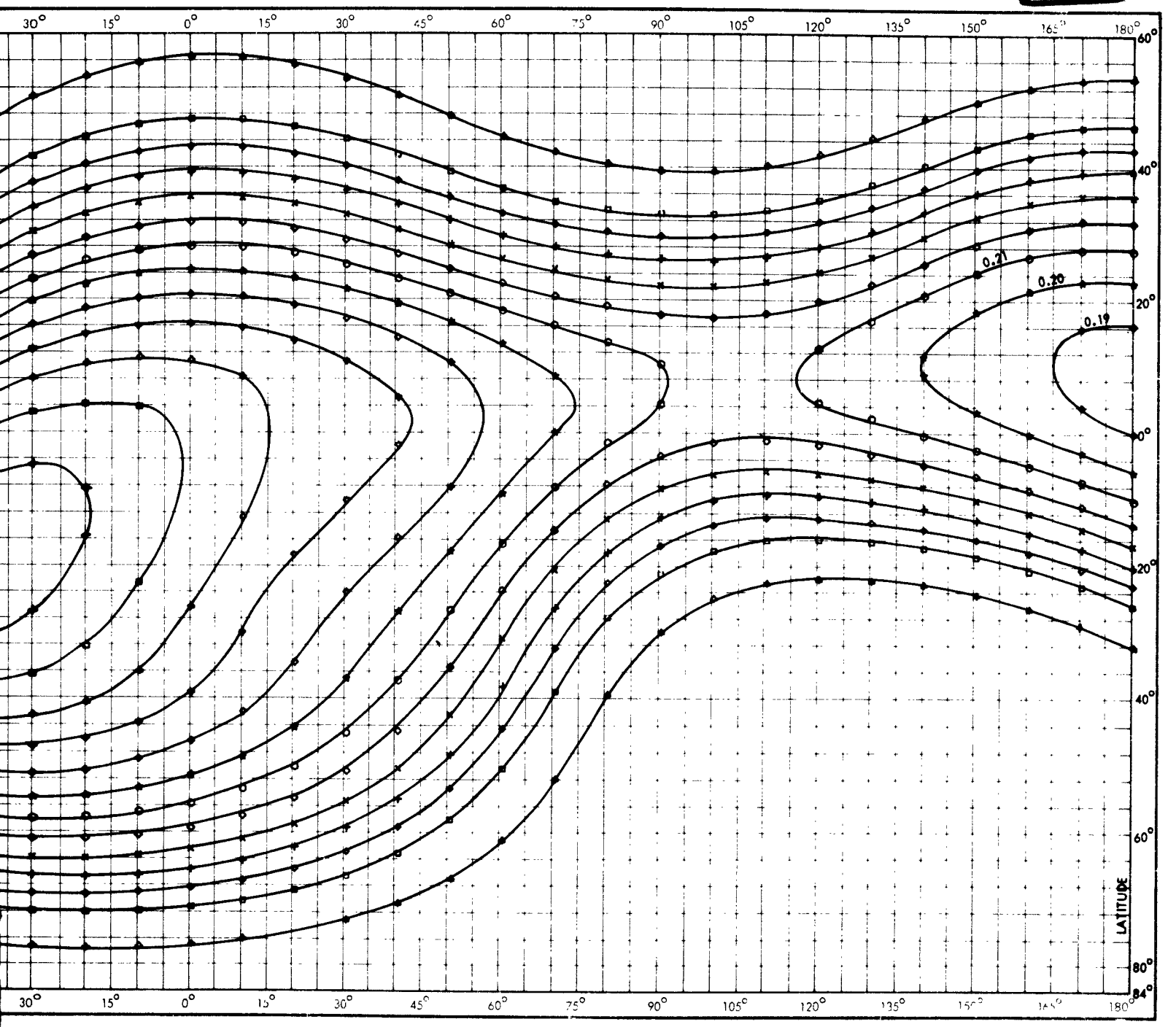

ity, B (Gauss), in the Region of the South Atlantic Anomaly at Altitude 1400 km

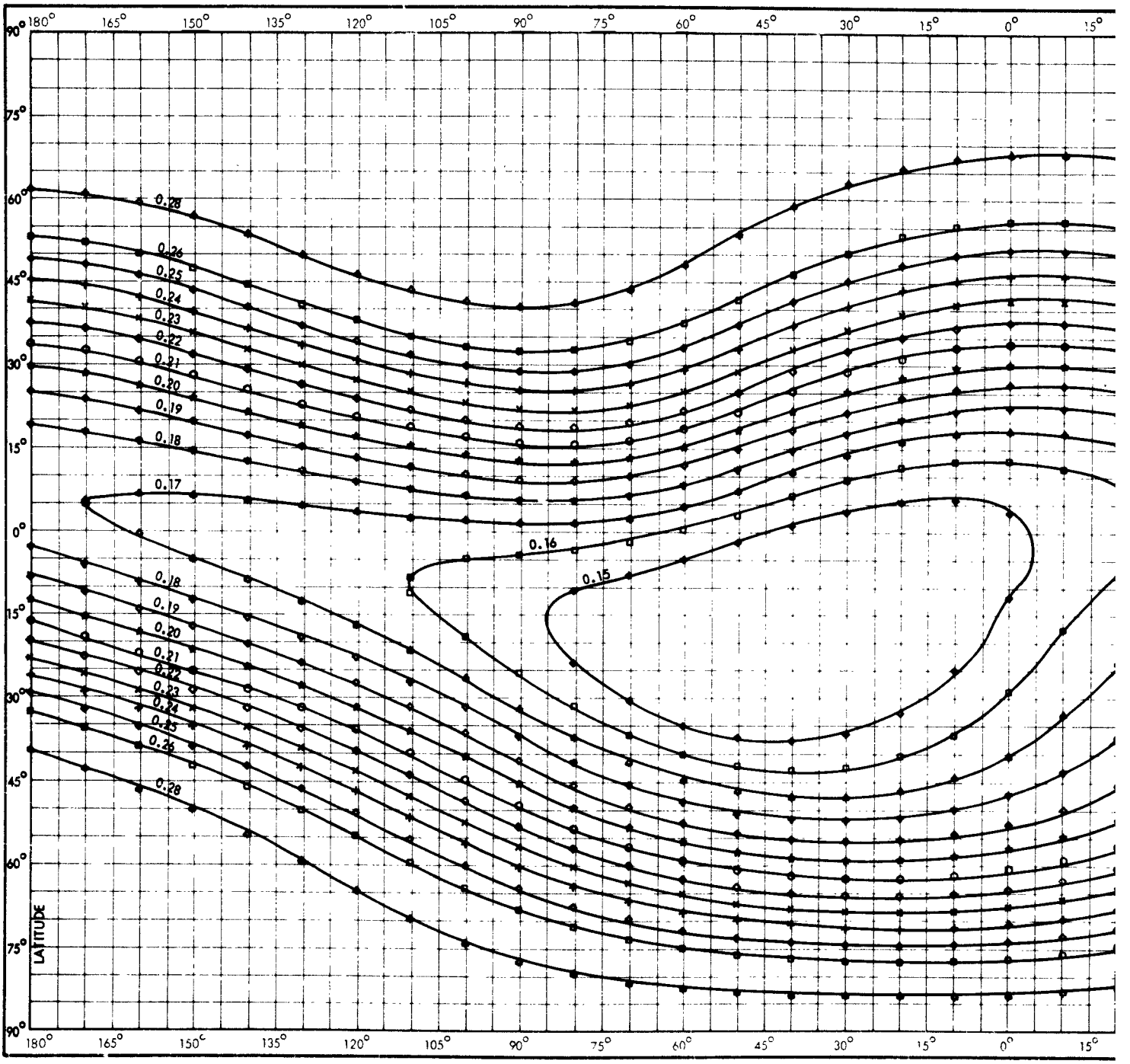

Figure 30. Constant Magnetic Field Intensity, B (Gauss), in the Region of the Sc

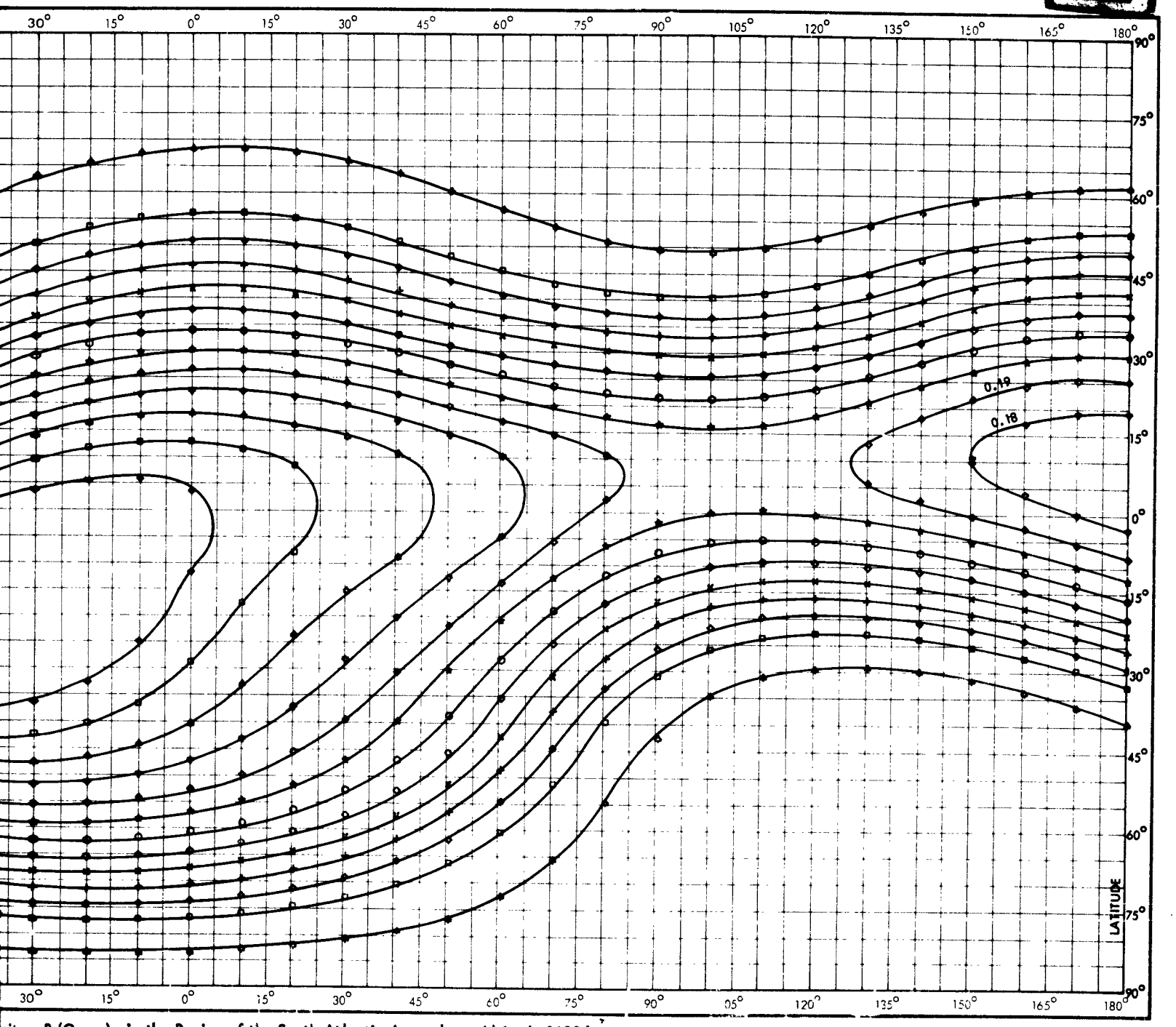

sity, B (Gauss), in the Region of the South Atlantic Anomaly at Altitude 1600 km

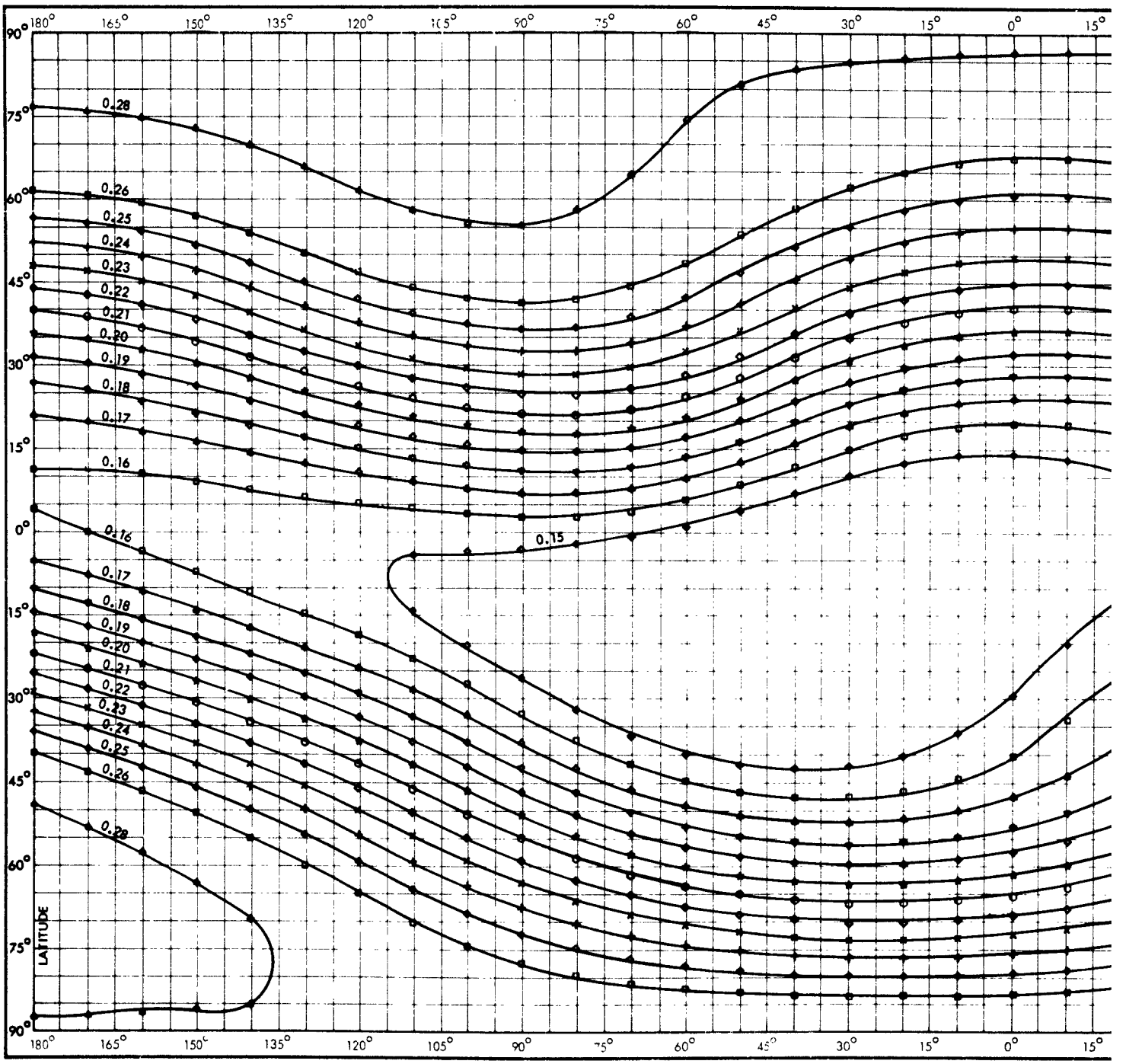

Figure 31. Constant Magnetic Field Intensity, B (Gauss), in the Region of the S

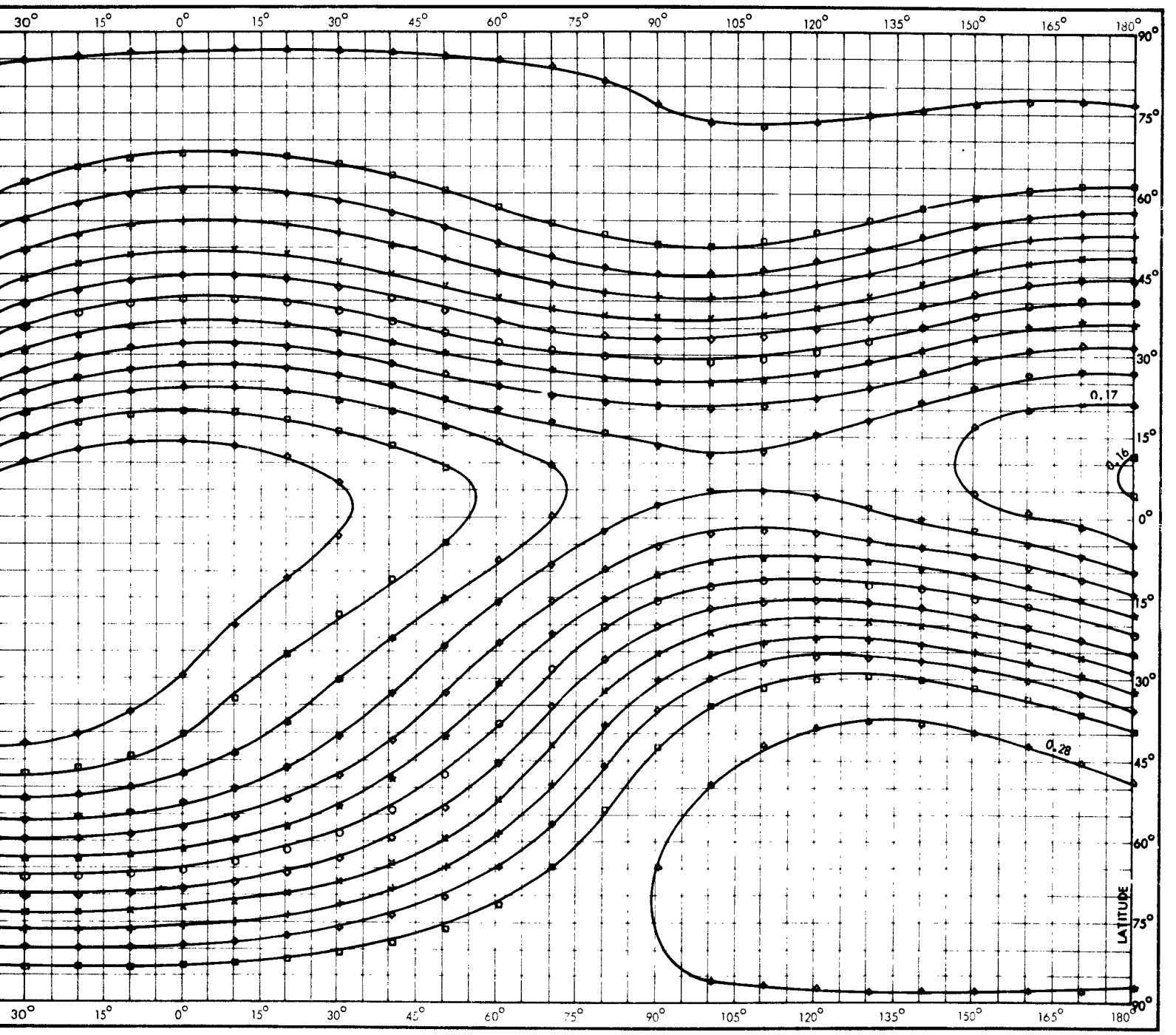

ity, B (Gauss), in the Region of the South Atlantic Anomaly at Altitude 1800 km

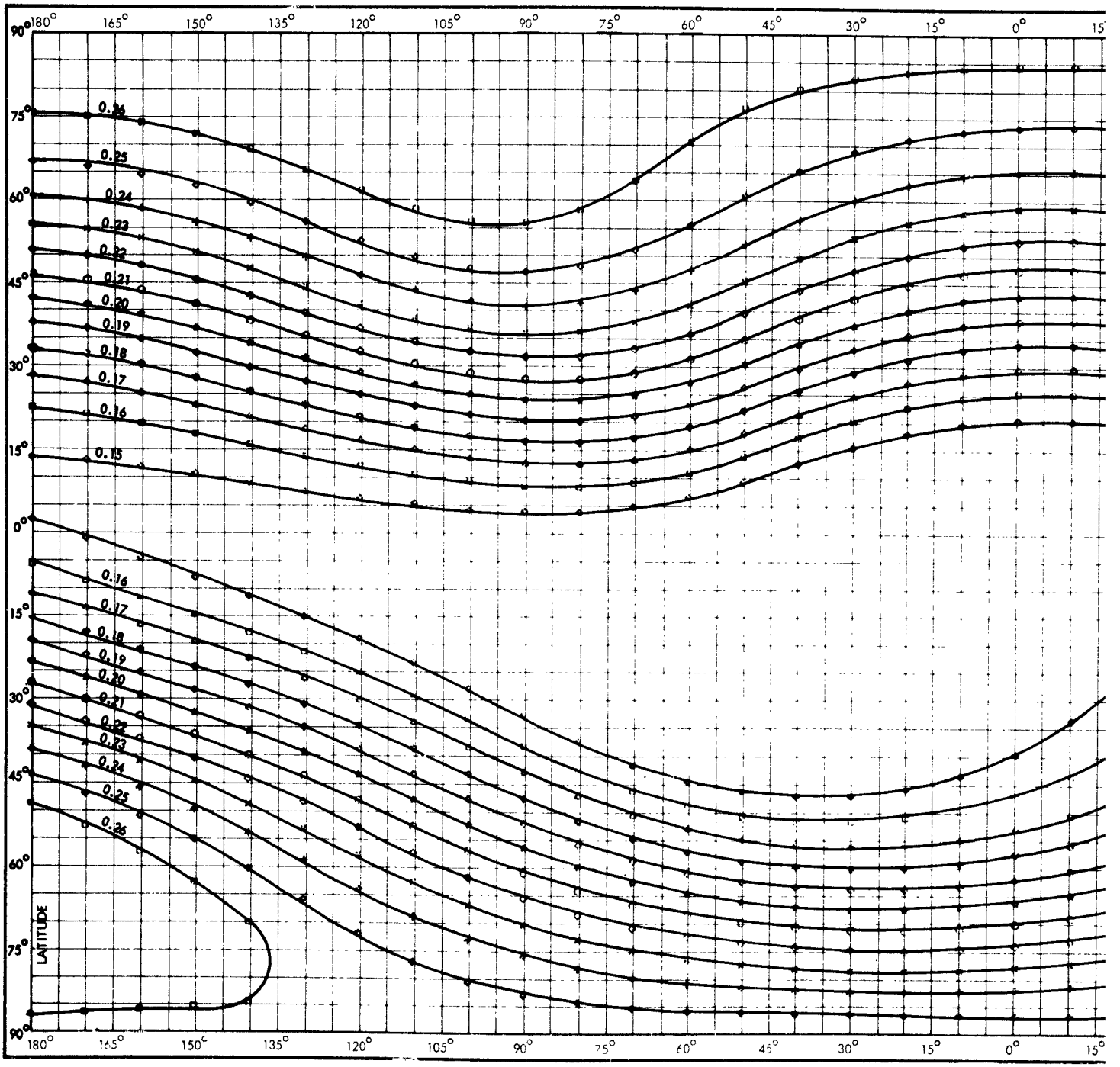

Figure 32. Constant Magnetic Field Intensity, B (Gauss), in the Region of t

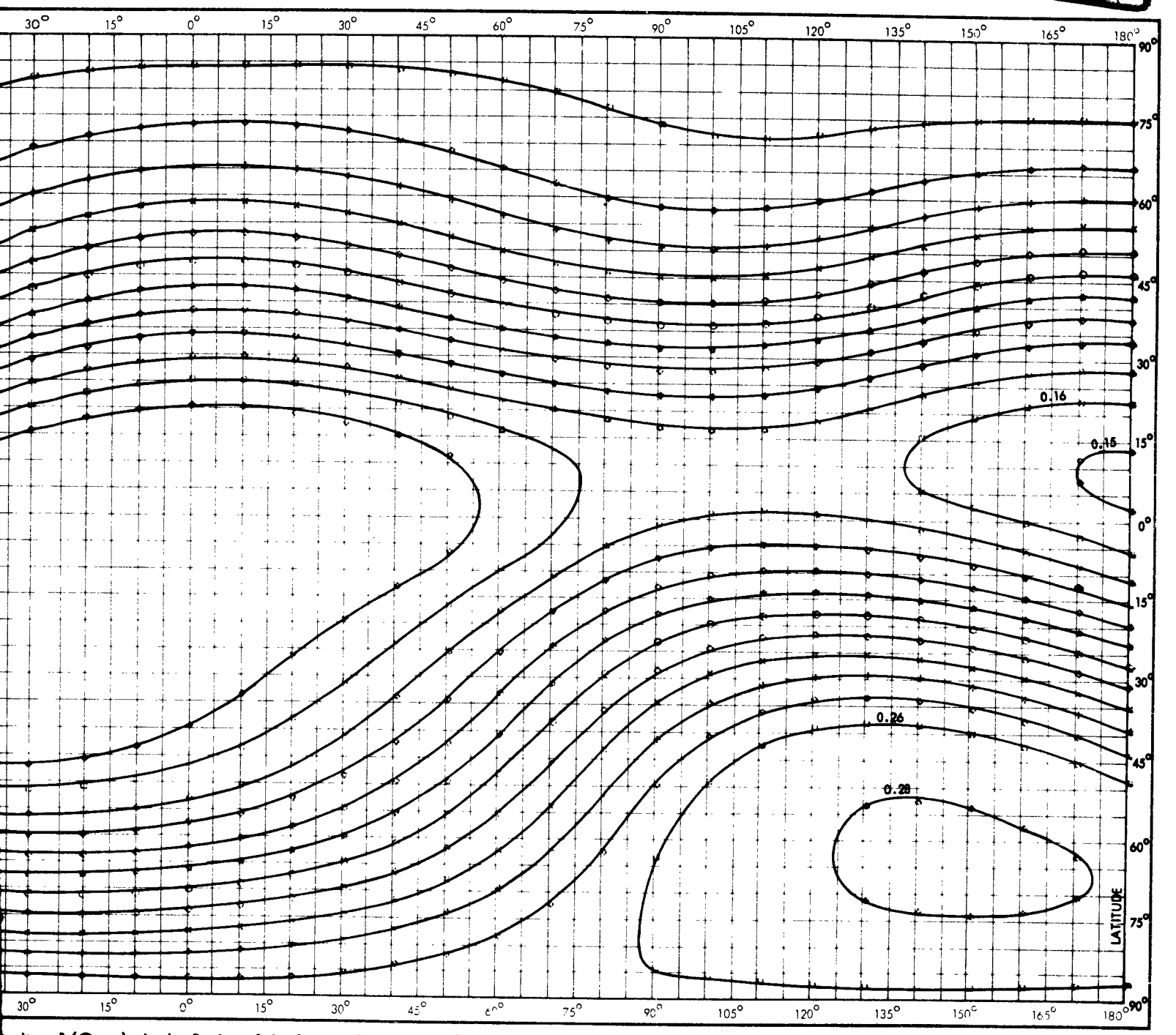

nsity, B (Gauss), in the Region of the South Atlantic Anomaly at Altitude 2000 Kilometers.

C. CONTOURS OF B AND L
(Jensen and Whitaker Coefficients)

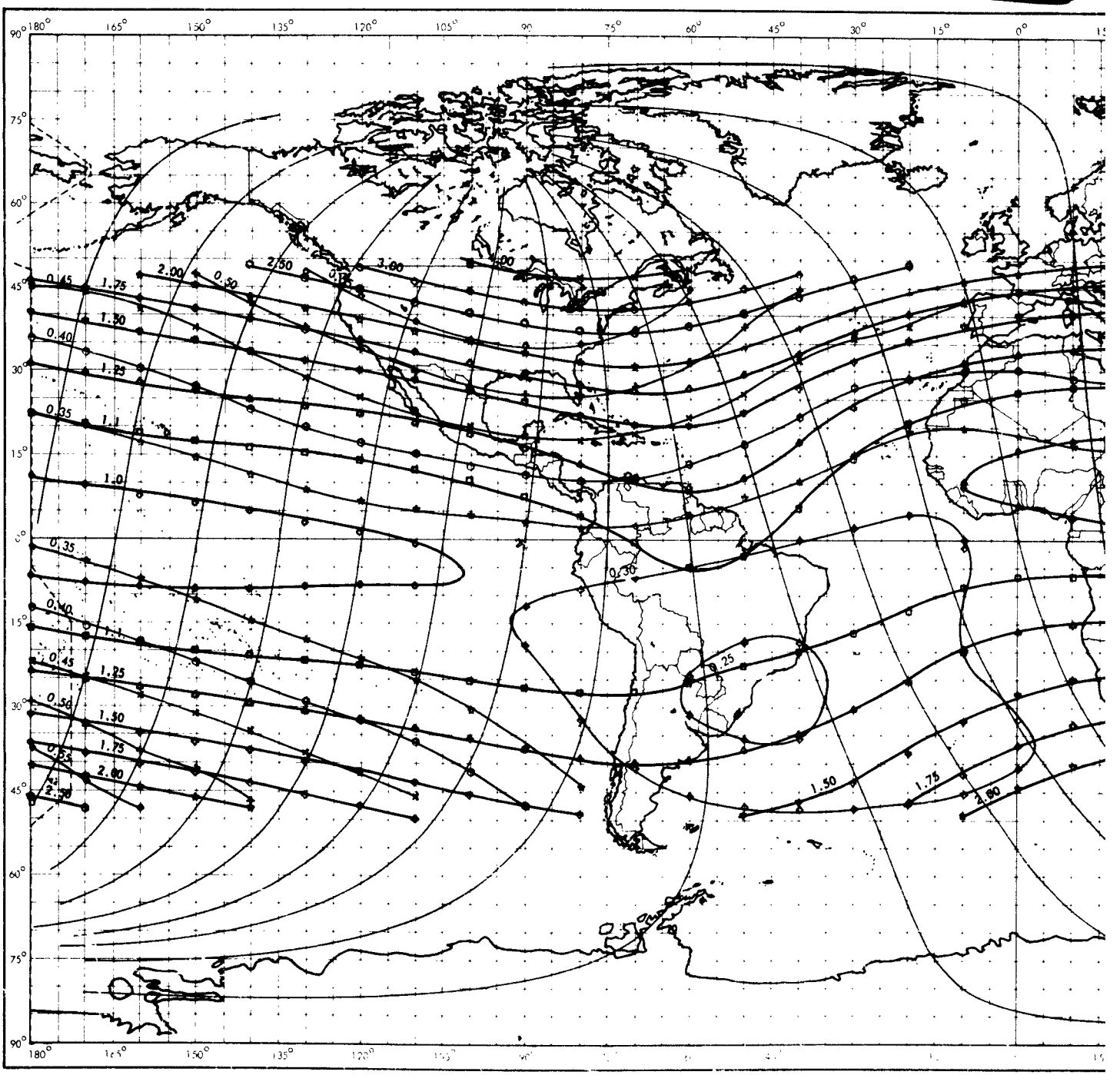

Figure 33. Constant Magnetic Field Intensity, B (Gauss), and Constant Magnetic

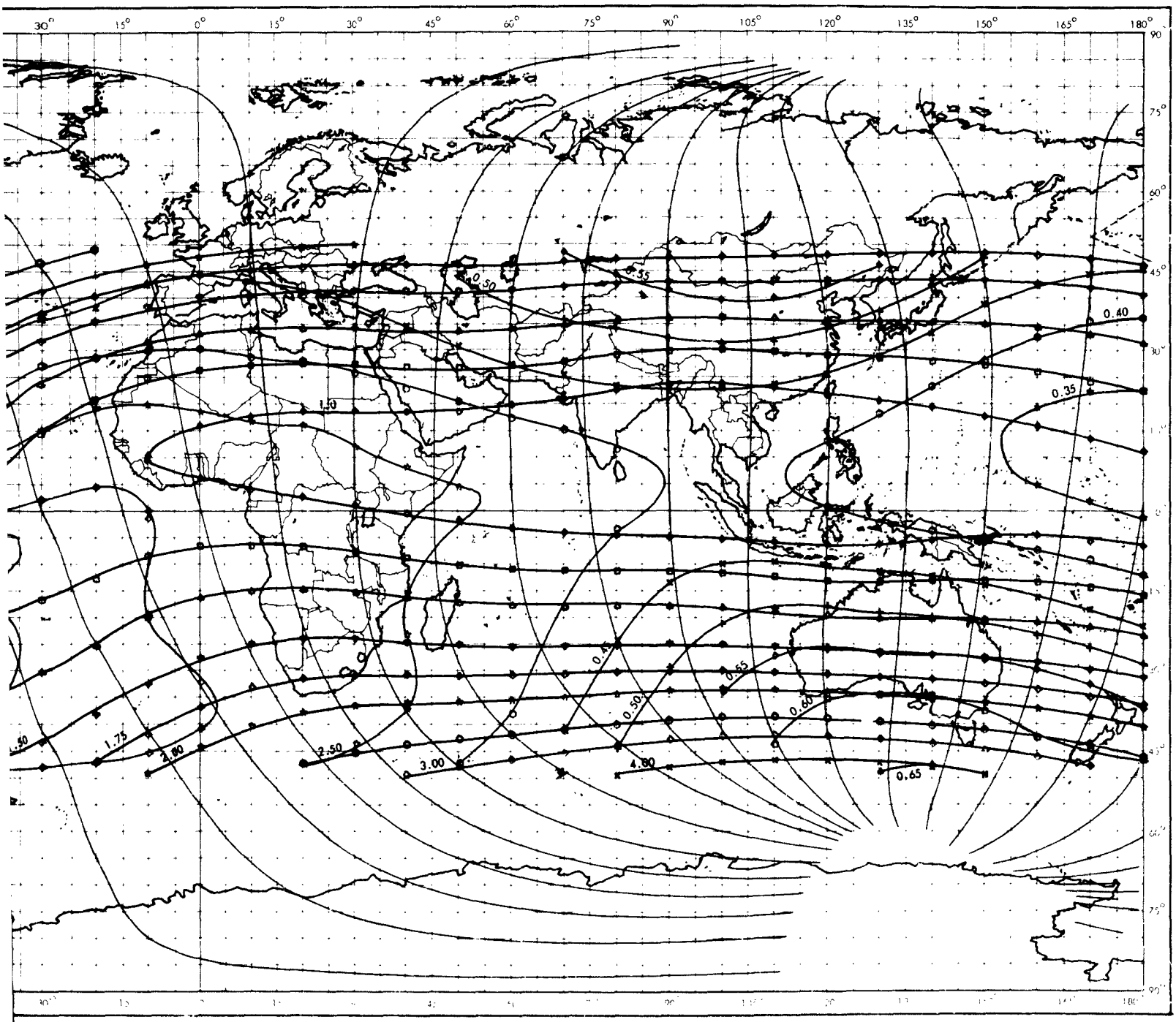

B (Gauss), and Constant Magnetic Shell Parameter, L (Earth Radii), At Altitude 0 Kilometers.

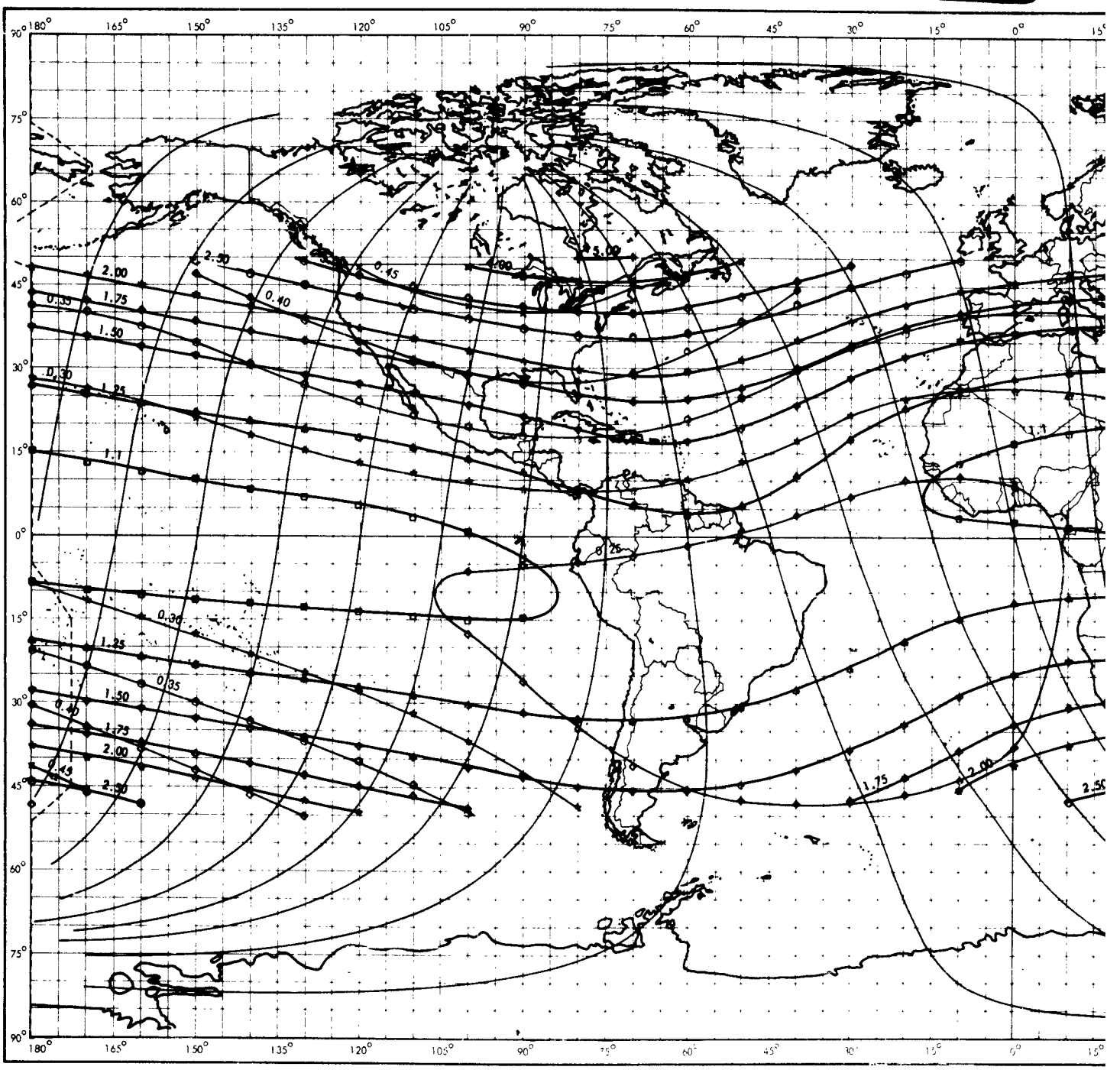

Figure 34. Constant Magnetic Field Intensity, B (Gauss), and Constant Magnetic

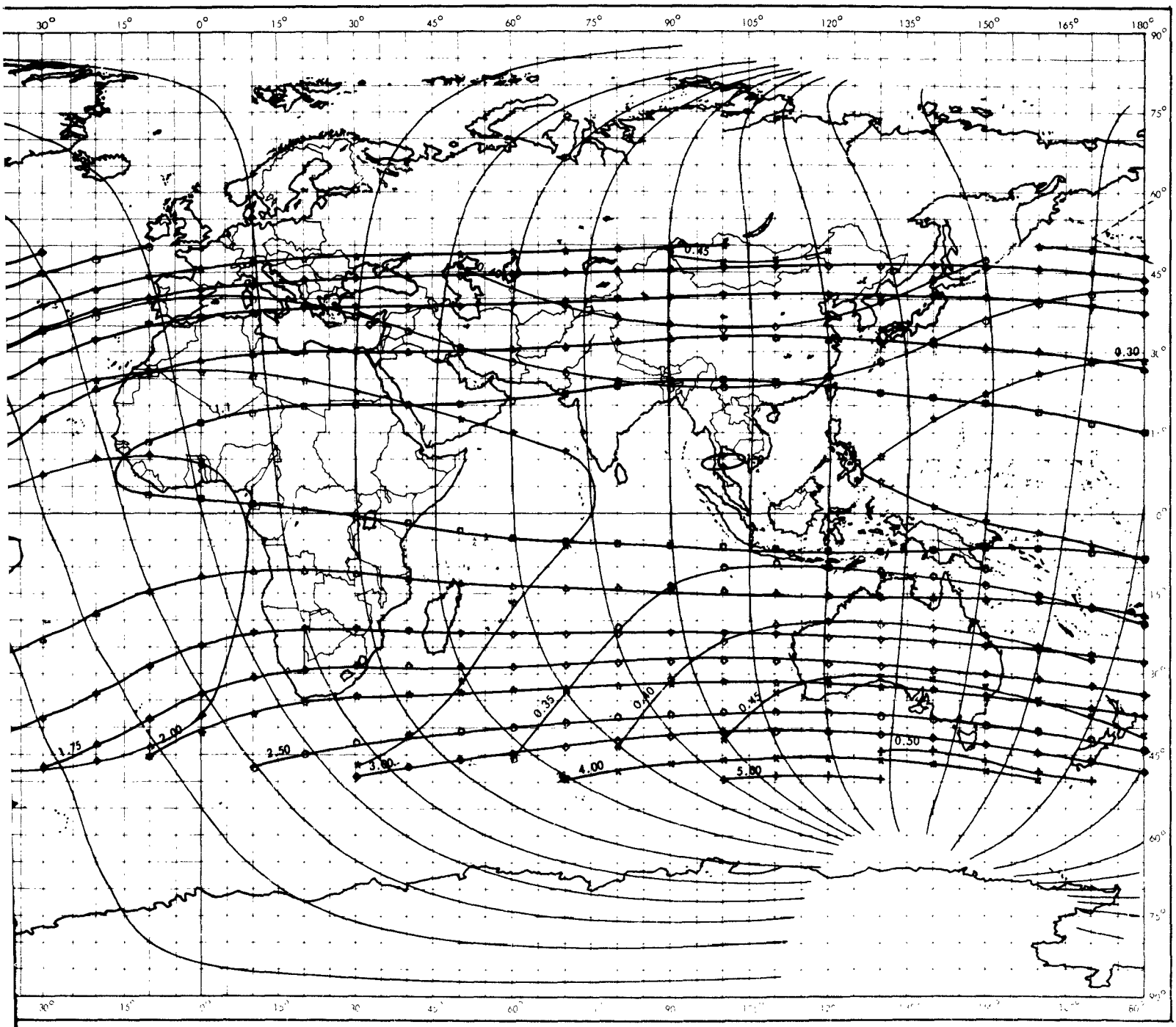

B (Gauss), and Constant Magnetic Shell Parameter, L (Earth Radii), At Altitude 500 Kilometers.

D. COMPARISON BETWEEN CONTOURS

(as Calculated from the Jensen and Cain Coefficients and as Calculated by the Jensen and Whitaker Coefficients)

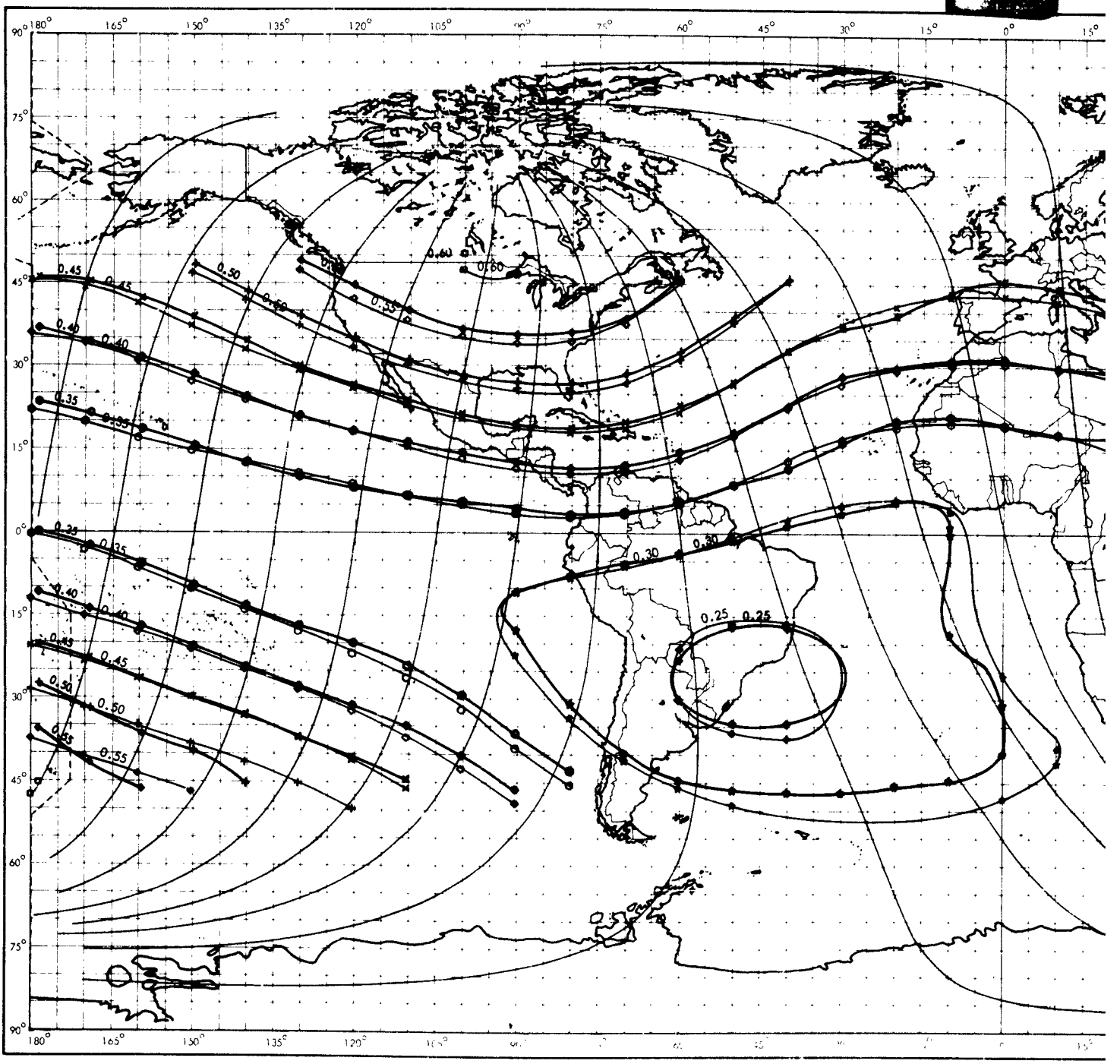

Figure 35. Constant Magnetic Field Intensity B,(Gauss), Using Jensen an
Field Intensity, B (Gauss), Using Jensen and Whitaker's 512 Co

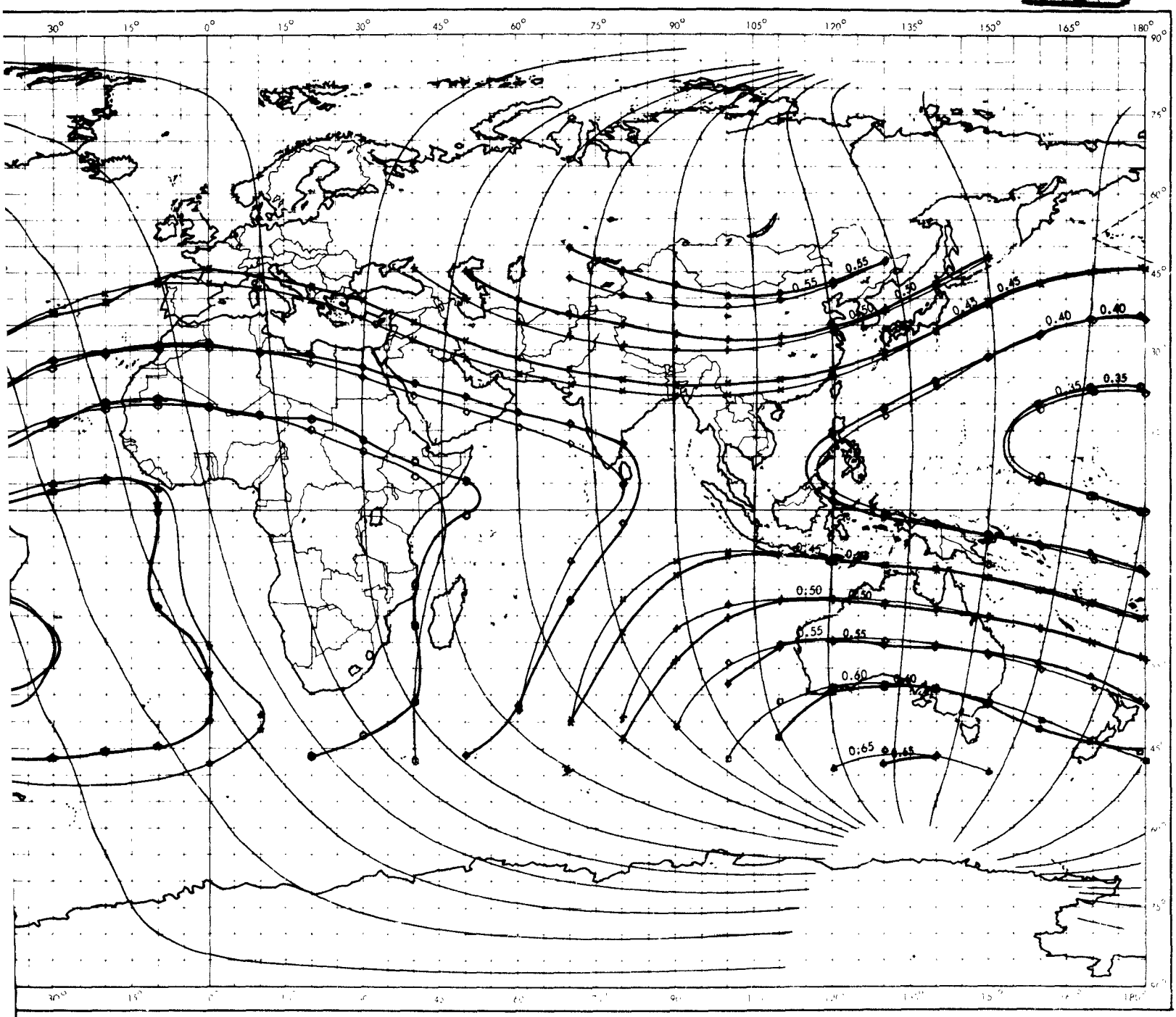

d Intensity B,(Gauss), Using Jensen and Cain's 48 Coefficients and Constant Magnetic
), Using Jensen and Whitaker's 512 Coeficients at Altitude 0 Kilometers.

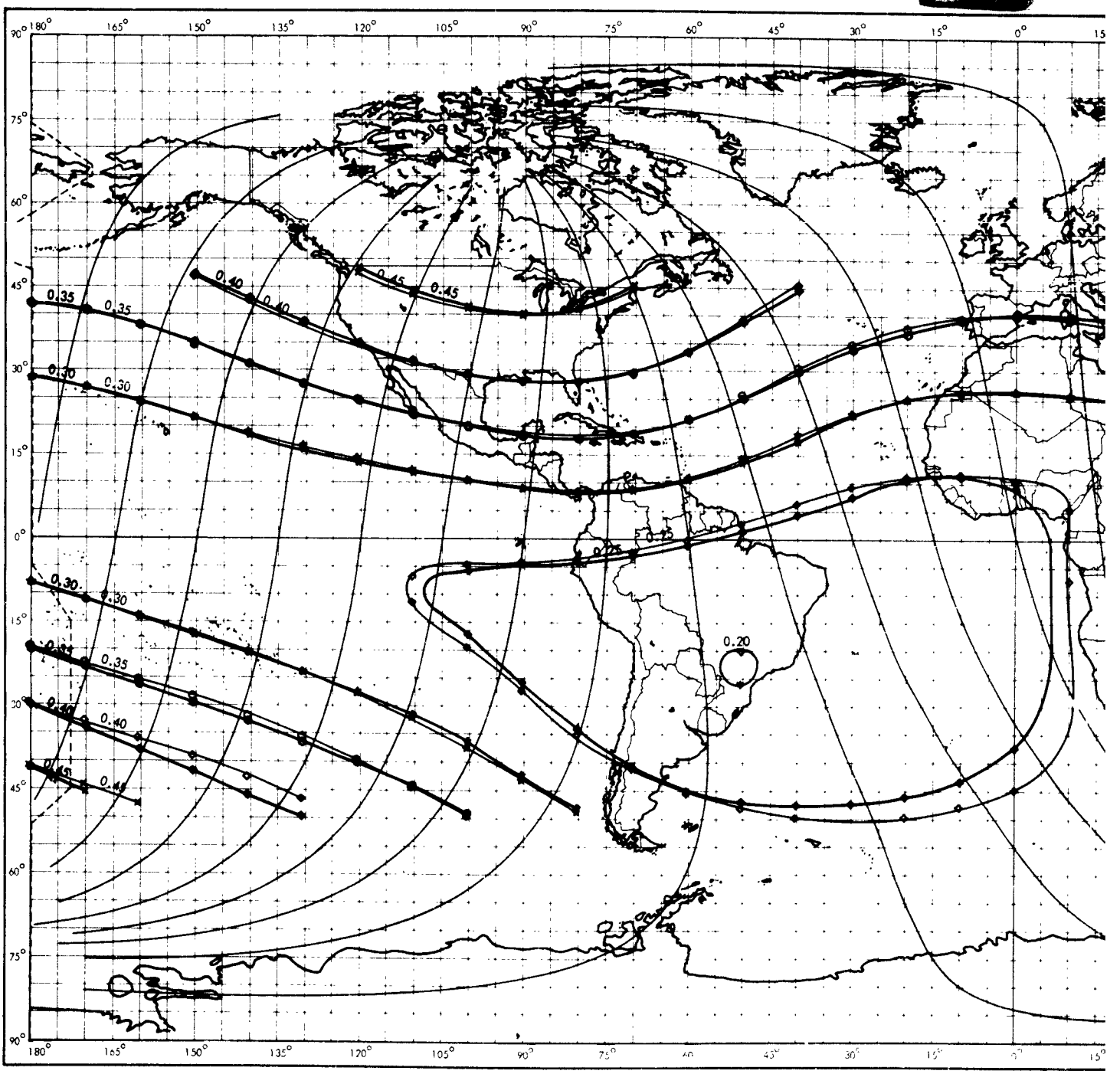

Figure 36. Constant Magnetic Field Intensity B,(Gauss), Using Jensen ar
Field Intensity, B (Gauss), Using Jensen and Whitaker's 512 (

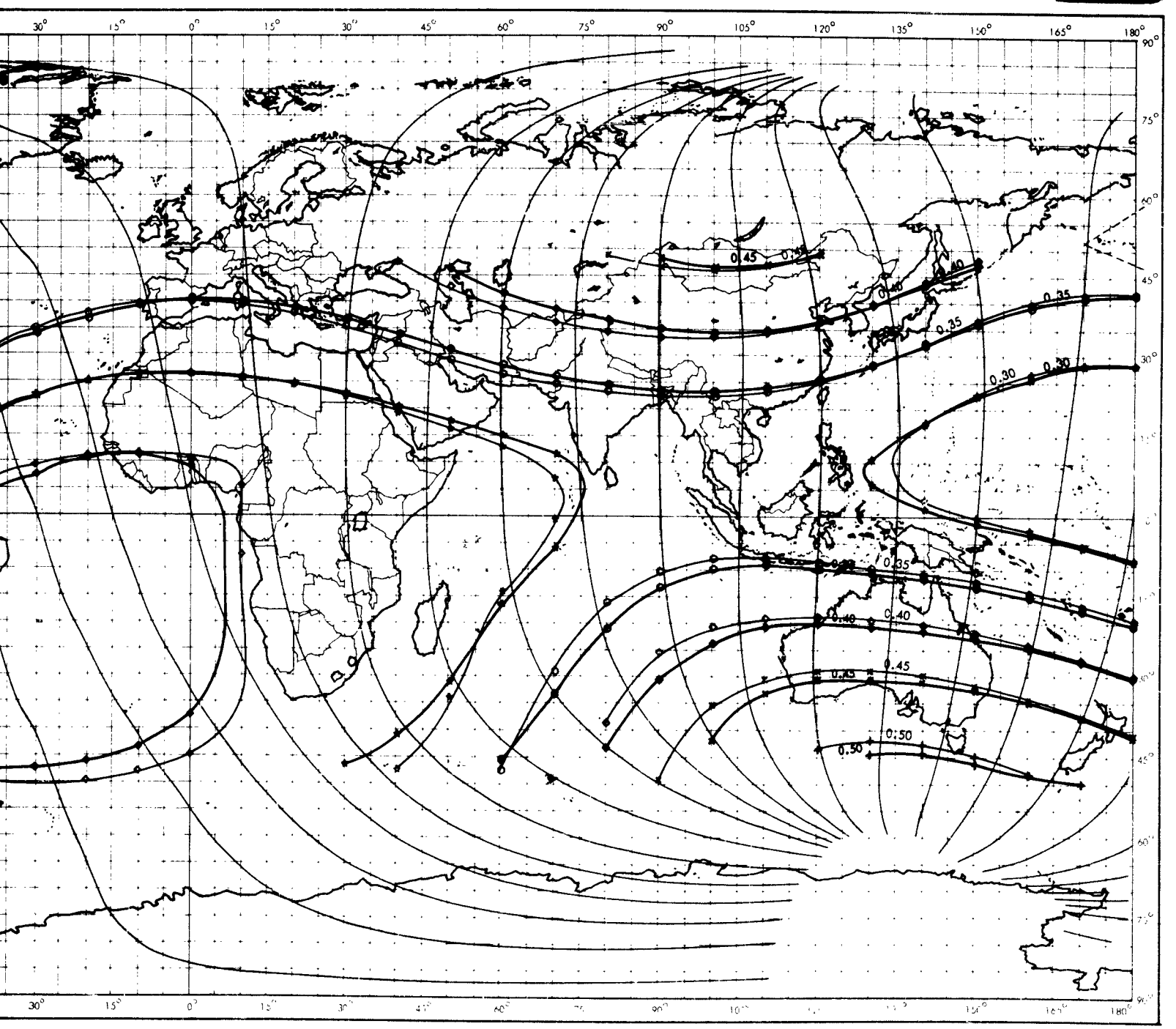

Intensity B,(Gauss), Using Jensen and Cain's 48 Coefficients and Constant Magnetic
), Using Jensen and Whitaker's 512 Coefficients at Altitude 500 Kilometers.

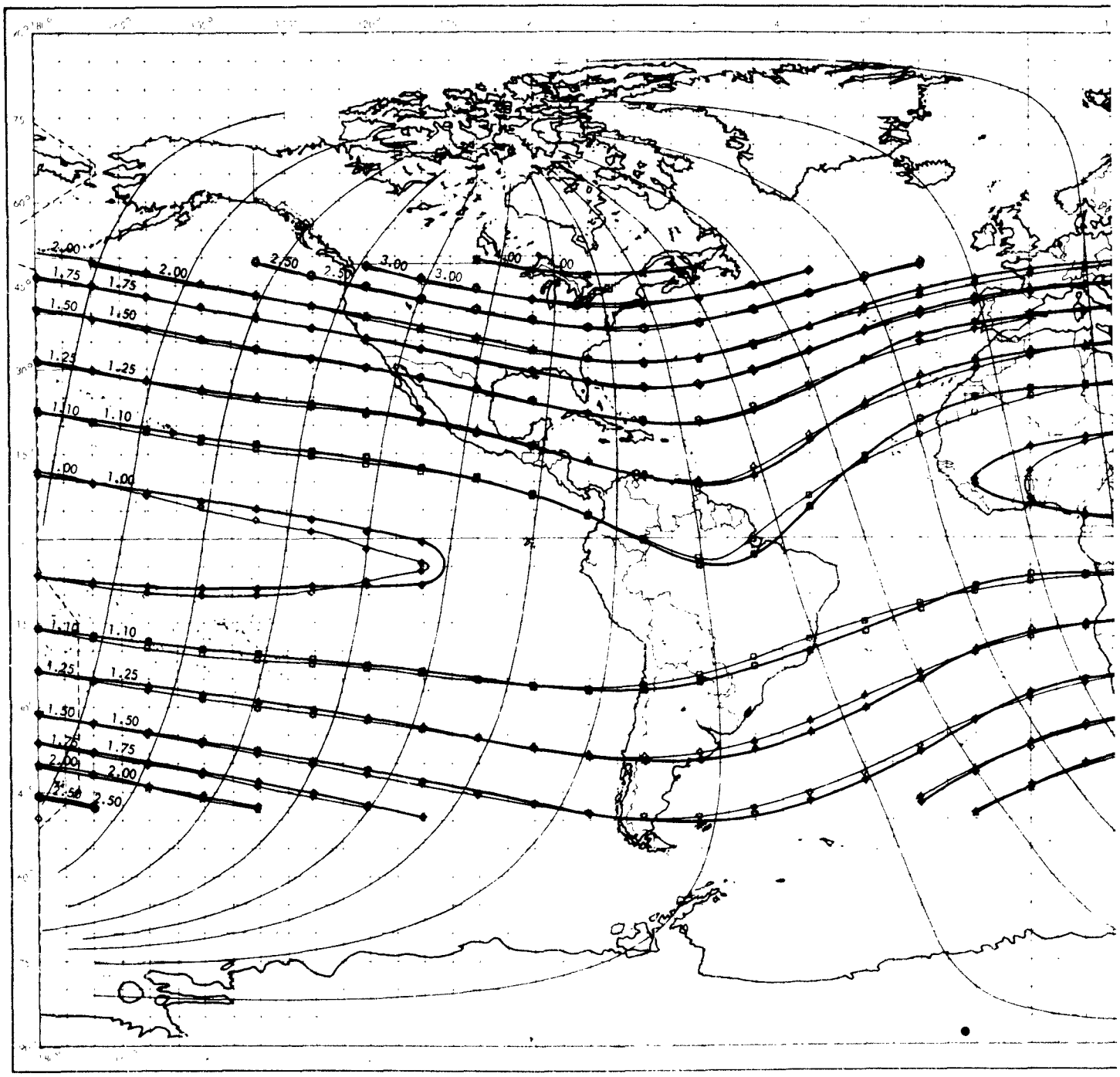

Figure 37. Constant Magnetic Shell Parameter, L (Earth Radii)
and Constant Magnetic Shell Parameter, L (Earth Radii), Using
Altitude 0 Kilometers

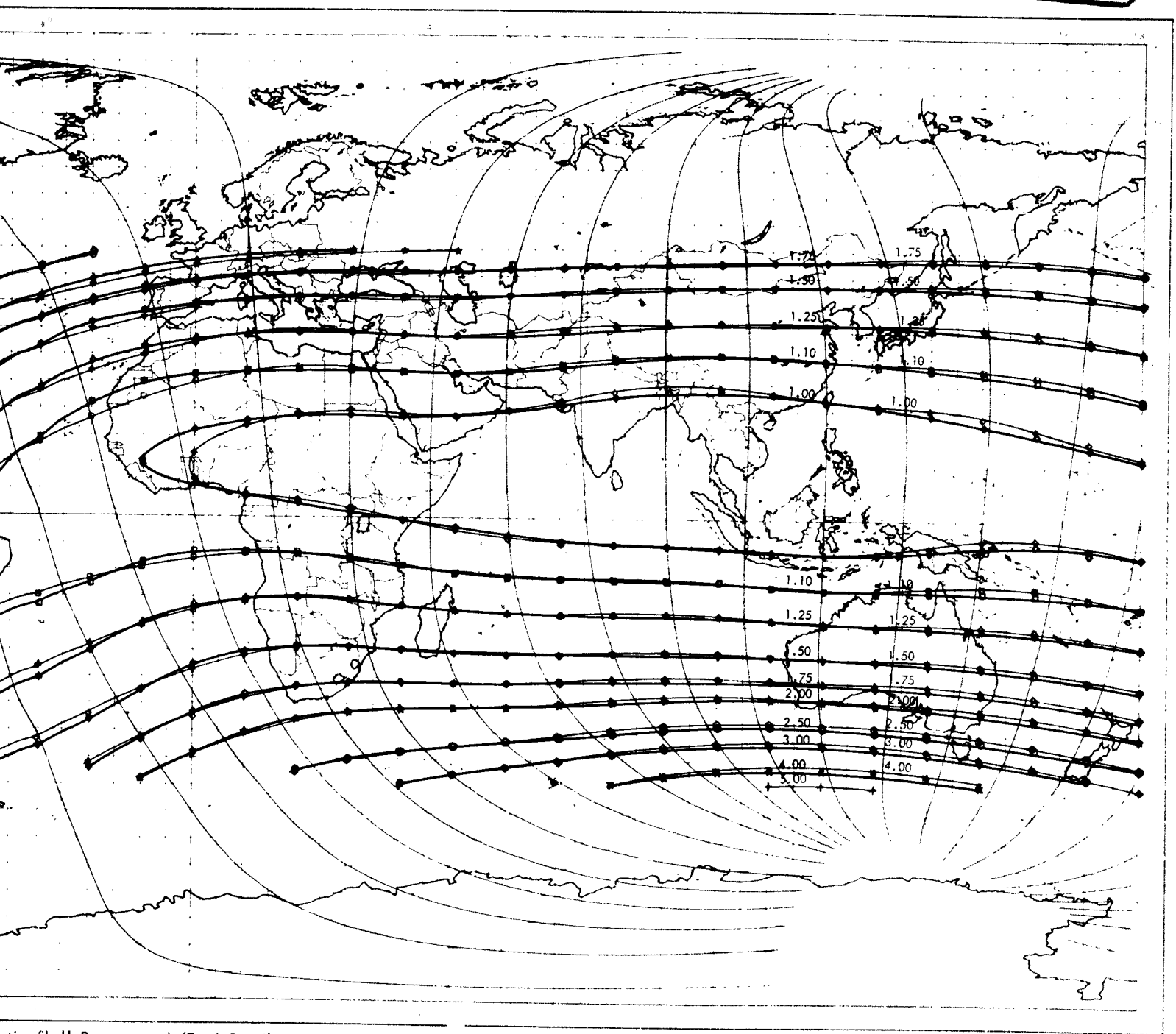

etic Shell Parameter, L (Earth Radii), Using Jensen and Cain's 48 Coefficients

ell Parameter, L (Earth Radii), Using Jensen and Whitaker's 512 Coefficients at Altitude 0 Kilometers.

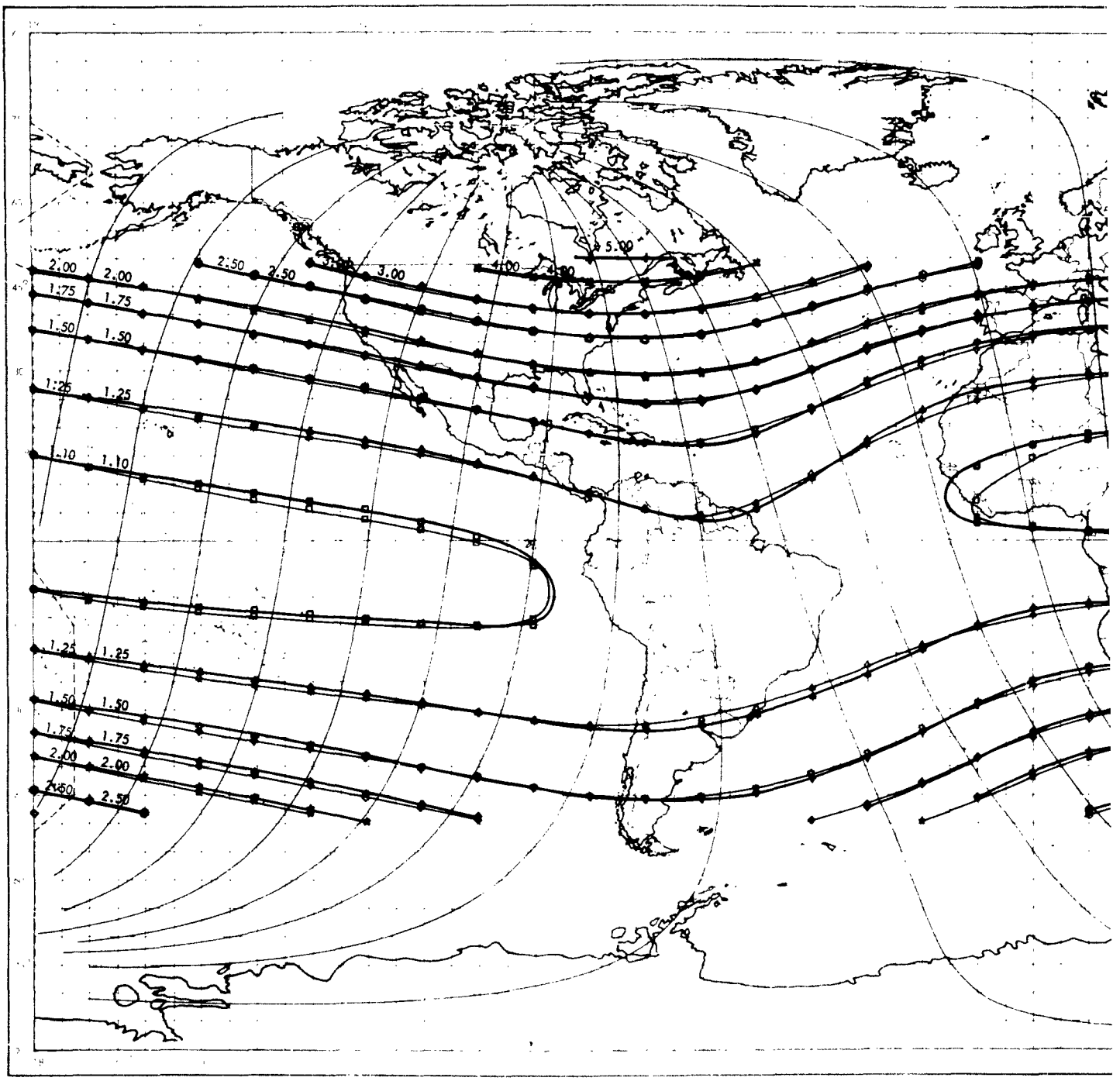

Figure 38. Constant Magnetic Shell Parameter, L (Earth Radi
and Constant Magnetic Shell Parameter, L (Earth Radii), Usi
at Altitude 500 Kilome

2

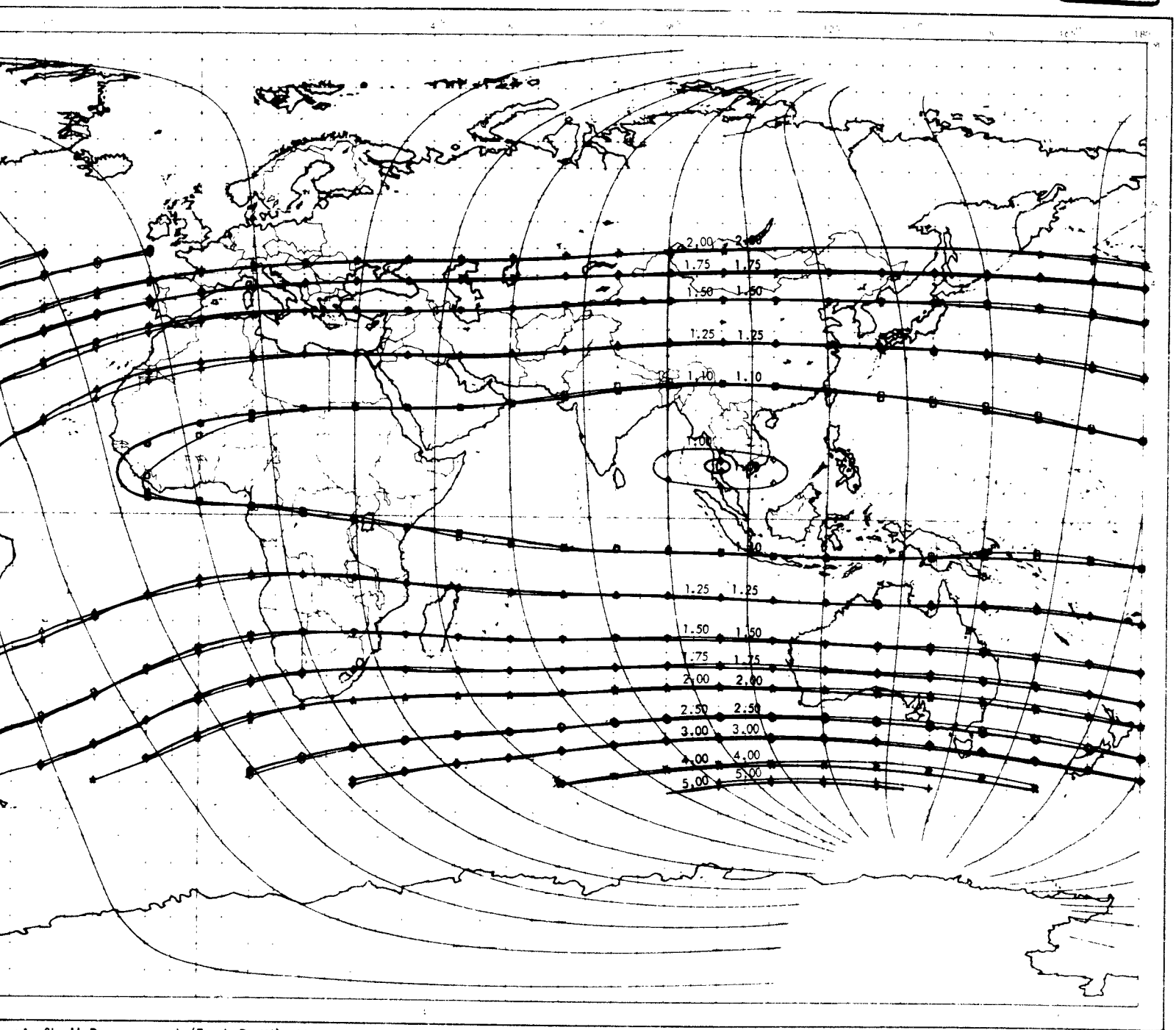

netic Shell Parameter, L (Earth Radii), Using Jensen and Cain's 48 Coefficients
hell Parameter, L (Earth Radii), Using Jensen and Whitaker's 512 Coefficients at Altitude 500 Kilometers.

E. CONSTANT B-L TRACES

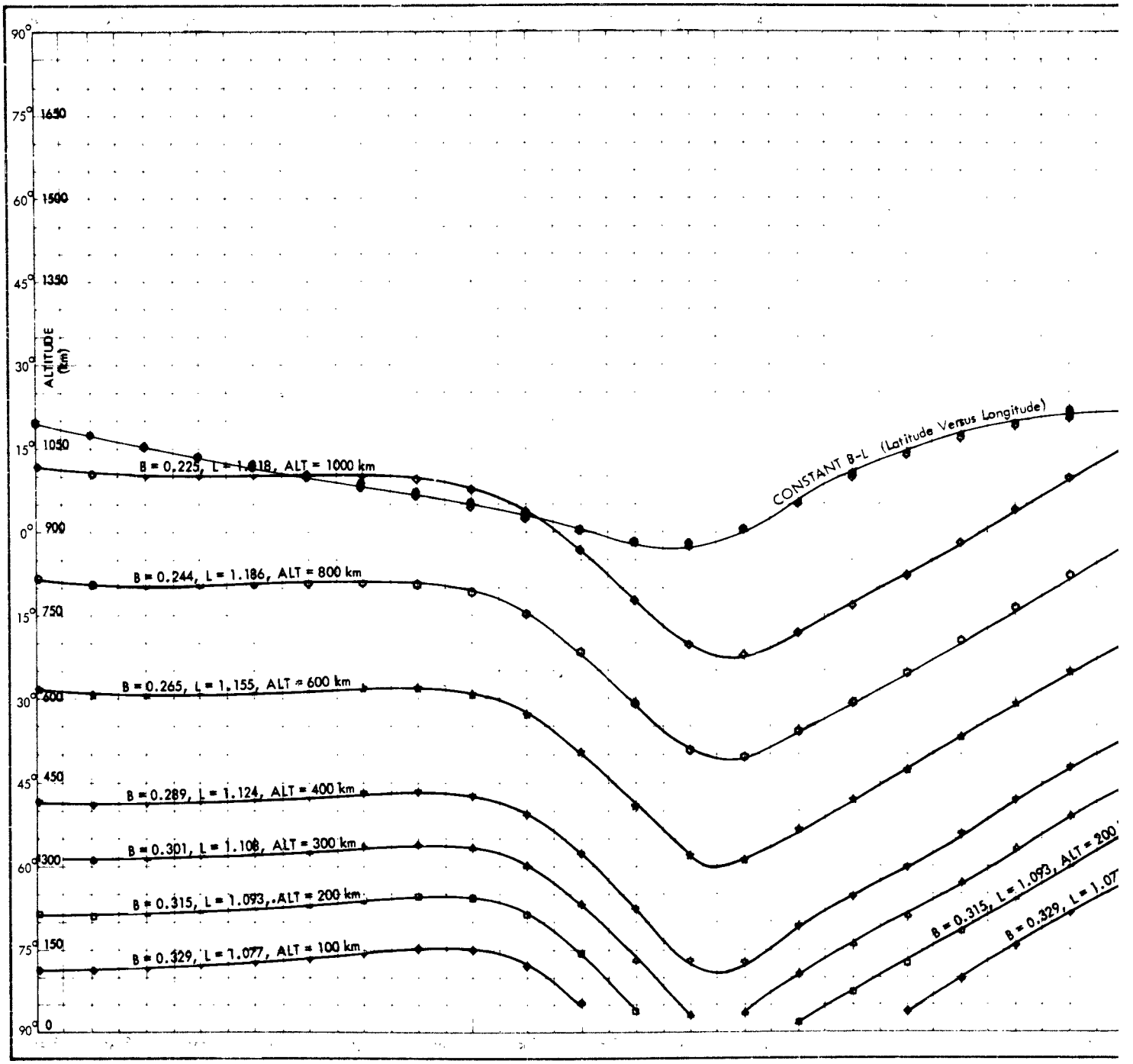

Figure 39. Constant B-L Traces in the Northern Hemisphere at Initial Latitude 17.5
Where B is the Magnetic Field Intensity (Gauss) and L is the Ma
Note: Above the Earth's Surface the Latitude Versus Longitude Plot is Common (within c

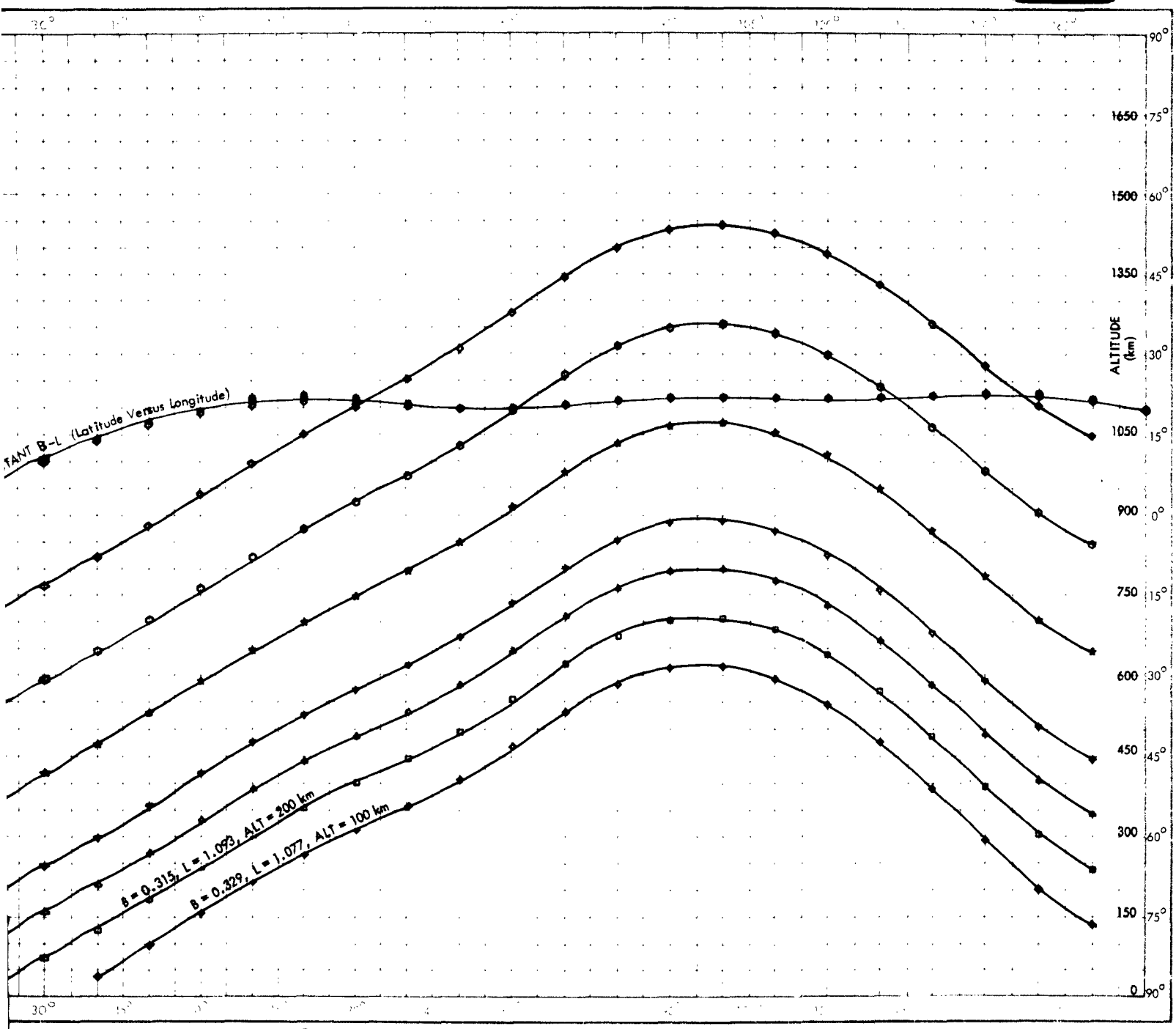

ern Hemisphere at Initial Latitude 17.5° N, Initial Longitude 190° E at Various Initial Altitudes
Field Intensity (Gauss) and L is the Magnetic Shell Parameter (in Earth Radii)
rsus Longitude Plot is Common (within a maximum deviation ± 1.5° Latitude) for all Altitude Considered

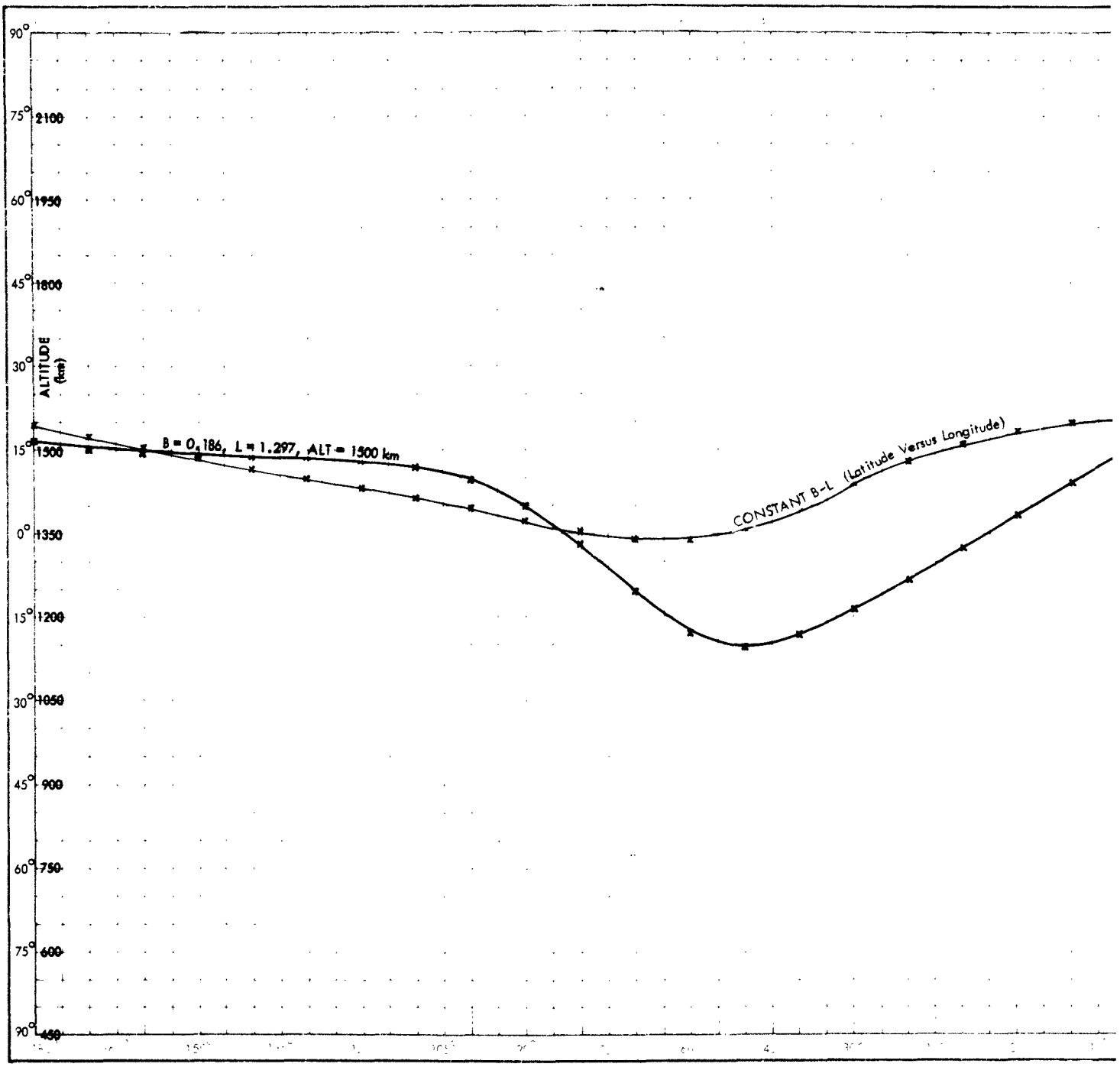

Figure 40. Constant B-L Trace in the Northern Hemisphere at Initial Latitude 17.5° N In
Where B is the Magnetic Field Intensity (Gauss) and L is the Magnetic

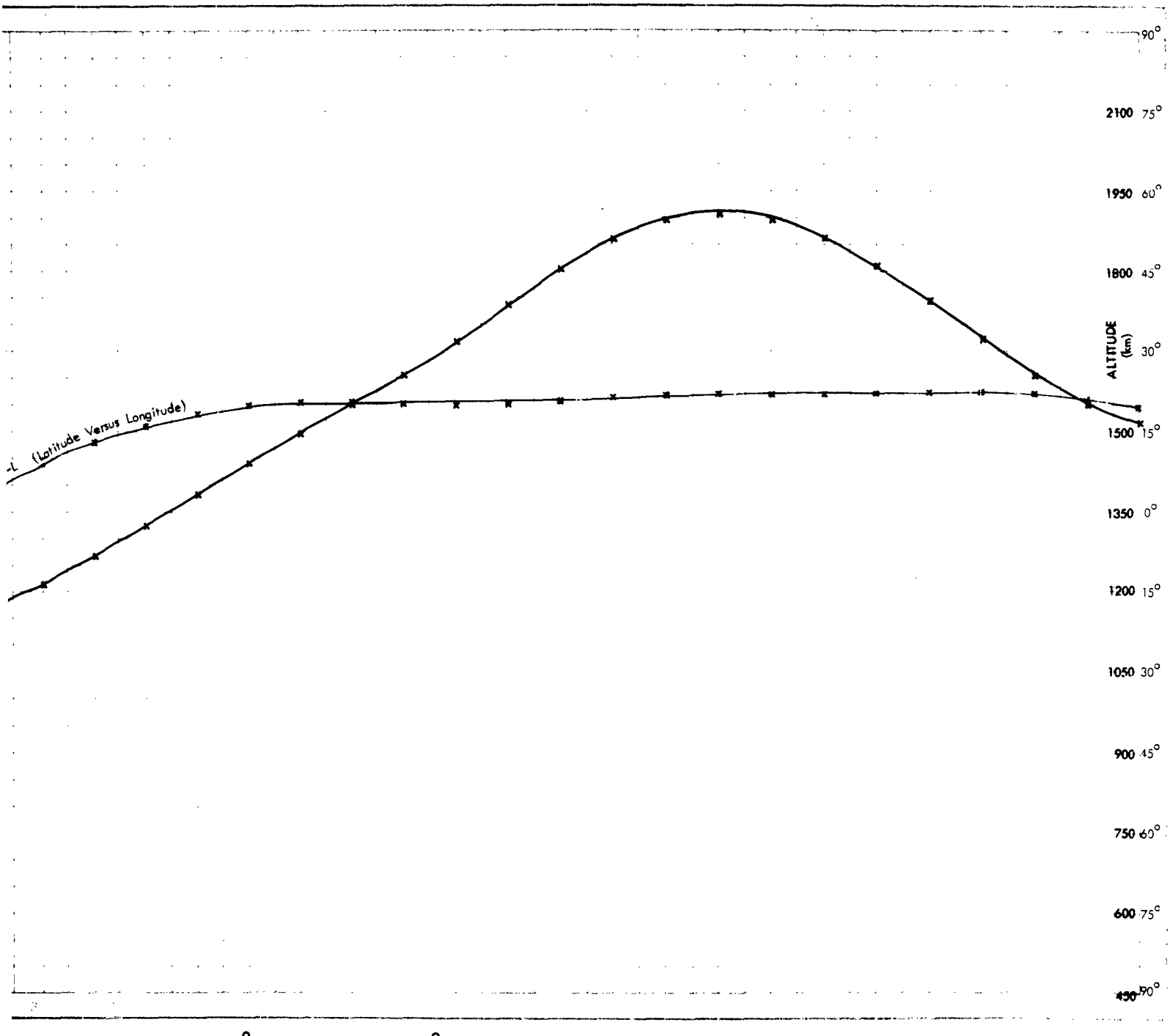

sphere at Initial Latitude 17.5° N Initial Longitude 190° E and Initial Altitude 1500 km
ensity (Gauss) and L is the Magnetic Shell Parameter (in Earth Radii)

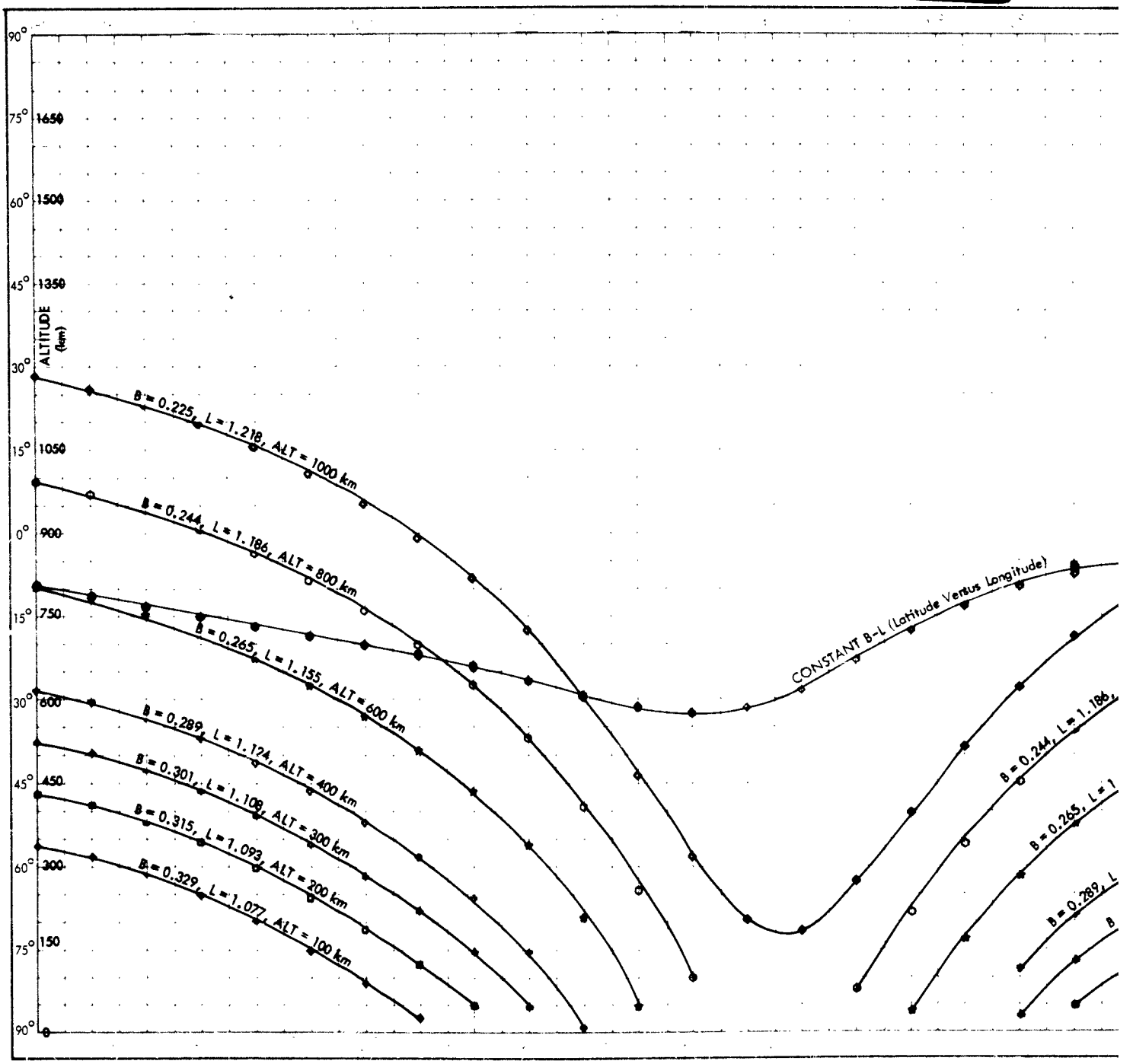

Figure 41. Constant B-L Traces in the Southern Hemisphere of the Conjugate to the Traces at Ir
Where B is the Magnetic Field Intensity (Gauss) and L is the M
Note: Above the Earth's Surface the Latitude Versus Longitude Plot is Common (within a

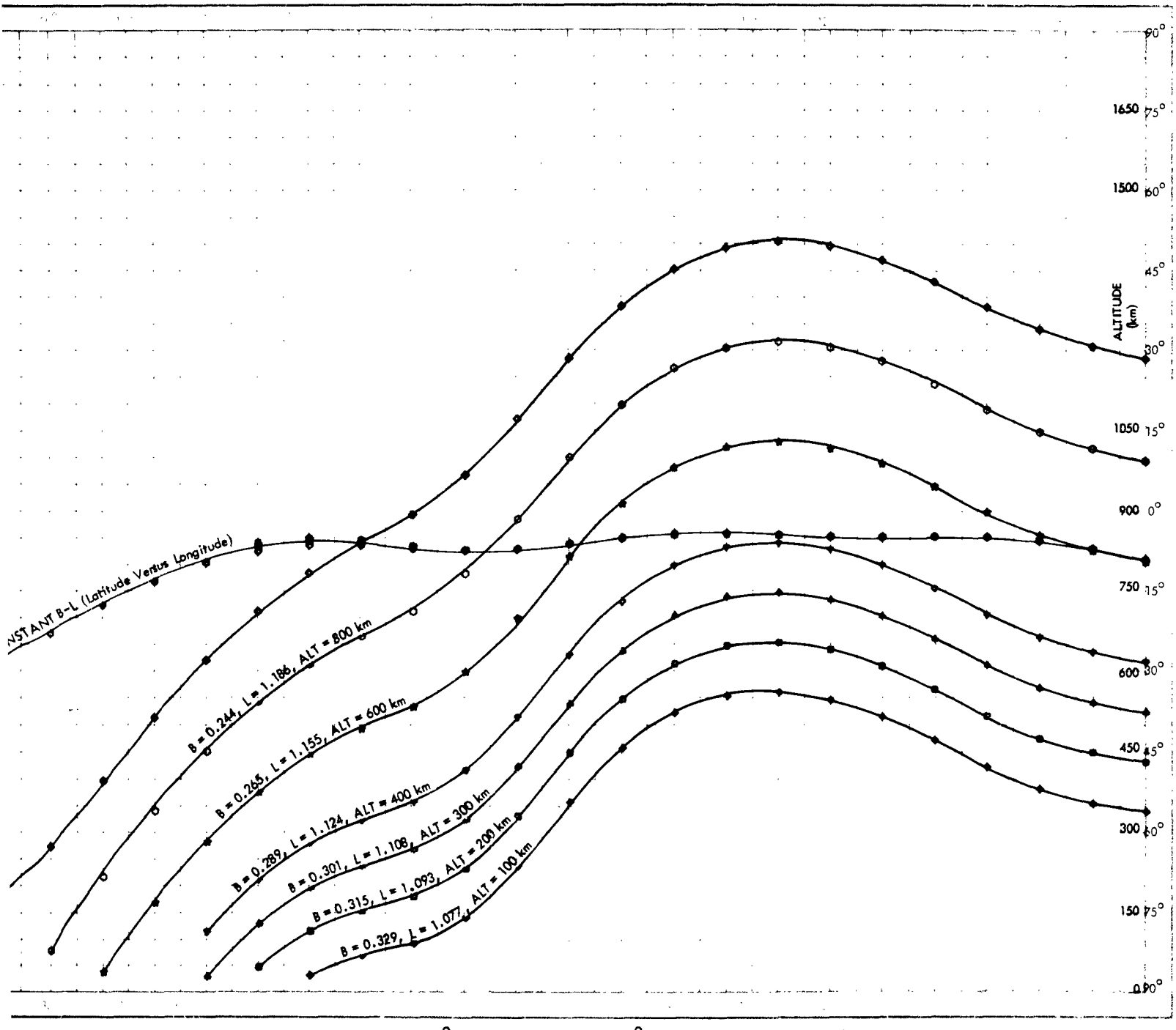

ıre of the Conjugate to the Traces at Initial Latitude 17.5° N, Initial Longitude 190° E at various Initial Altitudes
l Field Intensity (Gauss) and L is the Magnetic Shell Parameter (in Earth Radii)
ı Longitude Plot is Common (within a maximum Deviation of ± 1.5° Latitude) for all Altitudes Considered.

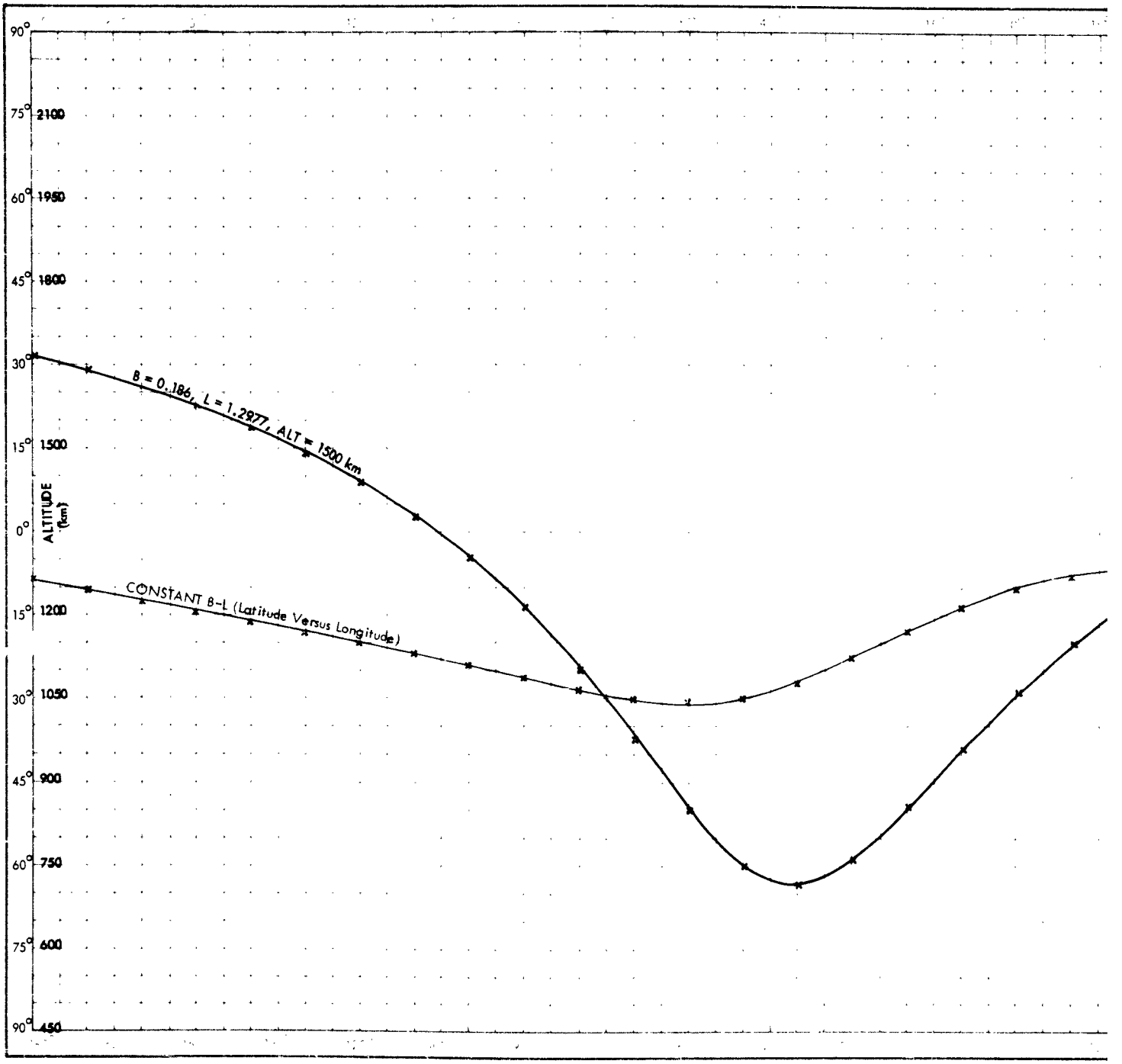

Figure 42. Constant B-L Trace in the Southern Hemisphere of the Conjugate to the Trace at Init
Where B is the Magnetic Field Intensity (Gauss) and L is the M

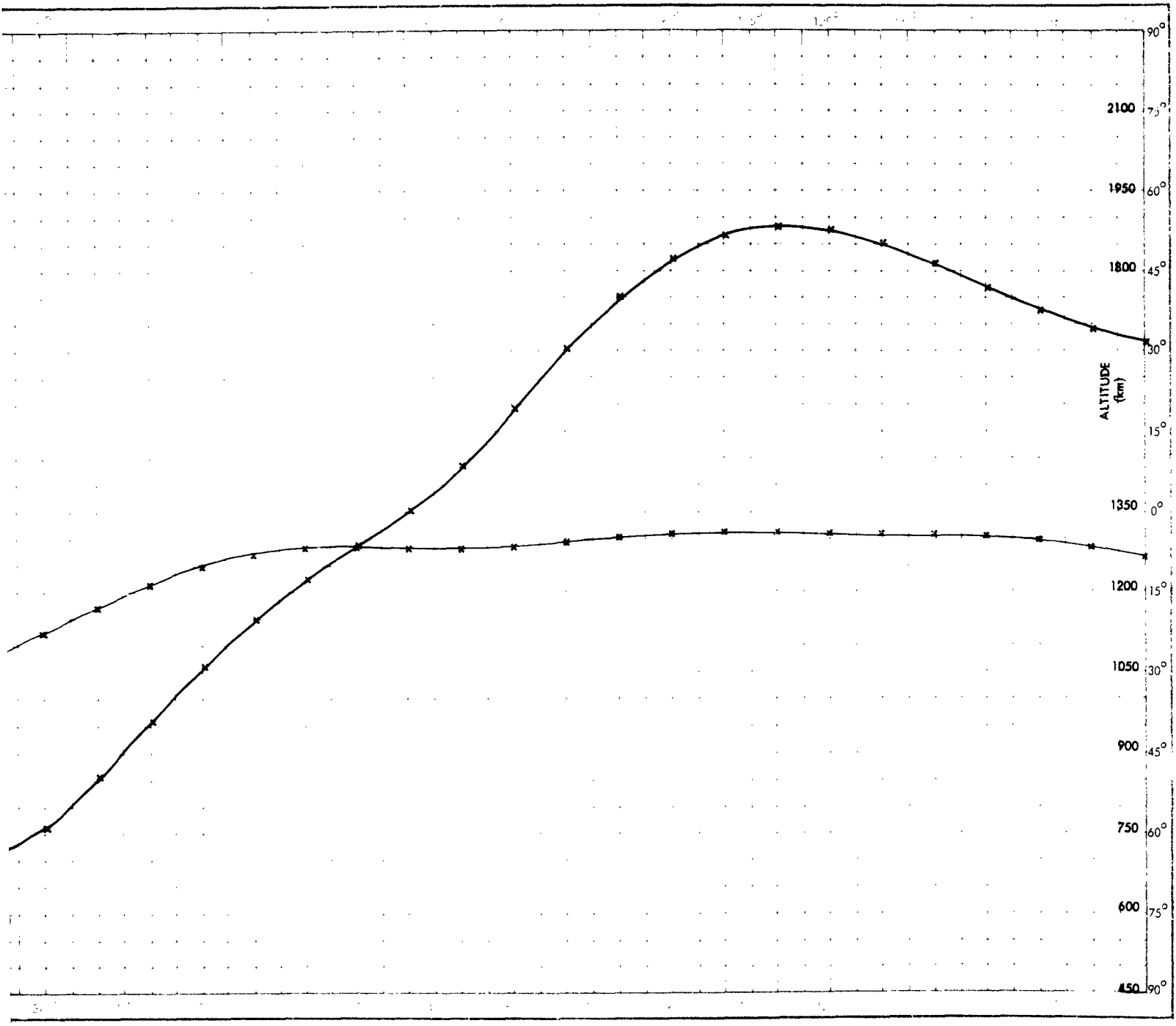

of the Conjugate to the Trace at Initial Latitude 17.5° N Initial Longitude 190° E at Initial Altitude 1500 km
Field Intensity (Gauss) and L is the Magnetic Shell Parameter (in Earth Radii)

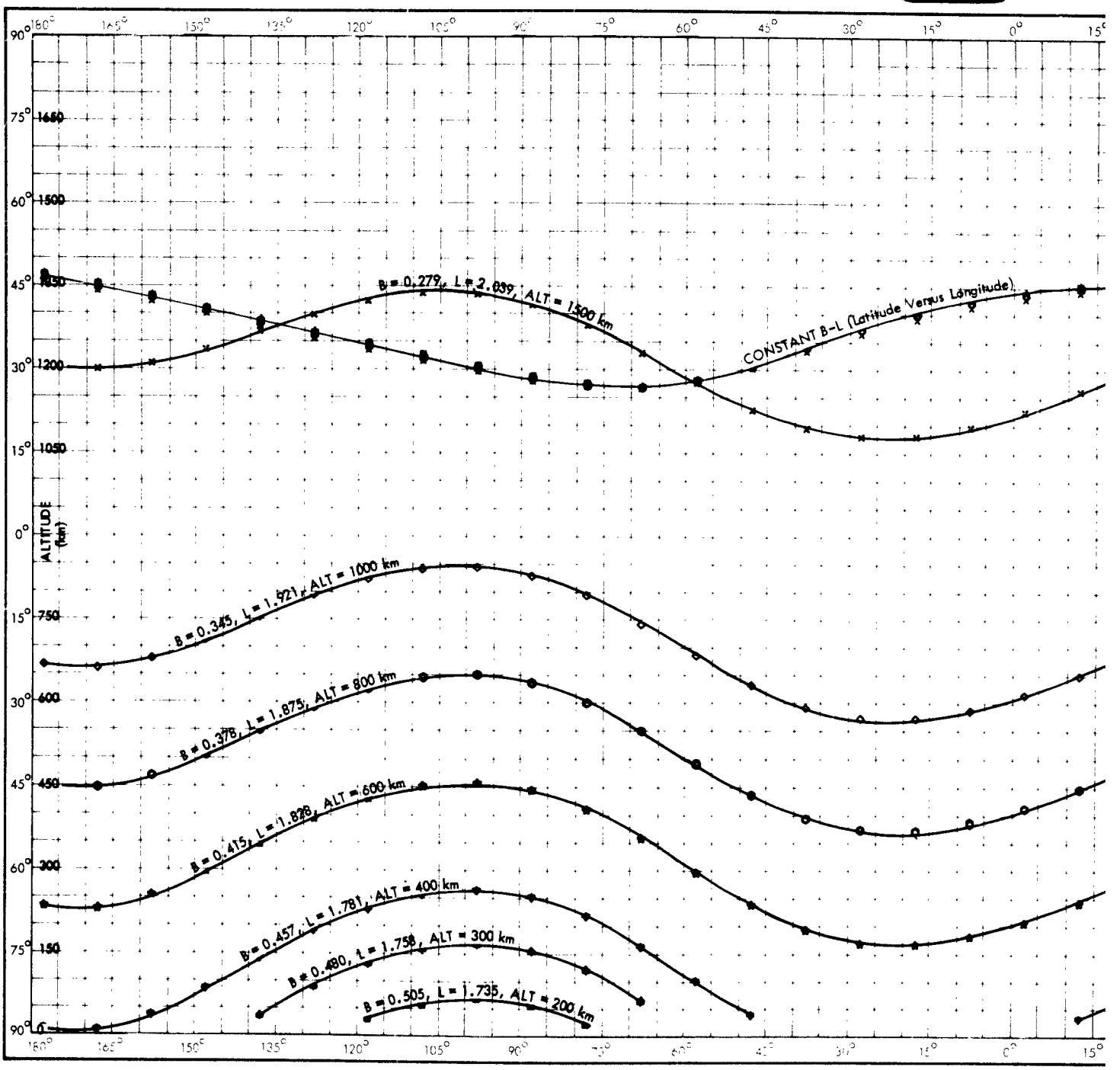

Figure 43. Constant B-L Traces in the Northern Hemisphere at Initial Latitud
Where B is the Magnetic Field Intensity (Gauss) and L is the
Note: Above the Earth's Surface the Latitude Versus Longitude Plot is Common (withi

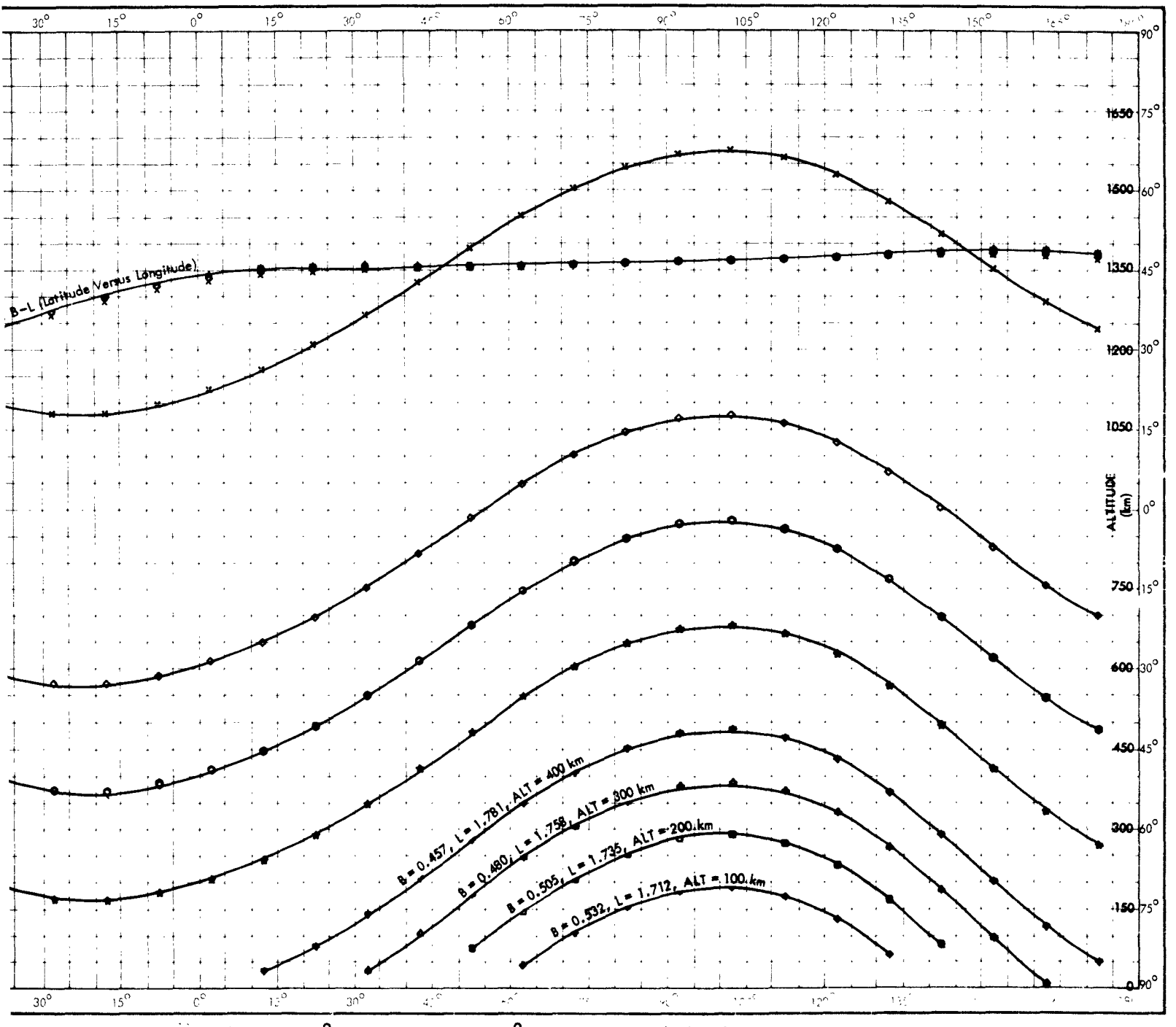

lorthern Hemisphere at Initial Latitude 46° N, Initial Longitude 72° E at Various Initial Altitudes
lc Field Intensity (Gauss) and L is the Magnetic Shell Parameter (in Earth Radii)
rsus Longitude Plot is Common (within a maximum deviation of ± 1.5° Latitude) for all Altitudes Considered

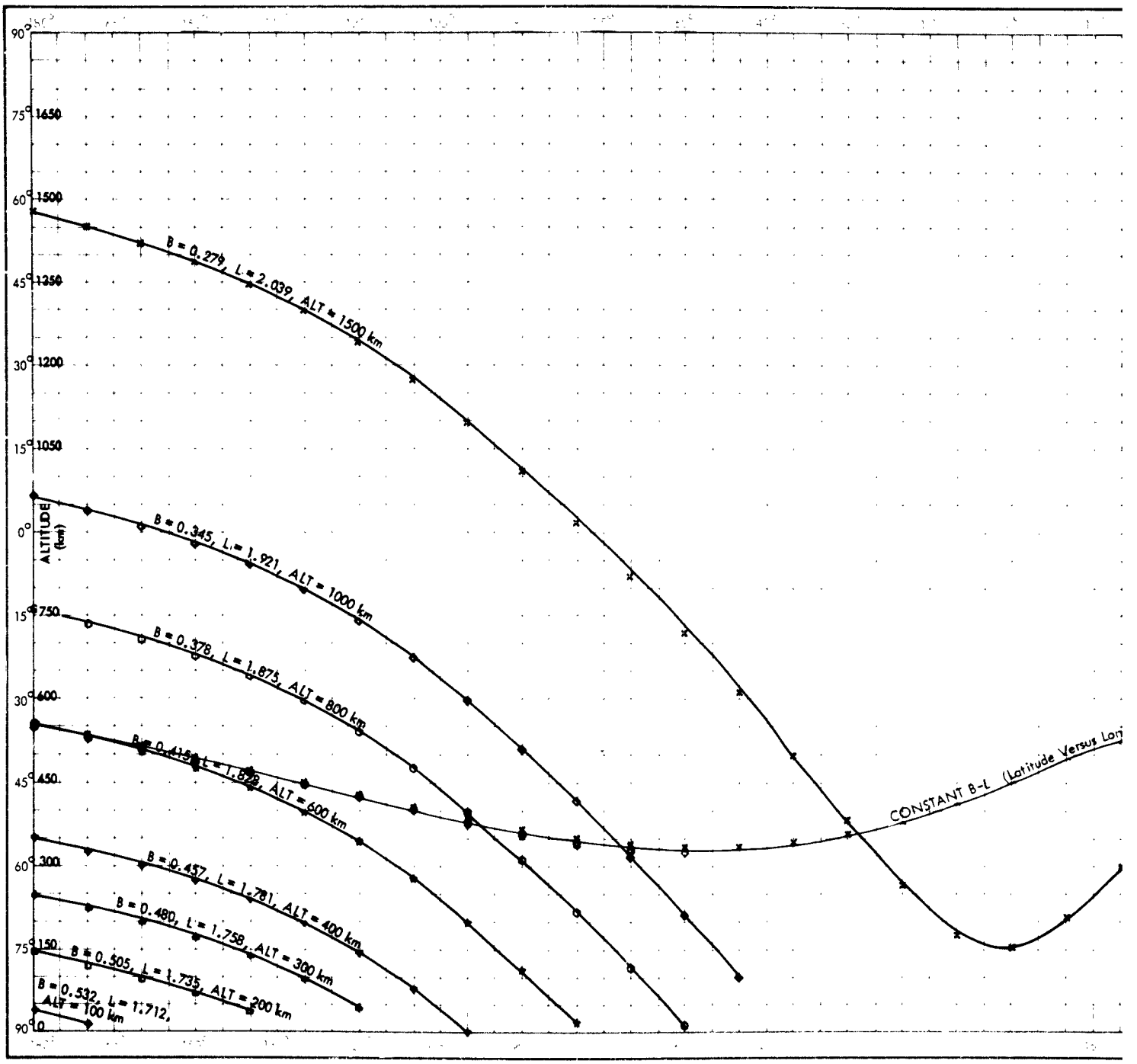

Figure 44. Constant B-L Traces in the Southern Hemisphere of the Conjugate to the Traces at
Where B is the Magnetic Field Intensity (Gauss) and L is the Magr
Note: Above the Earth's Surface the Latitude Versus Longitude Plot is Common (within a maxi

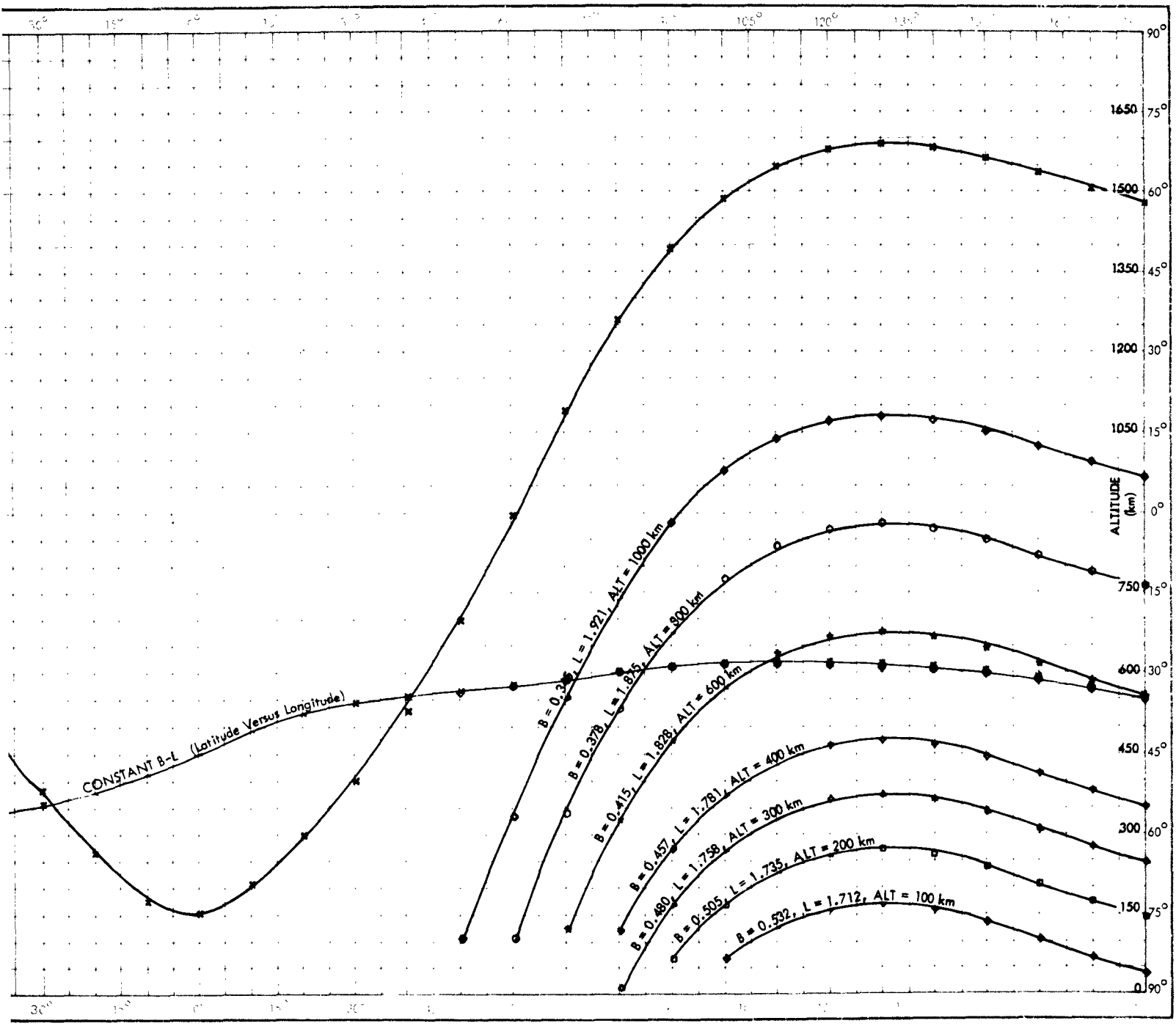

phere of the Conjugate to the Traces at Initial Latitude 46° N Initial Longitude 72° E at Various Initial Altitudes
eld Intensity (Gauss) and L is the Magnetic Shell Parameter (in Earth Radii)
ongitude Plot is Common (within a maximum Deviation of ± 1.5° Latitude) for all Altitudes Considered

F. DIFFERENCES BETWEEN CONSTANT B-L TRACES

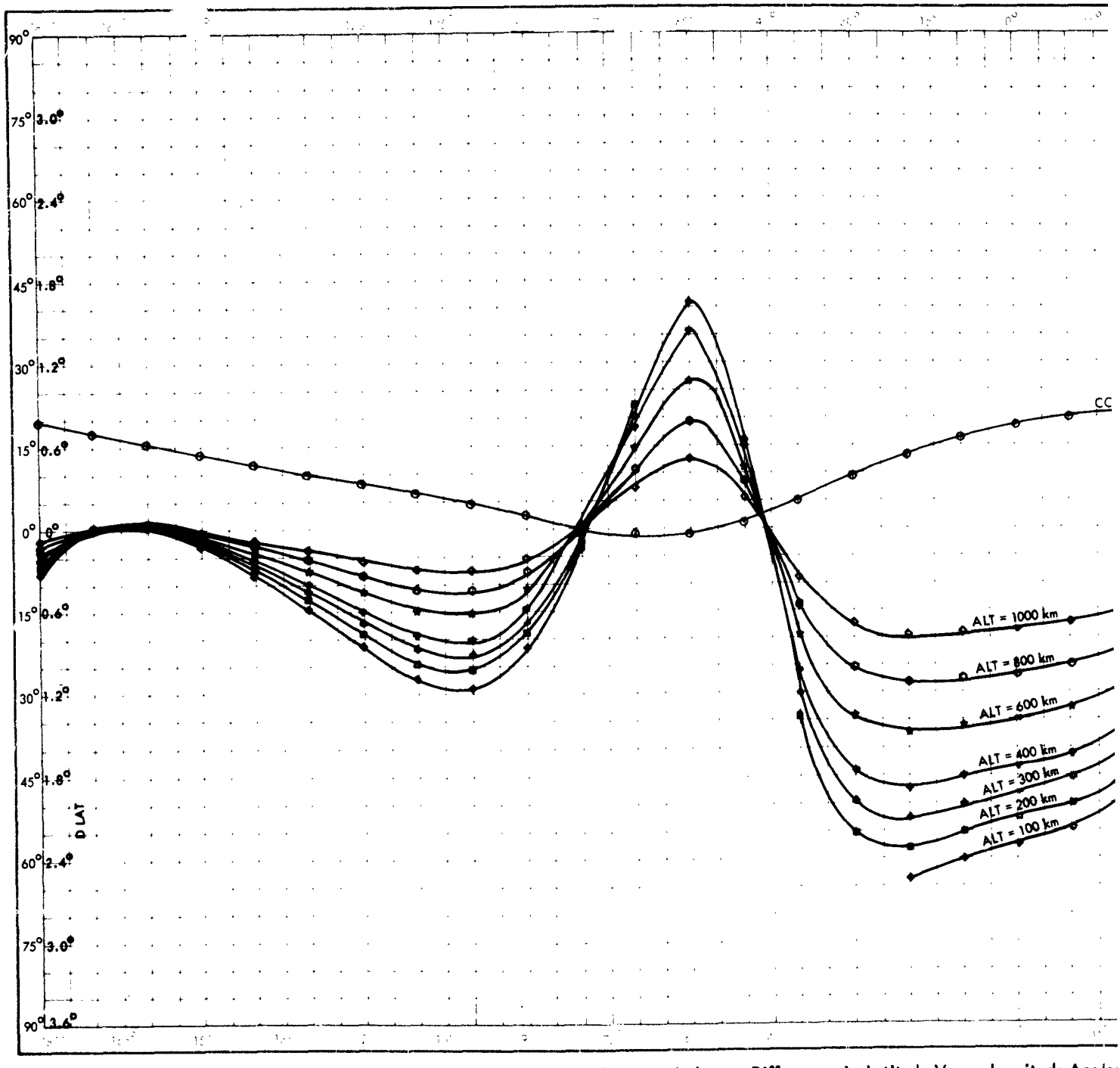

Figure 45. Northern Hemisphere - Differences in Latitude Versus Longitude Angles and Those Traces Having the Same Initial Latitude 17.5° N, Longit

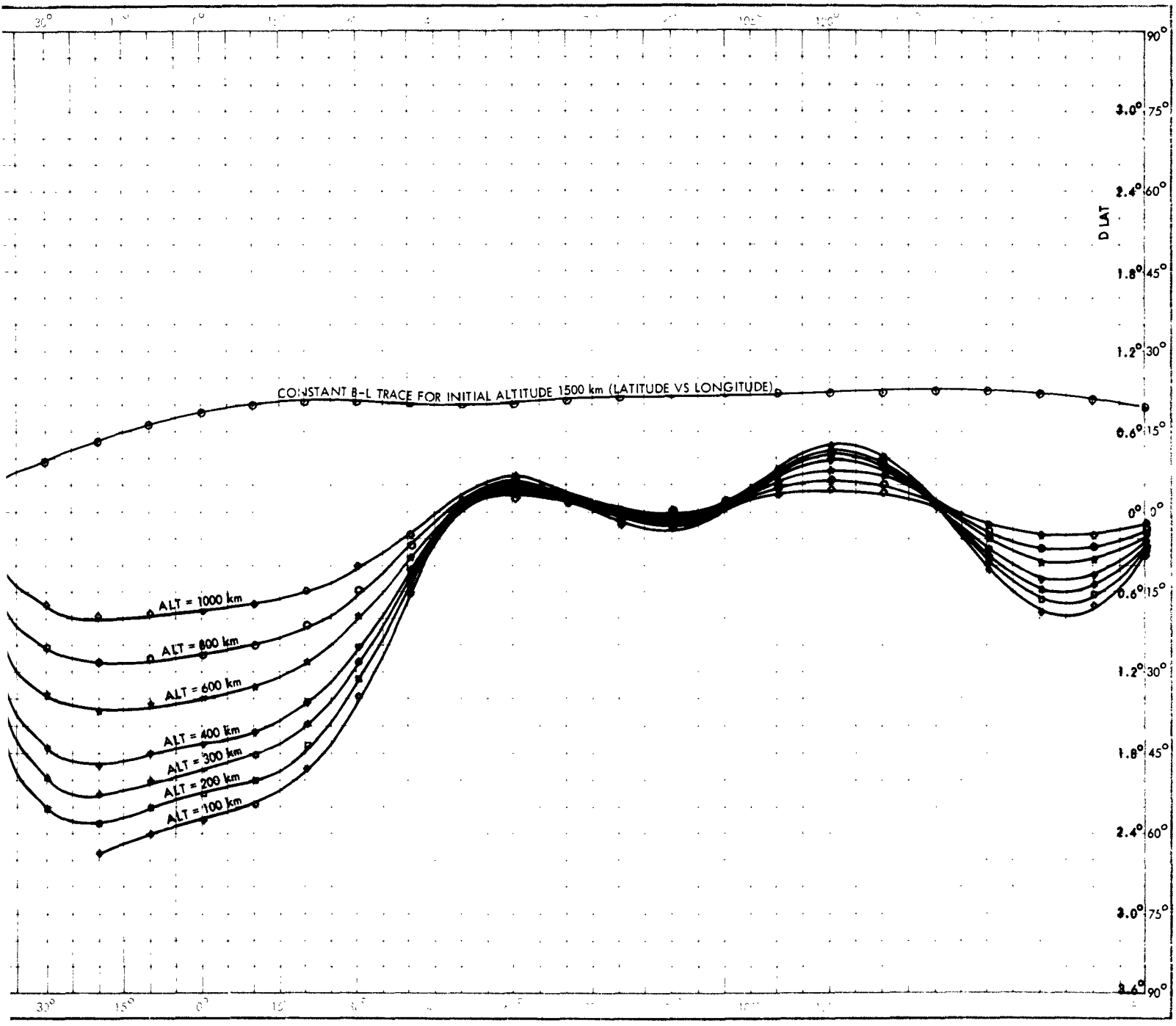

es in Latitude Versus Longitude Angles from the Constant B-L Trace at Initial Altitude of 1500 km
Same Initial Latitude 17.5° N, Longitude 190° E but Different Initial Altitudes

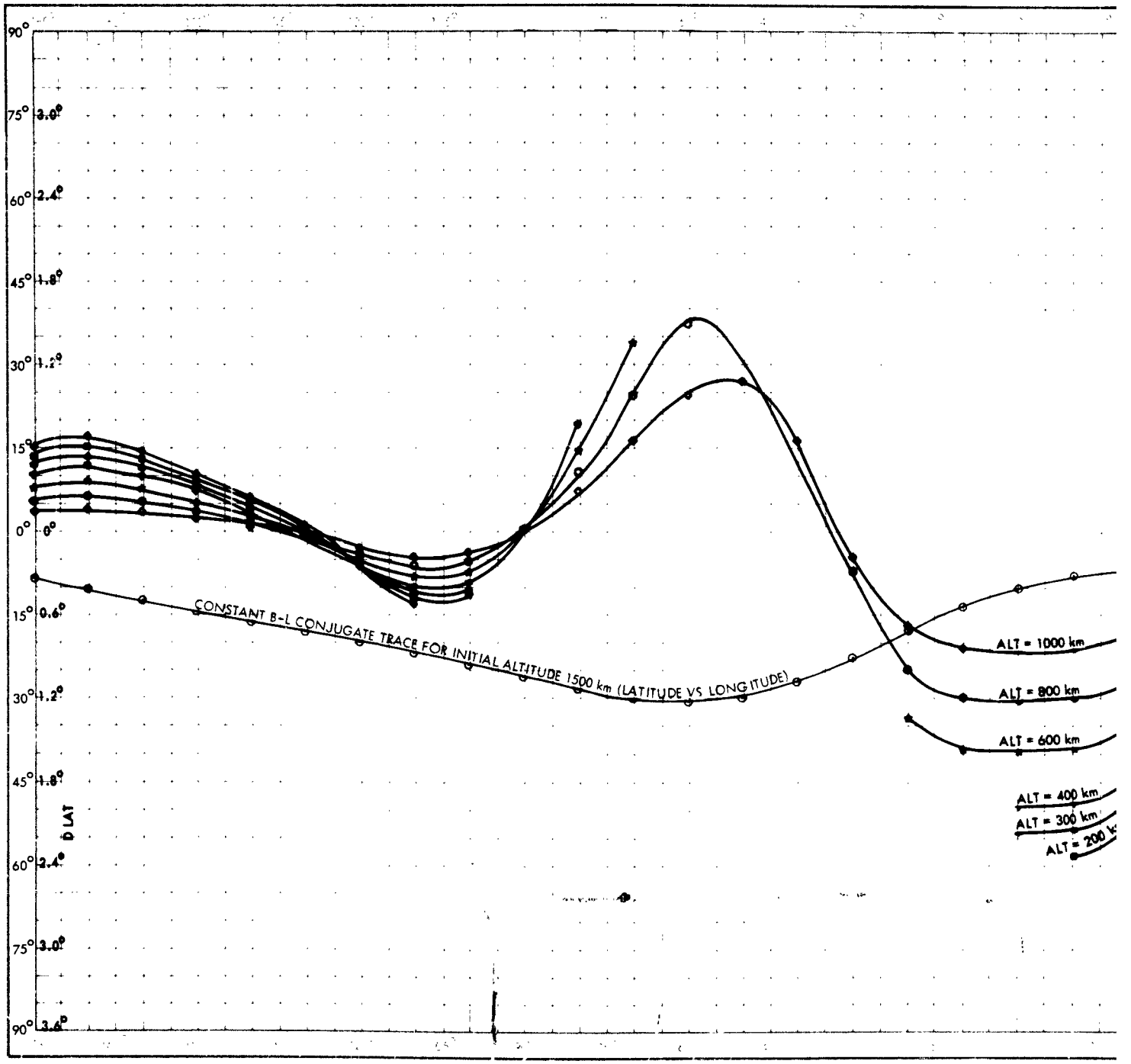

Figure 46. Southern Hemisphere - Differences in Latitude Versus Longitude Angles of 1500 km and Those Conjugate Traces Having the Same Initial Latitude 17.5°

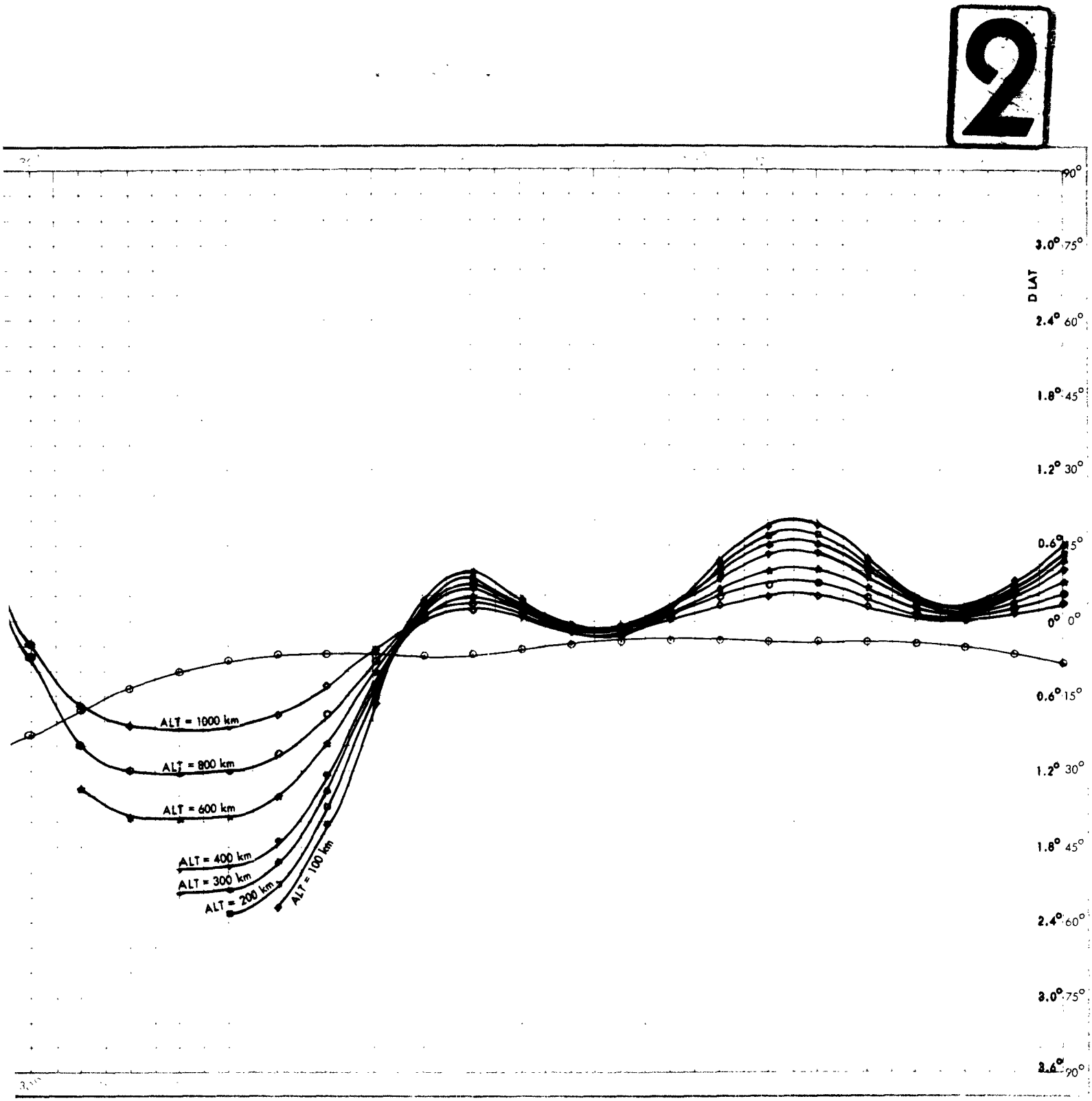

in Latitude Versus Longitude Angles from the Constant B-L Conjugate Trace at Initial Altitude
ving the Same Initial Latitude 17.5° N, Longitude 190° E but at Different Initial Altitudes

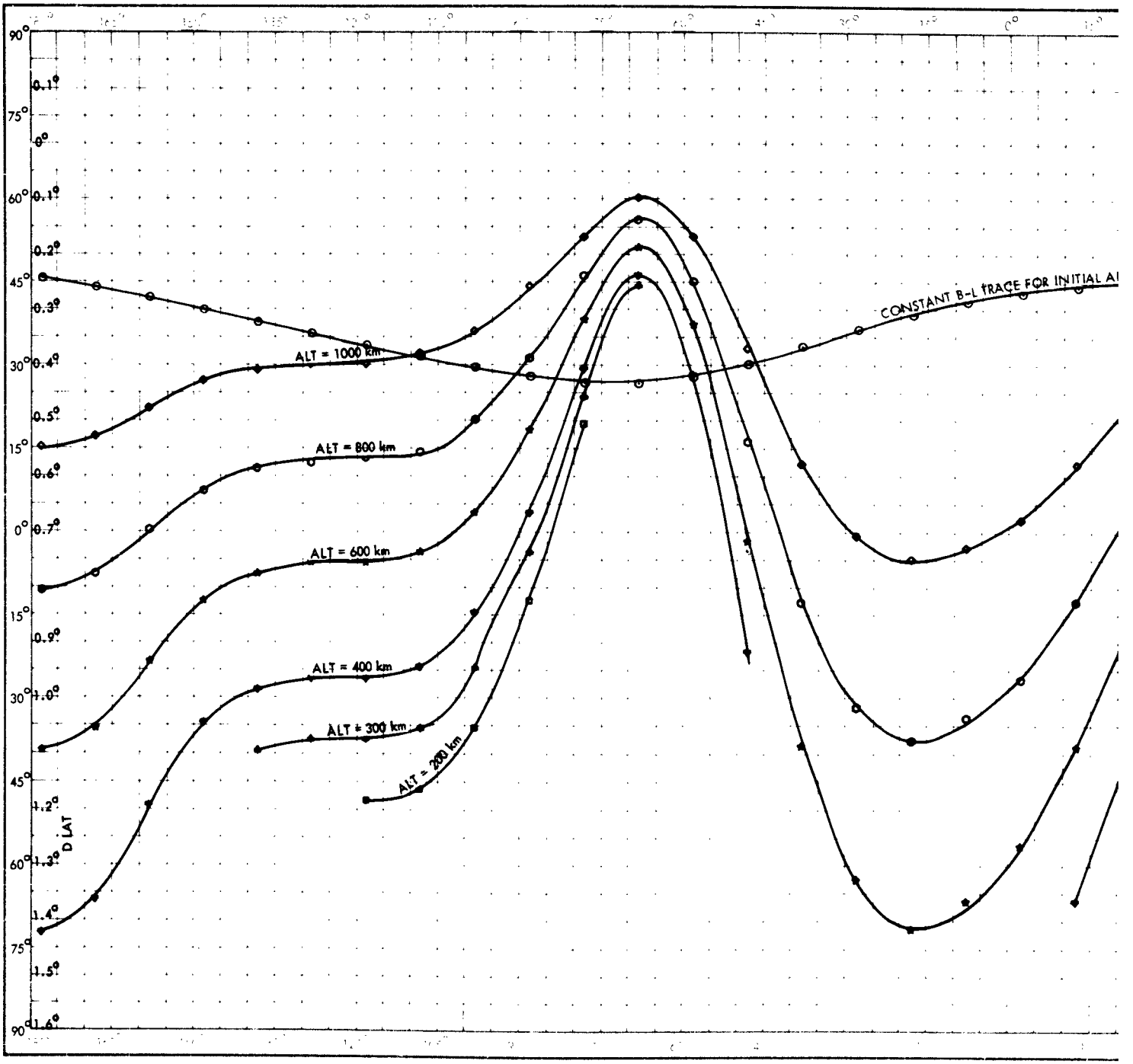

Figure 47. Northern Hemisphere - Differences in Latitude Versus Longitude Angles
and Those Traces Having the Same Initial Latitude 46° N, Longitud

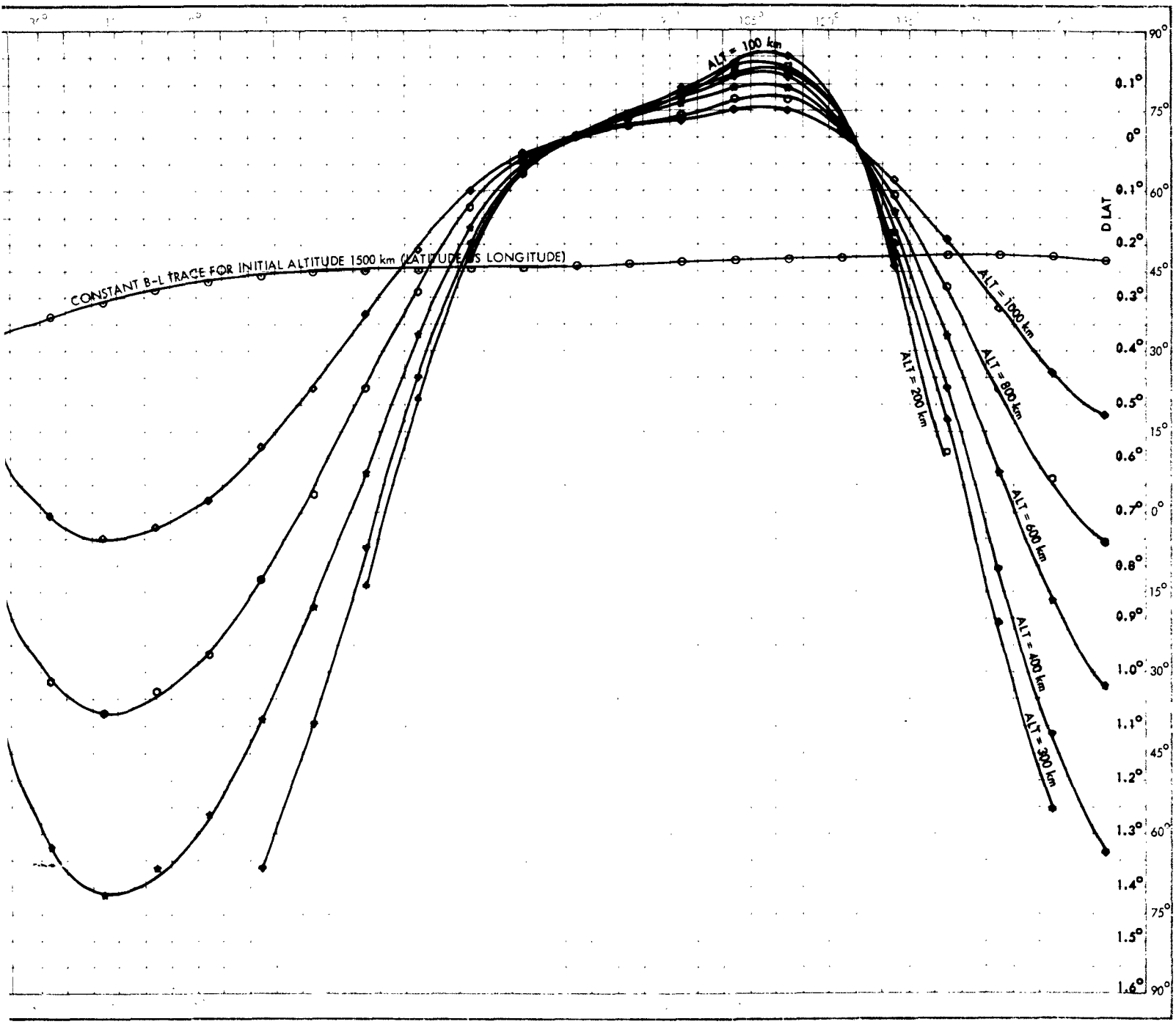

ls in Latitude Versus Longitude Angles from the Constant B-L Trace at Initial Altitude of 1500 km
Same Initial Latitude 46° N, Longitude 72° E but Different Initial Altitudes

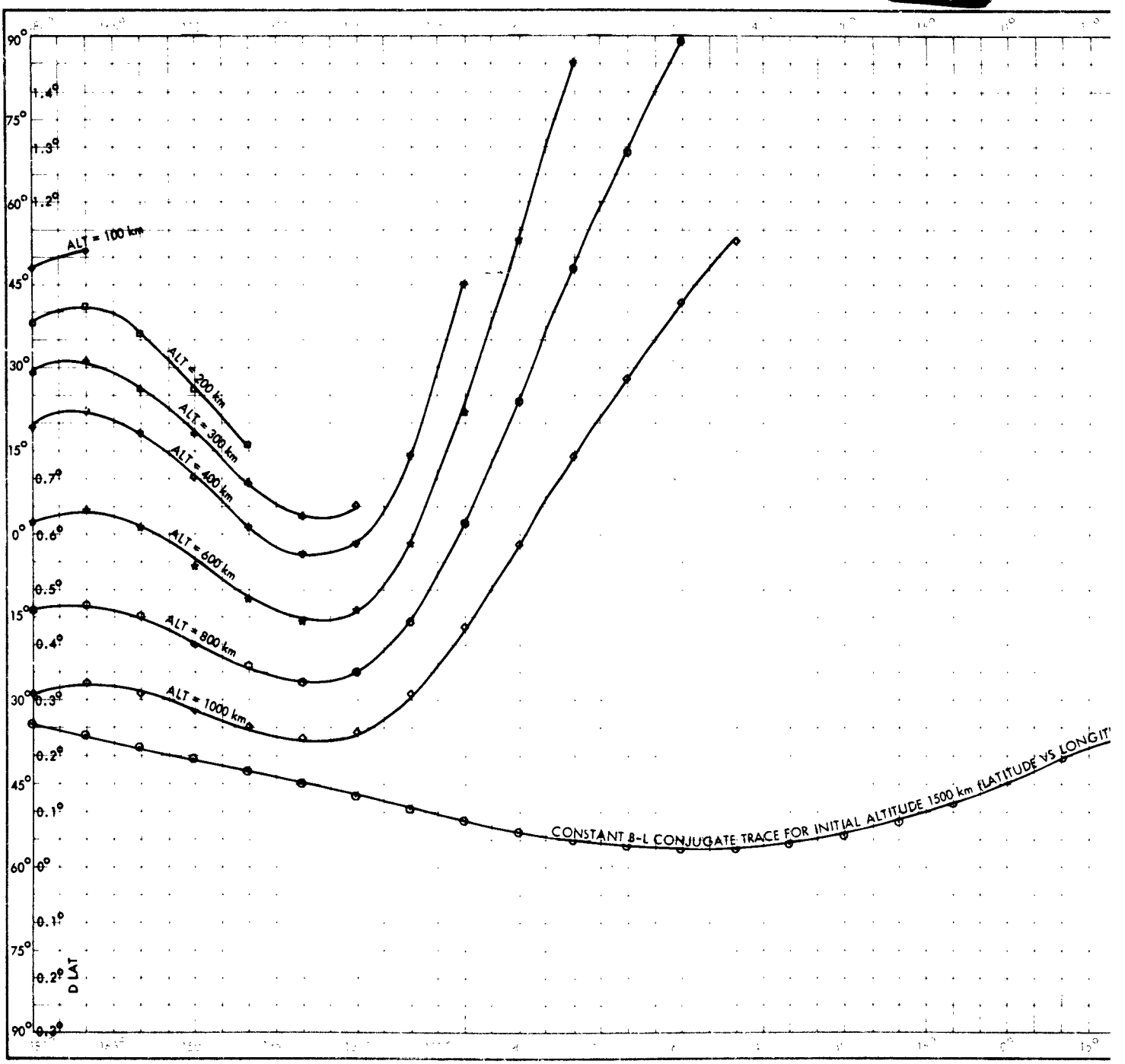

Figure 48. Southern Hemisphere - Differences in Latitude Versus Longitude Angles f
of 1500 km and Those Conjugate Traces Having the Same Initial Latitude 46° N,

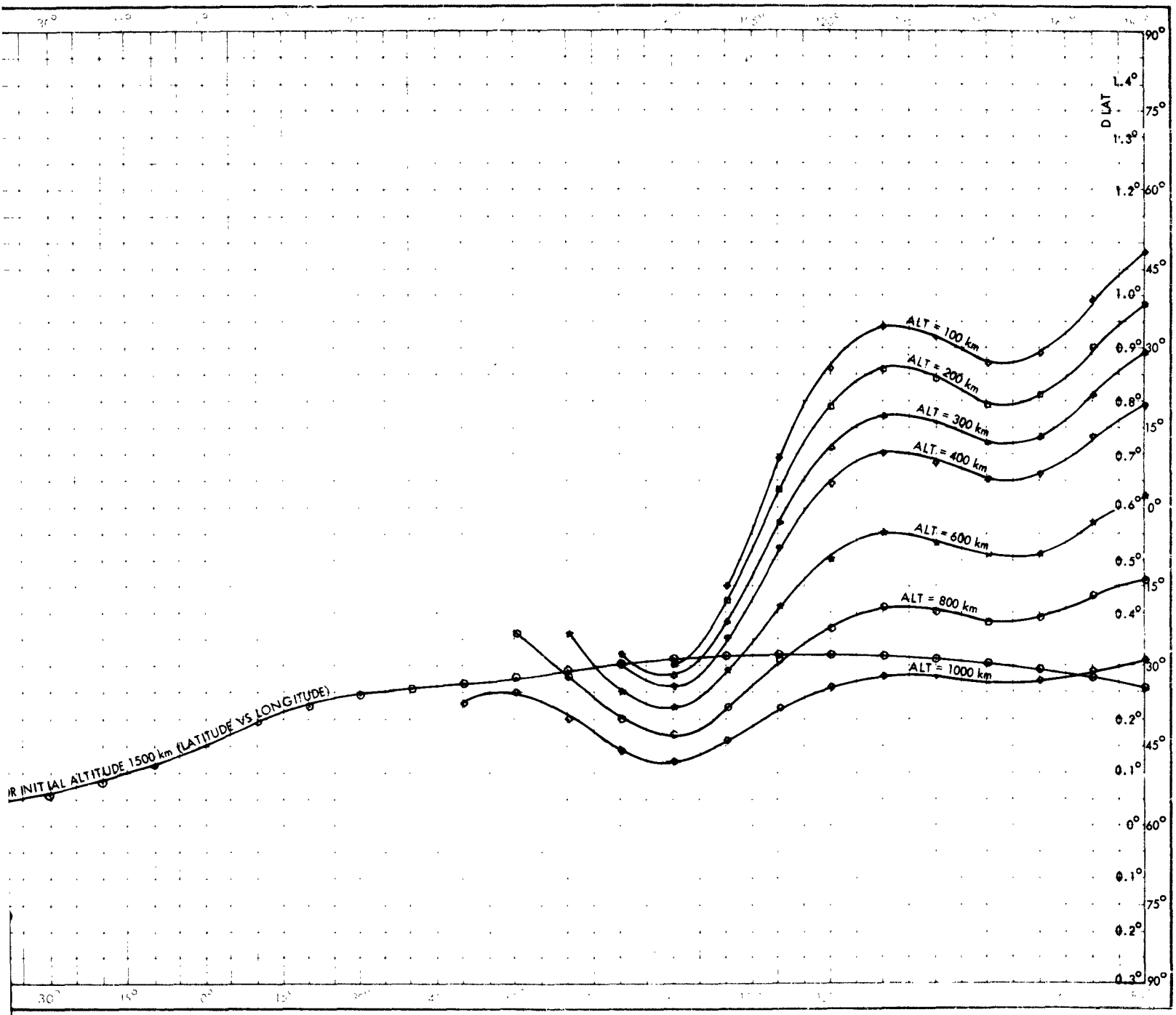

s in Latitude Versus Longitude Angles from the Constant B-L Conjugate Trace at Initial Altitude
having the Same Initial Latitude 46° N, Longitude 72° E but at Different Initial Altitudes

G. PAIRS OF CONJUGATE B-L TRACES

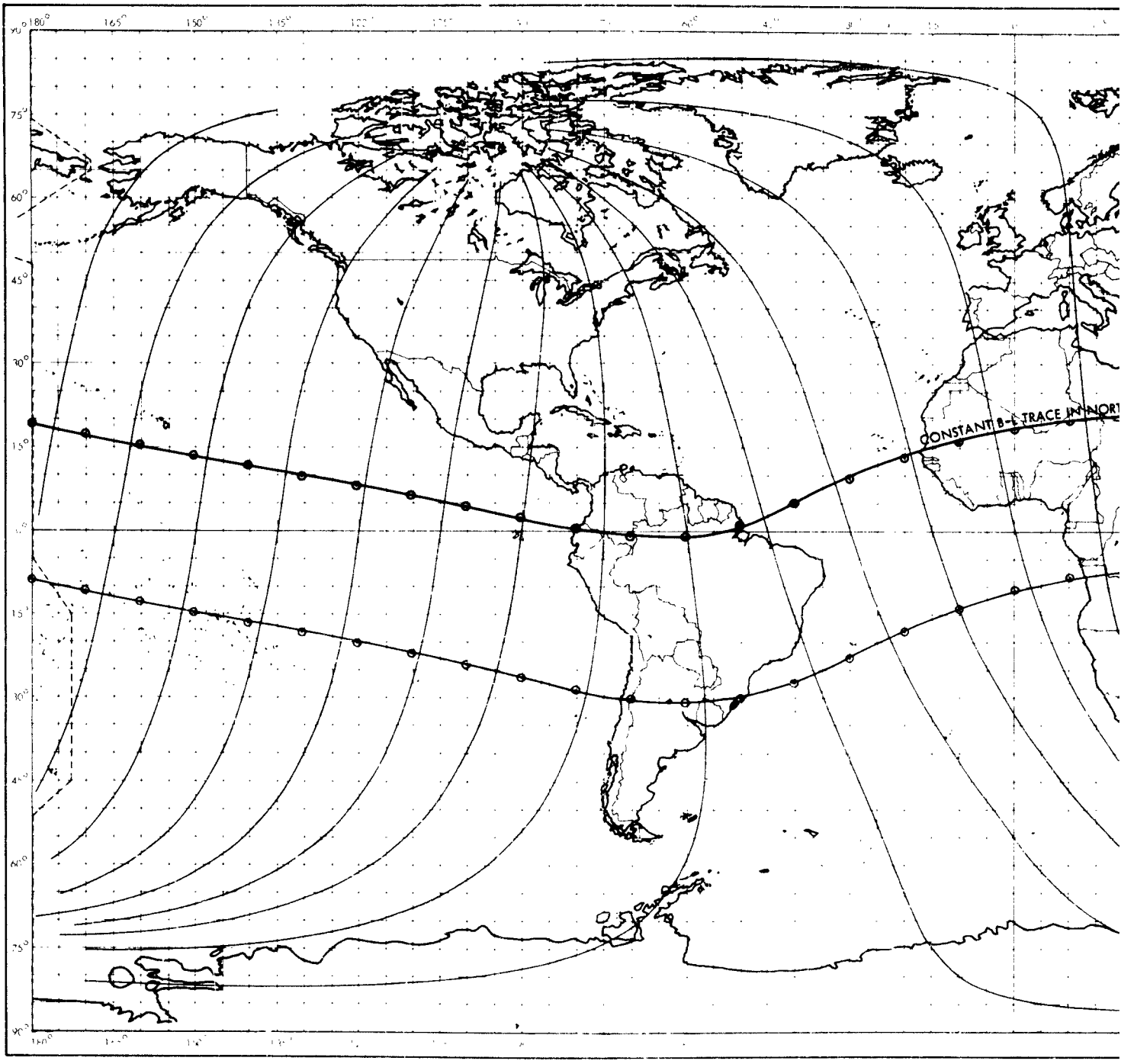

Figure 49. Constant B-L Trace in the Northern Hem
of 1500 km, Initial Latitude 17.5° N and Initial L
Conjugate Trace in the Southern He

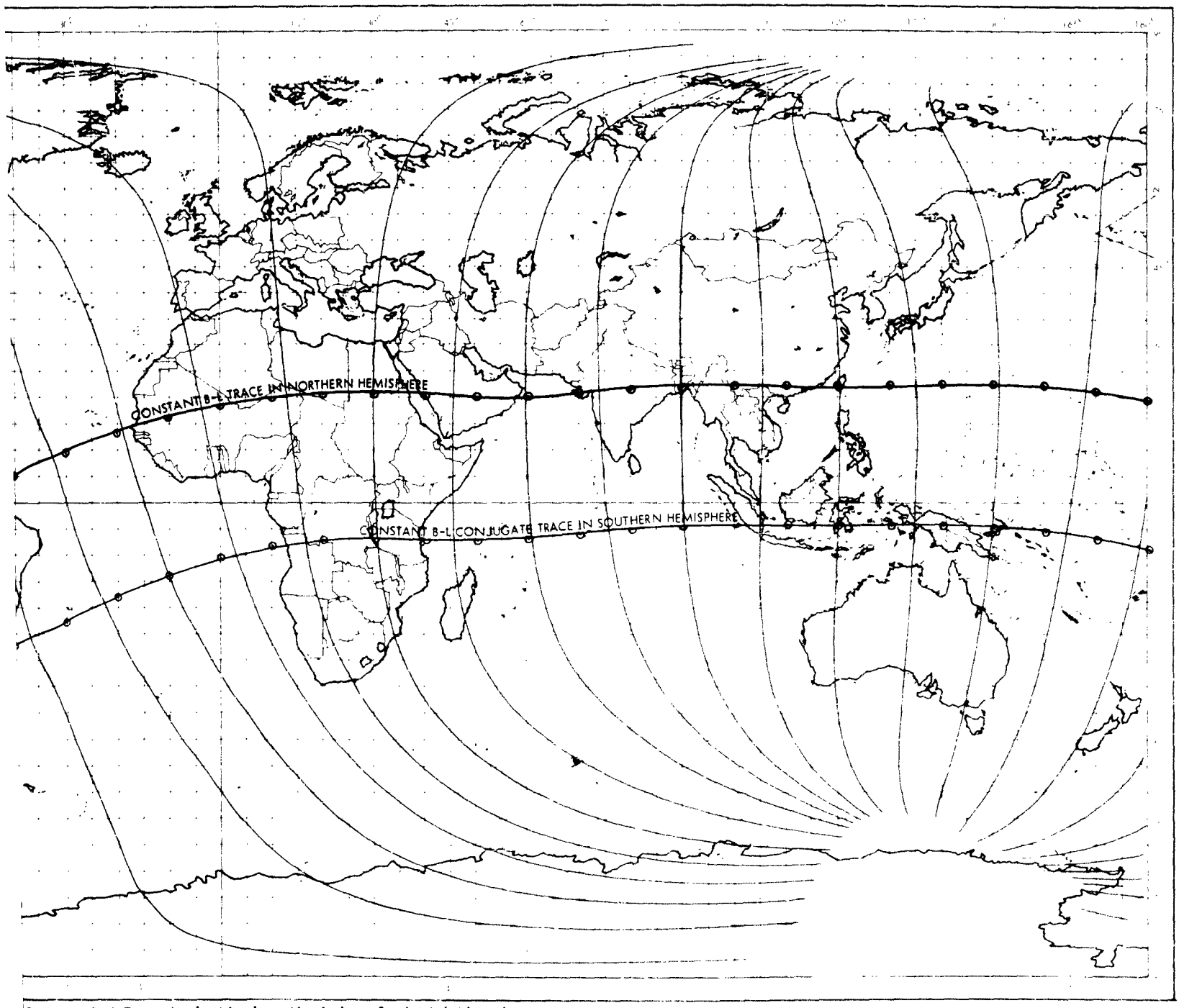

Constant B-L Trace in the Northern Hemisphere for Initial Altitude
, Initial Latitude 17.5° N and Initial Longitude 190° E Also its
Conjugate Trace in the Southern Hemisphere

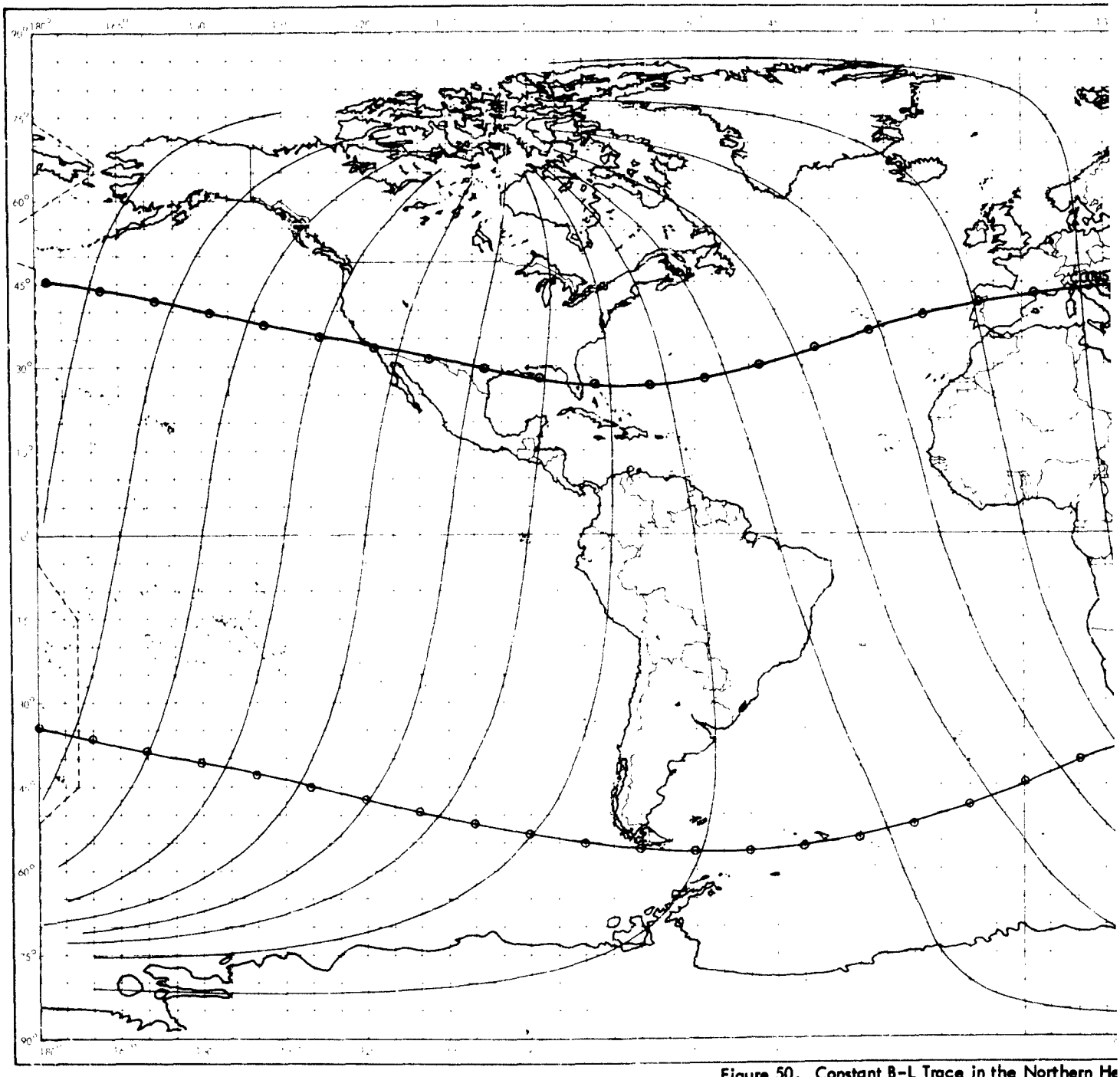

Figure 50. Constant B-L Trace in the Northern He
of 1500 km, Initial Latitude 46° N and Initial
Conjugate Trace in the Southern

2

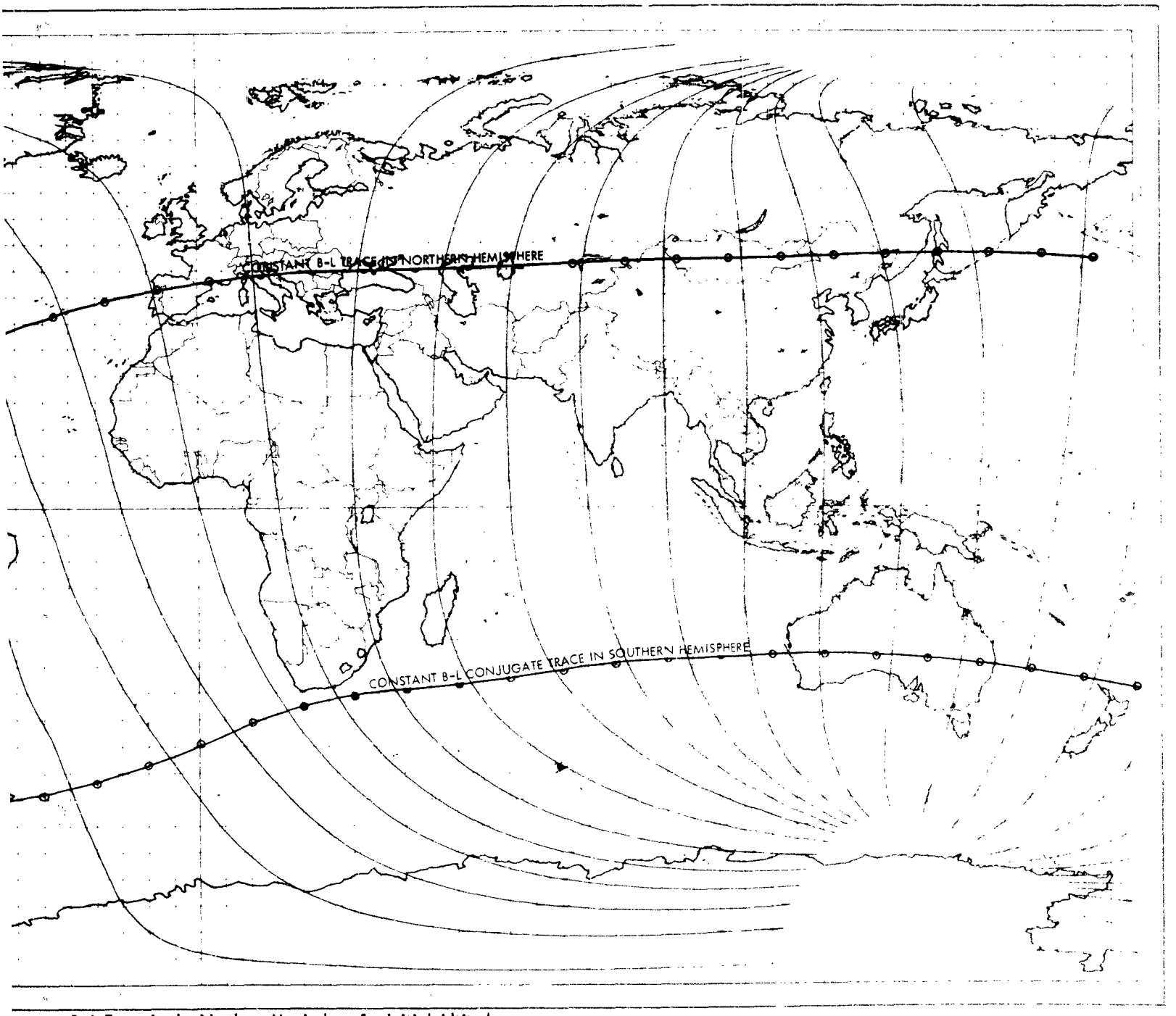

onstant B-L Trace in the Northern Hemisphere for Initial Altitude
Initial Latitude 46° N and Initial Longitude 72° E Also its
Conjugate Trace in the Southern Hemisphere

H. THE GEOMAGNETIC EQUATOR

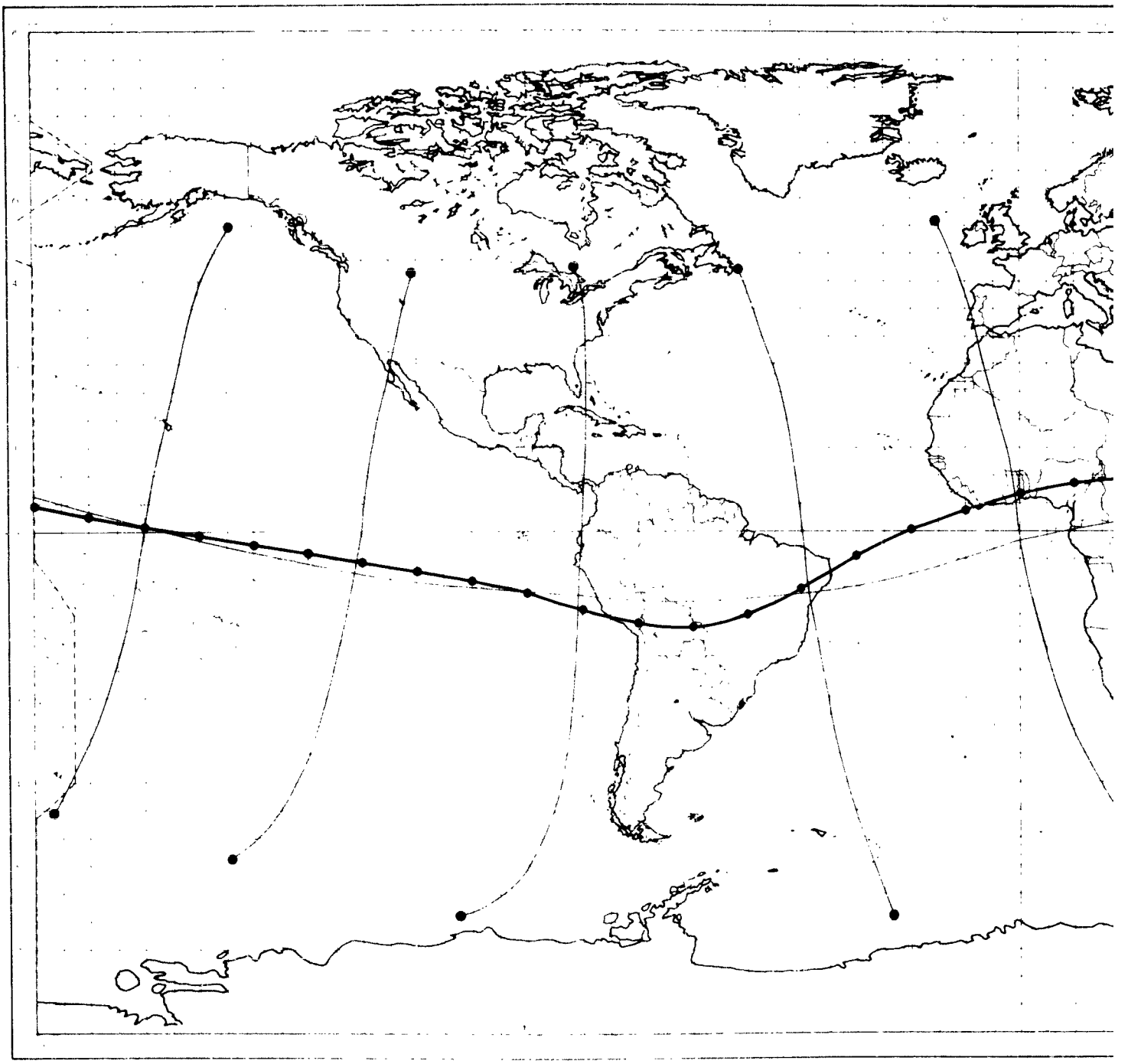

NOTE: THE EQUATOR AT 1500 km ALTITUDE DIFFERS FROM THIS BY LESS THAN 3° OF LATITUDE

Figure 51. Position of the Geomagnetic Equat

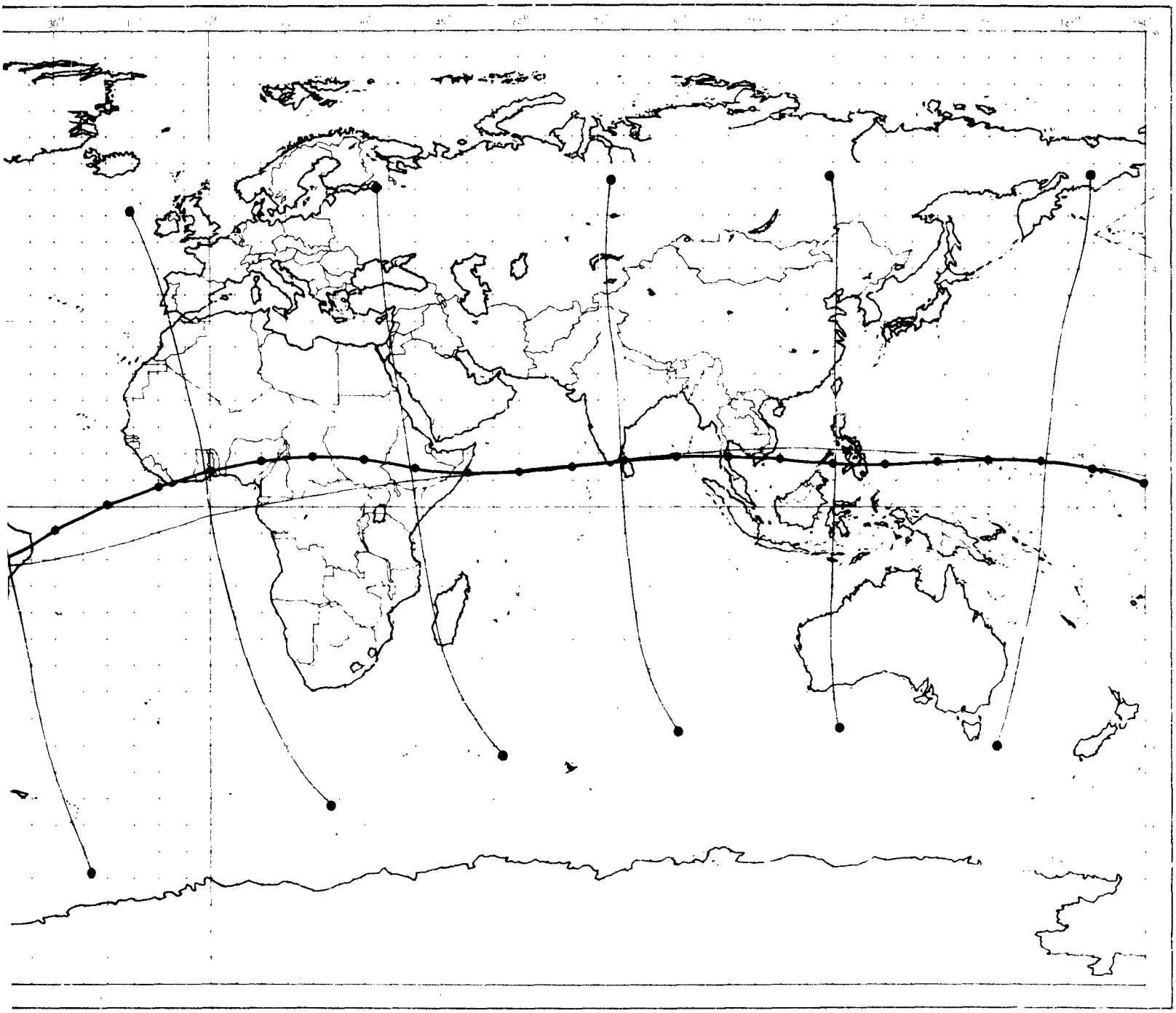

51. Position of the Geomagnetic Equator at 100km. Altitude

I. APPROXIMATE GEOMAGNETIC SHELL LATITUDES

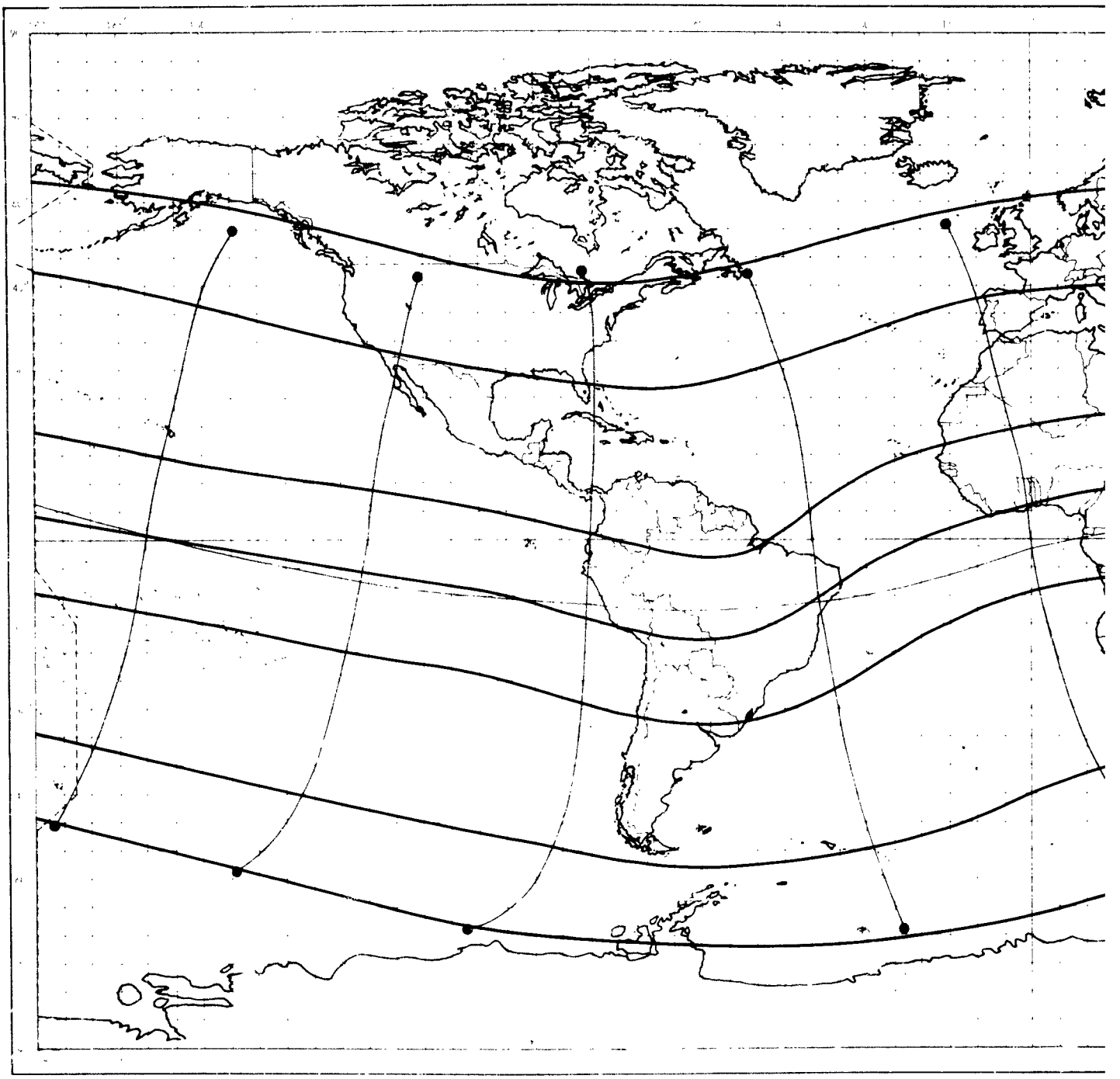

Figure 52. Approximate Geomagne

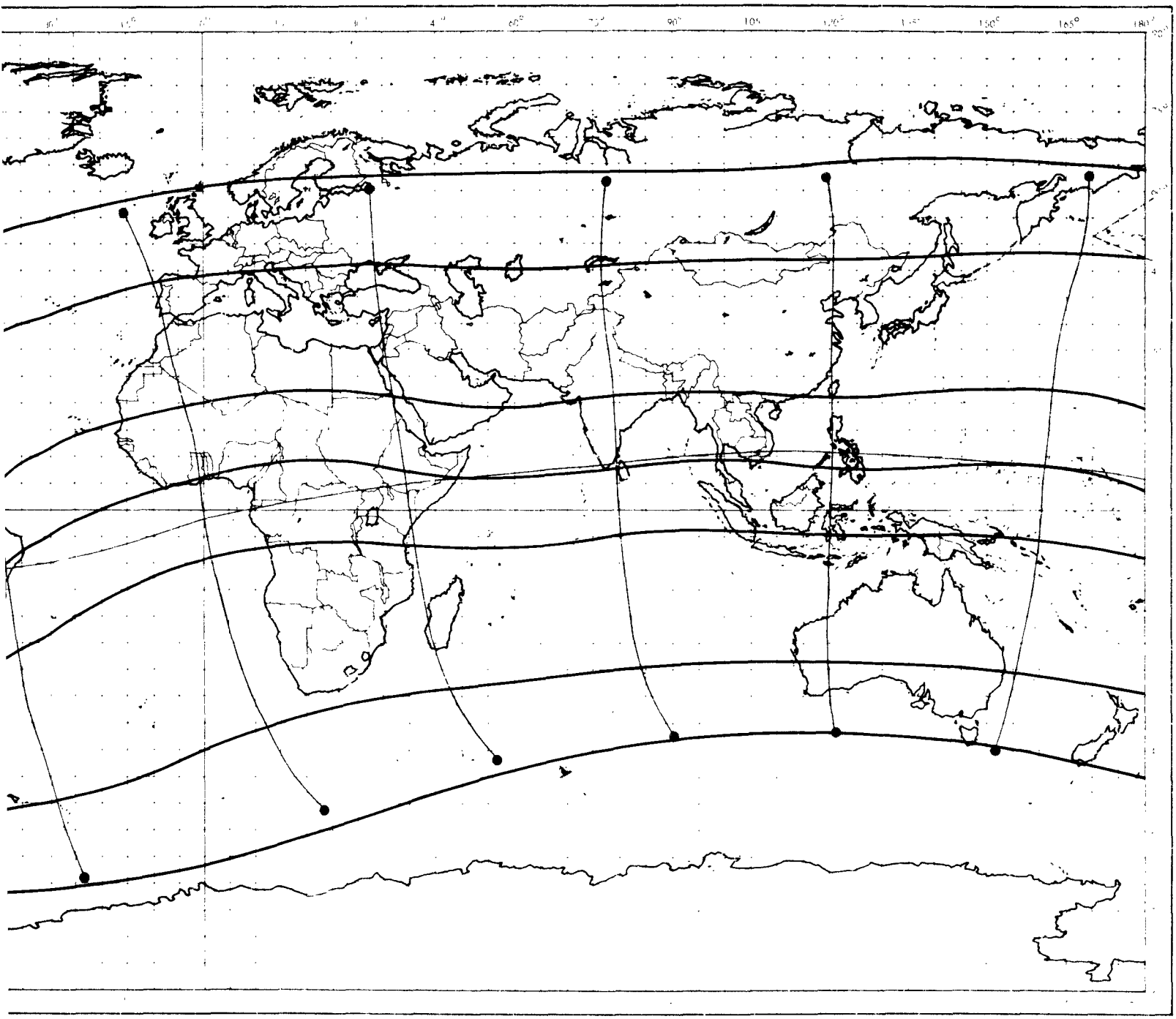

Figure 52. Approximate Geomagnetic Shell Latitudes

J. CONJUGATE AURORAL GRIDS

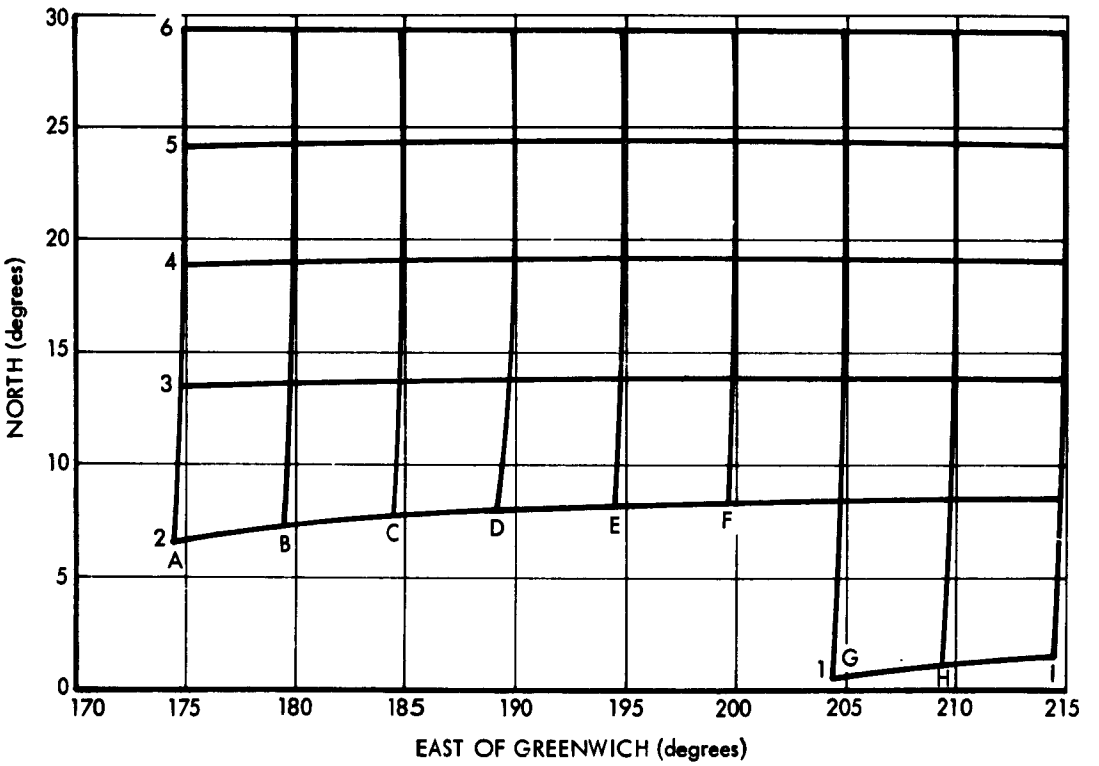

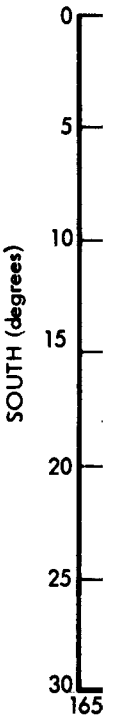

Figure 53. Auroral Conjugate Grids for Pacifi

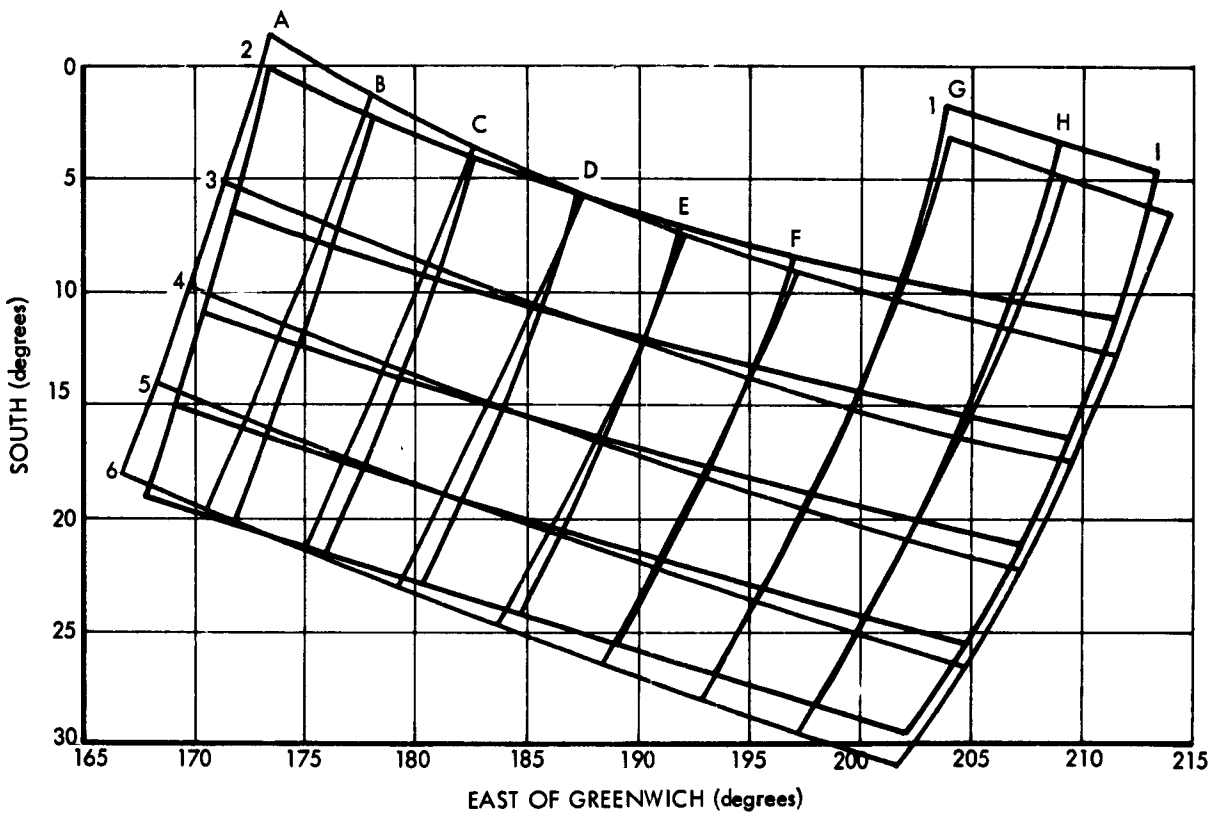

NOTE: Southern Conjugate Grids are Calculated Using Jensen and Whitaker Coefficients and Using Jensen and Cain Coefficients

). Auroral Conjugate Grids for Pacific Area at 70 km

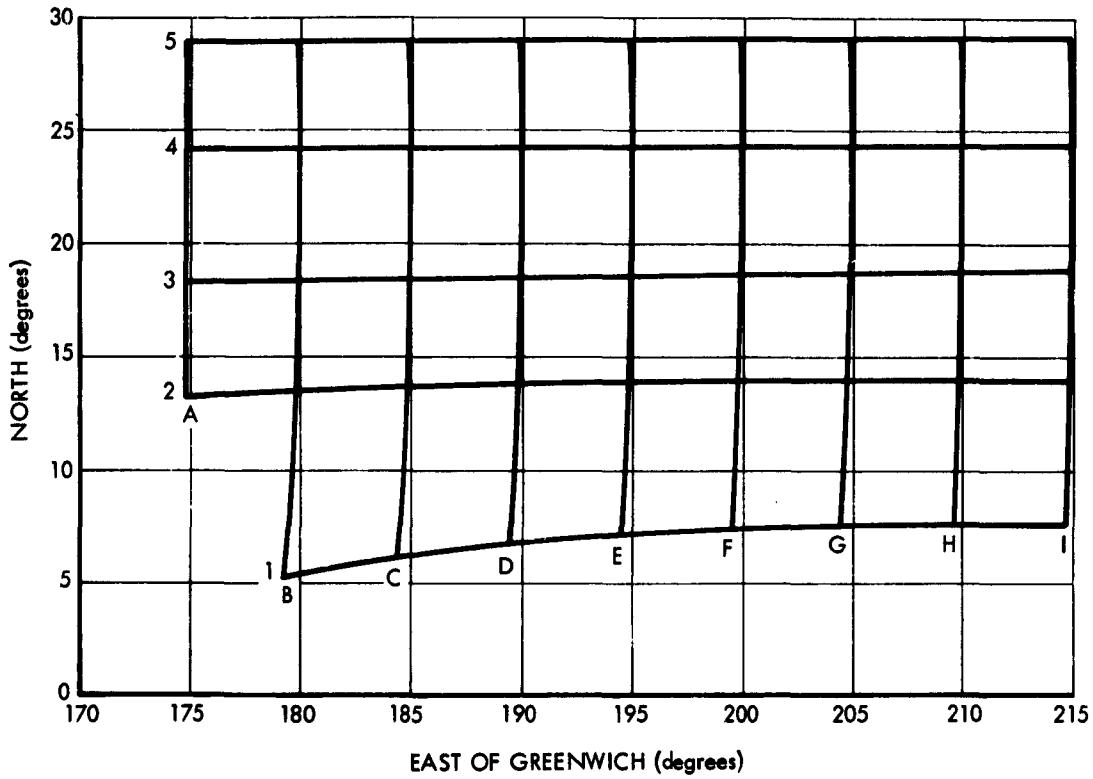

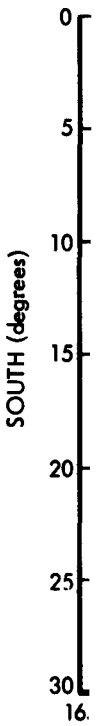

Figure 54. Auroral Conjugate Grids for Pacific

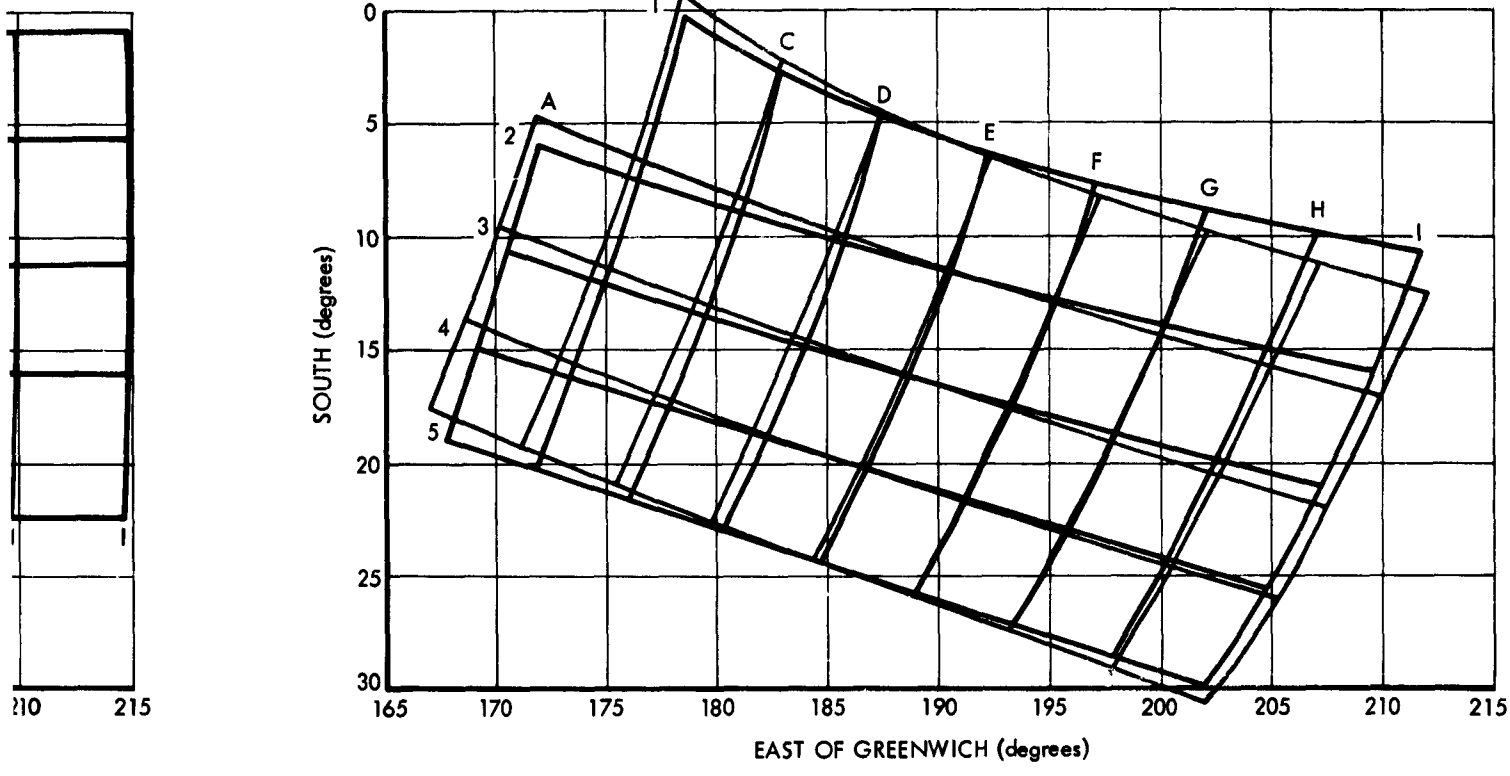

NOTE: Southern Conjugate Grids are Calculated Using Jensen and Whitaker Coefficients and Using Jensen and Cain Coefficients

Auroral Conjugate Grids for Pacific Area at 100 km

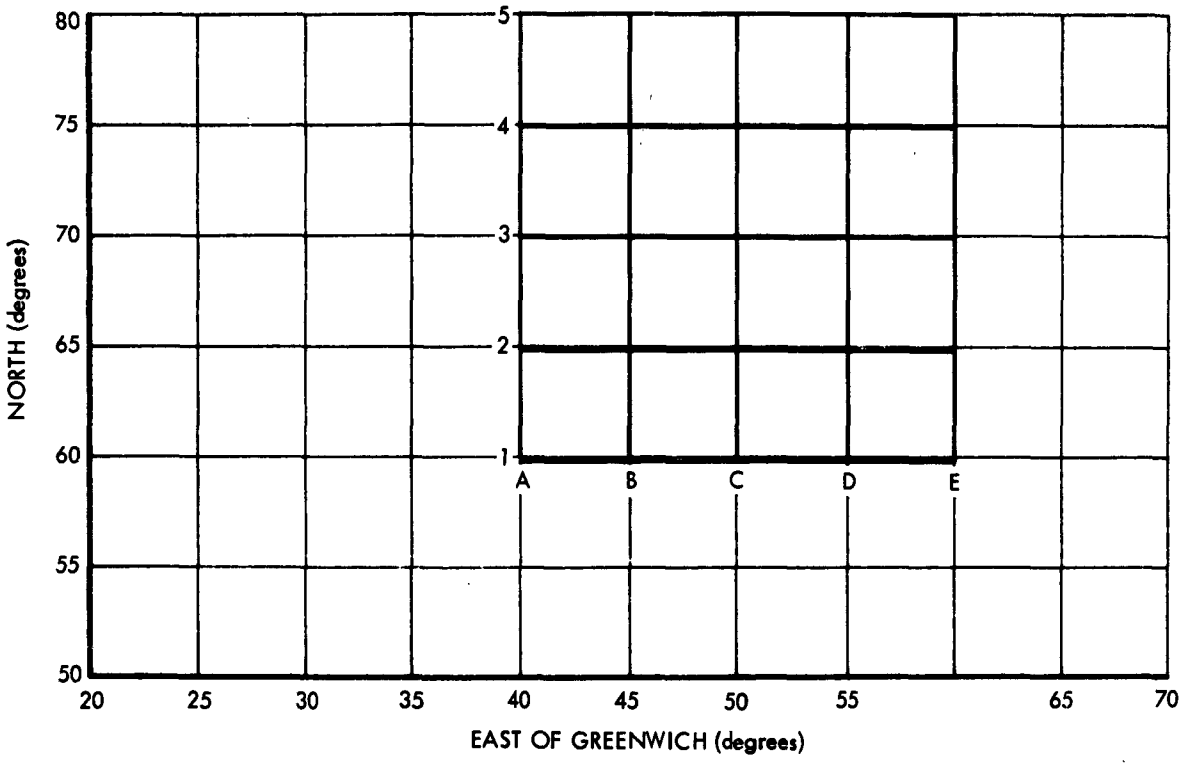

Figure 55. Auroral Conjugate Grids for North

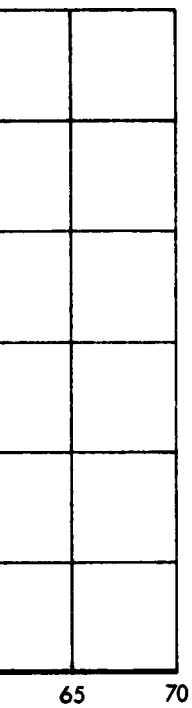

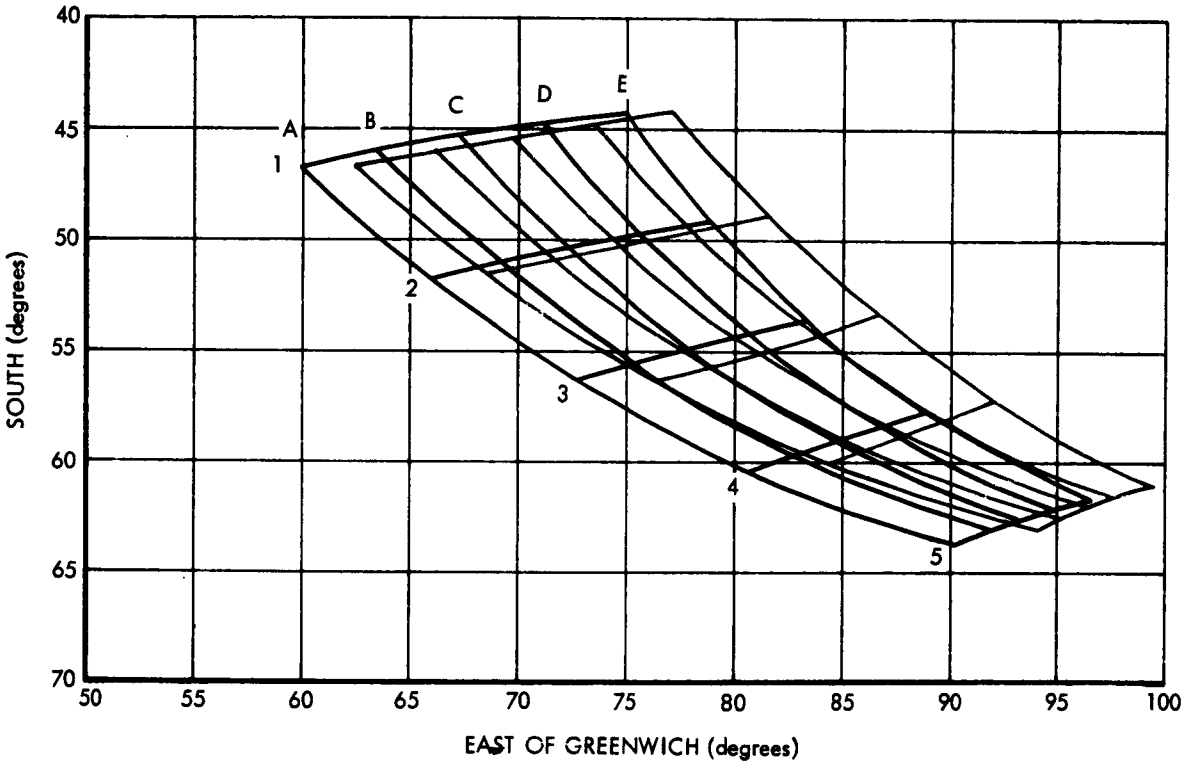

NOTE: Southern Conjugate Grids are Calculated Using Jensen and Whitaker Coefficients and Using Jensen and Cain Coefficients

. Auroral Conjugate Grids for North Eurasian Area at 70 km

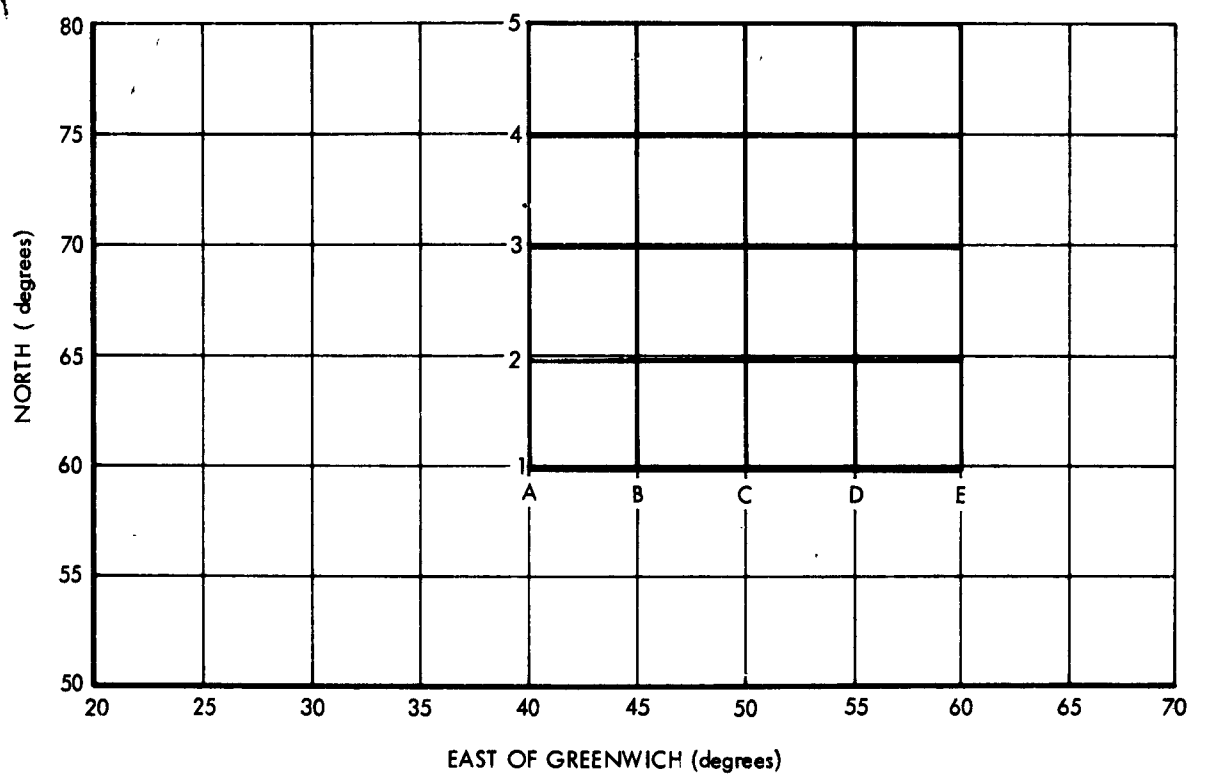

SOUTH (degrees)

Figure 56. Auroral Conjugate Grids for North

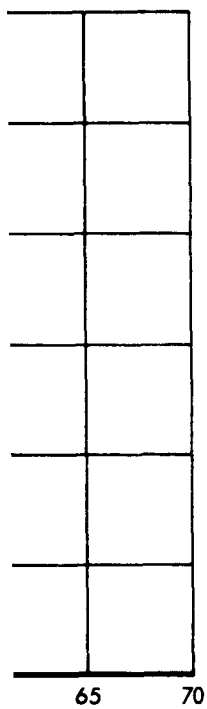

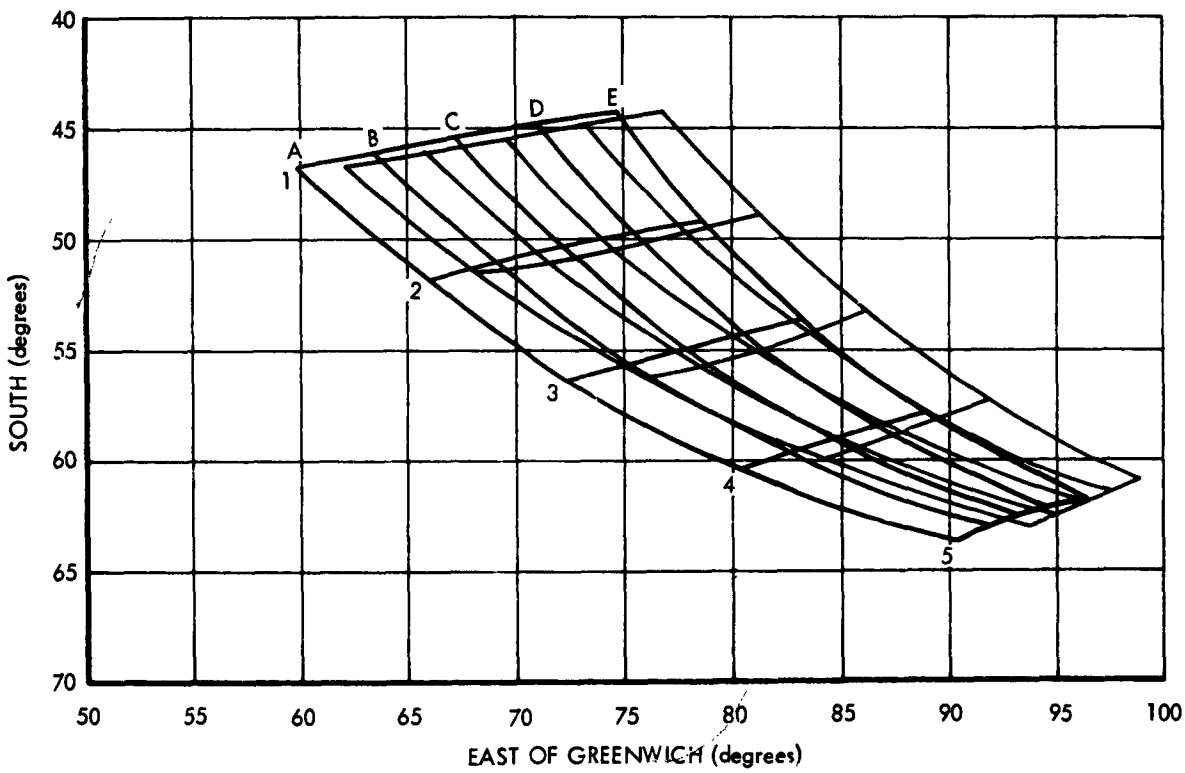

NOTE: Southern Conjugate Grids are Calculated Using Jensen and Whitaker Coefficients and Using Jensen and Cain Coefficients

Auroral Conjugate Grids for North Eurasian Area at 100 km

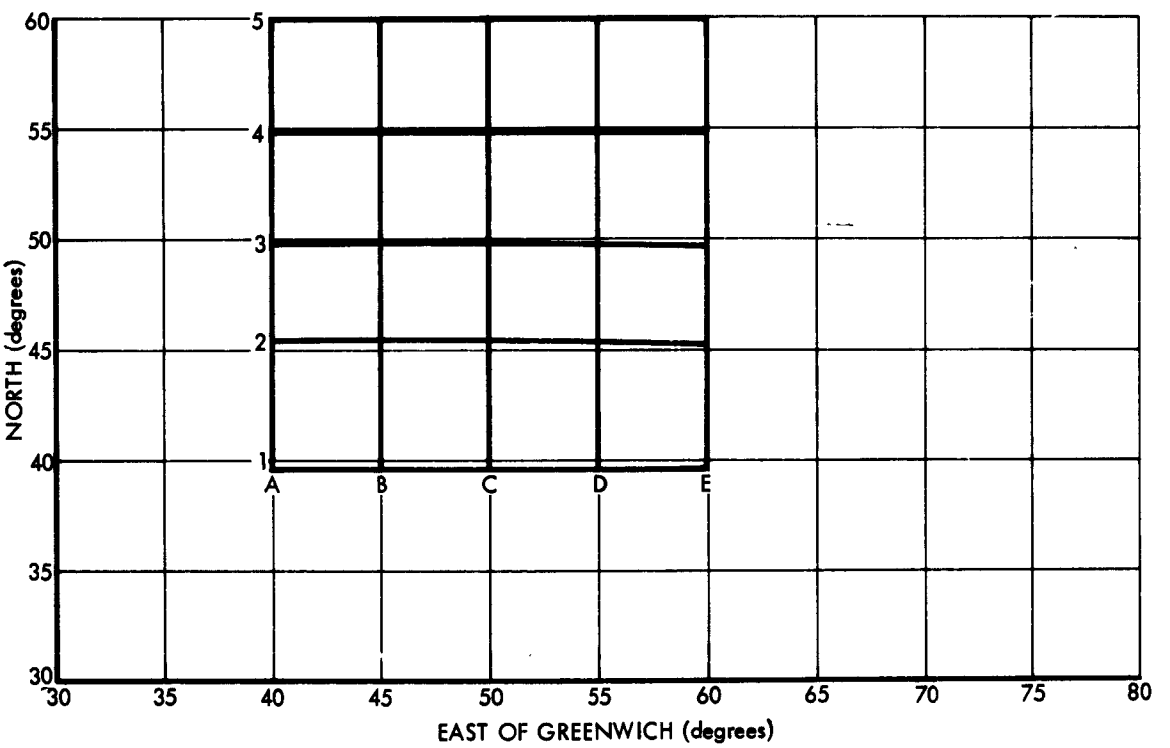

Figure 57. Auroral Conjugate Grids for W

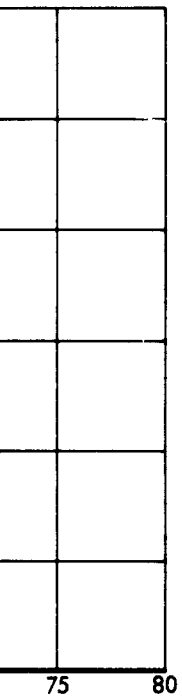

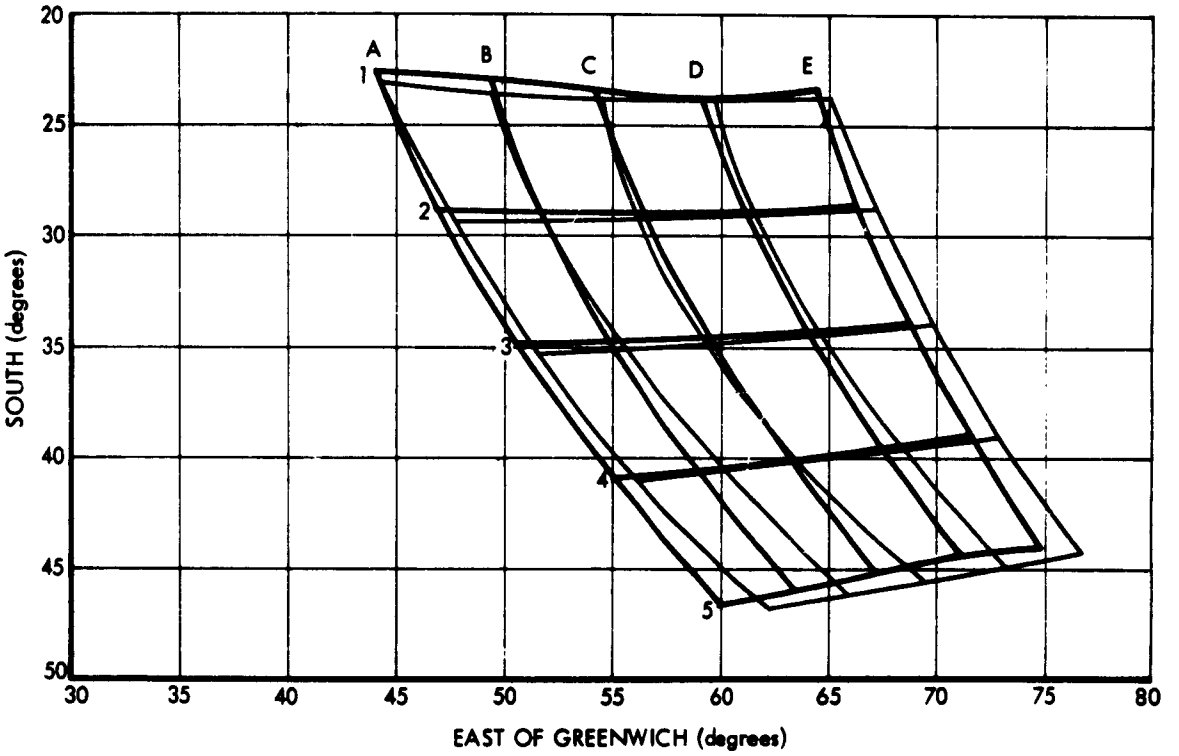

NOTE: Southern Conjugate Grids are Calculated Using Jensen and Whitaker Coefficients and Using Jensen and Cain Coefficients

57. Auroral Conjugate Grids for West Eurasian Area at 70 km

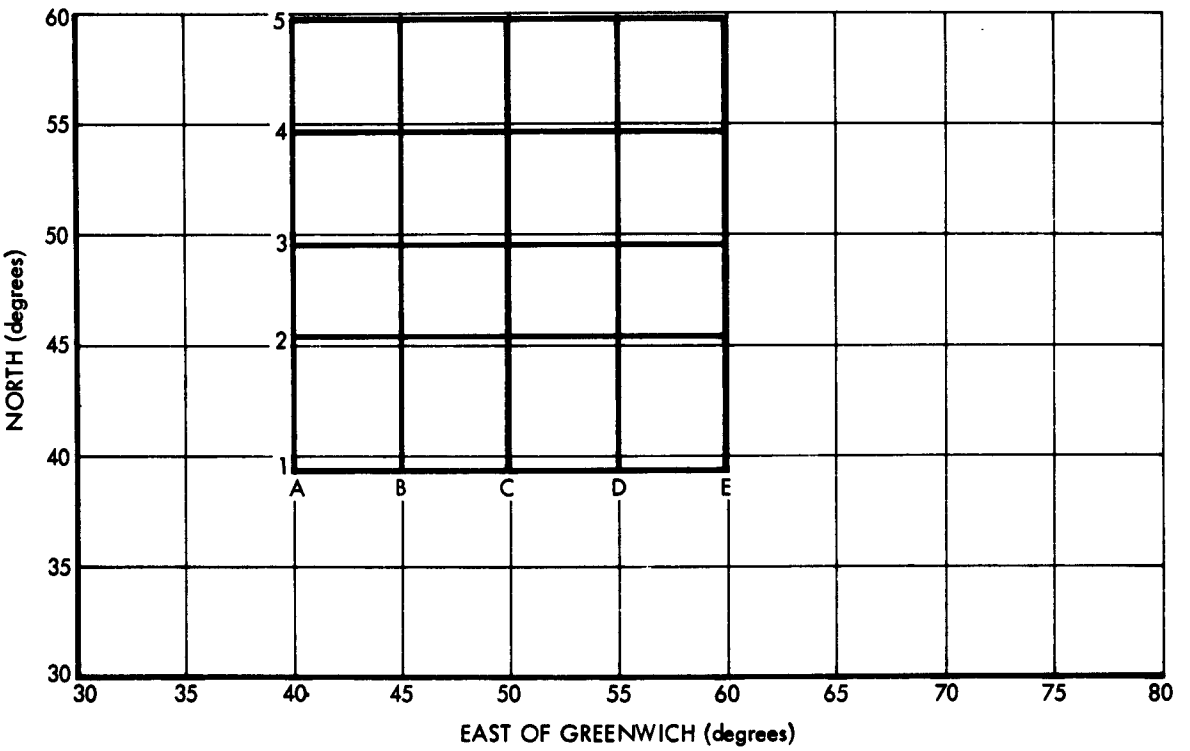

Figure 58. Auroral Conjugate Grids for West Eu

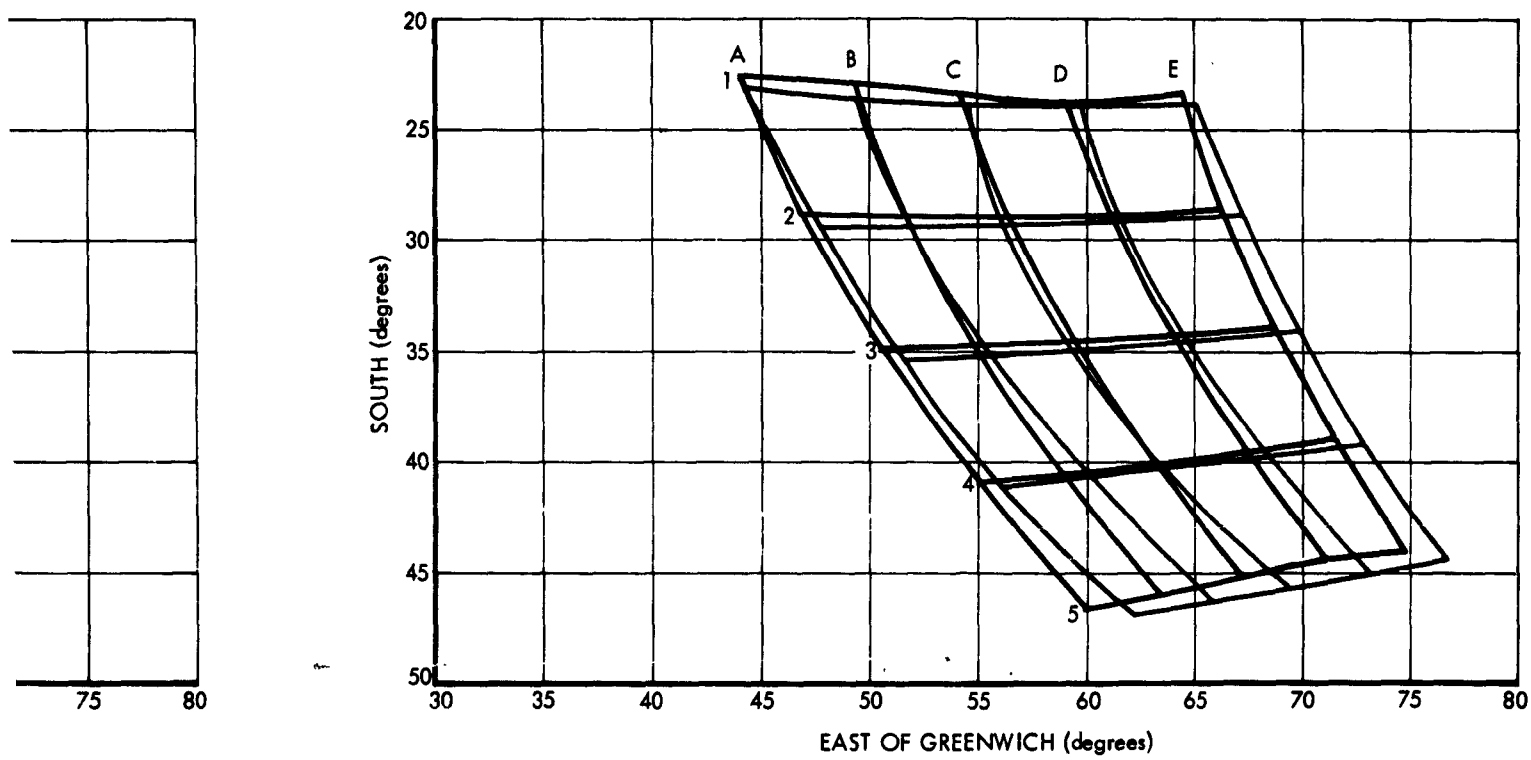

NOTE: Southern Conjugate Grids are Calculated Using Jensen and Whitaker Coefficients and Using Jensen and Cain Coefficients

Auroral Conjugate Grids for West Eurasian Area at 100 km

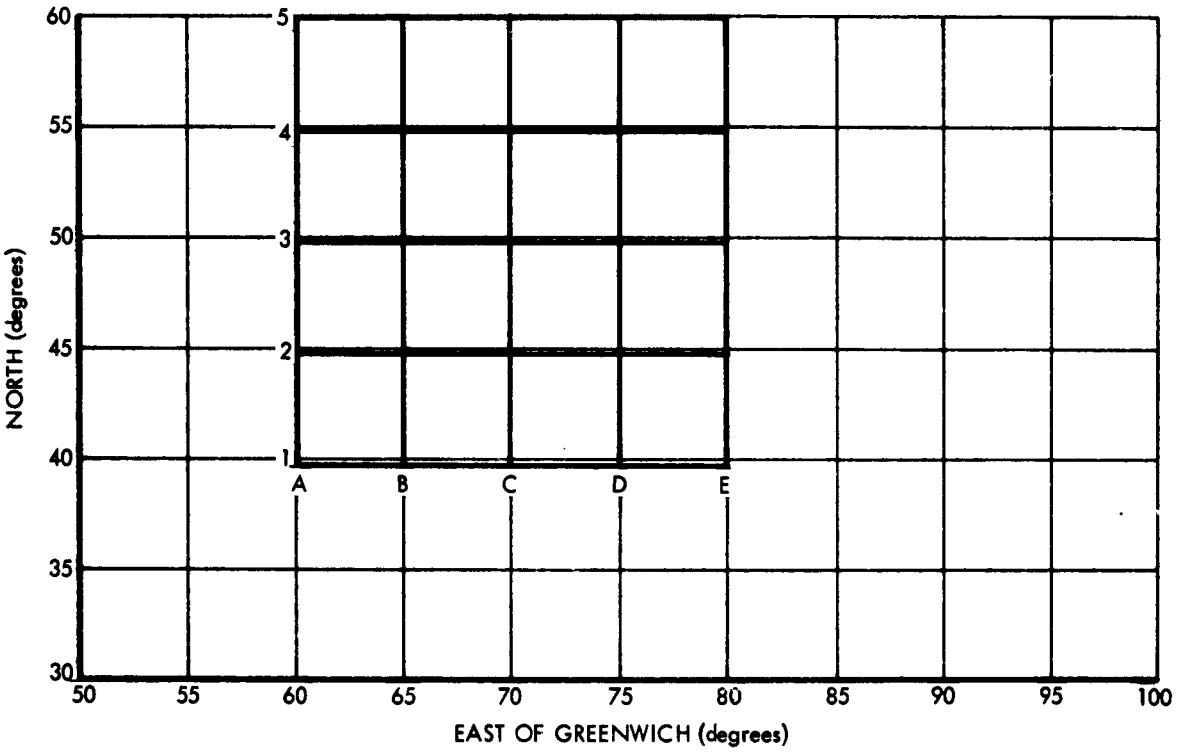

Figure 59. Auroral Conjugate Grids for East E

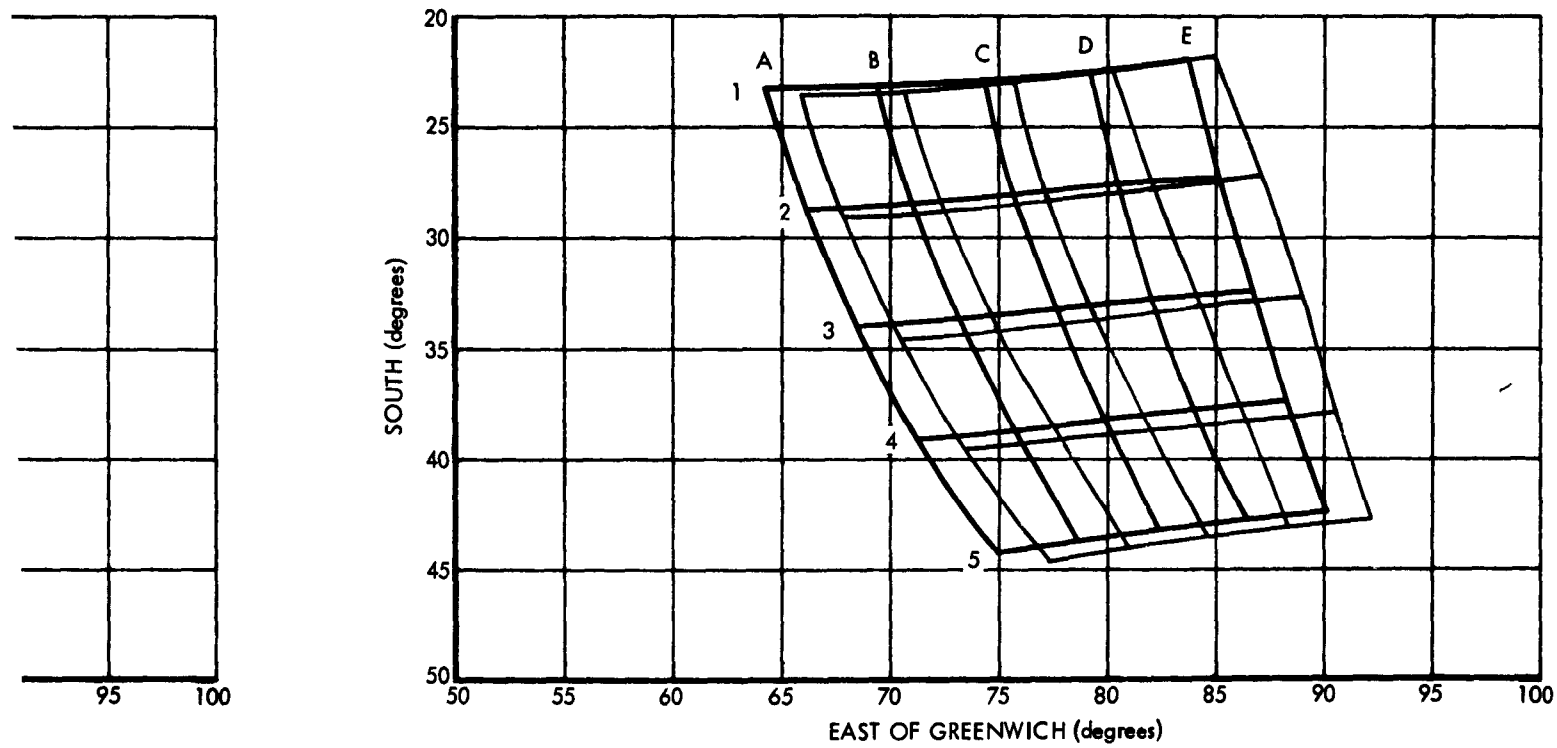

NOTE: Southern Conjugate Grids are Calculated Using Jensen and Whitaker Coefficients and Using Jensen and Cain Coefficients

Auroral Conjugate Grids for East Eurasian Area at 70 km

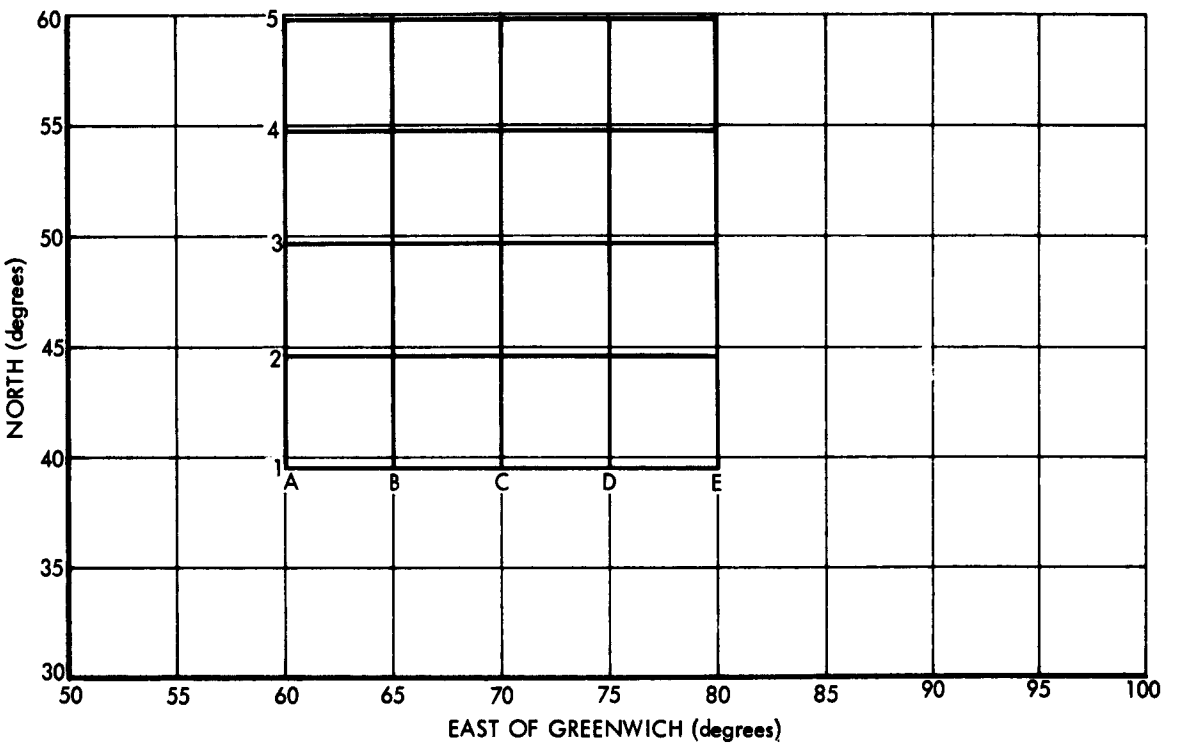

SOUTH (degrees)

Figure 60. Auroral Conjugate Grids for East E

NOTE: Southern Conjugate Grids are Calculated Using Jensen and Whitaker Coefficients and Using Jensen and Cain Coefficients

j0. Auroral Conjugate Grids for East Eurasian Area at 100 km